

UNCERTAINTY BASED ANALYSIS OF SEEPAGE THROUGH EARTH-FILL  
DAMS

A THESIS SUBMITTED TO  
THE GRADUATE SCHOOL OF NATURAL AND APPLIED SCIENCES  
OF  
MIDDLE EAST TECHNICAL UNIVERSITY

BY

MELİH ÇALAMAK

IN PARTIAL FULFILLMENT OF THE REQUIREMENTS  
FOR  
THE DEGREE OF DOCTOR OF PHILOSOPHY  
IN  
CIVIL ENGINEERING

DECEMBER 2014



Approval of the thesis:

**UNCERTAINTY BASED ANALYSIS OF SEEPAGE THROUGH  
EARTH-FILL DAMS**

submitted by **MELİH ÇALAMAK** in partial fulfillment of the requirements for the degree of **Doctor of Philosophy in Civil Engineering Department, Middle East Technical University** by,

Prof. Dr. Gülbin Dural Ünver  
Dean, Graduate School of **Natural and Applied Sciences**

Prof. Dr. Ahmet Cevdet Yalçınır  
Head of Department, **Civil Engineering**

Prof. Dr. A. Melih Yanmaz  
Supervisor, **Civil Engineering Department, METU**

Assoc. Prof. Dr. Elçin Kentel  
Co-supervisor, **Civil Engineering Department, METU**

**Examining Committee Members:**

Assoc. Prof. Dr. Şahnaz Tiğrek  
Civil Engineering Dept., METU

Prof. Dr. A. Melih Yanmaz  
Civil Engineering Dept., METU

Asst. Prof. Dr. Nejan Huvaj Sarihan  
Civil Engineering Dept., METU

Asst. Prof. Dr. Koray K. Yılmaz  
Geological Engineering Dept., METU

Assoc. Prof. Dr. Serhat Küçükali  
Civil Engineering Dept., Çankaya University

**Date:** December 24, 2014

**I hereby declare that all information in this document has been obtained and presented in accordance with academic rules and ethical conduct. I also declare that, as required by these rules and conduct, I have fully cited and referenced all material and results that are not original to this work.**

Name, Last name: Melih Çalamak

Signature :

## ABSTRACT

### UNCERTAINTY BASED ANALYSIS OF SEEPAGE THROUGH EARTH-FILL DAMS

Çalamak, Melih

Ph.D., Department of Civil Engineering

Supervisor : Prof. Dr. A. Melih Yanmaz

Co-Supervisor: Assoc. Prof. Dr. Elçin Kentel

December 2014, 195 pages

The steady-state and transient seepage through embankment dams are investigated considering the uncertainty of hydraulic conductivity and van Genuchten fitting parameters,  $\alpha$  and  $n$  used for unsaturated flow modeling. A random number generation algorithm producing random values for these parameters is coupled with a finite element software, SEEP/W to analyze seepage through earth-fill dams. Monte Carlo simulation is adopted for stochastic seepage analyses. The variability effects of the random parameters on seepage are investigated conducting sensitivity analyses. The variation effects of hydraulic conductivity are found to be significant, whereas those of fitting parameters are shown to be negligible or minor. Considering these, the statistical and probabilistic properties of the seepage are assessed for different embankment dam types and boundary conditions. The degree of uncertainty and statistical randomness of the seepage are evaluated. In general, it is found that the seepage through embankment dams can be characterized by generalized extreme value or three-parameter log-normal distributions.

Keywords: Seepage analysis, Embankment dams, Spatial variability, Uncertainty, Monte Carlo simulation

## ÖZ

### TOPRAK DOLGU BARAJLARIN GÖVDESİNDEKİ SIZMANIN BELİRSİZLİK ESASLI ANALİZİ

Çalamak, Melih

Doktora, İnşaat Mühendisliği Bölümü

Tez Yöneticisi : Prof. Dr. A. Melih Yanmaz

Ortak Tez Yöneticisi : Doç. Dr. Elçin Kentel

Aralık 2014, 195 sayfa

Dolgu barajların gövdesindeki kararlı ve kararsız sızma, hidrolik iletkenlik ve doygun olmayan akım modellemesinde kullanılan van Genuchten parametreleri  $\alpha$  ve  $n$ 'nin belirsizliği göz önünde bulundurularak araştırılmıştır. Bu parametrelerin rasgele değişkenlerini üreten bir rasgele sayı üreticisi algoritma, sonlu elemanlar programı olan ve dolgu barajların gövdesindeki sızma analizlerinde kullanılan SEEP/W ile birleştirilmiştir. Stokastik sızma analizleri için Monte Carlo benzeşimi tekniği kullanılmıştır. Rasgele parametrelerin değişkenliğinin sızma üzerine olan etkileri duyarlılık analizleri ile incelenmiştir. Hidrolik iletkenlik değişkenliği etkisinin önemli olduğu bulunurken  $\alpha$  ve  $n$ 'nin değişkenlik etkilerinin ihmal edilebilir ya da çok küçük oldukları gösterilmiştir. Bunlar göz önünde bulundurularak, farklı dolgu baraj tipleri ve sınır koşulları için, sızmanın istatistiksel ve olasılıksal özellikleri belirlenmiştir. Sızmanın belirsizlik derecesi ve istatistiksel rasgeleliği değerlendirilmiştir. Genel olarak dolgu barajlardaki sızmanın genelleştirilmiş ekstrem değer ya da üç parametrelili log-normal dağılım ile tanımlanabileceği sonucuna varılmıştır.

Anahtar Kelimeler: Sızma analizi, Dolgu barajlar, Yersel değişkenlik, Belirsizlik, Monte Carlo benzeşimi

*To my parents Selma & Yaşar Çalamak*

## ACKNOWLEDGEMENTS

First, I would like to thank my supervisor, Professor Dr. A. Melih Yanmaz, for his guidance and support during my doctoral studies. Professor Yanmaz's mentorship throughout my research and teaching has added tremendously to my academic experience. I have benefited a lot from his wisdom. If this thesis has any academic merit, it is mainly thanks to the experience that I gained from him. I consider myself very lucky to have studied with Professor Yanmaz.

I would like to express my sincere gratitude to Assoc. Prof. Dr. Elçin Kentel who contributed the study with her valuable comments.

I would also like to thank the thesis monitoring committee members Assist. Prof. Dr. Nejan Huvaj Sarihan and Assist. Prof. Dr. Koray K. Yılmaz for their constructive suggestions, which helped improve the study.

My colleagues, fellow assistants, and my friends at METU were always there for me when I needed them. I have always been happy to work, discuss and spend time with Cem Sonat, Göker Türkakar, Meriç Selamoğlu, Dr. M. Tuğrul Yılmaz, and Onur Arı. Also, I appreciate faculty members and administrative staff of METU Water Resources Laboratory for providing me a perfect working environment.

I owe much to my colleague, my best friend and my brother Semih Çalamak for sharing the good and bad in my life. I also thank my sister Müjgan and nephew Rüzgar for making my life happier.

Finally, my dearest family deserves the special thanks. My parents are in the behind of all the achievements and success of my life. I appreciate their endless love, encouragement and tolerance. I undoubtedly could not have done this without them.

## TABLE OF CONTENTS

ABSTRACT .....	v
ÖZ.....	vi
ACKNOWLEDGEMENTS .....	viii
TABLE OF CONTENTS .....	ix
LIST OF TABLES .....	xii
LIST OF FIGURES.....	xiv
LIST OF SYMBOLS AND ABBREVIATIONS.....	xxi
1. INTRODUCTION.....	1
1.1 General.....	1
1.2 The Aim and Scope of the Study.....	2
2. LITERATURE REVIEW.....	5
3. THE METHODOLOGY .....	11
3.1 Hydraulic Model for Seepage Analysis.....	11
3.1.1 Theory and Solution Tools.....	11
3.1.1.1 The Software SEEP/W .....	13
3.1.2 Basics of Unsaturated Flow.....	14
3.2 Random Variable Model and Uncertainty Quantification.....	18
3.3 Monte Carlo Simulation .....	23
3.4 The Statistical Properties of van Genuchten Parameters.....	25
4. UNCERTAINTY BASED STEADY SEEPAGE ANALYSES .....	29

4.1	Preliminary Analysis.....	29
4.2	Uncertainty Based Analyses .....	32
4.2.1	Hypothetical Example 1: Dam 1 .....	36
4.2.2	Hypothetical Example 2: Dam 2 .....	39
4.2.3	Hypothetical Example 3: Dam 3 .....	42
4.3	Discussion .....	45
5.	UNCERTAINTY BASED TRANSIENT SEEPAGE ANALYSES .....	47
5.1	Rapid Drawdown Case .....	49
5.2	Rapid Fill Case.....	71
5.3	Discussion .....	92
6.	APPLICATIONS.....	95
6.1	Rapid Drawdown Case .....	98
6.2	Rapid Fill Case.....	116
6.3	Combined Fill and Drawdown Case .....	130
6.3.1	Homogeneous Embankment Dam .....	131
6.3.2	Simple Zoned Embankment Dam .....	142
7.	DISCUSSION.....	161
8.	CONCLUSIONS .....	165
8.1	Summary .....	165
8.2	Novelty of the Study .....	166
8.3	Conclusions.....	167
8.4	Suggested Future Research .....	168
	REFERENCES .....	171
	APPENDICES .....	183

APPENDIX A: The C# code.....	183
APPENDIX B: Supplementary codes .....	188
CURRICULUM VITAE .....	193

## LIST OF TABLES

### TABLES

Table 4.1 The properties of hypothetical dams considered for sensitivity analyses of steady-state seepage.....	33
Table 4.2 Cases considered for sensitivity analyses of steady-state seepage and corresponding statistical properties of soils. ....	35
Table 4.3 The descriptive statistics of the seepage rate for Case 1 to Case 9. ....	38
Table 4.4 The descriptive statistics of the seepage rate for Case 10 to Case 27. ...	41
Table 4.5 The descriptive statistics of the seepage rate for Case 28 to Case 36. ...	44
Table 5.1 Cases considered for sensitivity analyses of transient seepage and corresponding statistical properties of the soil. ....	48
Table 6.1 The statistical properties of the dam material considered for the application problems given in Section 6.1, Section 6.2 and Section 6.3.1 of Chapter 6. ....	98
Table 6.2 The descriptive statistics of the seepage rate for the rapid drawdown case. ....	99
Table 6.3 Goodness of fit results for PDFs of the seepage for the rapid drawdown case. ....	102
Table 6.4 The descriptive statistics of the seepage rate for the rapid fill case. ....	117
Table 6.5 Goodness of fit results for PDFs of the seepage for the rapid fill case.	119
Table 6.6 The descriptive statistics of the seepage through the homogeneous dam for the combined fill and drawdown case.....	132
Table 6.7 Goodness of fit results for PDFs of seepage through the homogeneous dam for the combined fill and drawdown case.....	134
Table 6.8 The statistical properties of the simple zoned dam material considered for the combined fill and drawdown case. ....	143

Table 6.9 The descriptive statistics of the seepage through the simple zoned dam for the combined fill and drawdown case. .... 145

Table 6.10 Goodness of fit results for PDFs of seepage through the simple zoned dam for the combined fill and drawdown case..... 147

## LIST OF FIGURES

### FIGURES

Figure 3.1 A typical soil-water characteristic curve.....	16
Figure 3.2 The $\alpha$ and $n$ relationship obtained from SoilVision for “Clay”. .....	21
Figure 3.3 The $\alpha$ and $n$ relationship obtained from SoilVision for “Sandy clay”. .	21
Figure 3.4 The SWCCs obtained from SoilVision for “Clay”. .....	27
Figure 3.5 The SWCCs obtained from SoilVision for “Sandy clay”. .....	28
Figure 4.1 The cross-sectional lay-out details of a sample dam.....	30
Figure 4.2 The seepage field for the dam having a height of 25 m. ....	30
Figure 4.3 The seepage field for the dam having a height of 40 m. ....	30
Figure 4.4 The average flow velocities at particular $x/B$ ratios for the dams having heights of 25 m and 40 m. ....	31
Figure 4.5 The change of coefficient of variation of the flow rate with respect to number of Monte Carlo simulations. ....	34
Figure 4.6 The geometry and boundary conditions of Dam 1.....	36
Figure 4.7 The box-plots of the seepage rate for Case 1 to Case 9. ....	38
Figure 4.8 The geometry and boundary conditions of Dam 2.....	39
Figure 4.9 The box-plots of the seepage rate for Case 10 to Case 27. ....	41
Figure 4.10 The geometry and boundary conditions of Dam 3.....	42
Figure 4.11 The box-plots of the seepage rate for Case 28 to Case 36. ....	44
Figure 5.1 The geometry, sections and initial conditions of the dam considered for sensitivity analyses on transient seepage.....	48
Figure 5.2 The upstream boundary condition for the rapid drawdown case .....	50
Figure 5.3 The change of the deterministic flow rate with respect to time for the rapid drawdown case. ....	50

Figure 5.4 The phreatic surface, pore water pressure contours and velocity vectors of deterministic seepage for rapid drawdown when $t=68$ days. ....	52
Figure 5.5 The phreatic surface, pore water pressure contours and velocity vectors of deterministic seepage for rapid drawdown when $t=1152$ days. ....	53
Figure 5.6 The phreatic surface, pore water pressure contours and velocity vectors of deterministic seepage for rapid drawdown when $t=2500$ days. ....	54
Figure 5.7 The box-plots of stochastic seepage for rapid drawdown when $t=68$ days at Section 1. ....	56
Figure 5.8 The box-plots of stochastic seepage for rapid drawdown when $t=68$ days at Section 2. ....	57
Figure 5.9 The box-plots of stochastic seepage for rapid drawdown when $t=68$ days at Section 3. ....	58
Figure 5.10 The box-plots of stochastic seepage for rapid drawdown when $t=68$ days at Section 4. ....	59
Figure 5.11 The box-plots of stochastic seepage for rapid drawdown when $t=68$ days at Section 5. ....	60
Figure 5.12 The box-plots of stochastic seepage for rapid drawdown when $t=1152$ days at Section 1. ....	61
Figure 5.13 The box-plots of stochastic seepage for rapid drawdown when $t=1152$ days at Section 2. ....	62
Figure 5.14 The box-plots of stochastic seepage for rapid drawdown when $t=1152$ days at Section 3. ....	63
Figure 5.15 The box-plots of stochastic seepage for rapid drawdown when $t=1152$ days at Section 4. ....	64
Figure 5.16 The box-plots of stochastic seepage for rapid drawdown when $t=1152$ days at Section 5. ....	65
Figure 5.17 The box-plots of stochastic seepage for rapid drawdown when $t=2500$ days at Section 1. ....	66
Figure 5.18 The box-plots of stochastic seepage for rapid drawdown when $t=2500$ days at Section 2. ....	67

Figure 5.19 The box-plots of stochastic seepage for rapid drawdown when $t=2500$ days at Section 3. ....	68
Figure 5.20 The box-plots of stochastic seepage for rapid drawdown when $t=2500$ days at Section 4. ....	69
Figure 5.21 The box-plots of stochastic seepage for rapid drawdown when $t=2500$ days at Section 5. ....	70
Figure 5.22 The upstream boundary condition for the rapid fill case. ....	71
Figure 5.23 The change of the deterministic flow rate with respect to time for the rapid fill case. ....	72
Figure 5.24 The phreatic surface, pore water pressure contours and velocity vectors of deterministic seepage for rapid fill when $t=50$ days. ....	73
Figure 5.25 The phreatic surface, pore water pressure contours and velocity vectors of deterministic seepage for rapid fill when $t=500$ days. ....	74
Figure 5.26 The phreatic surface and velocity vectors of deterministic seepage for rapid fill when $t=1000$ days. ....	75
Figure 5.27 The box-plots of stochastic seepage for rapid fill when $t=50$ days at Section 1. ....	77
Figure 5.28 The box-plots of stochastic seepage for rapid fill when $t=50$ days at Section 2. ....	78
Figure 5.29 The box-plots of stochastic seepage for rapid fill when $t=50$ days at Section 3. ....	79
Figure 5.30 The box-plots of stochastic seepage for rapid fill when $t=50$ days at Section 4. ....	80
Figure 5.31 The box-plots of stochastic seepage for rapid fill when $t=50$ days at Section 5. ....	81
Figure 5.32 The box-plots of stochastic seepage for rapid fill when $t=500$ days at Section 1. ....	82
Figure 5.33 The box-plots of stochastic seepage for rapid fill when $t=500$ days at Section 2. ....	83

Figure 5.34 The box-plots of stochastic seepage for rapid fill when $t=500$ days at Section 3. ....	84
Figure 5.35 The box-plots of stochastic seepage for rapid fill when $t=500$ days at Section 4. ....	85
Figure 5.36 The box-plots of stochastic seepage for rapid fill when $t=500$ days at Section 5. ....	86
Figure 5.37 The box-plots of stochastic seepage for rapid fill when $t=1000$ days at Section 1. ....	87
Figure 5.38 The box-plots of stochastic seepage for rapid fill when $t=1000$ days at Section 2. ....	88
Figure 5.39 The box-plots of stochastic seepage for rapid fill when $t=1000$ days at Section 3. ....	89
Figure 5.40 The box-plots of stochastic seepage for rapid fill when $t=1000$ days at Section 4. ....	90
Figure 5.41 The box-plots of stochastic seepage for rapid fill when $t=1000$ days at Section 5. ....	91
Figure 6.1 The change of (a) $\mu(Q)$ and (b) $\sigma(Q)$ with respect to time for the rapid drawdown case. ....	101
Figure 6.2 Frequency histogram of $Q$ for rapid drawdown case when $t=68$ days at Section 1. ....	103
Figure 6.3 Frequency histogram of $Q$ for rapid drawdown case when $t=68$ days at Section 2. ....	104
Figure 6.4 Frequency histogram of $Q$ for rapid drawdown case when $t=68$ days at Section 3. ....	105
Figure 6.5 Frequency histogram of $Q$ for rapid drawdown case when $t=68$ days at Section 4. ....	106
Figure 6.6 Frequency histogram of $Q$ for rapid drawdown case when $t=68$ days at Section 5. ....	107
Figure 6.7 Frequency histogram of $Q$ for rapid drawdown case when $t=1152$ days at Section 1. ....	108

Figure 6.8 Frequency histogram of Q for rapid drawdown case when t=1152 days at Section 2. ....	109
Figure 6.9 Frequency histogram of Q for rapid drawdown case when t=1152 days at Section 4. ....	110
Figure 6.10 Frequency histogram of Q for rapid drawdown case when t=1152 days at Section 5. ....	111
Figure 6.11 Frequency histogram of Q for rapid drawdown case when t=2500 days at Section 1. ....	112
Figure 6.12 Frequency histogram of Q for rapid drawdown case when t=2500 days at Section 2. ....	113
Figure 6.13 Frequency histogram of Q for rapid drawdown case when t=2500 days at Section 4. ....	114
Figure 6.14 Frequency histogram of Q for rapid drawdown case when t=2500 days at Section 5. ....	115
Figure 6.15 The change of (a) $\mu(Q)$ and (b) $\sigma(Q)$ with respect to time for the rapid fill case.....	118
Figure 6.16 Frequency histogram of Q for rapid fill case when t=28 days at Section 1. ....	120
Figure 6.17 Frequency histogram of Q for rapid fill case when t=28 days at Section 2. ....	121
Figure 6.18 Frequency histogram of Q for rapid fill case when t=461 days at Section 2. ....	122
Figure 6.19 Frequency histogram of Q for rapid fill case when t=461 days at Section 3. ....	123
Figure 6.20 Frequency histogram of Q for rapid fill case when t=461 days at Section 4. ....	124
Figure 6.21 Frequency histogram of Q for rapid fill case when t=461 days at Section 5. ....	125
Figure 6.22 Frequency histogram of Q for rapid fill case when t=1000 days at Section 2. ....	126

Figure 6.23 Frequency histogram of Q for rapid fill case when t=1000 days at Section 3.....	127
Figure 6.24 Frequency histogram of Q for rapid fill case when t=1000 days at Section 4.....	128
Figure 6.25 Frequency histogram of Q for rapid fill case when t=1000 days at Section 5.....	129
Figure 6.26 The upstream boundary condition for the combined fill and drawdown case.....	130
Figure 6.27 The change of (a) $\mu(Q)$ and (b) $\sigma(Q)$ with respect to time for homogeneous dam subjected to combined fill and drawdown case.....	133
Figure 6.28 Frequency histogram of Q through the homogeneous dam for the combined fill and drawdown case when t=1 days at Section 1.....	135
Figure 6.29 Frequency histogram of Q through the homogeneous dam for the combined fill and drawdown case when t=2 days at Section 1.....	136
Figure 6.30 Frequency histogram of Q through the homogeneous dam for the combined fill and drawdown case when t=2 days at Section 2.....	137
Figure 6.31 Frequency histogram of Q through the homogeneous dam for the combined fill and drawdown case when t=4 days at Section 1.....	138
Figure 6.32 Frequency histogram of Q through the homogeneous dam for the combined fill and drawdown case when t=4 days at Section 2.....	139
Figure 6.33 Frequency histogram of Q through the homogeneous dam for the combined fill and drawdown case when t=6 days at Section 1.....	140
Figure 6.34 Frequency histogram of Q through the homogeneous dam for the combined fill and drawdown case when t=6 days at Section 2.....	141
Figure 6.35 The geometry, sections and initial conditions of the simple zoned dam considered for combined fill and drawdown case.....	142
Figure 6.36 The change of (a) $\mu(Q)$ and (b) COV(Q) with respect to time for simple zoned dam subjected to combined fill and drawdown case.....	146
Figure 6.37 Frequency histogram of Q through the simple zoned dam for the combined fill and drawdown case when t=1 days at Section 1.....	148

Figure 6.38 Frequency histogram of Q through the simple zoned dam for the combined fill and drawdown case when t=1 days at Section 2.....	149
Figure 6.39 Frequency histogram of Q through the simple zoned dam for the combined fill and drawdown case when t=2 days at Section 1.....	150
Figure 6.40 Frequency histogram of Q through the simple zoned dam for the combined fill and drawdown case when t=2 days at Section 2.....	151
Figure 6.41 Frequency histogram of Q through the simple zoned dam for the combined fill and drawdown case when t=2 days at Section 3.....	152
Figure 6.42 Frequency histogram of Q through the simple zoned dam for the combined fill and drawdown case when t=4 days at Section 1.....	153
Figure 6.43 Frequency histogram of Q through the simple zoned dam for the combined fill and drawdown case when t=4 days at Section 2.....	154
Figure 6.44 Frequency histogram of Q through the simple zoned dam for the combined fill and drawdown case when t=4 days at Section 3.....	155
Figure 6.45 Frequency histogram of Q through the simple zoned dam for the combined fill and drawdown case when t=4 days at Section 4.....	156
Figure 6.46 Frequency histogram of Q through the simple zoned dam for the combined fill and drawdown case when t=6 days at Section 1.....	157
Figure 6.47 Frequency histogram of Q through the simple zoned dam for the combined fill and drawdown case when t=6 days at Section 2.....	158
Figure 6.48 Frequency histogram of Q through the simple zoned dam for the combined fill and drawdown case when t=6 days at Section 3.....	159
Figure 6.49 Frequency histogram of Q through the simple zoned dam for the combined fill and drawdown case when t=6 days at Section 4.....	160

## LIST OF SYMBOLS AND ABBREVIATIONS

B	The base width of the dam
CDF	Cumulative distribution function
CLR	Common Language Runtime
COV	Coefficient of variation
$D_{\max}$	The Kolmogorov-Smirnov statistics
FEM	Finite element method
G-3P	Three-parameter gamma distribution
GEV	Generalized extreme value distribution
H	Total head
h	Pressure head
$K_r$	Relative hydraulic conductivity
$K_s$	Saturated hydraulic conductivity
$K_x$	Hydraulic conductivity in x-direction
$K_y$	Hydraulic conductivity in y-direction
LN-3P	Three-parameter log-normal distribution
LPT3	Log-Pearson type 3 distribution
m	A fitting parameter of van Genuchten method
$m_w$	The slope of the water content curve
MCS	Monte Carlo simulation
N	Normal distribution
n	A fitting parameter of van Genuchten method
PDF	Probability density function
Q	Seepage rate
Q'	The boundary flux
r	The correlation coefficient

$r'$	Normally distributed random number
$t$	Time
$t_c$	The crest thickness
$u_1$	Independent random variable 1
$u_2$	Independent random variable 2
$V_{ave}$	The depth averaged flow velocity
$x$	The distance along the dam base measured from the heel
$X^2$	The Chi-square statistics
$Z$	The dam height
$z$	Elevation head
$\alpha$	A fitting parameter of van Genuchten method
$\alpha'$	The level of significance
$\gamma_{sub}$	The submerged specific weight of the soil
$\gamma_w$	The specific weight of water
$\theta$	The volumetric water content
$\theta_r$	The residual water content
$\theta_s$	The saturated water content
$\Theta$	Dimensionless water content
$\mu$	Mean
$\sigma$	Standard deviation

# CHAPTER 1

## INTRODUCTION

### 1.1 General

Dams made of natural earthen materials are commonly susceptible to seepage through their body. Underestimation or misleading estimation of seepage may result in failure of these types of dams. Many dam failures were observed due to seepage related problems, such as internal erosion and piping in the history. The related statistics showed that 43% of dam failures were caused by piping, and 66% of piping incidents were caused by the seepage through the dam body (Foster et al. 2000). Therefore, estimation of seepage through the body is crucial for the safety of the embankment dams.

In practical applications, the prediction of seepage quantity is generally handled with deterministic models using uniformly constant soil properties in space. These studies disregard the variation of both hydraulic and geotechnical properties of soils. However, it is a fact that all soils are heterogeneous in some degree and their properties show variability. Therefore, deterministic models may lead to unrealistic results in predicting the seepage characteristics.

The soil heterogeneities may be considered under two main categories (Elkateb et al. 2003): (1) The lithological heterogeneity, which can be defined as the form of thin soil layers embedded in another soil medium having a more uniform soil mass; (2) The inherent heterogeneity caused by the variation of soil properties (i.e. the

change of soil properties from one point to another) due to various deposition conditions and loading histories.

Along with the inherent uncertainties, there may be other reasons causing uncertainties in soil properties (Husein Malkawi et al. 2000):

- measurement errors caused by the equipment or human being,
- insufficient geotechnical site explorations due to high cost of measurements,
- disregarded soil properties that are hard to assess.

These uncertainties in soil properties may have strong effects on the seepage through the media. Preferential flow paths or unexpectedly high or low seepage fluxes may occur due to variations. Therefore, uncertainties in soil parameters should be taken into consideration to determine the realistic properties of the seepage. This can be achieved by the use of stochastic models. In stochastic modeling, input parameters of the system are considered to be non-deterministic (i.e. random). Due to the randomness of input parameters, output parameters of the system become random, which can be defined with statistical moments and a probability density function.

For the realistic prediction of the seepage characteristics, stochastic modeling is needed considering the randomness of the hydraulic and transport properties, such as hydraulic conductivity, porosity, soil water retention characteristics, etc. of the soil. Along with the consideration of uncertainties, a hydraulic model regarding both unsaturated and saturated flow is required for realistic results. Because, the mechanism of unsaturated flow is highly nonlinear and it may have important effects on the seepage behavior of systems.

## **1.2 The Aim and Scope of the Study**

The main goal of this study is to consider the soil uncertainties in the analysis of seepage through embankment dams and investigate their effects on the flow. In this study, inherent heterogeneity caused by the variation of soil parameters in space are considered as the source of uncertainty. The uncertainty of soils are simulated by

generating random variables of hydraulic conductivity,  $K$  and soil water characteristic curve fitting parameters of van Genuchten method (van Genuchten 1980),  $\alpha$  and  $n$ . The uncertainty of hydraulic conductivity may be resulted from the uncertainty of grain composition, extent of fine particles, irregularities of particle shapes and changes of properties due to compactness. Also, the randomness of  $\alpha$  and  $n$  can be related to the uncertainty of pore size and grain size distributions and clay and organic material contents of the soil. The random variables are used in the computation of the hydraulic conductivity (i.e. saturated or unsaturated hydraulic conductivity) and the soil-water content to simulate the variations in the soil.

The random inputs are generated using their probability density functions defined with a mean and a coefficient of variation (COV). The probabilistic properties of random inputs are determined from the related literature and a large soil database system called SoilVision (Fredlund 2005). The statistics of hydraulic conductivity and soil-water characteristic curve fitting parameters are determined for all soil types considered in the study, i.e. clay, sandy clay, gravelly sand. No previous stochastic model for seepage analysis reported in the literature has utilized such a large database in determination of the statistical properties of their random variables.

A random number generation algorithm is written in C# language. The random variables are generated using Box-Muller transformation method (Box and Muller 1958). The algorithm generates random values for the desired soil property (i.e.  $K$ ,  $\alpha$  and  $n$ ), and compute random hydraulic conductivity and soil-water content. This algorithm is coupled with a finite element software, SEEP/W (Geo-Slope Int Ltd 2013), which is used for the groundwater and seepage problems. Stochastic modeling of the seepage is handled with Monte Carlo simulation technique.

In the scope of the study, sensitivity analyses are conducted for both steady-state and transient unsaturated seepage through embankment dams. In these analyses, one-at-a-time sensitivity analyses are conducted keeping one parameter (i.e.  $K$  or  $\alpha$  or  $n$ ) random and others constant at their mean values. The individual effects of variation of the parameters on seepage are discussed for both states of the flow. The

parameters, whose variability have significant effects on seepage are presented. Also, comparisons are made between the results of sensitivity analyses and deterministic analyses of the seepage. Then, the parameters to be treated as stochastic variables in seepage computations are identified. To our knowledge, no previous study in the literature has presented the individual effects of above-mentioned parameters on the seepage through the embankment dams.

Afterwards, stochastic seepage analyses are conducted on homogeneous and simple zoned embankment dams for the transient flow considering the findings of the sensitivity analyses. The seepage rates obtained from these analyses are evaluated statistically. Their descriptive statistics and frequency histograms are obtained. Also, probability density functions are fitted to the seepage rates to statistically represent the data. The results of stochastic analyses are discussed to reveal the uncertainty of the seepage.

Finally, some suggestions are made for the future studies which will be based on stochastic modeling of seepage problems through embankment dams.

## **CHAPTER 2**

### **LITERATURE REVIEW**

The stochastic modeling of groundwater problems have been extensively studied for the last five decades. One of the first studies of the phenomenon was held by Warren and Price (1961). In this pioneering study, set of simulations, which are a kind of Monte Carlo simulations, and laboratory experiments were performed to investigate the effects of several probability distributions of hydraulic conductivity on steady-state and transient flow through one and three dimensional heterogeneous porous media. Then, the relationship between hydraulic conductivity variation and hydraulic head variation in groundwater flow systems was investigated by McMillan (1966) using numerical simulations. Wu et al. (1973) computed the seepage through an existing dam assuming the locations and dimensions of porous layers as random variables, whose statistical properties are obtained from the field data. Freeze (1975) stochastically analyzed steady-state groundwater flow through a one dimensional porous domain, and transient consolidation of a clay layer, regarding the randomness of hydraulic conductivity, compressibility and porosity. Monte Carlo simulation technique was adopted and it was concluded that the uncertainty degree of the predicted hydraulic heads was relatively large. Bakr et al. (1978) considered the correlation structure of hydraulic conductivity variation in a stochastic analysis of unidirectional flows. The relationship between hydraulic conductivity variation and head variance were investigated. Gutjahr et al. (1978) studied the difference between exact and approximate solutions of stochastic

differential equations of one dimensional flow in statistically homogeneous porous media and concluded that approximate solutions can be used for systems having lower standard deviations of hydraulic conductivity. Smith and Freeze (1979 a; b) conducted stochastic analyses for one and two dimensional steady-state groundwater flows adopting Monte Carlo simulation, and it was found that the standard deviation of hydraulic head increases when the standard deviation of hydraulic conductivity increases. Gutjahr and Gelhar (1981) compared the head variation results of one-dimensional flow through a porous medium obtained from the developed analytical solution and Monte Carlo simulation. It was found that the results obtained from two approaches were in agreement.

Then, studies considering the unsaturated flow in stochastic analysis of groundwater flow problems were introduced into the literature. Bresler and Dagan (1983 a; b), and Dagan and Bresler (1983) assumed the saturated hydraulic conductivity as a random parameter and related moisture content with suction using an analytical model. The variability of hydraulic conductivity, heads and water flux were investigated. Yeh et al. (1985 a; b) stochastically analyzed unsaturated steady-state flow using a perturbation method, which decomposes the random parameters into a mean part and a random fluctuation part. In the first study, only the saturated hydraulic conductivity is considered as a random parameter; in the second one, both hydraulic conductivity and a soil parameter,  $\alpha$ , which was used for relating the saturated and unsaturated hydraulic conductivity, regarded as random. It was concluded that, the degree of variability of hydraulic conductivity depends on its correlation scale, the mean capillary pressure and the mean hydraulic gradient. Mantoglou and Gelhar (1987), Mantoglou (1992), and Zhang (1999) extended the perturbation method used in Yeh et al. (1985 a; b) to transient unsaturated flow. The perturbation method was also used in studies of Tartakovsky (1999), Zhang and Lu (2002) and Lin and Chen (2004). However, this technique is stated to be insufficient in generating random variables having higher variances (Fenton and Griffiths 1996).

The mechanism of unsaturated flow is more complicated than that of the saturated flow. The water flow through an unsaturated soil is governed by some soil properties, such as soil type, grain size, pore size distribution and water retention in the unsaturated soil (Lu and Likos 2004). The behavior of the unsaturated soil is described by the relationship between its soil-water content and matric pressure, which is represented by a function called soil-water characteristic curve. This curve is used to assess the unsaturated hydraulic conductivity in groundwater and seepage flow problems. The functional relationship between pressure and water content is generally estimated using mathematical fitting methods. In most of the previous studies mentioned above, the unsaturated flow is modeled using Gardner's model (Gardner 1956). However, it is well known that van Genuchten model (van Genuchten 1980) is generally better in defining soil-water characteristics. Several researchers including Ahmed (2008), Ahmed et al. (2014), Cheng et al. (2008), Cho (2012), Fu and Jin (2009), Le et al. (2012), Li et al. (2009), Lu and Godt (2008), Soraganvi et al. (2005), Tan et al. (2004), and Thieu et al. (2001) adopted van Genuchten method for modeling unsaturated seepage in their studies.

Besides, liquid-phase configuration in an unsaturated soil is very complex and the relationship between water content and soil suction is not unique: it shows hysteresis. The water content at a given soil suction for a wetting process is less than that of a drying part (Maqsoud et al. 2004; Pham et al. 2005). A number of researchers studied hysteresis effect of unsaturated soils on seepage and groundwater flows (Hoa et al. 1977; Yang et al. 2012, 2013). Also, the uncertainty and relationship between van Genuchten parameters of wetting and drying paths was investigated by Likos et al. (2014).

The most of the previous work applied analytical methods for stochastic analyses. These analyses generally have simplifying assumptions for the solution, which made these methods rarely applicable to realistic hydraulic and geotechnical engineering problems. Because, in real cases, the geometry or problem domain is generally complex. Also, the initial and boundary conditions are complicated.

Therefore, the solution of the governing differential equation using analytical methods may not be possible. Recently, numerical methods are used to simulate systems without simplifications and obtain realistic results. The Finite Element Method (FEM) is the most common technique among numerical methods, which is widely used for modeling of seepage-related problems. The method consists of following main steps: defining the problem geometry, meshing (i.e. discretization), definition of material property, definition of initial and boundary conditions, and solution of finite element equations (Liu and Quek 2003). Many researchers starting from Neuman and Witherspoon (1970, 1971), Neuman (1973), Bathe and Khoshgoftaar (1979), Aral and Maslia (1983) and Lam and Fredlund (1984) have utilized FEM for the analysis of steady, unsteady and saturated, unsaturated seepage.

In the scope of their studies, some researchers established their own finite element model for the analysis, whereas the others adopted package programs or software. The software SEEP/W is one of the comprehensive tools using FEM to analyze seepage and groundwater flow problems occurring in porous media. The software is extensively used for pore water pressure computations (Chu-Agor et al. 2008; Ng and Shi 1998 a, b; Oh and Vanapalli 2010; Zhang et al. 2005) and seepage estimations (Foster et al. 2014; Money 2006; Soleymani and Akhtarapur 2011; Tan et al. 2004) in the literature. This software is also adopted in the present study.

Commonly, for the stochastic analysis of seepage and groundwater flow problems, FEM is coupled with Monte Carlo simulation (MCS) technique. This technique is based on repeated sampling of random variables of input parameters to investigate the probabilistic behavior of the systems. Numerous researchers have applied FEM and MCS in stochastic analysis of seepage through or beneath embankment dams (Ahmed 2012, 2009; Cho 2012; Fenton and Griffiths 1996, 1997; Griffiths and Fenton 1993; Le et al. 2012). Among these, Le et al. (2012) and Cho (2012) studied the stochastic analysis of unsaturated seepage through embankments. Both studies adopted van Genuchten method for unsaturated flow modeling. Le et al. (2012) randomly varied the porosity which resulted in uncertainty in hydraulic conductivity

and water retention properties (i.e. the degree of saturation) of the soil. The influence of correlation lengths of porosity field and the statistics of the seepage rate were investigated and it was resulted that flow rate can be reasonably defined by log-normal probability density function. Cho (2012) considered the variation of hydraulic conductivity of layered soils having independent autocorrelation functions. The effects of correlation distances and anisotropic heterogeneity are investigated and it was found that the seepage behavior of the embankment is dependent on the dominant component of the flow vector.

The generation of the random input in Monte Carlo simulation is one of the main steps of the technique. There are a number of sampling or transformation methods for random number generation. One of the most popular methods for sampling random numbers from a normal distribution is Box-Muller transformation (Golder and Settle 1976). The method can be effectively used within Monte Carlo simulation (Caflisch 1998). There are a number of uncertainty based analysis using Box-Muller transformation with MCS in the areas of both hydraulic and geotechnical engineering (Chalermyanont and Benson 2004; Chang et al. 1994; Eykholt et al. 1999).

In many geotechnical engineering studies, the spatial variation in properties of soils were described using a correlation function. In these research studies, the soil properties were assumed to be correlated over distances. For probabilistic slope stability calculations studies of Cho (2007), Griffiths and Fenton (2004), Griffiths et al. (2009), Gui et al. (2000), Jiang et al. (2014), Srivastava and Babu (2009), and Vanmarcke (1980) have considered the correlation of hydraulic conductivity or strength parameters of soils. Besides, for stochastic analysis of seepage through or beneath embankments, studies of Ahmed (2012, 2009), Cho (2012), Fenton and Griffiths (1996) and Griffiths and Fenton (1997, 1998, 1993) have utilized a correlation function for hydraulic conductivity. Commonly, Gauss-Markov spatial correlation function defined in the study of Fenton and Vanmarcke (1990) was used in these studies. The function governs the degree of correlation between two points

of the field. According to the correlation theory, if the points are closer to each other, they are expected to have similar hydraulic conductivity values. Alternatively, if the points are widely separated, the correlation is expected to be weak. The parameter describing the degree of spatial correlation in the random field is called scale of fluctuation. When the scale of fluctuation goes to infinity, the random field is completely correlated, having uniform hydraulic conductivity field. Among these studies, Fenton and Griffiths (1996) and Ahmed (2009) analyzed seepage through embankment dams stochastically. They considered the random field of hydraulic conductivity having a log-normal distribution function and a correlation structure. The random field theory was used to characterize the uncertainty of the hydraulic conductivity. The random field generation was handled using local average subdivision method defined in Fenton and Vanmarcke (1990). The former study investigated the descriptive statistics of the flow rate through the embankment dam and the latter one compared the seepage results through an earth dam obtained from deterministic and stochastic solutions.

Many of the researchers stated above have considered only the randomness of the hydraulic conductivity in their stochastic seepage or groundwater flow models. However, Li et al. (2009) considered not only the random field of hydraulic conductivity, but also the random fields of van Genuchten fitting parameters,  $\alpha$  and  $n$ . The random fields of fitting parameters were independently generated using Karhunen-Loeve expansion technique. Stochastic analyses were conducted for two-dimensional steady-state and transient flows through a porous medium. The study was focused on the efficiency of probabilistic collocation method and resulted that this method can accurately estimate the seepage rate statistics with a smaller effort when compared with MCS.

## CHAPTER 3

### THE METHODOLOGY

#### 3.1 Hydraulic Model for Seepage Analysis

##### 3.1.1 Theory and Solution Tools

The governing differential equation for the seepage through a two-dimensional domain can be expressed assuming that flow follows Darcy's law (Richards 1931; Papagianakis and Fredlund 1984; Geo-Slope Int Ltd 2013):

$$\frac{\partial}{\partial x} \left( K_x \frac{\partial H}{\partial x} \right) + \frac{\partial}{\partial y} \left( K_y \frac{\partial H}{\partial y} \right) + Q' = \frac{\partial \theta}{\partial t} \quad (3.1)$$

where  $K_x$  and  $K_y$  are the hydraulic conductivities in x and y directions, respectively,  $H$  is the total head being the summation of pressure head ( $h$ ) and elevation head ( $z$ ),  $Q'$  is the boundary flux,  $\theta$  is the volumetric water content and  $t$  is the time. The equation states that the summation of the change of flow in x and y directions and applied external flux is equal to the rate of change of the soil storage (i.e. the volumetric water content) with respect to time.

For steady-state conditions, there is no change in the storage of the soil; therefore, Eq. (3.1) is reduced to the following equation for this condition:

$$\frac{\partial}{\partial x} \left( K_x \frac{\partial H}{\partial x} \right) + \frac{\partial}{\partial y} \left( K_y \frac{\partial H}{\partial y} \right) + Q' = 0 \quad (3.2)$$

The changes in volumetric water content of Eq. (3.1) are derived by the changes in the stress and soil properties (Fredlund and Morgenstern 1976; Fredlund and Morgenstren 1977). Briefly, the change in the volumetric water content can be related with the change in the pore-water pressure of the soil:

$$\partial\theta = m_w \partial u_w \quad (3.3)$$

where,  $m_w$  is the slope of the water content curve and  $u_w$  is the pore water pressure.

Eq. (3.3) can be expressed in terms of the total head and elevation head by:

$$\partial\theta = m_w \gamma_w \partial(H - z) \quad (3.4)$$

In above equation,  $\gamma_w$  is the specific weight of water. As the elevation is constant, the derivative of  $z$  with respect to time will be zero. Then, the partial differential equation given in Eq. (3.1) can be written as (Geo-Slope Int Ltd 2013):

$$\frac{\partial}{\partial x} \left( K_x \frac{\partial H}{\partial x} \right) + \frac{\partial}{\partial y} \left( K_y \frac{\partial H}{\partial y} \right) + Q' = m_w \gamma_w \frac{\partial H}{\partial t} \quad (3.5)$$

The governing partial differential equation of the seepage can be solved using finite element method. This method is based on dividing the problem domain into small sections called elements, describing the behavior of each individual element with element equations and connecting all element equations to characterize the behavior of the whole domain. The element equations are approximated from the original nonlinear equation. Most commonly, Galerkin's weighted residual approach is used to obtain the finite element form of the original equation. In this approach, an integral is formed for the residual of all nodes using a weight function and the residual is set to zero (Liu and Quek 2003).

The governing differential equation of the seepage can be approximated using Galerkin's weighted residual method. The finite element seepage equation can be expressed in a general form using (Geo-Slope Int Ltd 2013):

$$[K]\{H\} + [M]\{H\} = \{Q\} \quad (3.6)$$

in which  $[K]$  is the element characteristics matrix,  $\{H\}$  is the vector of nodal heads,  $[M]$  the element mass matrix,  $\{Q\}$  is the applied flux vector. The detailed finite element formulation can be found in Geo-Slope Int. Ltd. (2013).

#### **3.1.1.1 The Software SEEP/W**

In this study, the software SEEP/W (Geo-Slope Int Ltd 2013) is used to conduct seepage analyses. It is a comprehensive computer aided design software, developed by Geo-Slope International Ltd., for analyzing groundwater flow, seepage, excess pore-water pressure dissipation problems within porous media (Geo-Slope Int Ltd 2014). The software allows modeling of both saturated and unsaturated flows. The steady, transient, confined and unconfined flow problems having various boundary conditions can be analyzed via this software.

The software adopts finite element method to solve the nonlinear governing differential equation of the seepage given in Eq. (3.5). The finite element formulation of the software is briefly described in the previous section. The solution is conducted in an iterative manner in the software. Hydraulic conductivity of an element or the size of the seepage face are iteratively calculated. For example, in an iteration, hydraulic conductivity of an element is computed using the average pore water pressure of its nodes. For the next iteration, resulting hydraulic conductivity is used to compute the pore water pressures of the element nodes. This, procedure is repeated until the convergence is reached in the computations.

SEEP/W can compute hydraulic conductivity, total head, pore water pressure, flow velocity magnitudes and gradients at the nodes of the finite element domain. Also, the seepage rates across desired sections can be obtained from the software. Some views from the interface of the software and its full capabilities can be found in Geo-Slope Int Ltd (2014).

SEEP/W allows the use of add-in functions which are used to define soil properties, boundary conditions, etc. This is the main reason for selecting this software as the simulation tool of this study. The problems can be modeled without limitations by

using add-in functions. This also allowed this study to quantify uncertainties in soil properties in the seepage analyses.

The add-in functions which are to be used in SEEP/W should be based on Microsoft .NET CLR (Common Language Runtime) (Geo-Slope Int. Ltd 2012). Any programming language which can generate CLR code can be used to create an add-in including C# and Visual Basic .NET.

### **3.1.2 Basics of Unsaturated Flow**

Soil part above the phreatic surface of the seepage is in partially saturated or unsaturated condition. The pore water saturation is less than unity in the unsaturated zone and there exists suction in the soil matrix. Due to the suction, some saturated mechanical properties of the soil, such as the hydraulic conductivity, the shear strength, the compression index etc., change (Sako and Kitamura 2006).

In the unsaturated zone of the soil, some quantity of flow takes place due to the suction or capillary action. In relatively high values of the suction and correspondingly low values of water content soil-water-air systems, the flow is governed by the adsorption effects caused by the surface properties of the soil particles. Oppositely, in relatively high values of water content and correspondingly low values of the suction, the flow is governed by the capillary action which directly depends on pore structure and pore size distribution (Lu and Likos 2004).

The relationship between the soil suction and water content is described with soil water characteristic curve (SWCC). The shape of a SWCC is determined by the density, pore size distribution, grain size distribution, clay content, organic material content, etc., of the soil (Lu and Likos 2004). The SWCC of an existing soil can be obtained by experimental methods both in sites and in a laboratory medium. Discrete data points showing the water content and the corresponding suction are obtained from direct measurements. Data points are generally plotted on semi-log graphs and a representative curve is fitted to the points. However, the direct measurement of SWCC may be difficult and expensive in some cases. Sampling, transporting and

preparation of specimens in laboratory tests, and installation, maintenance and monitoring in field measurements may be costly, time consuming and complex (Lu and Likos 2004). Therefore, generally mathematical functions which are fitted to soil water characteristics data are used for the sake of simplicity. There are many mathematical models proposed in the literature for presenting SWCC. They are namely, Brooks and Corey (1964) model, Brutsaert (1966) model, Burdine (1953) model, Fredlund and Xing (1994) model, Gardner (1956) model, van Genuchten (1980) model, Mualem (1976) model, and Tani (1982) model. In this study, van Genuchten (1980) model is adopted to estimate the unsaturated hydraulic conductivity and it is explained below. The detailed information and reviews on other models can be found in Sillers et al. (2001).

The van Genuchten (1980) model is based on prediction of the unsaturated hydraulic conductivity from the information of the soil water characteristic curve and saturated hydraulic conductivity. In the model, an equation for the soil water content and suction relationship is described. Also, closed-form analytical expressions are defined for unsaturated hydraulic conductivity using the equation of soil water characteristics curve. The equation of the SWCC contains three fitting parameters; namely,  $\alpha$ ,  $n$ , and  $m$ . The parameter  $\alpha$  is the inverse of the air entry pressure which is the suction where the air first starts to enter to the largest pore of the soil. Therefore, it is related with the largest pore size of the soil (Lu and Likos 2004). The  $n$  parameter is related to the slope of SWCC at its inflection point which shows the rate of change of the desaturation zone. It depends on the pore size distribution (Sillers et al. 2001). The parameter  $m$  is related to the asymmetry of the SWCC about its inflection point. A typical SWCC illustrating the air-entry value, saturated and residual water contents and the inflection point is given in Figure 3.1.

The water content of a soil can be expressed with a dimensionless variable by normalizing it with its saturated and residual values. The function of the dimensionless water content,  $\theta$  is in the following form:

$$\Theta = \frac{\theta - \theta_r}{\theta_s - \theta_r} \quad (3.7)$$

where  $\theta$  is the volumetric water content, and  $s$  and  $r$  indicates the saturated and residual values of the water content, respectively.

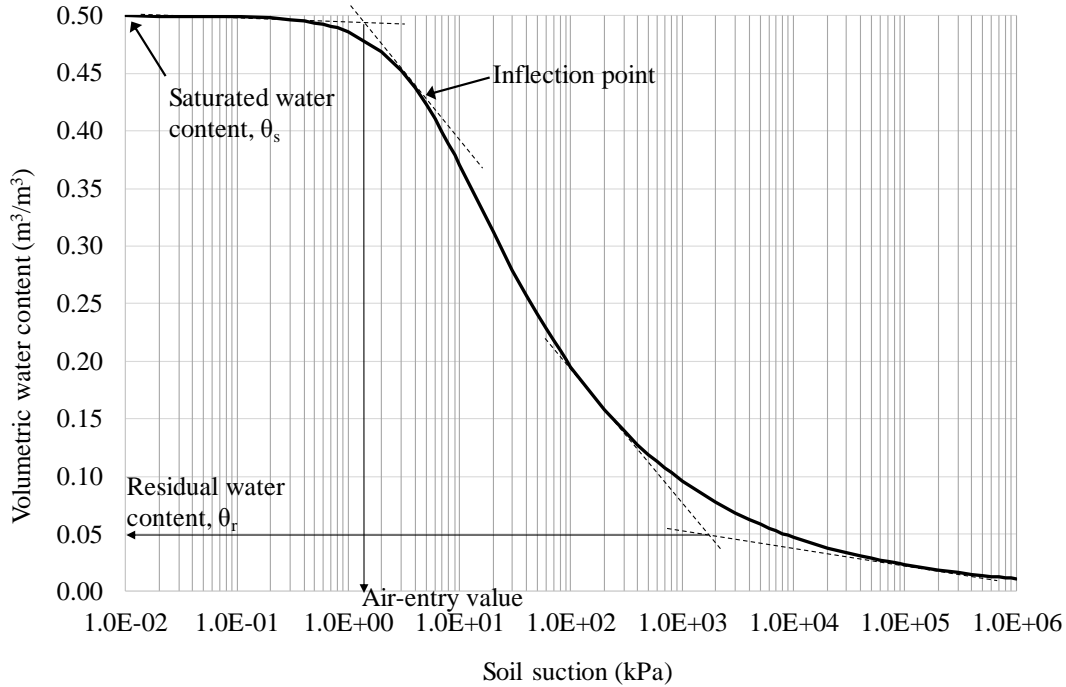


Figure 3.1 A typical soil-water characteristic curve.

van Genuchten (1980) proposed a closed form, three-parameter equation for the estimation of the dimensionless water content:

$$\Theta = \frac{I}{\left(1 + (\alpha h)^n\right)^m} \quad (3.8)$$

where  $\alpha$ ,  $n$  and  $m$  are fitting parameters and  $h$  is the pressure head. The parameter  $m$  is related to  $n$  with the following equation (van Genuchten 1980):

$$m = 1 - \frac{1}{n} \quad (3.9)$$

The pressure term in the right-hand side of Eq. (3.8) can be expressed in either units of pressure or head, which can be taken as kPa and m, respectively in SI unit system. If it is expressed with the unit of pressure,  $\alpha$  has the inverse unit of pressure (i.e. kPa<sup>-1</sup>). In the other case,  $\alpha$  has the inverse unit of head (i.e. m<sup>-1</sup>). Then, by using equations (3.7) and (3.8) the water content can be defined with the following function:

$$\theta = \theta_r + \frac{\theta_s - \theta_r}{\left(1 + (\alpha h)^n\right)^m} \quad (3.10)$$

In the prediction of unsaturated hydraulic conductivity, a variable called,  $K_r$ , relative hydraulic conductivity is used. It is the normalized form of the unsaturated hydraulic conductivity with respect to saturated hydraulic conductivity:

$$K_r = \frac{K}{K_s} \quad (3.11)$$

where  $K_s$  is the saturated hydraulic conductivity. For the prediction of the relative hydraulic conductivity Mualem (1976) proposed the following equation:

$$K_r = \Theta^{1/2} \left[ \frac{\int_0^\Theta \frac{1}{h(x)} d(x)}{\int_0^1 \frac{1}{h(x)} d(x)} \right]^2 \quad (3.12)$$

van Genuchten (1980) utilized Eq. (3.12) to derive a closed form equation for the relative hydraulic conductivity. The equation is obtained using equations (3.8), (3.9) and (3.12) with some restrictions (van Genuchten 1980):

$$K_r(\Theta) = \Theta^{1/2} \left[ 1 - \left(1 - \Theta^{1/m}\right)^m \right]^2 \quad (3.13)$$

When Eq. (3.8) is substituted into Eq. (3.13), the relative hydraulic conductivity can be expressed in terms of the pressure head:

$$K_r(h) = \frac{\left\{ 1 - (\alpha h)^{n-1} \left[ 1 + (\alpha h)^n \right]^{-m} \right\}^2}{\left[ 1 + (\alpha h)^n \right]^{m/2}} \quad (3.14)$$

Then, one may compute the hydraulic conductivity using the function given below.

$$K(h) = \begin{cases} K_s K_r(r) & (h < 0) \\ K_s & (h \geq 0) \end{cases} \quad (3.15)$$

### 3.2 Random Variable Model and Uncertainty Quantification

The purpose of modeling variables of the seepage process as random numbers is to treat the uncertainties in the problem. In seepage-related problems, there may be uncertainties in soil properties, such as hydraulic conductivity, porosity, fitting parameters of the SWCC, etc. Also, initial and/or boundary conditions may be uncertain. For example, the inflow into the reservoir of an embankment dam is generally uncertain due to the randomness of hydrological parameters (Vanmarcke 2010). These uncertainties can be represented by using random variables. The random input generation is one of the main parts of the Monte Carlo simulation approach.

In computational statistics, random variable generation is mainly handled in two steps (L'Ecuyer 2012): (1) generation of independent and uniformly distributed random variables over the interval (0,1) and (2) applying transformations to these random variables to generate random numbers from desired probability distributions. The process in step (1) is called pseudo random number generation. There are different transformation methods for step (2), depending on the probability distribution of the random number.

In the study, soil uncertainty is modeled by treating hydraulic conductivity and van Genuchten fitting parameters  $\alpha$  and  $n$  as random inputs. These random inputs have non-uniform density functions. One of the comprehensive transformation techniques for non-uniform, particularly Gaussian, random variable generation is

Box-Muller method (Box and Muller 1958). This method is adopted for the random number generation in this study. Random variables for hydraulic conductivity,  $K$  and van Genuchten fitting parameters  $\alpha$  and  $n$  are generated using their probability density functions (PDFs) defined with a mean and coefficient of variation (COV).

A brief information on the basic statistical definitions frequently used in this study are introduced herein. The mean is the expected value of the data set and it is the first moment. The variance is the second central moment and shows how the data is distributed about the mean. The coefficient of variation is the ratio of standard deviation to the mean, being a dimensionless measure of the variability of the data set. The skewness is the third central moment and gives the information about the symmetry of the probability distribution of the data set. The fourth moment is kurtosis, being the measure of peakedness or flatness of the probability distribution (Ang and Tang 1975).

Before generating random variables of parameters  $\alpha$  and  $n$ , the correlation between two variables is investigated. In the study of Phoon et al. (2010), the parameters  $\alpha$  and  $n$  for sandy clay loam, loam, loamy sand, clay and silty clay are stated to be negatively correlated with correlation coefficients -0.268, -0.251, -0.409, -0.487 and -0.308, respectively. The correlation coefficients were determined using the data of 55 soils for loamy sand, 50 soils for sandy clay loam, 67 soils for loam, 17 soils for clay, and 24 soils for silty clay. It can be said that the statistical analyses conducted in the study were based on limited number of soils. Also, absolute values of the correlation coefficients are smaller than 0.35 indicate weak or low correlations (Rumsey 2011; Taylor 1990).

In the scope of the present study, a statistical analysis is held to investigate the correlation between  $\alpha$  and  $n$  for clay and sandy clay soil types. The data of these parameters are gathered from the database of SoilVision software (Fredlund 2005). The software has a comprehensive soil database containing detailed information of over 6000 soils (SoilVision Systems Ltd. 2014). The soil water characteristic curves, saturated permeabilities, soil compression and compaction data, etc., of numerous

soil types can be found in the software. For the statistical analysis, the data of  $\alpha$  and  $n$  are obtained from 100 soils for clay and 103 soils for sandy clay. The relationship and correlation between  $\alpha$  and  $n$  are investigated using scatterplots given in Figure 3.2 and Figure 3.3 for clay and sandy clay, respectively. In these figures,  $r$  stands for the Pearson product-moment correlation coefficient (Pearson 1895). The correlation coefficients are calculated as 0.24 for clay and 0.34 for sandy clay. Similarly, it can be said that these coefficients represent weak correlations between two parameters (Rumsey 2011; Taylor 1990).

On the other hand, the parameters  $\alpha$  and  $n$  are expressed to be independent in the study of van Genuchten (1980). Also, in the study of Li et al. (2009) random variables of these parameters were sampled independently from their prescribed probability distributions. The independence between two parameters can be explained by the fact that the parameter  $\alpha$  is determined by the largest pore size of the soil, whereas the parameter  $n$  is determined by the pore size distribution of the soil (Lu and Likos 2004). Besides, the weak correlation between two parameters were found to be negative in the study of Phoon et al. (2010) and positive in this study, which is inconsistent in view of statistical dependence. Therefore, weak correlations between parameters  $\alpha$  and  $n$  are neglected and they are assumed as independent variables in this study.

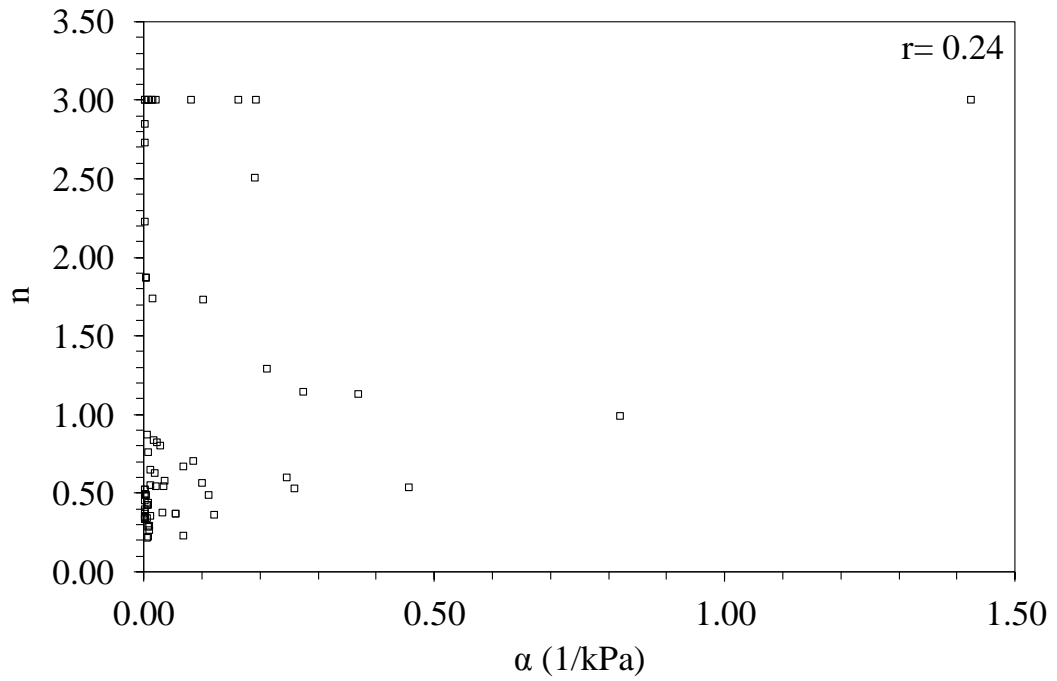


Figure 3.2 The  $\alpha$  and  $n$  relationship obtained from SoilVision for "Clay".

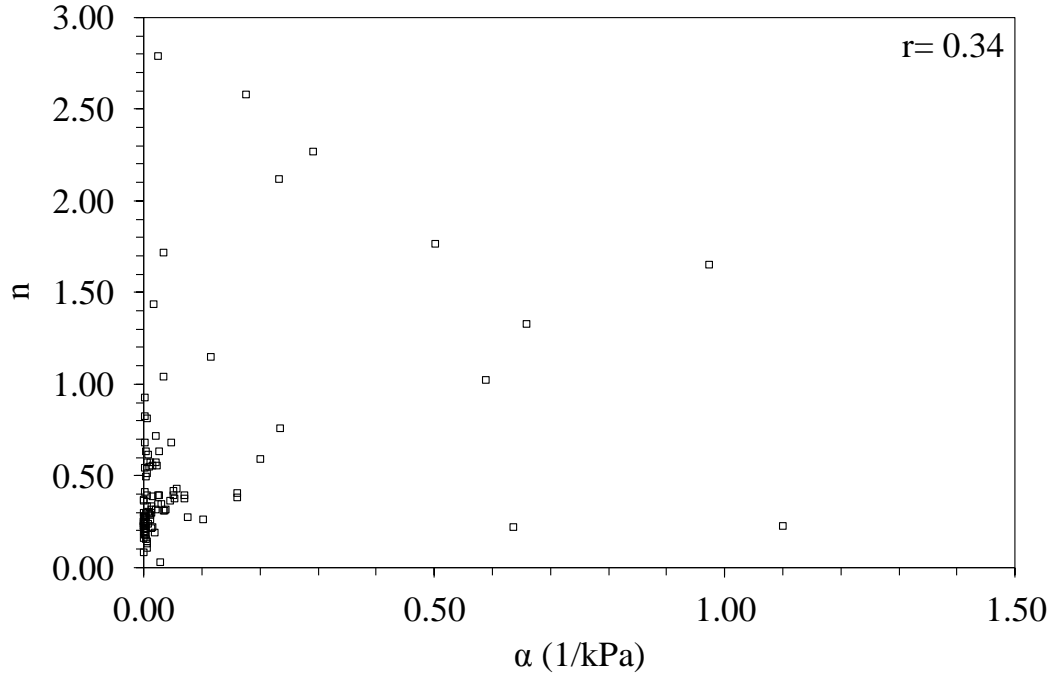


Figure 3.3 The  $\alpha$  and  $n$  relationship obtained from SoilVision for "Sandy clay".

The random variable generation method of the study is used for all random parameters: hydraulic conductivity,  $K$  and SWCC fitting parameters,  $\alpha$  and  $n$ . The procedure for random saturated hydraulic conductivity generation is explained below. The same steps are also used for random variable generation of  $\alpha$  and  $n$ .

The parameters  $\alpha$  and  $n$  are shown to follow log-normal distribution for many types of soils (Carsel and Parrish 1988; Phoon et al. 2010). Also, hydraulic conductivity follows log-normal distribution (Bennion and Griffiths 1966; Bulnes 1946; Law 1944; Warren and Price 1961; Willardson and Hurst 1965). The probability density function of saturated hydraulic conductivity can be defined with mean,  $\mu_{K_s}$  and variance,  $\sigma_{K_s}^2$ . Then, natural logarithm of  $K_s$  (i.e.  $\ln K_s$ ) can be said to follow normal distribution with a mean  $\mu_{\ln K_s}$  and a variance  $\sigma_{\ln K_s}^2$ . The following transformations can be used to obtain the mean and variance of the normalized PDF (Ang and Tang 1975; Fenton and Griffiths 1996):

$$\sigma_{\ln K_s}^2 = \ln \left( 1 + \frac{\sigma_{K_s}^2}{\mu_{K_s}^2} \right) \quad (3.16)$$

$$\mu_{\ln K_s} = \ln(\mu_{K_s}) - \frac{1}{2} \sigma_{\ln K_s}^2 \quad (3.17)$$

Then, the random variables for hydraulic conductivity having log-normal distribution can be obtained using:

$$K_s = \exp(\mu_{\ln K_s} + \sigma_{\ln K_s} r') \quad (3.18)$$

in which  $r'$  is the standard normally distributed random number obtained from Box-Muller transformation (Box and Muller 1958):

$$r' = (-2 \ln u_1)^{1/2} \sin 2\pi u_2 \quad (3.19)$$

where  $u_1$  and  $u_2$  are independent random variates from the same uniform probability density function on the interval (0, 1).

The random number generation algorithm described here is implemented in a code written in C# language. The code runs as an add-in within the SEEP/W software. The code consist of two sub-functions: one is for calculating the relative hydraulic conductivity using van Genuchten method, and the other one is for computing the soil-water content using van Genuchten method. Two main parts handle the generation of random variables for  $\alpha$ ,  $n$  and  $K$  and call the sub-functions to compute random hydraulic conductivity and water content, separately.

### **3.3 Monte Carlo Simulation**

For many real world problems, input parameters, initial and boundary conditions are random in nature. Due to these random variables, the behavior of the systems may be different than they are expected. Generally, statistical properties of these random variables are known from previous observations based on field or laboratory measurements. To fully investigate such systems, a set of simulations can be conducted using artificially generated random variables from their known statistical properties. The solution of each simulation yields an output. If numerous numbers of simulations are conducted, a set of outputs can be obtained. Then, the outputs can be statistically analyzed to understand the behavior of the system. This method is named as Monte Carlo simulation (MCS) (Singh et al. 2007).

Monte Carlo simulation is generally used for determination of the output properties of complex systems whose behavior are nonlinear. For these systems, analytical solutions may need unrealistic assumptions or even may not be possible. The systems can be modeled very close to the reality using MCS. It allows detailed description of the system without using any assumptions or simplifications. This is the main advantage of this approach.

Monte Carlo simulation is the most frequently used approach in stochastic analysis of seepage and groundwater problems in porous medium. The modeling of such type of problems requires the detailed definition of the problem geometry, soil properties, such as hydraulic conductivity function, volumetric water content function, and

initial and boundary conditions. MCS allows the detailed description of the problems and the use of desired numerical solution technique in analyses. There are also a number of other stochastic methods for probabilistic analysis of seepage and groundwater related problems, such as perturbation and probabilistic collocation methods; however MCS is relatively simple and reliable. One disadvantage of this technique may be the computational effort needed for numerous number of simulations. However, the recent growth in computer processors and speed made MCS a less time consuming and powerful tool.

For above-mentioned reasons, Monte Carlo simulation technique is adopted in this study. The problems are solved repeatedly for the same geometry and boundary conditions; but for different random inputs (i.e. hydraulic conductivity and/or van Genuchten fitting parameters,  $\alpha$  and  $n$ ). The random inputs are generated from their probability density functions defined with a mean and a coefficient of variation (COV). The generated random variables are consistent and they represent the uncertainties in some properties of a certain soil type. The repeated simulations yield a set of seepage rate values having the same number with the number of simulations. Then, the set of output is statistically analyzed by obtaining its descriptive statistics, frequency histogram, probability distribution function or box-plot.

The steps followed for MCS of the study are as follows:

- 1) A probability density function having a mean and a coefficient of variation is determined for the random parameter (i.e. hydraulic conductivity, or  $\alpha$  or  $n$ ) from the related literature and the database of SoilVision software (Fredlund 2005).
- 2) The geometry, initial and boundary conditions, the materials and their statistical properties are defined for the problem in the finite element software SEEP/W.
- 3)  $N$ , being the number of MCS, number of copies of the SEEP/W simulation file are generated using a batch file written in Windows command line (see Appendix B for the related batch file).

- 4) N number of copies are solved individually for steady-state or transient seepage using another batch file. During the solution of copies, the random variables are individually generated for each simulation file using the C# code which can work as an add-in in SEEP/W (see Appendix A and Appendix B for the C# code and the related batch file, respectively).
- 5) N number of SEEP/W simulation files are extracted using a different batch file (see Appendix B for the related batch file).
- 6) N number of seepage rate values are gathered in one final Microsoft Excel file using a code written in Visual Basic language (see Appendix B for the related supplementary code).

For the sensitivity analyses and the applications of the study, the above procedure is applied for the stochastic solution of the problems.

### **3.4 The Statistical Properties of van Genuchten Parameters**

Monte Carlo simulation requires the probability density functions of model input parameters which can be defined with a mean and a coefficient of variation. These properties have significant effects on the output parameters and play an important role in determination of the behavior of the systems.

This study considers the uncertainty of hydraulic conductivity and SWCC fitting parameters, which is defined by van Genuchten method. In the study, the probability density function properties of the hydraulic conductivity of different soil types are directly obtained from the related literature. However, a different approach is followed for the fitting parameters,  $\alpha$  and  $n$ . Because for these parameters, the deterministic values are extensively supplied for different soil types in the literature (Ghanbarian-Alavijeh et al. 2010; Yates et al. 1989). However, the distributional information and statistical properties of  $\alpha$  and  $n$  is often lacking or not well established. There are only a few studies providing this information (Carsel and Parrish 1988; Zeng et al. 2012). In the scope of this study, both the related literature and the database of SoilVision software (Fredlund 2005) are utilized to obtain and

justify the probabilistic characteristics of  $\alpha$  and  $n$ . The use of SoilVision database is as follows: the data (i.e. location, physical properties, etc., and van Genuchten fitting parameters) of 100 soils for clay and 103 soils for sandy clay are extracted from the database. Then, SWCC of every sampled soil are drawn using Eq. (3.8) for each soil type (i.e. clay and sandy clay). A few soils having extreme values of fitting parameters are eliminated to determine a reasonable range for SWCCs. The obtained SCWWs are given in Figure 3.4 and Figure 3.5 for clay and sandy clay, respectively.

As can be seen from Figure 3.4 and Figure 3.5 the upper and lower bounds are determined for SWCCs of clay and sandy clay. Then, the mean SWCC obtained using the mean  $\alpha$ ,  $\mu_\alpha$  and the mean  $n$ ,  $\mu_n$  given in Carsel and Parrish (1988) is drawn for clay and sandy clay on these figures. It is seen that, the mean SWCC stays inside the lower and upper bounds for both soil types. Also, the coefficient of variation values of fitting parameters (i.e. for clay,  $COV(\alpha)=0.80$ ,  $COV(n)=0.07$ ; for sandy clay,  $COV(\alpha)=0.63$ ,  $COV(n)=0.08$  (Carsel and Parrish 1988)) can be said to be relatively small. This means, randomly generated SWCCs having statistical properties defined in Carsel and Parrish (1988) will not be dispersed and commonly remain inside the determined bounds. Therefore, it is concluded that the use of statistical properties given in Carsel and Parrish (1988) yields realistic random SWCCs and reasonable for the rest of the analyses of the study.

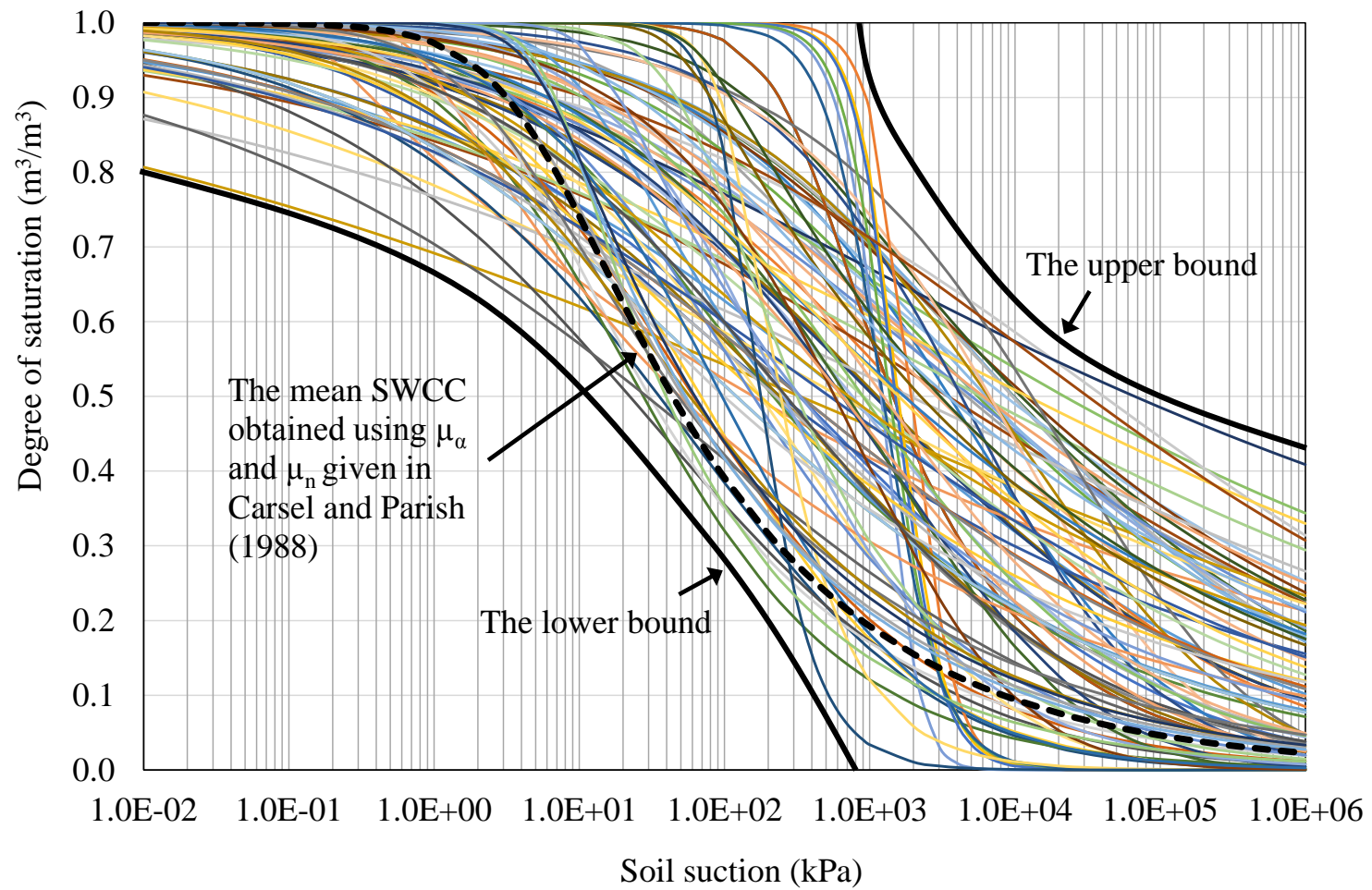


Figure 3.4 The SWCCs obtained from SoilVision for “Clay”.

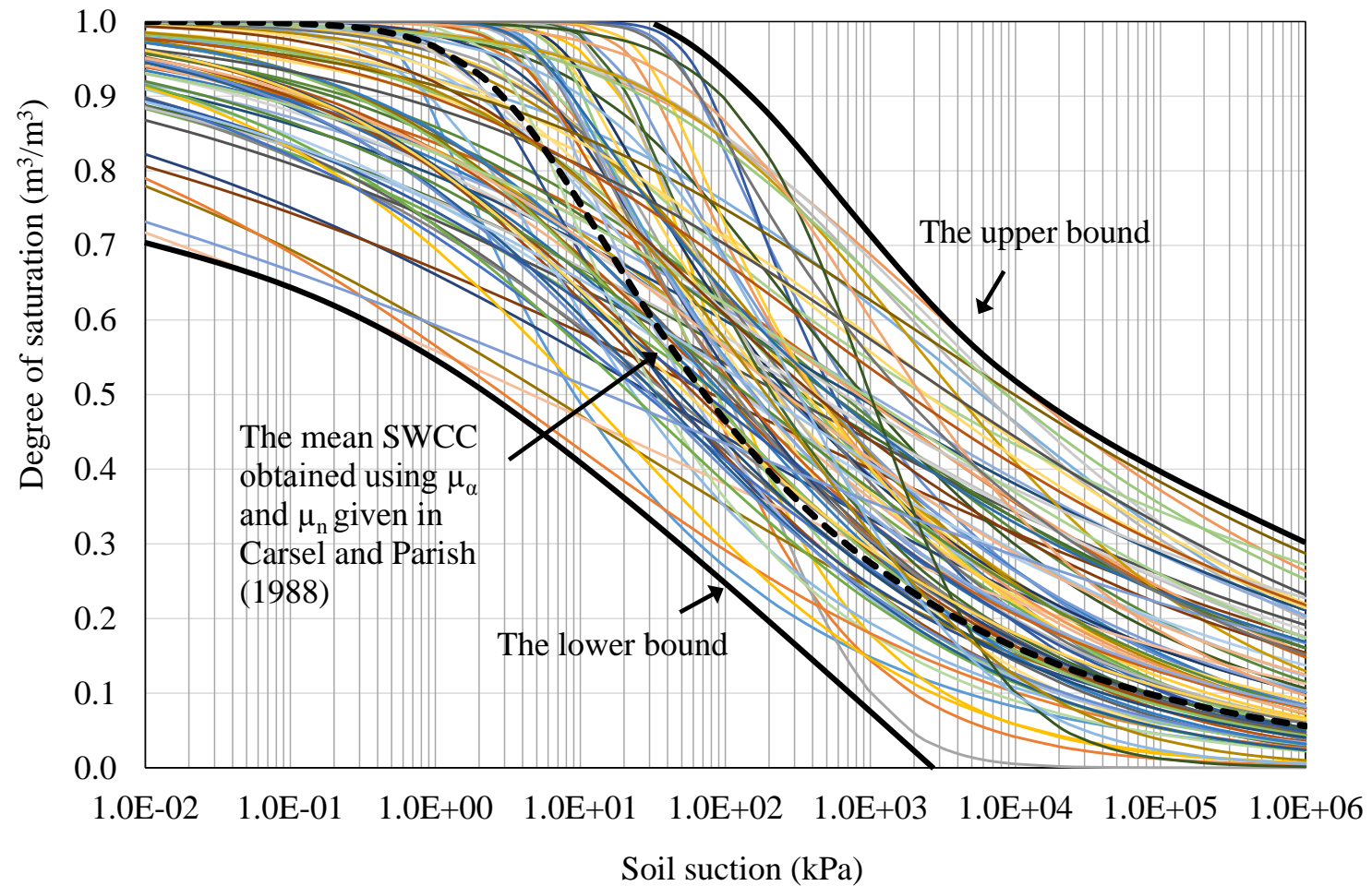


Figure 3.5 The SWCCs obtained from SoilVision for “Sandy clay”.

## CHAPTER 4

### UNCERTAINTY BASED STEADY SEEPAGE ANALYSES

#### 4.1 Preliminary Analysis

Series of simulations need to be conducted to assess the findings of uncertainty-based seepage analysis. In order to limit almost infinite number of configurations reflecting dam height, material type, and embankment zoning possibilities, the computations are desired to be conducted for various material arrangements for a given dam height. However, to evaluate the possible effect of dam height on the seepage field for a given dam geometry composed of a certain material arrangement, a preliminary analysis is carried out for two different heights of a dam having simple zoning as shown in Figure 4.1. In this figure,  $Z$  and  $H$  are the dam height and the total upstream head, respectively,  $B$  is the total width of the base of the dam,  $x$  is the distance along the dam base measured from the heel, and  $t_c$  is the crest thickness.

Dam geometric characteristics are decided according to USBR (1987) criteria. To this end, dams having heights of 25 m and 40 m are considered with the upstream total heads of 23 m, and 37 m, respectively. The SEEP/W software is executed for steady state conditions to determine the spatial distribution of the seepage field throughout the dam body (see Figure 4.2, and Figure 4.3).

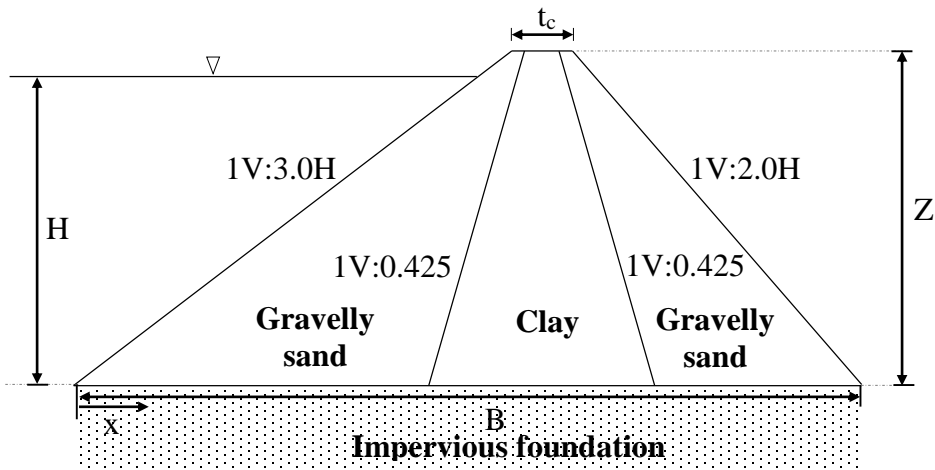


Figure 4.1 The cross-sectional lay-out details of a sample dam.

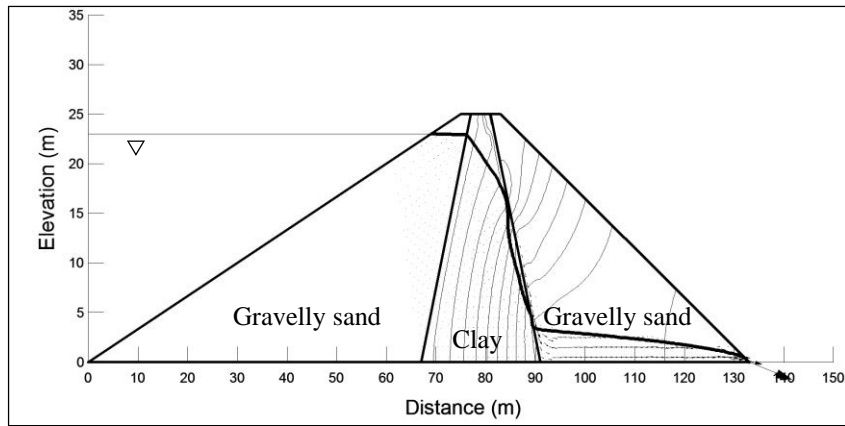


Figure 4.2 The seepage field for the dam having a height of 25 m.

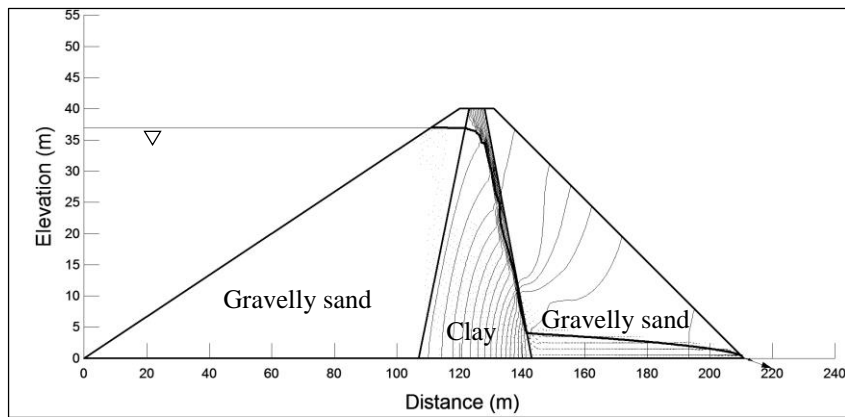


Figure 4.3 The seepage field for the dam having a height of 40 m.

For comparison purposes, the flow velocity values are determined throughout the vertical plane between the base and the phreatic line at given  $x/B$  values. Hence, at a particular  $x/B$  ratio, the depth averaged flow velocity ( $v_{ave}$ ) along the vertical direction is computed (see Figure 4.4).

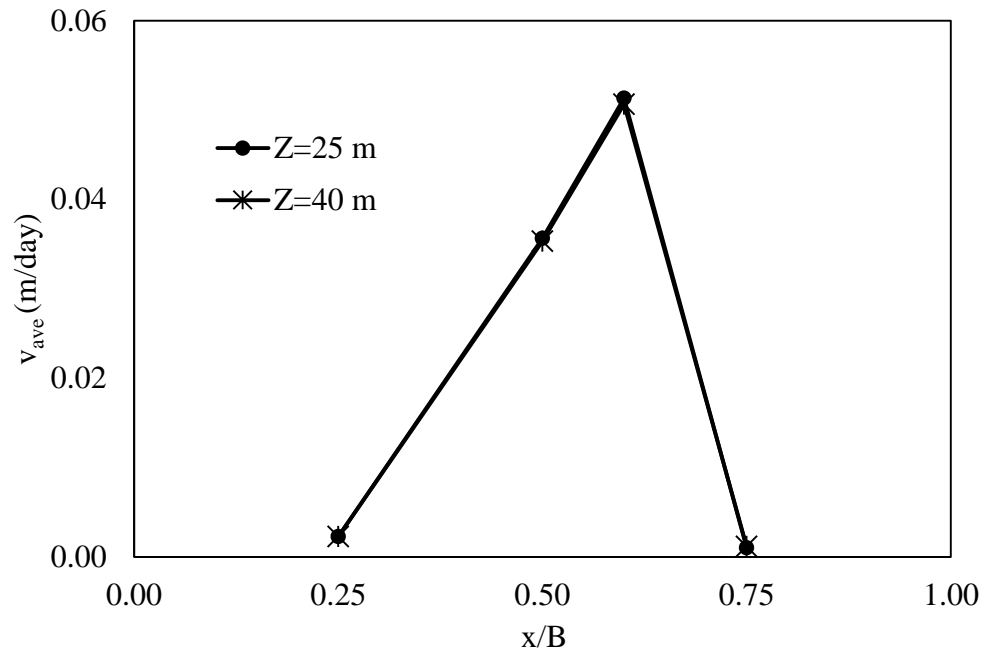


Figure 4.4 The average flow velocities at particular  $x/B$  ratios for the dams having heights of 25 m and 40 m.

As can be seen from Figure 4.4, with 60% increase of the dam height from 25 m to 40 m, the depth averaged velocities along the dam body are almost the same for both dam bodies. Therefore, it can be stated that the seepage fields at particular zones of an embankment dam would be similar to that of the corresponding zone of a dam of different height composed of the same material. This similarity may be due to the similarity of the seepage gradients, i.e. with the increase of the dam height, the width of the dam also increases. This may result in almost similar gradients, and hence velocities at the corresponding zones of the dams having different height. Since the type of the dam material is the same for different heights, the aforementioned similarity is also applicable in case of transient flow conditions. As a result of this

preliminary analysis, it is decided to carry out all the simulations throughout this study under a given constant dam height. However, this effect needs to be checked for relatively higher dams having proportional characteristics.

In the preliminary analysis, as a supplementary check, the piping condition is investigated for the embankment dams handled in this study. For this purpose, the critical hydraulic gradient is compared with the hydraulic gradient values observed throughout the bodies of dams. The critical hydraulic gradient is the gradient at which the internal erosion initiates in the soil. It is defined by:

$$i_c = \frac{\gamma_{sub}}{\gamma_w} \quad (4.1)$$

in which  $\gamma_{sub}$  is the submerged unit weight of the soil and  $\gamma_w$  is the unit weight of water. The critical hydraulic gradient, which initiates movement of soil particles ranges from 1.0 to 2.0 (Jacobson 2013). The hydraulic gradient values computed throughout the dam bodies considered in this study range from  $3 \times 10^{-3}$  to 0.90 for all the analyses. Therefore, it can be said that piping is not critical for the embankment dams taken into account in this research.

## 4.2 Uncertainty Based Analyses

This part of the study presents the sensitivity analyses for steady-state seepage through different types of embankment dams. One-at-a-time sensitivity analyses are conducted to investigate the individual effects of hydraulic conductivity and van Genuchten fitting parameters,  $\alpha$  and  $n$  on the steady-state seepage. In other words, the sensitivity of the flow to variation of these parameters is investigated. In each set of simulation, one selected parameter is kept random varying with three different coefficient of variation values, which are  $COV_r$ ,  $0.5COV_r$  and  $2.0COV_r$ , in which  $COV_r$  is the recommended COV value for the selected parameter in the literature. The other parameters are kept constant at their mean values. The variation of the parameters depend on many soil properties, such as texture, grain size distribution, water content distribution, etc., which are hard to accurately assess. By selecting

three COV values for each parameter, it is assumed that all possible variation degrees of parameters are accounted in simulations.

The algorithm presented in the previous chapter is applied on three hypothetical embankment dams, which are two homogeneous dams and a simple zoned dam. The geometric properties of dams are determined using related design specifications (United States Bureau of Reclamation (USBR) 1987) depending on their height and material types. The properties of the dams considered in the sensitivity analyses are presented in Table 4.1. The foundations of the embankments are considered to be impervious; therefore, only the seepage through their bodies are evaluated. A total number of 36 cases are investigated; 9 for Hypothetical example 1: Dam 1, 18 for Hypothetical example 2: Dam 2, and 9 for Hypothetical example 3: Dam 3. Each case represents spatial variation of a selected parameter (i.e.  $K$  or  $\alpha$  or  $n$ ) of a soil type (i.e. sandy clay or gravelly sand). The cases and their corresponding parameter properties are given in Table 4.2. This table also indicates the references which are used to obtain the statistical properties of the parameters (i.e. the mean and the COV). The determination of the statistical properties of the random variables was explained in Section 3.4.

Table 4.1 The properties of hypothetical dams considered for sensitivity analyses of steady-state seepage.

	Type	Material	Height (m)	Side slopes	
				U/S slope	D/S slope
Dam 1	Homogeneous	Sandy clay (SC)	25	1V:3.0H	1V:2.0H
Dam 2	Simple zoned	Shell: Gravelly sand (GS) Core: Clay (C)	20	1V:3.0H	1V:2.5H
Dam 3	Homogeneous	Gravelly sand (GS)	20	1V:3.0H	1V:2.5H

Note: U/S: Upstream; D/S: Downstream, V: Vertical, H: Horizontal

In Monte Carlo simulation technique, the number of the simulations affect the accuracy of the results. When the coefficient of variation of output parameter stabilizes, the number of the simulations can be said to be adequate. In this study, the adequacy of the number of realizations is checked by calculating the coefficient

of variation of the flow rate passing through the dam body for various simulation numbers.

Figure 4.5 shows the change of  $COV(Q)$  with respect to number of simulations for Hypothetical Example 1. From the figure it is clear that  $COV(Q)$  stabilizes after around 500 iterations. Therefore, for each application at least 500 Monte Carlo simulations are conducted.

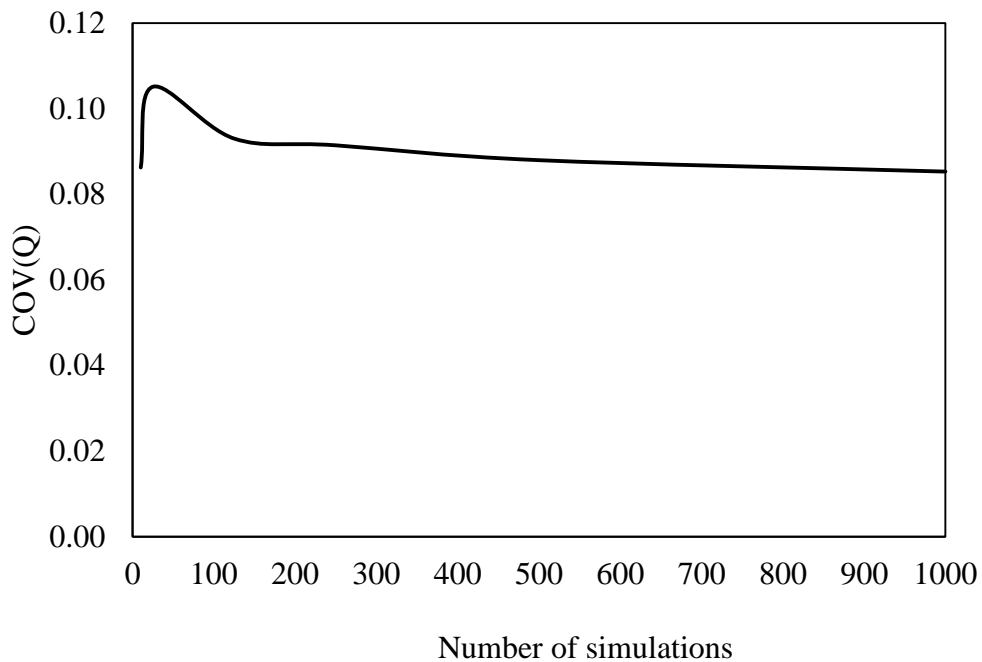


Figure 4.5 The change of coefficient of variation of the flow rate with respect to number of Monte Carlo simulations.

The results of the simulations are given in box-plots which enable presenting the statistical properties of data groups and comparisons in one figure. A box-plot presents the first and the third quartiles, the median and the maximum and minimum values of the data. Also the spread and symmetry of its distribution can be identified from a box-plot illustration (Williamson et al. 1989). In a box-plot, the lower and upper lines of the box indicates the first and the third quartiles, respectively, the line inside the box presents the median and the lower and upper line extends demonstrate the minimum and maximum of the data, respectively.

Table 4.2 Cases considered for sensitivity analyses of steady-state seepage and corresponding statistical properties of soils.

	Case No.	Parameter						Reference	
		K		$\alpha$		n			
		$\mu$ (m/s)	COV	$\mu$ (cm <sup>-1</sup> )	COV	$\mu$	COV		
Dam 1 (Sandy clay )	1	$3.33 \times 10^{-7}$	1.17	0.027	N/A	1.23	N/A	(Carsel and Parrish 1988; Fredlund 2005)	
	2	$3.33 \times 10^{-7}$	2.33	0.027	N/A	1.23	N/A		
	3	$3.33 \times 10^{-7}$	4.66	0.027	N/A	1.23	N/A		
	4	$3.33 \times 10^{-7}$	N/A	0.027	0.32	1.23	N/A		
	5	$3.33 \times 10^{-7}$	N/A	0.027	0.63	1.23	N/A		
	6	$3.33 \times 10^{-7}$	N/A	0.027	1.26	1.23	N/A		
	7	$3.33 \times 10^{-7}$	N/A	0.027	N/A	1.23	0.04		
	8	$3.33 \times 10^{-7}$	N/A	0.027	N/A	1.23	0.08		
	9	$3.33 \times 10^{-7}$	N/A	0.027	N/A	1.23	0.16		
Dam 2	Clay	10	$7.22 \times 10^{-7}$	1.35	0.02	N/A	1.31	N/A	(Carsel and Parrish 1988; Fredlund 2005)
		11	$7.22 \times 10^{-7}$	2.70	0.02	N/A	1.31	N/A	
		12	$7.22 \times 10^{-7}$	5.40	0.02	N/A	1.31	N/A	
		16	$7.22 \times 10^{-7}$	N/A	0.02	0.4	1.31	N/A	
		17	$7.22 \times 10^{-7}$	N/A	0.02	0.8	1.31	N/A	
		18	$7.22 \times 10^{-7}$	N/A	0.02	1.6	1.31	N/A	
		22	$7.22 \times 10^{-7}$	N/A	0.02	N/A	1.31	0.035	
		23	$7.22 \times 10^{-7}$	N/A	0.02	N/A	1.31	0.070	
		24	$7.22 \times 10^{-7}$	N/A	0.02	N/A	1.31	0.140	
	Gravelly sand	13	$8.80 \times 10^{-5}$	0.02	0.08	N/A	2.45	N/A	(Zeng et al. 2012)
14		$8.80 \times 10^{-5}$	0.04	0.08	N/A	2.45	N/A		
15		$8.80 \times 10^{-5}$	0.08	0.08	N/A	2.45	N/A		
19		$8.80 \times 10^{-5}$	N/A	0.08	0.02	2.45	N/A		
20		$8.80 \times 10^{-5}$	N/A	0.08	0.04	2.45	N/A		
21		$8.80 \times 10^{-5}$	N/A	0.08	0.08	2.45	N/A		
25		$8.80 \times 10^{-5}$	N/A	0.08	N/A	2.45	0.022		
26		$8.80 \times 10^{-5}$	N/A	0.08	N/A	2.45	0.044		
27	$8.80 \times 10^{-5}$	N/A	0.08	N/A	2.45	0.088			
Dam 3 (Gravelly sand)	28	$8.80 \times 10^{-5}$	0.02	0.08	N/A	2.45	N/A	(Zeng et al. 2012)	
	29	$8.80 \times 10^{-5}$	0.04	0.08	N/A	2.45	N/A		
	30	$8.80 \times 10^{-5}$	0.08	0.08	N/A	2.45	N/A		
	31	$8.80 \times 10^{-5}$	N/A	0.08	0.02	2.45	N/A		
	32	$8.80 \times 10^{-5}$	N/A	0.08	0.04	2.45	N/A		
	33	$8.80 \times 10^{-5}$	N/A	0.08	0.08	2.45	N/A		
	34	$8.80 \times 10^{-5}$	N/A	0.08	N/A	2.45	0.022		
	35	$8.80 \times 10^{-5}$	N/A	0.08	N/A	2.45	0.044		
	36	$8.80 \times 10^{-5}$	N/A	0.08	N/A	2.45	0.088		

Note: N/A (Not Applicable) indicates deterministic treatment of the corresponding variable with its mean value.

The use of box-plots helped interpretation of the effects of variation of the parameters on the seepage rate. Also, flow rates are compared with those obtained from the deterministic model to discuss the random variables whose variability have significant impacts on the seepage. This is to recommend which variables can be treated deterministically and others as random in future steady-state seepage analysis of embankment dams.

**4.2.1 Hypothetical Example 1: Dam 1**

In this example, the sensitivity of the steady-state seepage through a 25 m high homogeneous dam made of sandy clay, resting on an impervious foundation is examined. The geometry and the boundary conditions of the dam is shown in Figure 4.6. The constant upstream total head is 20 m and there is no tailwater. The cases considered for the analysis and their corresponding parameter statistics are shown in Table 4.2. A total of nine cases (i.e. Case 1 to Case 9 in Table 4.2) are considered for Dam 1. The effects of variation of;

- $K$  are investigated in Case 1 to Case 3,
- $\alpha$  are investigated in Case 4 to Case 6,
- $n$  are investigated in Case 7 to Case 9.

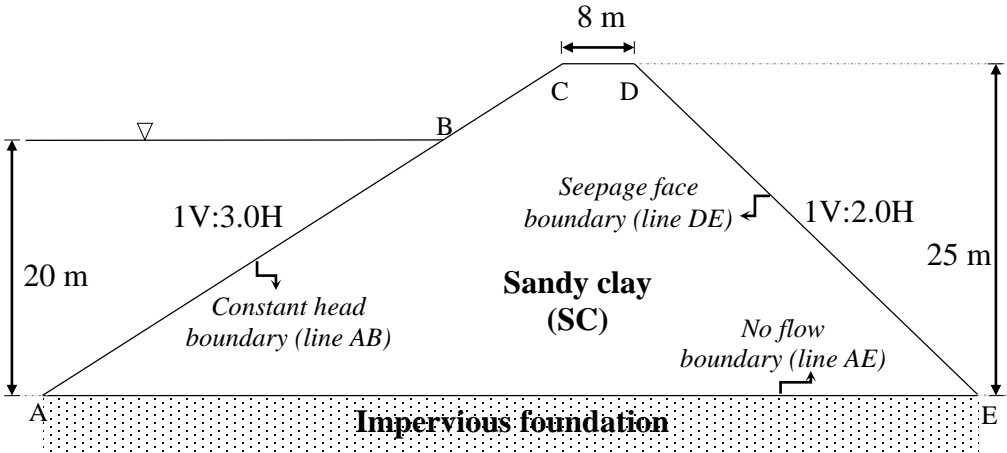


Figure 4.6 The geometry and boundary conditions of Dam 1.

In total, 4500 ( $9 \times 500$ ) simulations are conducted for the example. The seepage rate results obtained for these cases are presented with box-plots supplied in Figure 4.7. The seepage rate computed with the deterministic model, keeping the parameters constant at their mean values is presented with a continuous line on Figure 4.7. Also, descriptive statistics of the seepage rate for these cases are given in Table 4.3.

The results of Cases 1 to 3 showed that the variation of hydraulic conductivity have substantial impacts on the steady-state seepage. Particularly, the increase in variation of  $K$  results in sharp decrease in the flow rate. When COV of  $K$  increases, the variation of the flow rate (i.e.  $COV(Q)$ ) and its probability distribution skewness increases. Also, significant differences are observed between the deterministically computed flow rate and the mean flow rates of Cases 1 to 3. The difference between the mean and deterministic flow rates reaches up to 50% when variation coefficient of  $K$  is doubled. The reason for this result is explained in Section 4.3.

However, as it is clear from the results of Case 4 to 9 that, individual variabilities of  $\alpha$  and  $n$  cause negligible effects on the steady-state seepage. For these cases, the mean, minimum and maximum seepage rates are very close to each other and to the deterministic seepage rate. Also, no effect is observed on the probabilistic nature of the seepage. This means the uncertainty of  $\alpha$  and  $n$  has negligible effects on the steady-state seepage of the example problem (see Table 4.3).

It should be noted that, the hydraulic conductivity is varied between the COV values of 1.17 and 4.66; however, the variation of the output parameter,  $COV(Q)$  is computed to change between 0.05 and 0.12. Therefore, it can be said that the system has the ability of decreasing the variation of the input parameter.

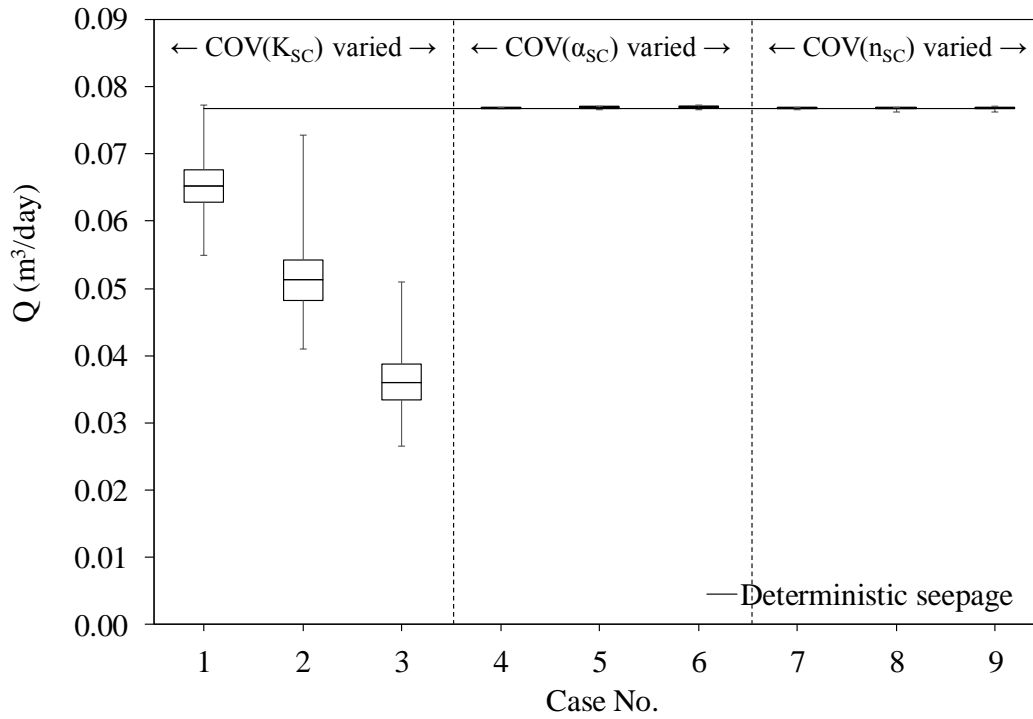


Figure 4.7 The box-plots of the seepage rate for Case 1 to Case 9.

Table 4.3 The descriptive statistics of the seepage rate for Case 1 to Case 9.

Case No.	Range and mean (m <sup>3</sup> /day)			COV(Q)	Skewness	Kurtosis	% difference b/w mean & deterministic Q
	Max	Min	$\mu$				
1	0.077	0.055	0.065	0.05	0.25	0.22	15.0
2	0.073	0.041	0.051	0.09	0.42	0.58	33.1
3	0.051	0.027	0.036	0.12	0.56	0.54	52.6
4	0.077	0.077	0.077	0.00	-0.49	-0.73	0.0
5	0.077	0.077	0.077	0.00	-0.04	-0.08	0.0
6	0.077	0.077	0.077	0.00	-0.46	0.90	0.2
7	0.077	0.077	0.077	0.00	-0.02	-0.10	0.0
8	0.077	0.076	0.077	0.00	-1.01	5.40	0.1
9	0.077	0.076	0.077	0.00	-0.19	1.74	0.1

#### 4.2.2 Hypothetical Example 2: Dam 2

A sensitivity analysis is conducted for steady-state seepage through a 20 m high simple zoned embankment dam given in Figure 4.8. The dam is composed of two materials: gravelly sand for the shell and clay for the core. A constant 16 m of total head is assigned as the upstream boundary condition, whereas there is no tailwater at the downstream. The cases considered for Dam 2 and their corresponding parameter statistics are given in Table 4.2. For eighteen cases (i.e. Case 10 to Case 27 in Table 4.2), a total number of 9000 (18×500) Monte Carlo simulations are held.

The influences of the variation degree of;

- $K$  are investigated for;
  - clay in Case 10 to Case 12,
  - gravelly sand in Case 13 to Case 15.
- $\alpha$  are investigated for;
  - clay in Case 16 to Case 18,
  - gravelly sand in Case 19 to Case 21.
- $n$  are investigated for;
  - clay in Case 22 to Case 24,
  - gravelly sand in Case 25 to Case 27.

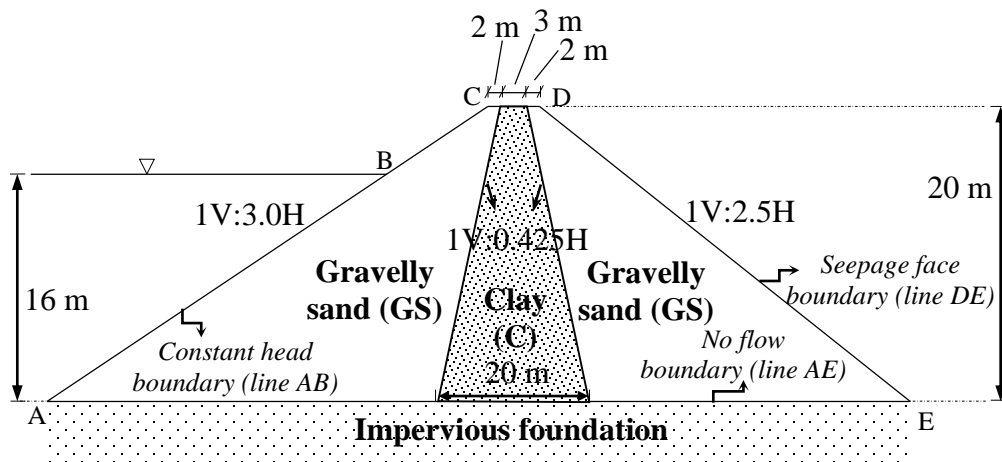


Figure 4.8 The geometry and boundary conditions of Dam 2.

The computed seepage rates for these cases together with the deterministic seepage result are illustrated with box-plots in Figure 4.9. The descriptive statistics of the flow rate are also supplied in Table 4.4. The box-plots of Cases 10 to 12 showed that the variation of hydraulic conductivity of the core material has considerable effects on steady-state seepage. Increase in COV of K results in a sharp decrease in the flux. The mean seepage rates resulting from the varying hydraulic conductivity of clay are 13% to 50% smaller than deterministically computed seepage (see Cases 10 to 12 in Table 4.4). For Case 12, even the maximum seepage rate that can be observed is smaller than the deterministically computed seepage. However, no similar effects are observed for the variation of hydraulic conductivity of the shell material. There is no significant difference between the mean flow rates computed for Cases 13 to 15 and the deterministic flux (see Table 4.4). This can be attributed to the difference between hydraulic conductivities and COV values of clay and gravelly sand. Gravelly sand has a lower variation in its properties, which result in insignificant effects on the seepage.

For the problem considered, the behavior of the seepage is highly dependent on the hydraulic characteristics of the core material. The flow quantity is found to be governed by the properties of the clay, which has much smaller permeability and higher variability. The increase in COV(K) of clay results in a decrease in seepage quantity and increase in its variation degree.

The investigation of Cases 16 to 27 shows that the variability in van Genuchten parameters,  $\alpha$  and  $n$  for clay and gravelly sand causes insignificant changes on the flow. The mean flow rates for these cases are very close to the deterministically computed flow rate, which make their impacts negligible. Although the COV of  $\alpha$  and  $n$  increased to certain levels, no change is observed in the variation of the flow rate.

It is also seen that there is no direct relationship between the asymmetry (i.e. skewness and kurtosis) of the probability distributions of the seepage rate and the variation of input parameters (see Table 4.4).

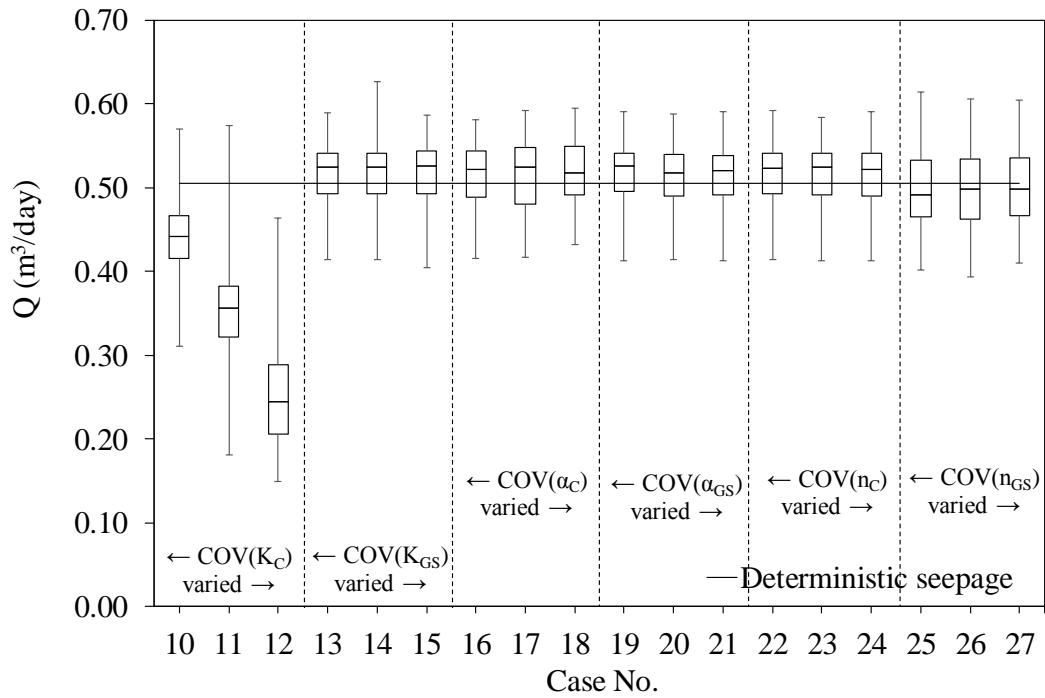


Figure 4.9 The box-plots of the seepage rate for Case 10 to Case 27.

Table 4.4 The descriptive statistics of the seepage rate for Case 10 to Case 27.

Case No.	Range and mean (m <sup>3</sup> /day)			COV(Q)	Skewness	Kurtosis	% difference b/w mean & deterministic Q
	Max	Min	μ				
10	0.570	0.311	0.441	0.09	-0.25	0.42	12.7
11	0.575	0.181	0.349	0.16	-0.10	1.71	30.8
12	0.464	0.149	0.252	0.24	0.74	0.29	50.1
13	0.590	0.414	0.517	0.07	-0.59	0.22	2.5
14	0.626	0.415	0.517	0.07	-0.51	0.29	2.4
15	0.587	0.405	0.518	0.07	-0.63	0.22	2.7
16	0.582	0.415	0.516	0.07	-0.48	-0.43	2.1
17	0.593	0.417	0.512	0.09	-0.49	-0.76	1.5
18	0.596	0.432	0.521	0.07	-0.01	-0.98	3.2
19	0.590	0.413	0.518	0.07	-0.67	0.35	2.7
20	0.588	0.414	0.514	0.07	-0.40	0.04	1.9
21	0.591	0.413	0.513	0.07	-0.73	0.43	1.7
22	0.592	0.414	0.516	0.07	-0.60	0.25	2.2
23	0.584	0.413	0.515	0.07	-0.64	0.15	2.1
24	0.591	0.413	0.516	0.07	-0.47	0.12	2.2
25	0.615	0.402	0.498	0.08	0.25	-0.75	1.4
26	0.606	0.394	0.499	0.09	0.09	-0.85	1.1
27	0.604	0.410	0.501	0.09	0.06	-0.87	0.8

### 4.2.3 Hypothetical Example 3: Dam 3

The sensitivity analysis of the current part is conducted to distinguish the variation effects of input parameters of different soil types. The starting point of this example is the results obtained from the sensitivity analysis held in the previous section (i.e. sensitivity analysis held on Dam 2). In this analysis, it was found that the variation of input parameters (i.e.  $K$ ,  $\alpha$  and  $n$ ) of gravelly sand has no substantial effects on steady-state seepage. To justify this finding, a homogeneous dam similar to Dam 2 is considered with a fill material composed of only gravelly sand. Although it is obvious that this is not a realistic dam material since it is highly permeable, it will provide a mean for investigating parameter variation effects of highly permeable materials. The cross-sectional view of the dam is presented in Figure 4.10. For the seepage through the dam, 4500 ( $9 \times 500$ ) number of samples are solved via MCS for nine cases, which are Case 28 to Case 36 in Table 4.2. The variation impacts of gravelly sand's;

- $K$  are investigated in Case 28 to Case 30,
- $\alpha$  are investigated in Case 31 to Case 33,
- $n$  are investigated in Case 34 to Case 36.

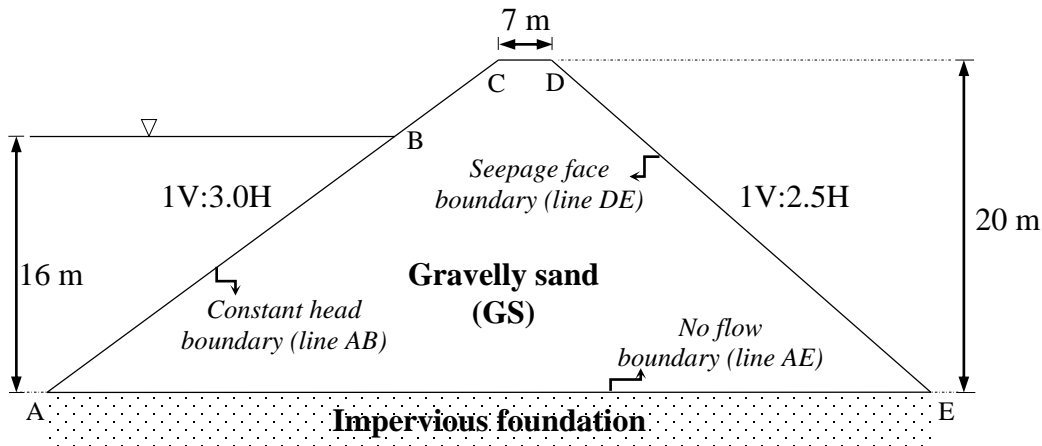


Figure 4.10 The geometry and boundary conditions of Dam 3.

The box-plots of the seepage rate data obtained from Monte Carlo simulations are illustrated in Figure 4.11. The figure also demonstrates the deterministically computed seepage rate through the dam body. The descriptive statistics of the flow are provided in Table 4.5.

It is observed from the figure that, the flow decreasing effect of hydraulic conductivity variation found in the previous analyses (i.e. sensitivity analyses held on Dam 1 and Dam 2) almost disappeared in this example. There is no difference between the mean seepage rates and the deterministically computed one for all cases. The reason for this may be the lower variation degree of the parameters of gravelly sand. Their COV values are smaller, resulting in slight changes in the parameter values assigned to the nodes of the domain. This may have caused a kind of homogeneity in the flow domain. The increase in the variation of K only results an increase in the range of observed flow rates.

Similarly and expectedly, the variation of  $\alpha$  and  $n$  resulted in no significant change in the flow rate. Although their variations are increased to certain levels, no change is observed in the mean flow rate and its variation.

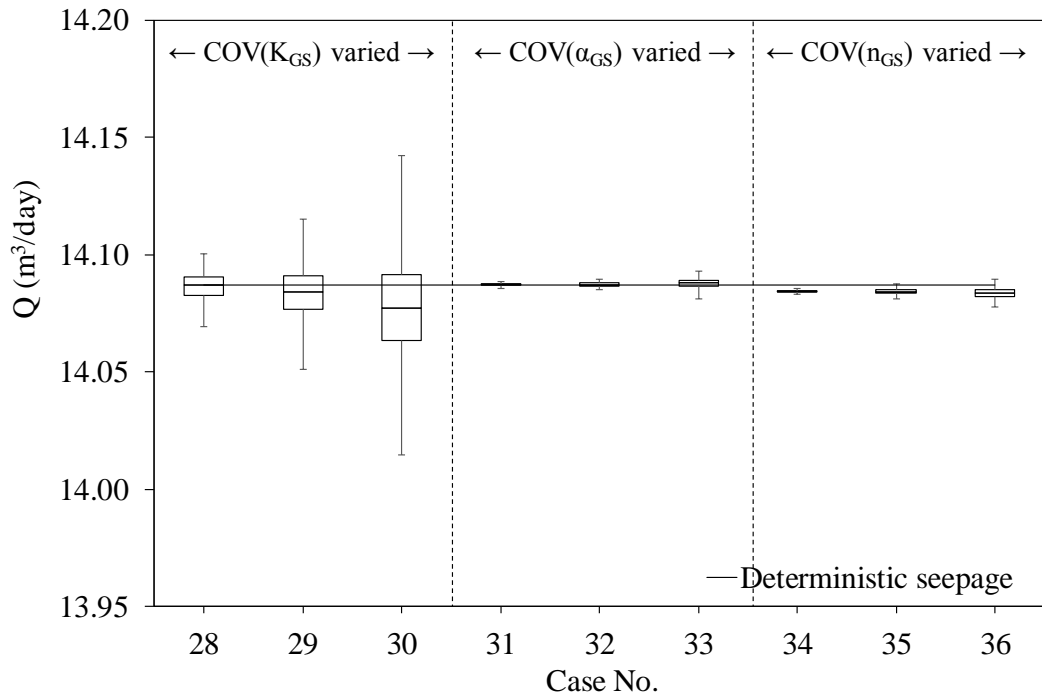


Figure 4.11 The box-plots of the seepage rate for Case 28 to Case 36.

Table 4.5 The descriptive statistics of the seepage rate for Case 28 to Case 36.

Case No.	Range and mean (m <sup>3</sup> /day)			COV(Q)	Skewness	Kurtosis	% difference b/w mean & deterministic Q
	Max	Min	$\mu$				
28	14.10	14.07	14.09	0.00	-0.15	-0.18	0.0
29	14.12	14.05	14.08		-0.16	-0.05	0.0
30	14.14	14.01	14.08		-0.04	0.22	0.1
31	14.09	14.09	14.09		0.04	0.10	0.0
32	14.09	14.09	14.09		0.07	-0.30	0.0
33	14.09	14.08	14.09		-0.18	0.49	0.0
34	14.09	14.08	14.08		0.02	0.03	0.0
35	14.09	14.08	14.08		-0.07	0.35	0.0
36	14.09	14.08	14.08		0.01	-0.08	0.0

### 4.3 Discussion

The sensitivity analyses conducted for different embankment dam geometries and material types showed that the effects of van Genuchten parameters on steady-state seepage is negligibly small for the tested COV ranges. The resulting mean seepage rates, when  $\alpha$  and  $n$  are varied, are seen to be very close to deterministic rate. The percent differences between these flows are computed to be smaller than 3.2% (see the last columns of Table 4.3, Table 4.4 and Table 4.5). Therefore, treatment of van Genuchten parameters as deterministic variables in steady-state seepage analysis of embankment dams appears to be reasonable for the material types considered in the study.

However, for fine grained materials having higher variations in its properties, the variation of hydraulic conductivity is found to have substantial effects; resulting a decrease in the mean seepage rate up to 50% when compared with the deterministic seepage. For these materials, the flow decreases as the variability of  $K$  increases. It is clear that when the variation of hydraulic conductivity is very high, the permeability of the nodes in the flow domain rapidly changes from one to another. This results in irregular and relatively long flow paths and consequently smaller seepage rates. Conversely, lower variations of  $K$  may result in homogeneity through the dam resulting a seepage behavior similar to that observed in the deterministic model. Similar results were found in the research of Ahmed (2009) and he concluded that a core may not be needed if highly variable materials are used as the fill material in embankment dams. It can be concluded that the hydraulic conductivity uncertainty should be considered by treating it as a random variable in steady-state seepage analyses through embankment dams.

It is seen that the degree of variation of  $K$ ,  $\alpha$  and  $n$  strongly depends on the material type. The coefficient of variation of parameters decreases when the grain size of the material increases (see Table 4.2). The sensitivity analysis conducted for Dam 3 showed that if the fill material of the embankment is only composed of coarse soil

particles having lower property variations, the steady-state seepage analysis can be conducted using deterministic models.

The hydraulic conductivity of soils having finer particles, such as clay, silt, silty and clayey soils, etc., is governed by highly variable space organization of their minerals or aggregates and varying pore sizes (Meunier 2005) which result in higher variations in the hydraulic conductivity. Therefore, treatment of hydraulic conductivity as a random variable is recommended if the embankment material is composed of such materials.

## CHAPTER 5

### UNCERTAINTY BASED TRANSIENT SEEPAGE ANALYSES

In this study, the sensitivity of the transient seepage is also investigated with a series of analyses which are similar to sensitivity analyses conducted for the steady-state seepage. The same procedure is applied here: one parameter is randomly varied while others are kept constant (i.e. one-at-a time analysis) to investigate what effects are produced on the transient seepage. To this end, a homogeneous embankment dam composed of sandy clay is considered. The dam height is 25 m, and its base width is 133 m. The upstream and downstream slopes are 1V:3.0H and 1V:2.0H, respectively. The bottom boundary of the flow domain is assumed to be no flow boundary, and there is no tailwater at the downstream side. Also, the surface along the downstream slope is considered as seepage face boundary. The dam is shown with its geometry and boundary conditions in Figure 5.1.

The dam is subjected to two different transient conditions: rapid drawdown and rapid fill. Therefore, the total head at the upstream changes with time depending on the condition. Both conditions are considered to occur individually. It is assumed that no successive event occurred after these conditions until steady-state flow conditions are reached. Therefore, they are purely independent events.

Nine different cases, each one investigating the variation effect of a parameter on the seepage, are analyzed. The cases and their parameter properties are given in Table 5.1. Similar to the previous sensitivity analysis conducted for the steady-state seepage, one parameter is made random with three COV values and others are kept

constant at their mean values. For example, for Case 1 to 3 parameters  $\alpha$  and  $n$  are fixed at their mean values  $0.027 \text{ cm}^{-1}$  and  $1.23$ , respectively, whereas the hydraulic conductivity,  $K$  is assumed to be random having a mean  $0.029 \text{ m/day}$  and COV values  $1.17$ ,  $2.33$  and  $4.66$ .

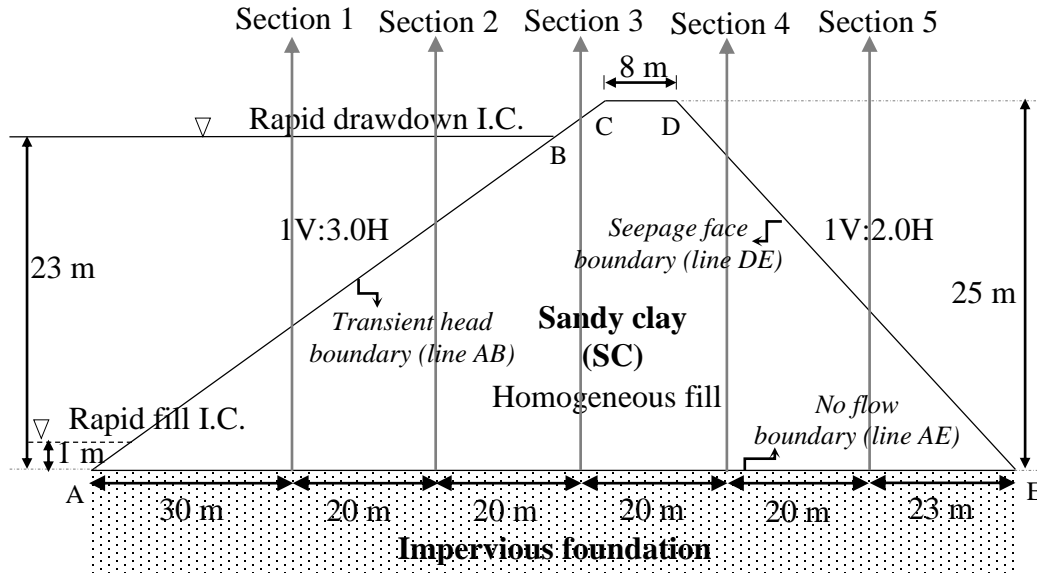


Figure 5.1 The geometry, sections and initial conditions of the dam considered for sensitivity analyses on transient seepage.

Table 5.1 Cases considered for sensitivity analyses of transient seepage and corresponding statistical properties of the soil.

Case No.	Parameter						Reference
	K		$\alpha$		n		
	$\mu$ (m/s)	COV	$\mu$ ( $\text{cm}^{-1}$ )	COV	$\mu$	COV	
1	$3.33 \times 10^{-7}$	1.17	0.027	N/A	1.23	N/A	(Carsel and Parrish 1988; Fredlund 2005)
2	$3.33 \times 10^{-7}$	2.33	0.027	N/A	1.23	N/A	
3	$3.33 \times 10^{-7}$	4.66	0.027	N/A	1.23	N/A	
4	$3.33 \times 10^{-7}$	N/A	0.027	0.32	1.23	N/A	
5	$3.33 \times 10^{-7}$	N/A	0.027	0.63	1.23	N/A	
6	$3.33 \times 10^{-7}$	N/A	0.027	1.26	1.23	N/A	
7	$3.33 \times 10^{-7}$	N/A	0.027	N/A	1.23	0.04	
8	$3.33 \times 10^{-7}$	N/A	0.027	N/A	1.23	0.08	
9	$3.33 \times 10^{-7}$	N/A	0.027	N/A	1.23	0.16	

Note: N/A (Not Applicable) indicates deterministic treatment of the corresponding variable with its mean value.

For each case, the transient seepage through the dam is stochastically analyzed conducting 500 number of MCS. Therefore, 4500 ( $9 \times 500$ ) samples are solved for each rapid drawdown and rapid fill cases. In total, 9000 simulations are held for the current sensitivity analyses.

During transient flow conditions, generally varying fluxes are observed through the dam body for a given time. For an instant, the seepage rate may both increase and decrease at different sections. Therefore, to consider the spatial variability the seepage, flow results are obtained for five sections through the dam body. The sections are located at 30 m, 50 m, 70 m, 90 m and 110 m from the heel of the structure. These sections are termed as Section 1, Section 2, Section 3, Section 4, and Section 5, respectively (see Figure 5.1). Also, the seepage results are derived for three time steps of the simulation duration: one from the initial state, one from the intermediate state and another from the final state. Similarly, results are presented in box-plots to examine the variation effects of the parameters. The deterministic model results are also used for comparison purposes.

### **5.1 Rapid Drawdown Case**

For the rapid drawdown case, a total head of 23 m is assigned to the upstream face of the dam given in Figure 5.1 as an initial condition. Then, the total head is decreased from 23 m to 1 m in four days, linearly. Such a drawdown rate is common for most flood detention dams subject to recession period of a flood. The graphical representation of the boundary condition is presented in Figure 5.2.

The duration of the simulation is determined as 2500 days, which is a sufficient time for the flow to reach a condition where almost no changes are observed between two successive time steps at all sections. In other words, at the end of the simulation, almost steady-state conditions are observed for the flow. The simulation duration of the analysis is determined from the deterministic model of the problem. The change of the deterministic seepage rate with respect to time at sections are given in

Figure 5.3 for the case. It clear from this figure that after 2500 days, the seepage rate at sections do not change considerably with respect to time.

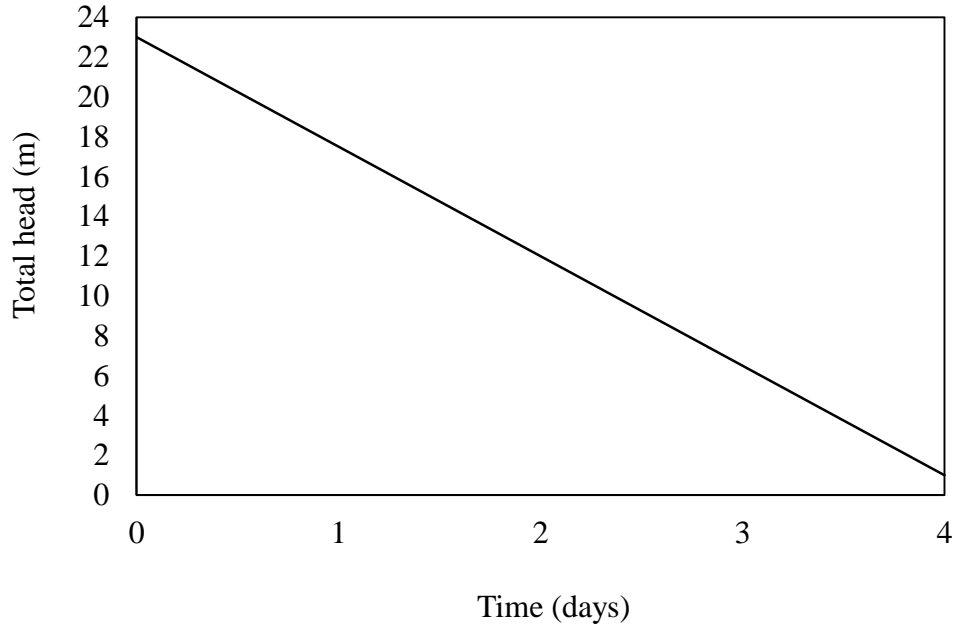


Figure 5.2 The upstream boundary condition for the rapid drawdown case

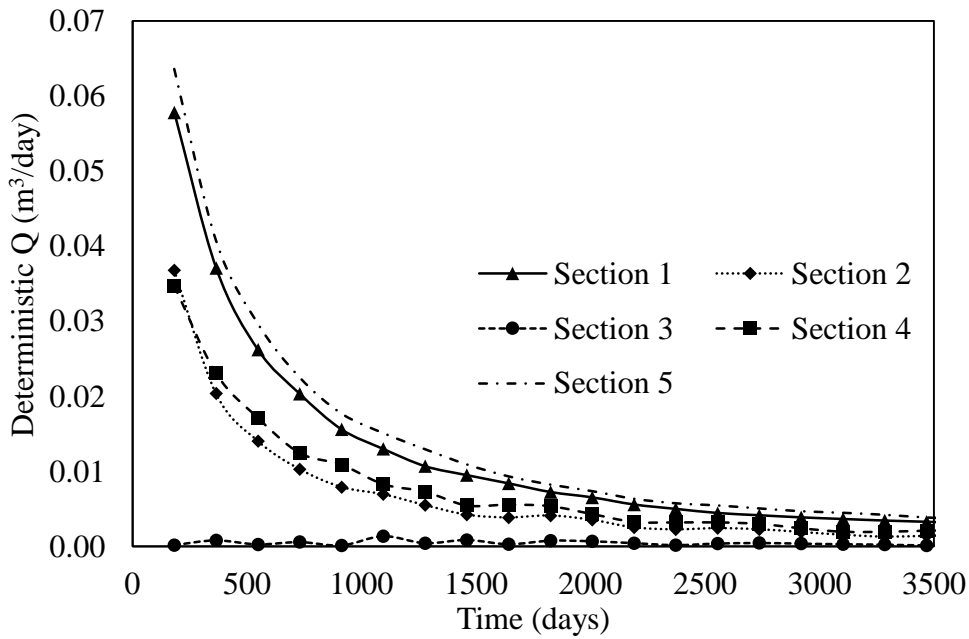


Figure 5.3 The change of the deterministic flow rate with respect to time for the rapid drawdown case.

The phreatic surface of the seepage obtained from the deterministic model for the rapid drawdown case is presented in Figure 5.4 to Figure 5.6. The phreatic surface and velocity vectors can be seen from these figures for times  $t= 68$  days, 1152 days and 2500 days, which correspond to 3%, 46% and 100% of the total simulation duration, respectively. This figure demonstrates the seepage tendency of the dam and enables analytical evaluation of results obtained from stochastic the analysis. For example, it is clear from this figure that the velocity vectors at Section 3 is considerably small for all times resulting in relatively and negligibly small flow rates at the section. Also, at the end of the simulation (i.e. when  $t=2500$  days) insignificantly low flow rates are observed for all sections. Similar results are expected and obtained from the stochastic analysis.

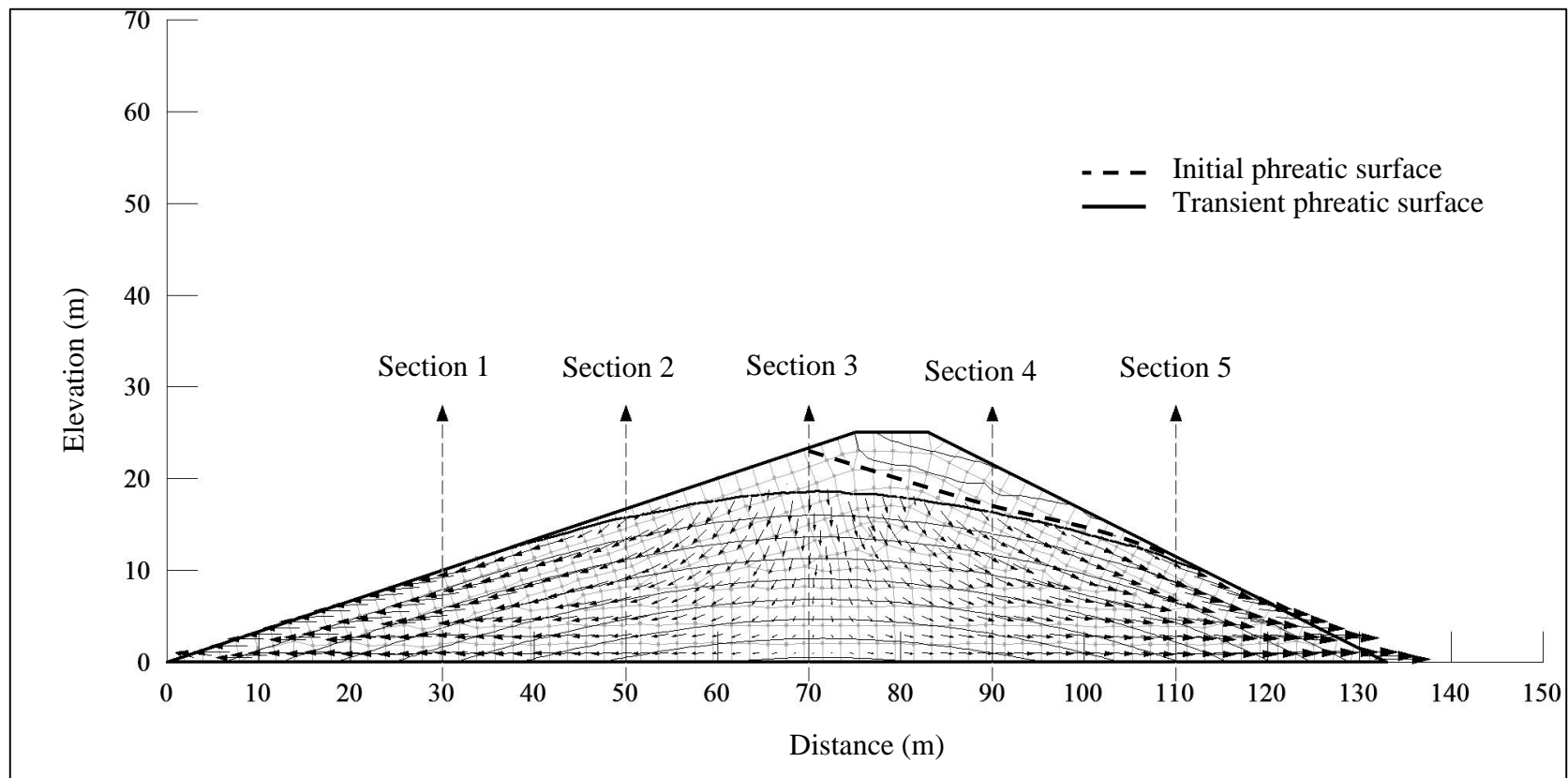


Figure 5.4 The phreatic surface, pore water pressure contours and velocity vectors of deterministic seepage for rapid drawdown when  $t=68$  days.

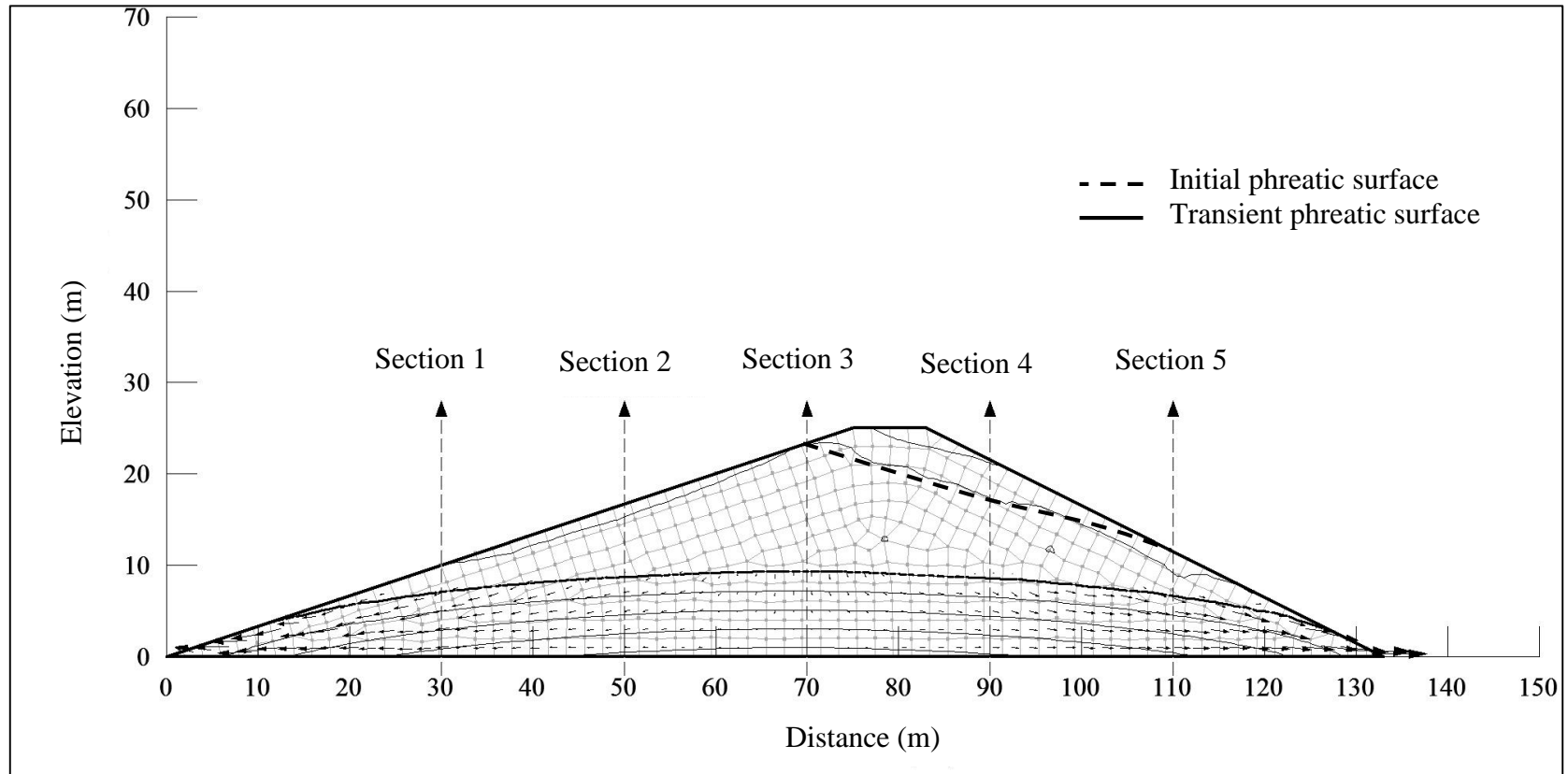


Figure 5.5 The phreatic surface, pore water pressure contours and velocity vectors of deterministic seepage for rapid drawdown when  $t=1152$  days.

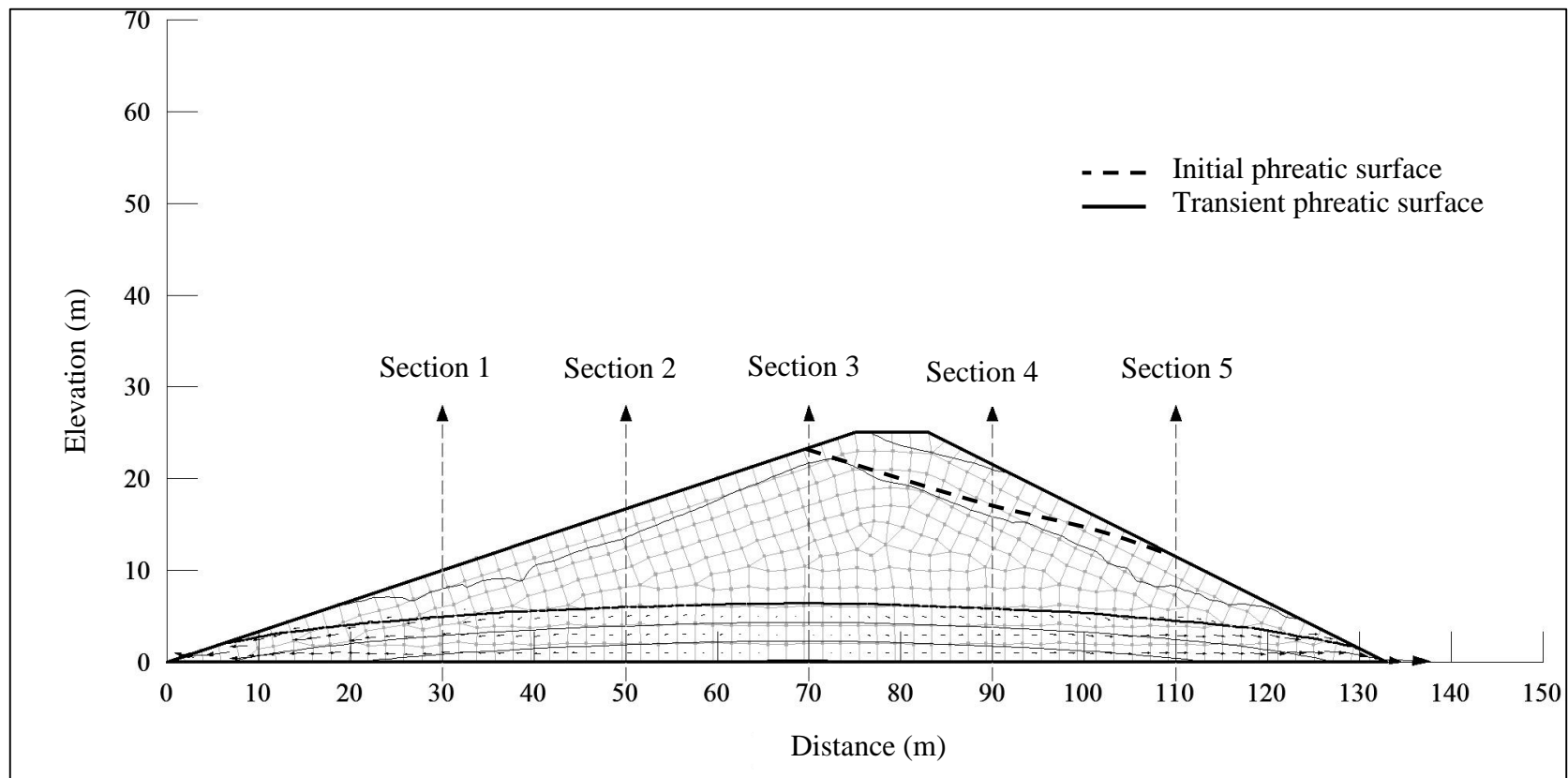


Figure 5.6 The phreatic surface, pore water pressure contours and velocity vectors of deterministic seepage for rapid drawdown when  $t=2500$  days.

The box-plots of the seepage rate for Case 1 to 9 for rapid drawdown are given in, Figure 5.7 to Figure 5.11 for  $t=68$  days, Figure 5.12 to Figure 5.16 for  $t=1152$  days, and Figure 5.17 to Figure 5.21 for  $t=2500$  days. The seepage rates computed from the deterministic model are also given on these figures for the related sections and times.

The results showed that the variation of hydraulic conductivity has significant effect on transient seepage. The flow rate decreases sharply when  $K$  is highly varied (see Case 1 to 3 in Figure 5.7 to Figure 5.11). However, when the results of Case 1 to 3 are compared in Figure 5.7 to Figure 5.21, it can be seen that the effect of variability of  $K$  on the seepage rate decreases as time increases. This effect almost disappears when the flow decreased to negligible rates at the end of the simulation (see Case 1 to 3 in Figure 5.17 to Figure 5.21). Therefore, it can be said that there is a direct relation between the effects of variability of  $K$  and the seepage rate. In other words, at a given section, when the flow rate increases, the effect of hydraulic conductivity variability pronounces.

The results showed that the variability of van Genuchten parameters (i.e.  $\alpha$  and  $n$ ) caused a slight decrease in the mean flow rate. This decrease can be attributed to the uncertainty of unsaturated hydraulic conductivity originating from the randomness of  $\alpha$  and  $n$ . However, the increase in variability of  $\alpha$  and  $n$  has almost no effects on transient seepage (see Case 4 to 9 in Figure 5.7 to Figure 5.21). Although the variations of these parameters are increased to certain levels (see Table 5.1) the decrease in the mean flow rate has not changed. Therefore, it can be said that the uncertainty of van Genuchten parameters has relatively smaller effects for studied COV value ranges which may be considered as insignificant for many seepage related problems.

It should be noted that the box-plots for Section 3 might be misleading in discussing the results. Because there exist negligibly small flow rates for all times at this section. Therefore, very small flow rates at Section 3 are considered as “no flow” case and no interpretation is made accordingly.

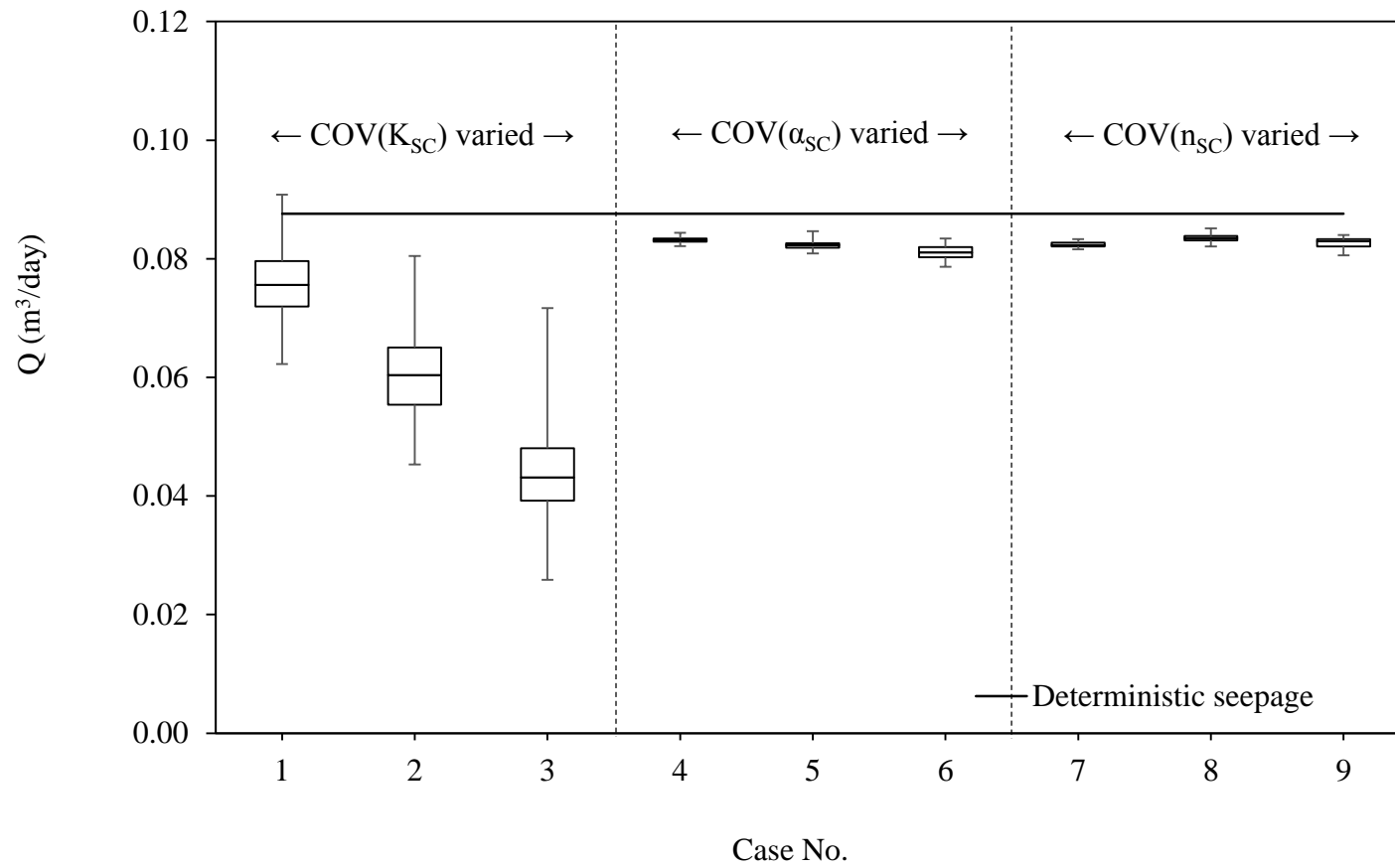


Figure 5.7 The box-plots of stochastic seepage for rapid drawdown when  $t=68$  days at Section 1.

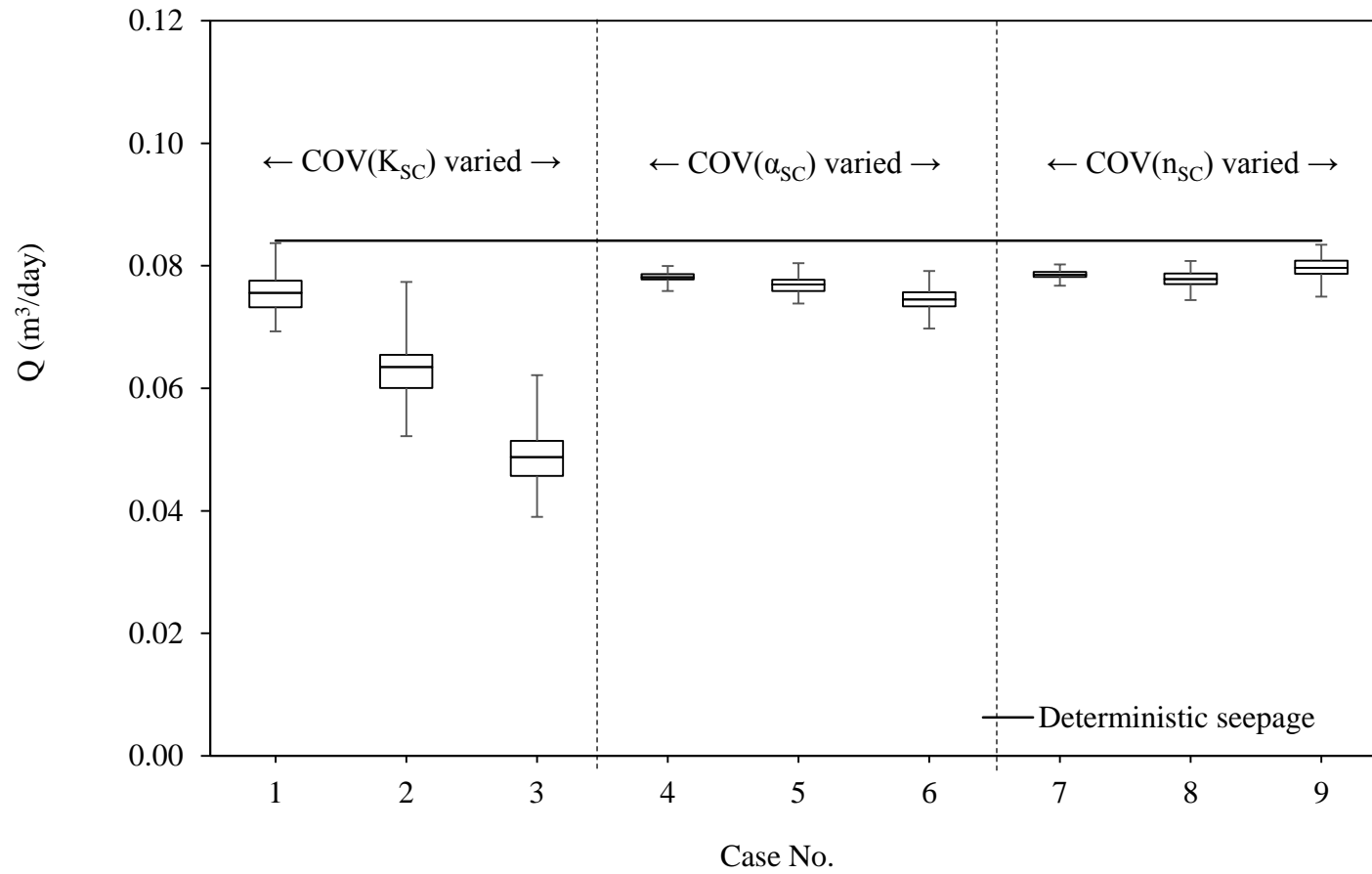


Figure 5.8 The box-plots of stochastic seepage for rapid drawdown when  $t=68$  days at Section 2.

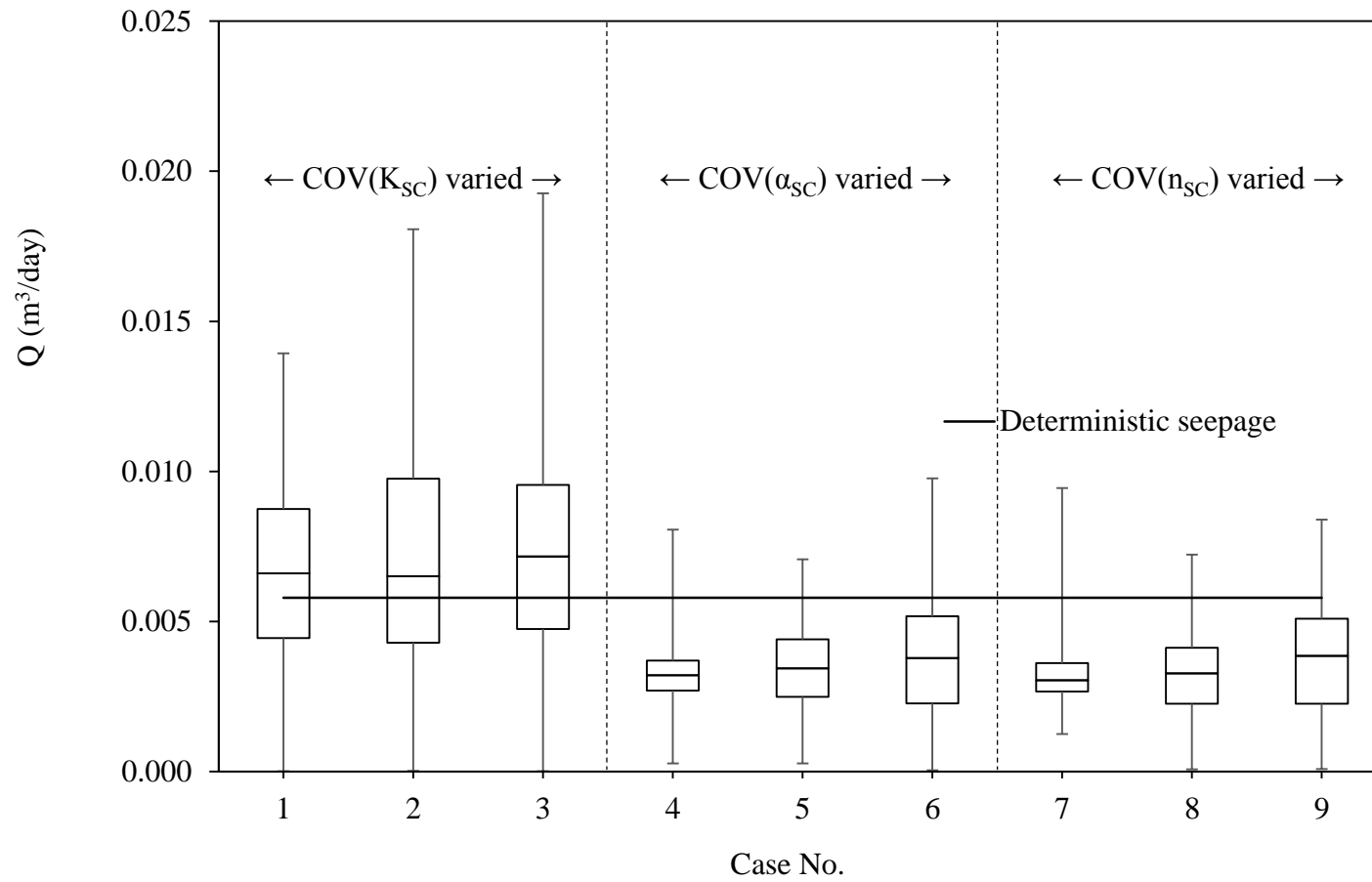


Figure 5.9 The box-plots of stochastic seepage for rapid drawdown when  $t=68$  days at Section 3.

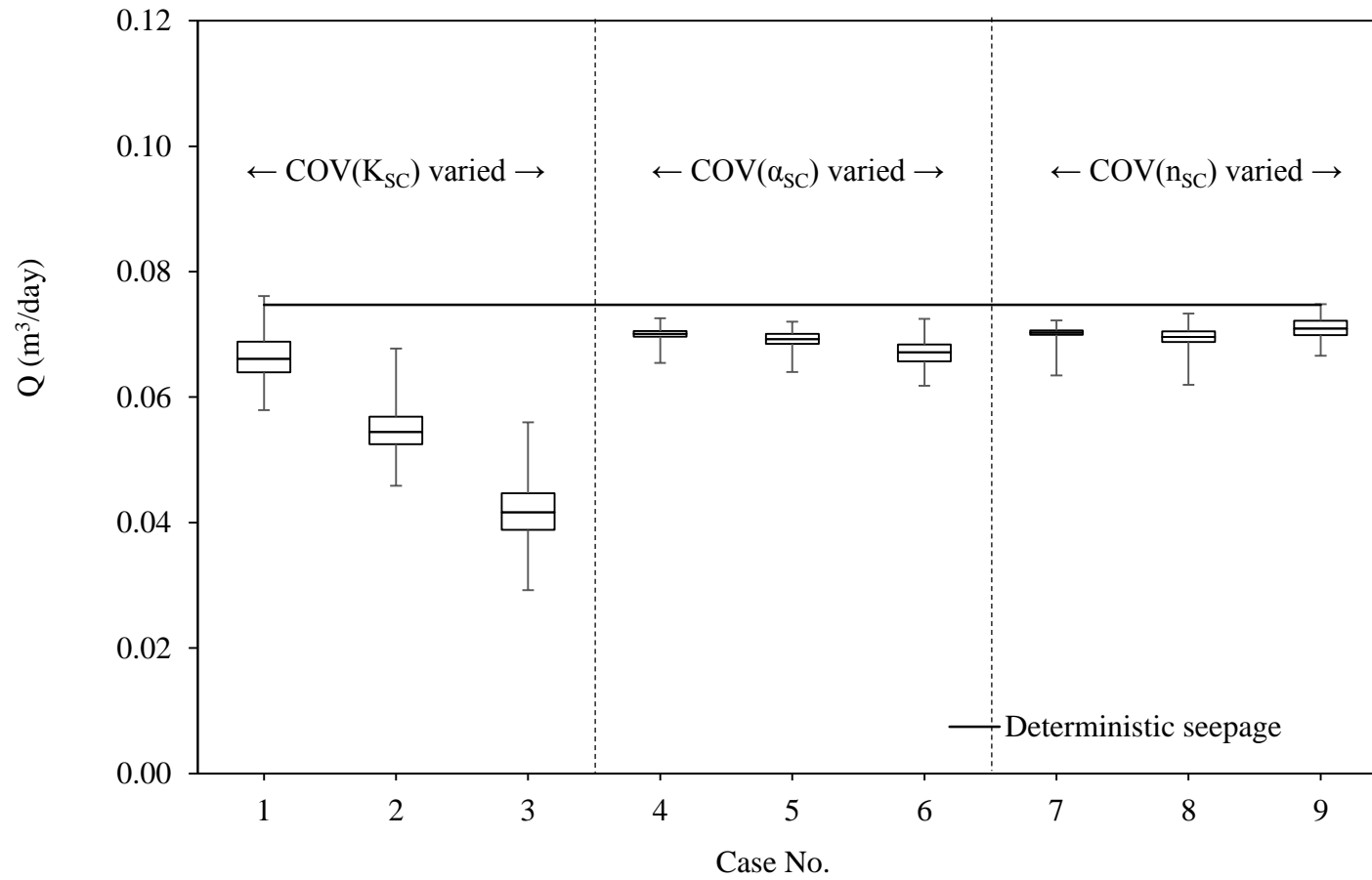


Figure 5.10 The box-plots of stochastic seepage for rapid drawdown when  $t=68$  days at Section 4.

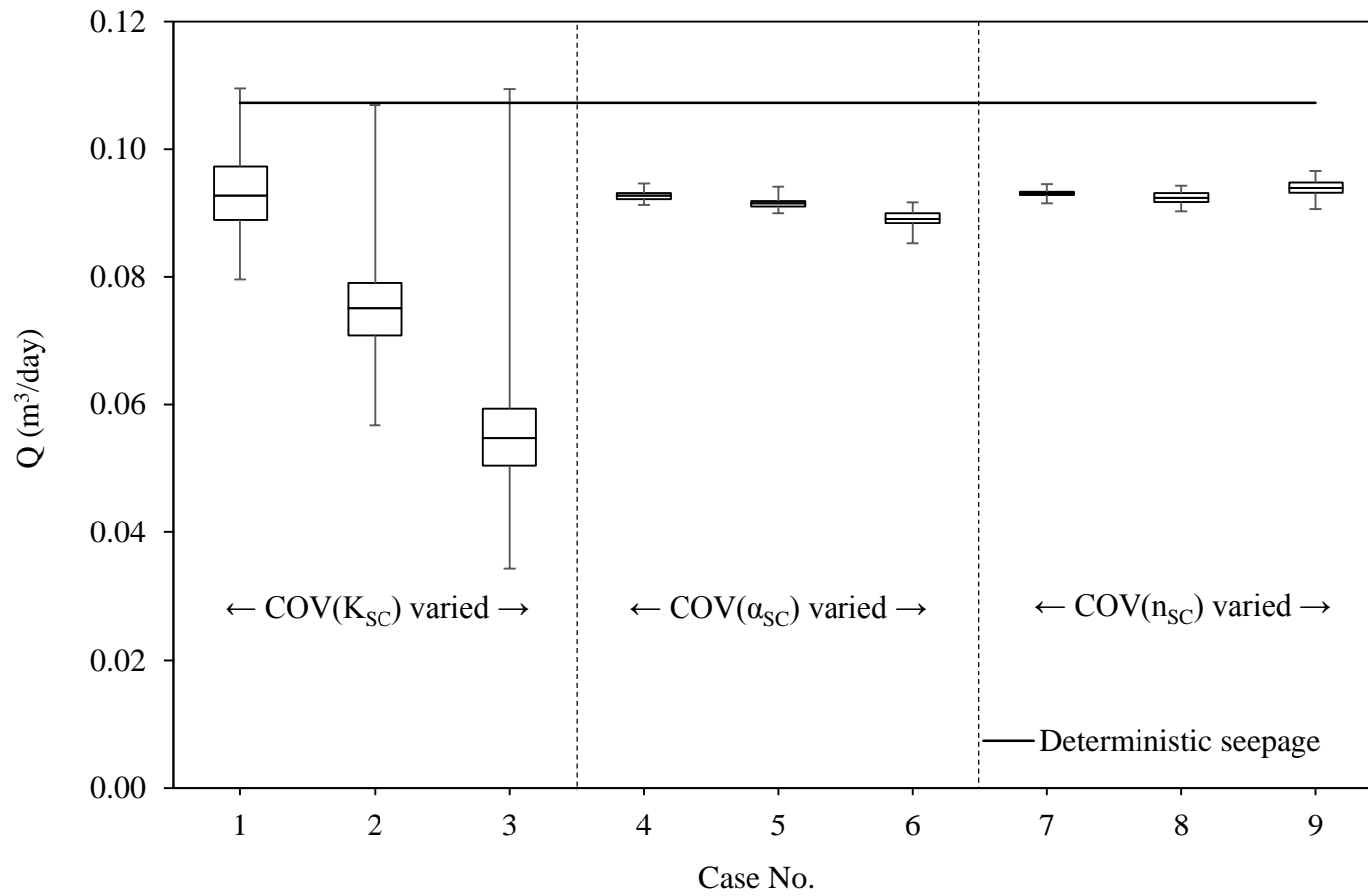


Figure 5.11 The box-plots of stochastic seepage for rapid drawdown when  $t=68$  days at Section 5.

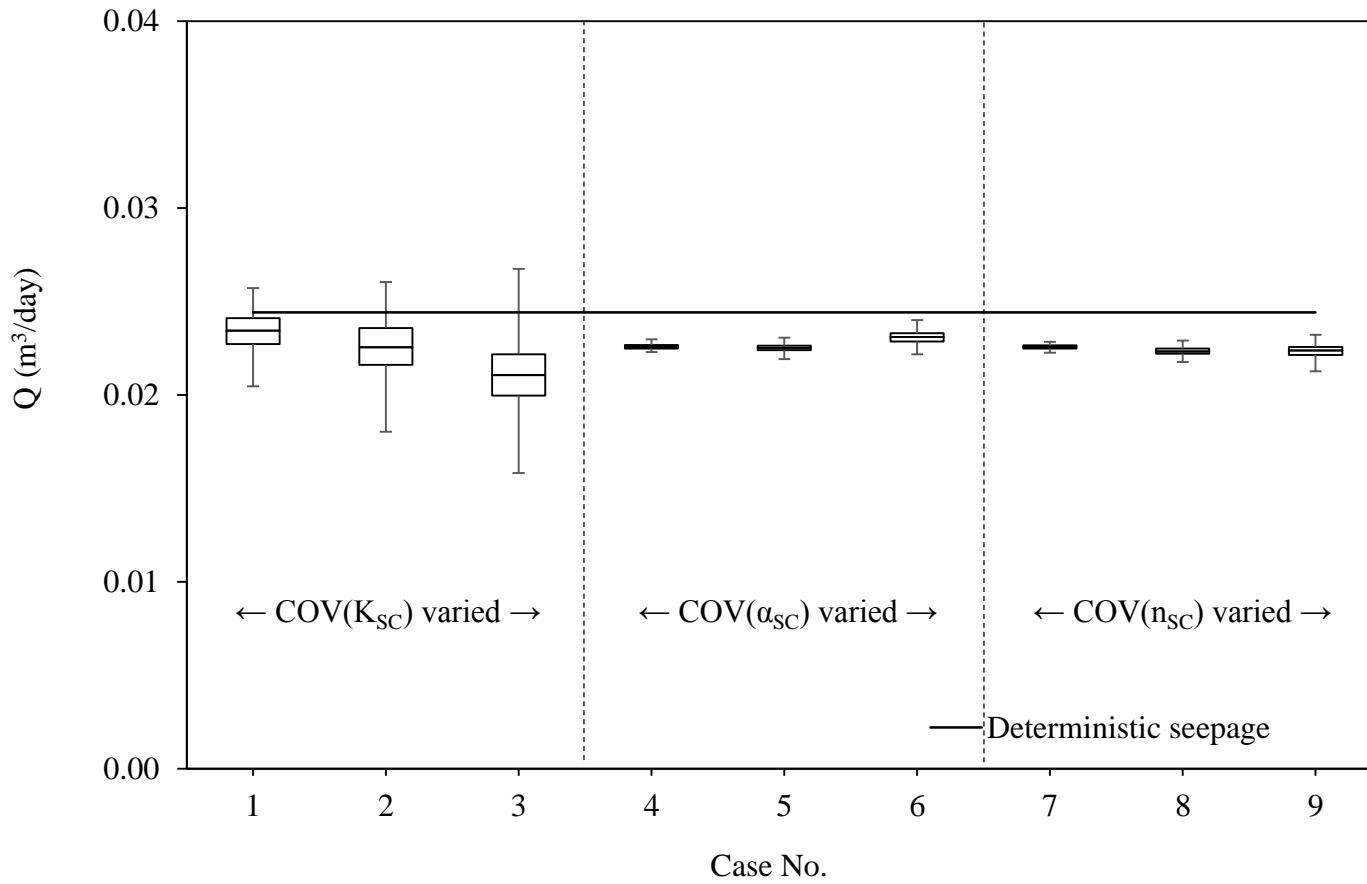


Figure 5.12 The box-plots of stochastic seepage for rapid drawdown when  $t=1152$  days at Section 1.

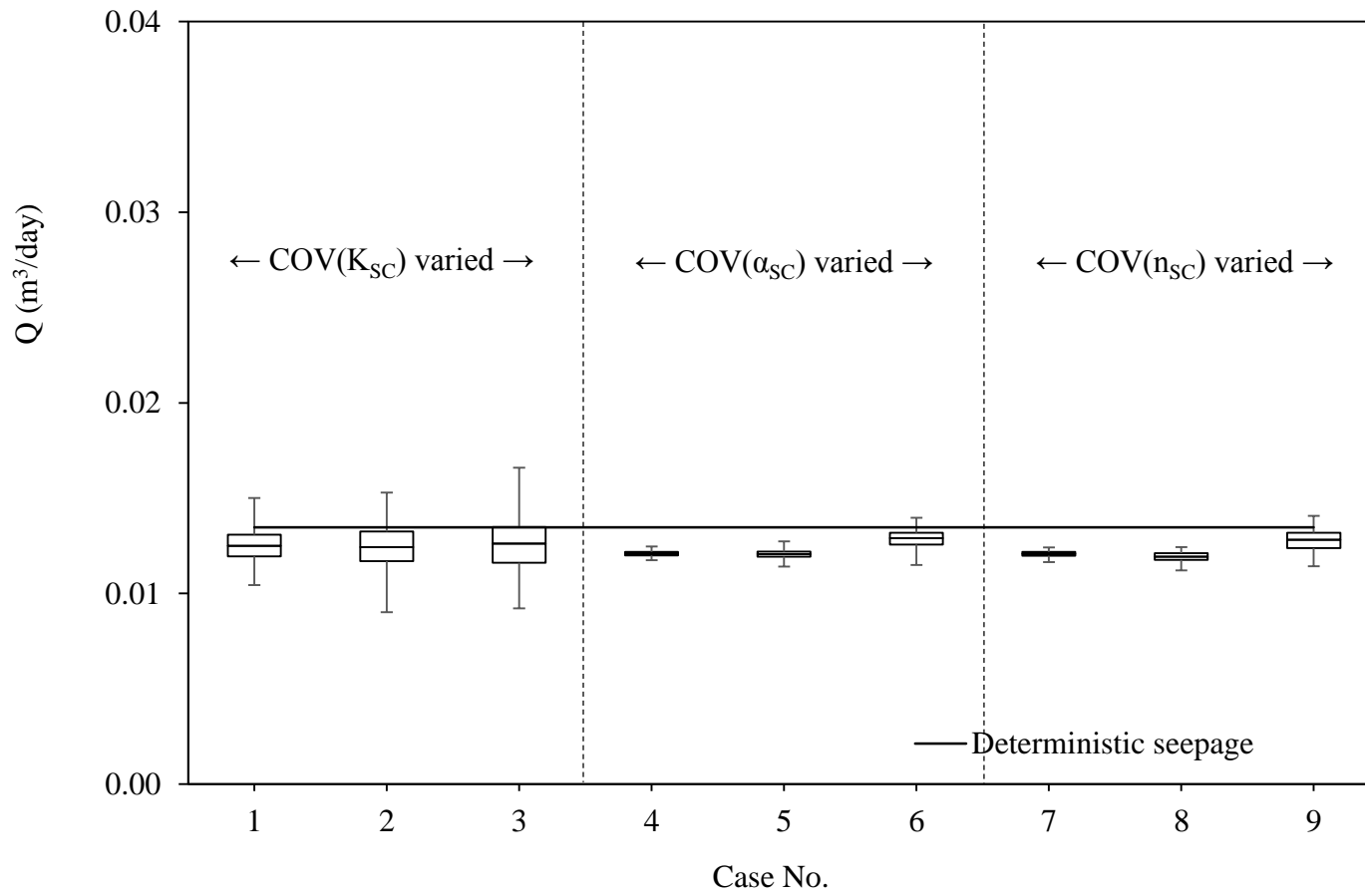


Figure 5.13 The box-plots of stochastic seepage for rapid drawdown when  $t=1152$  days at Section 2.

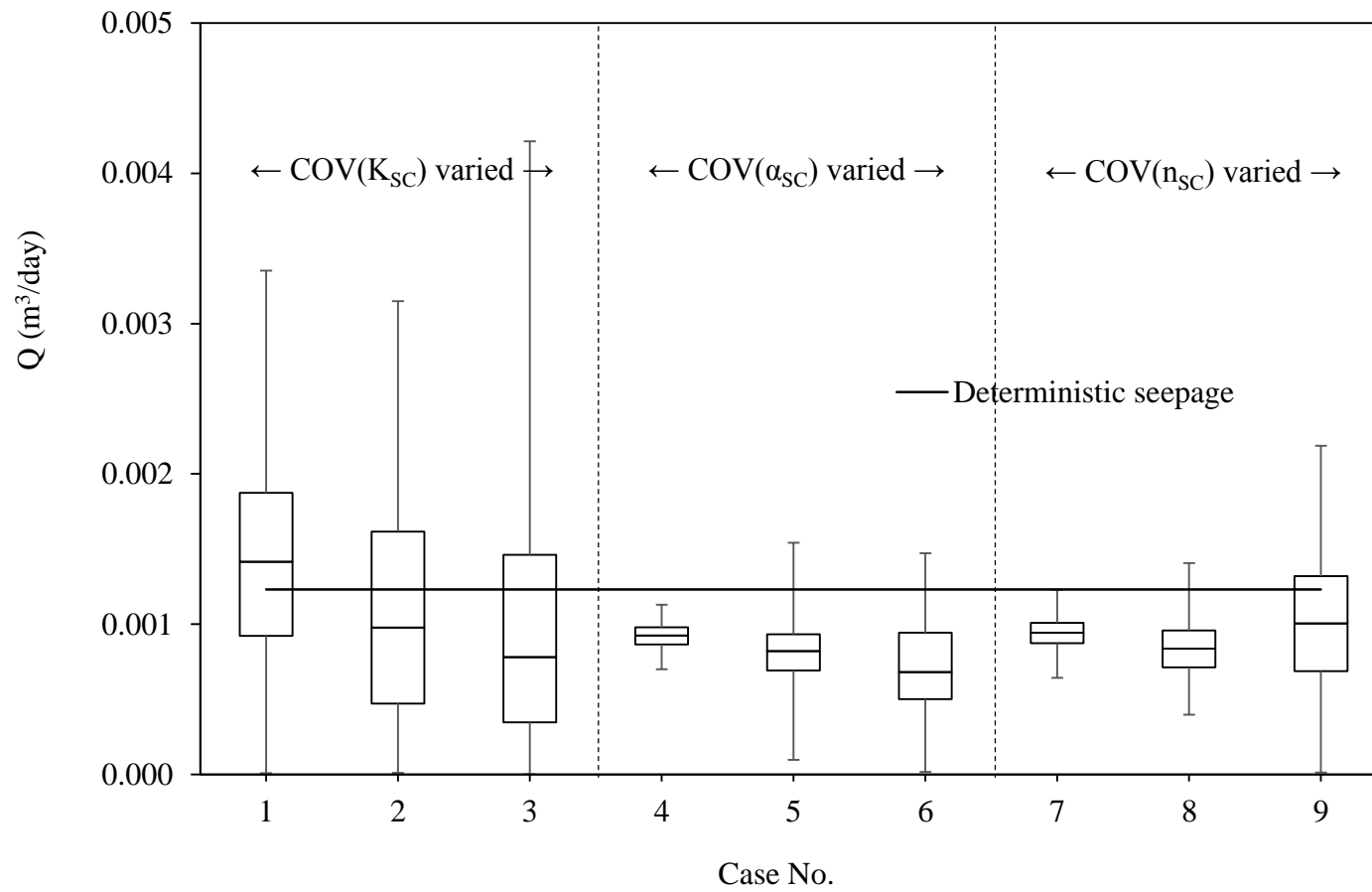


Figure 5.14 The box-plots of stochastic seepage for rapid drawdown when  $t=1152$  days at Section 3.

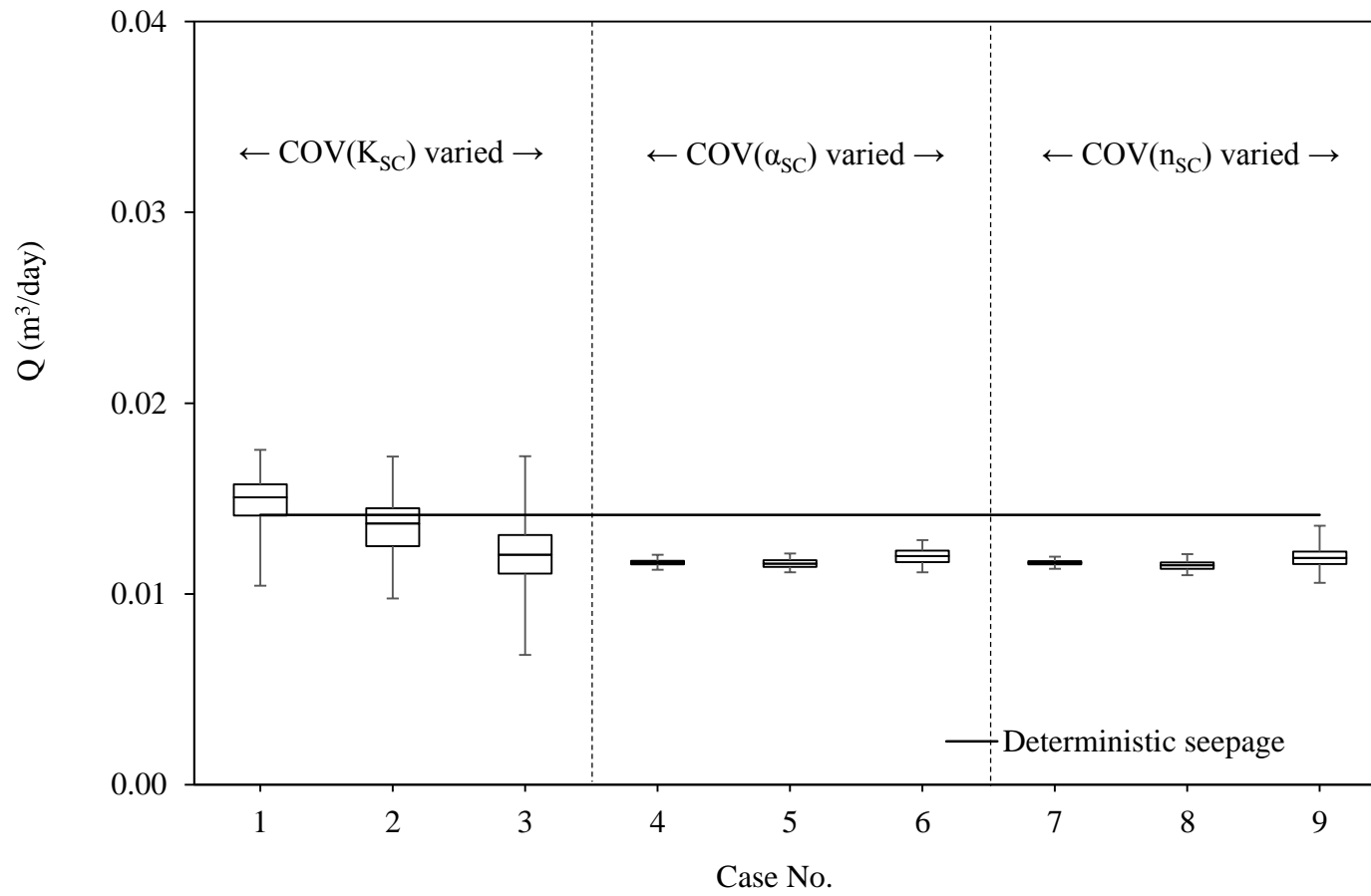


Figure 5.15 The box-plots of stochastic seepage for rapid drawdown when  $t=1152$  days at Section 4.

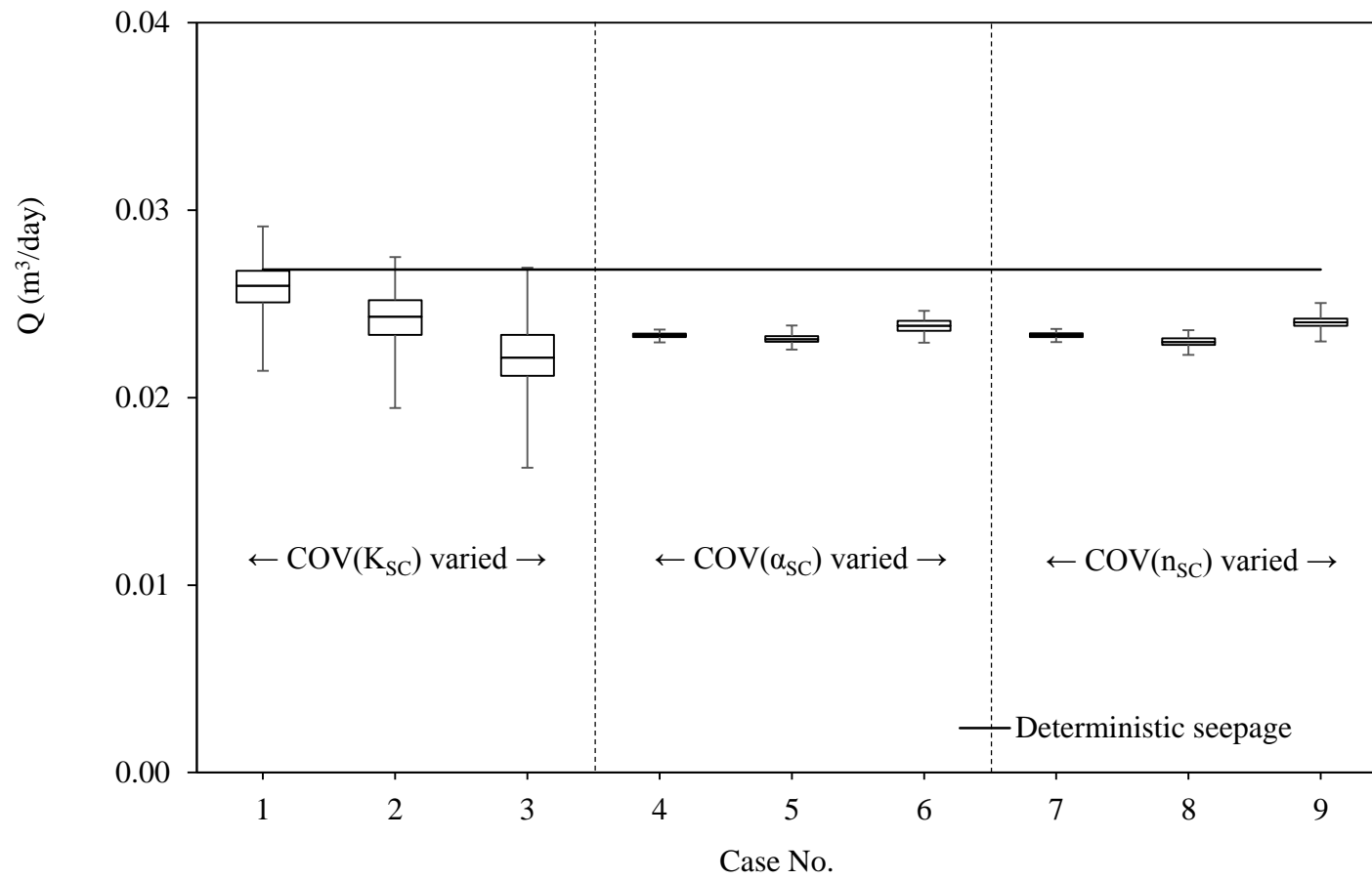


Figure 5.16 The box-plots of stochastic seepage for rapid drawdown when  $t=1152$  days at Section 5.

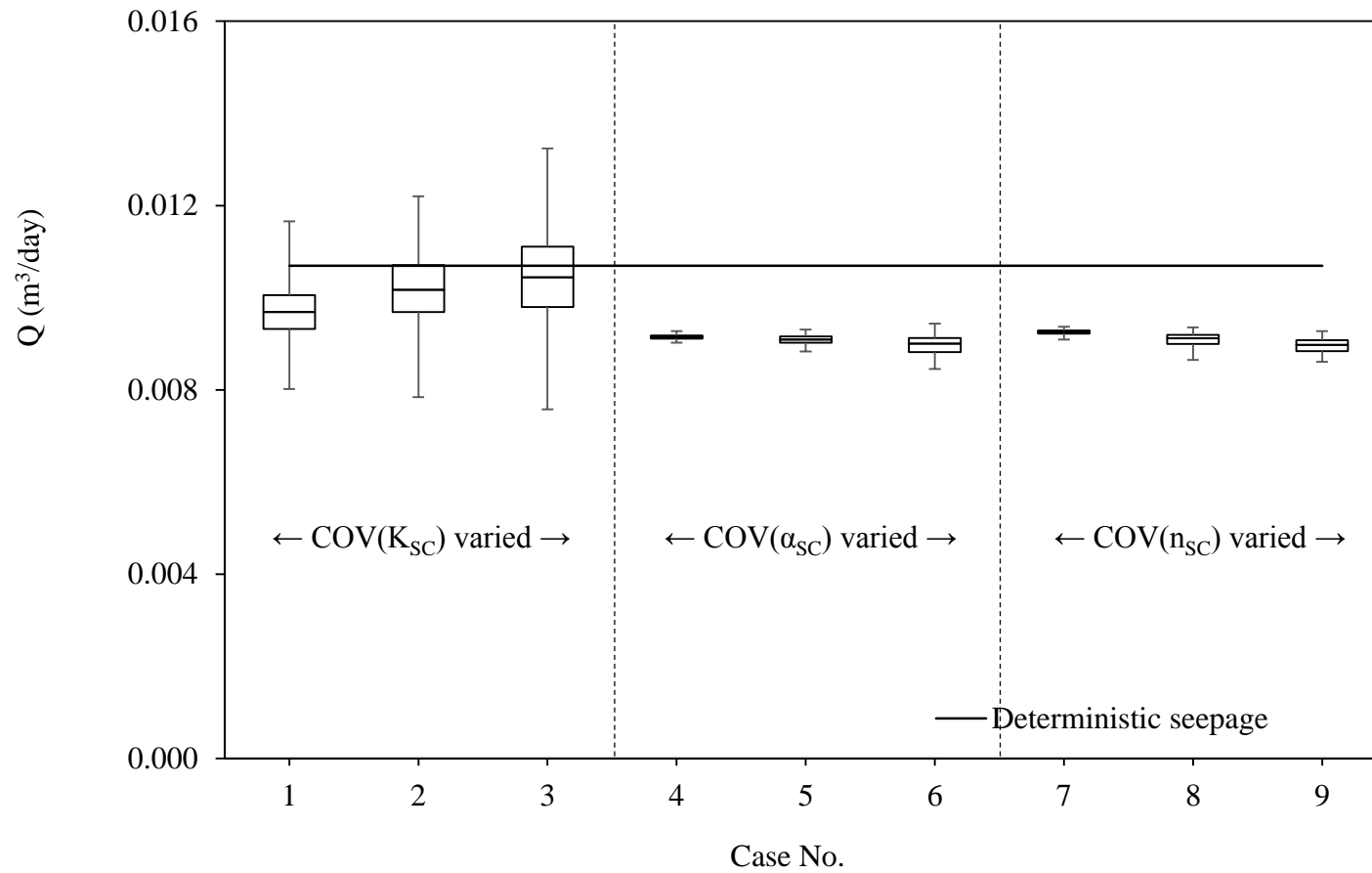


Figure 5.17 The box-plots of stochastic seepage for rapid drawdown when  $t=2500$  days at Section 1.

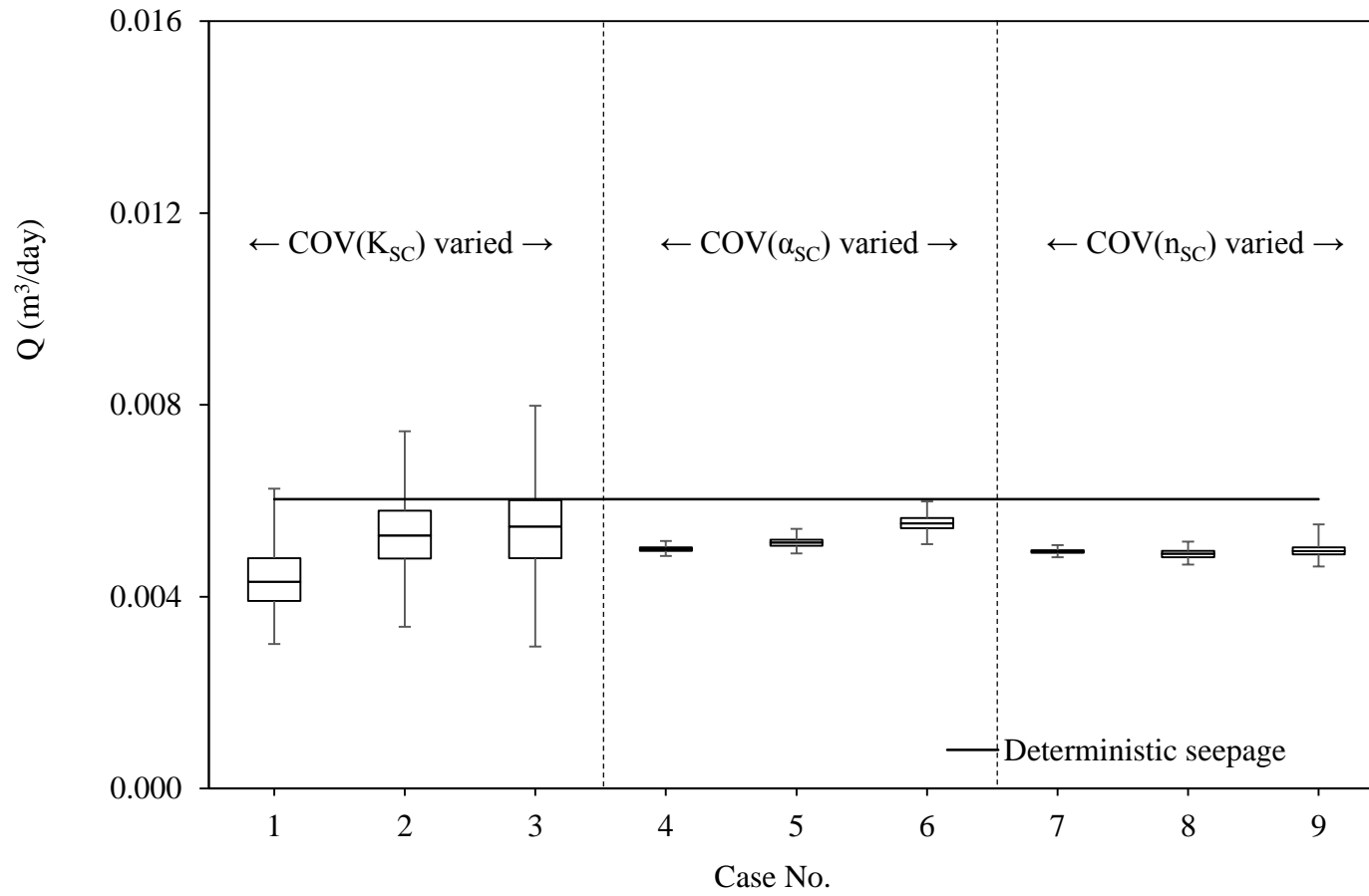


Figure 5.18 The box-plots of stochastic seepage for rapid drawdown when  $t=2500$  days at Section 2.

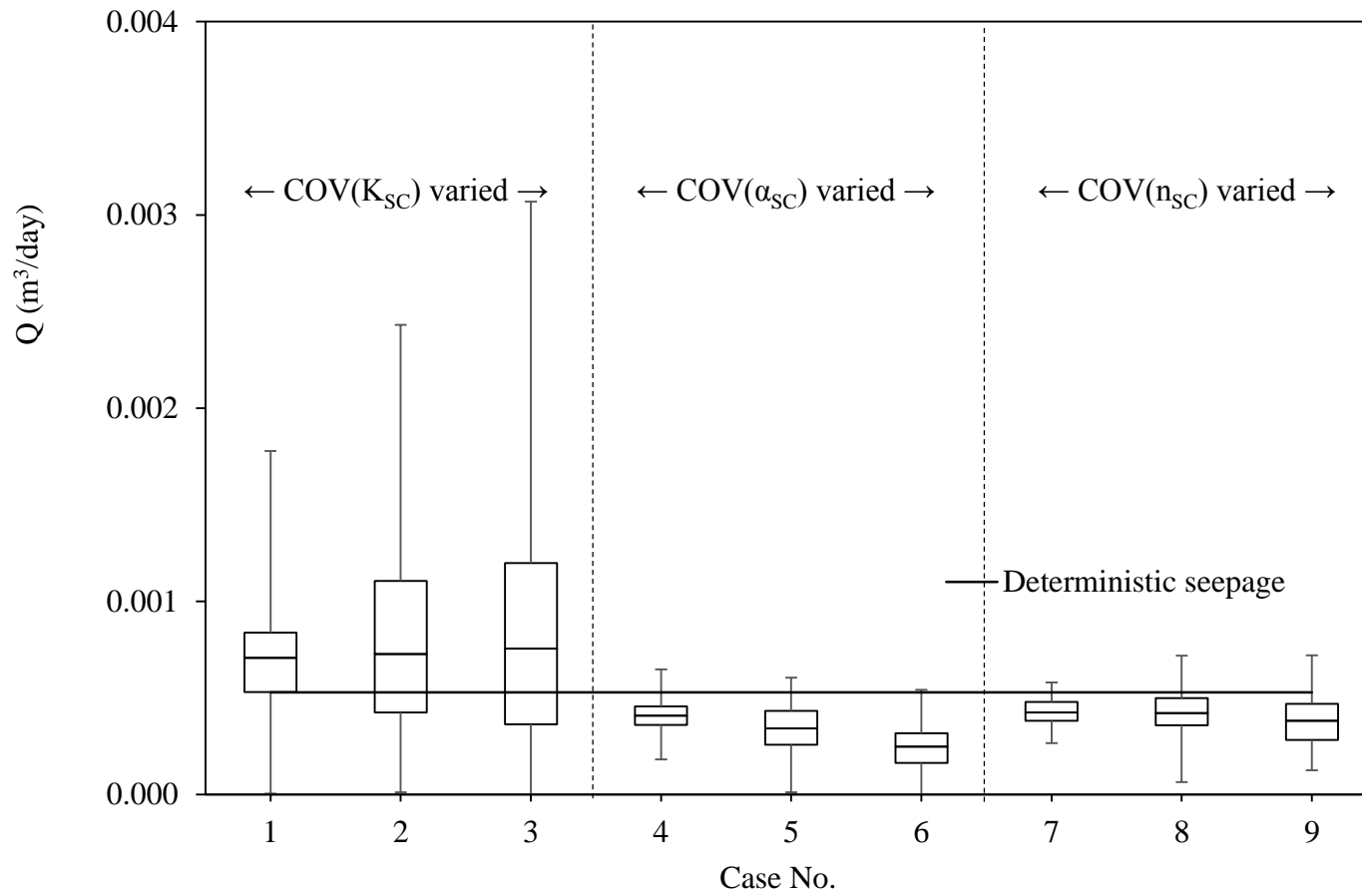


Figure 5.19 The box-plots of stochastic seepage for rapid drawdown when  $t=2500$  days at Section 3.

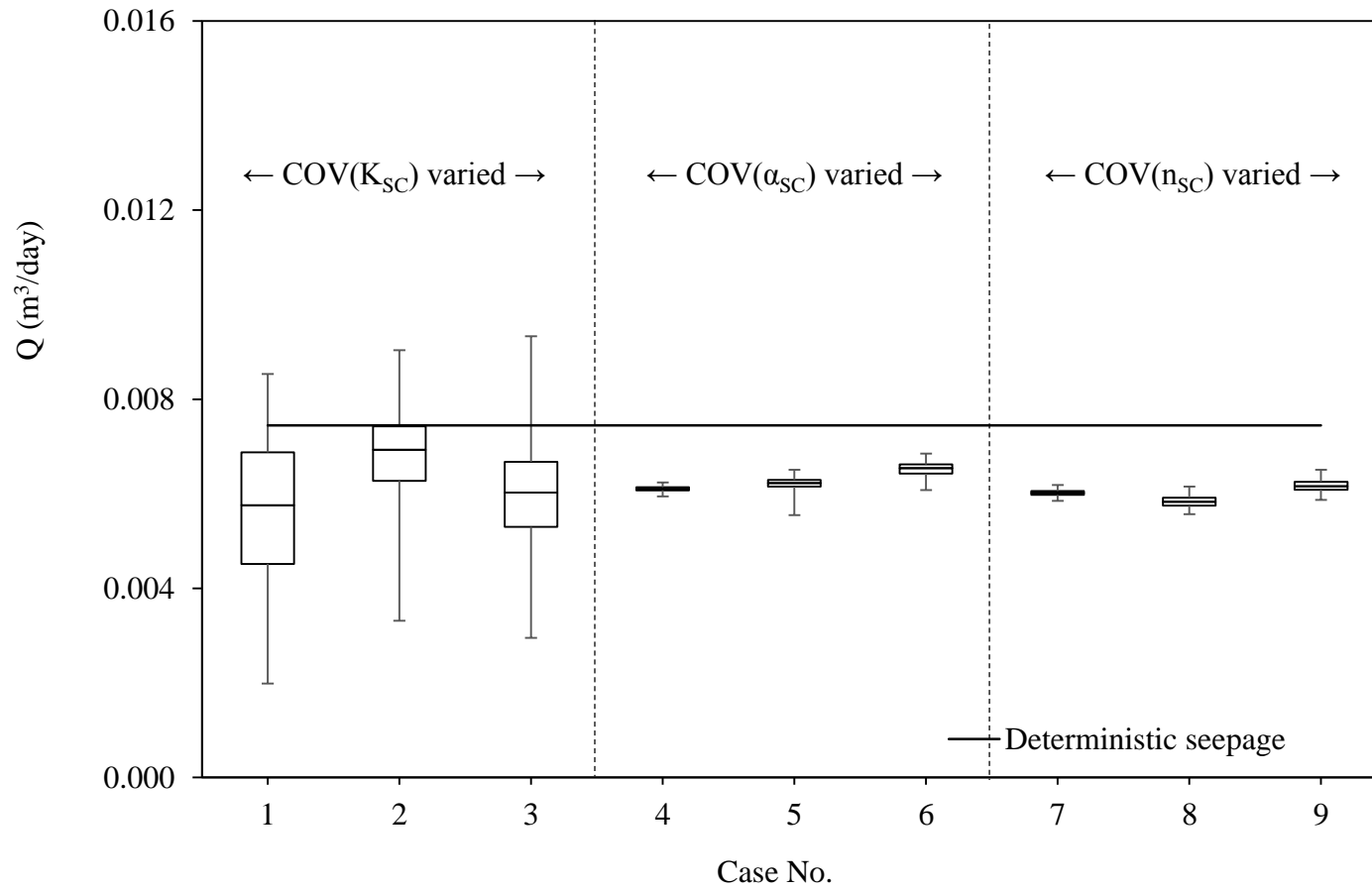


Figure 5.20 The box-plots of stochastic seepage for rapid drawdown when  $t=2500$  days at Section 4.

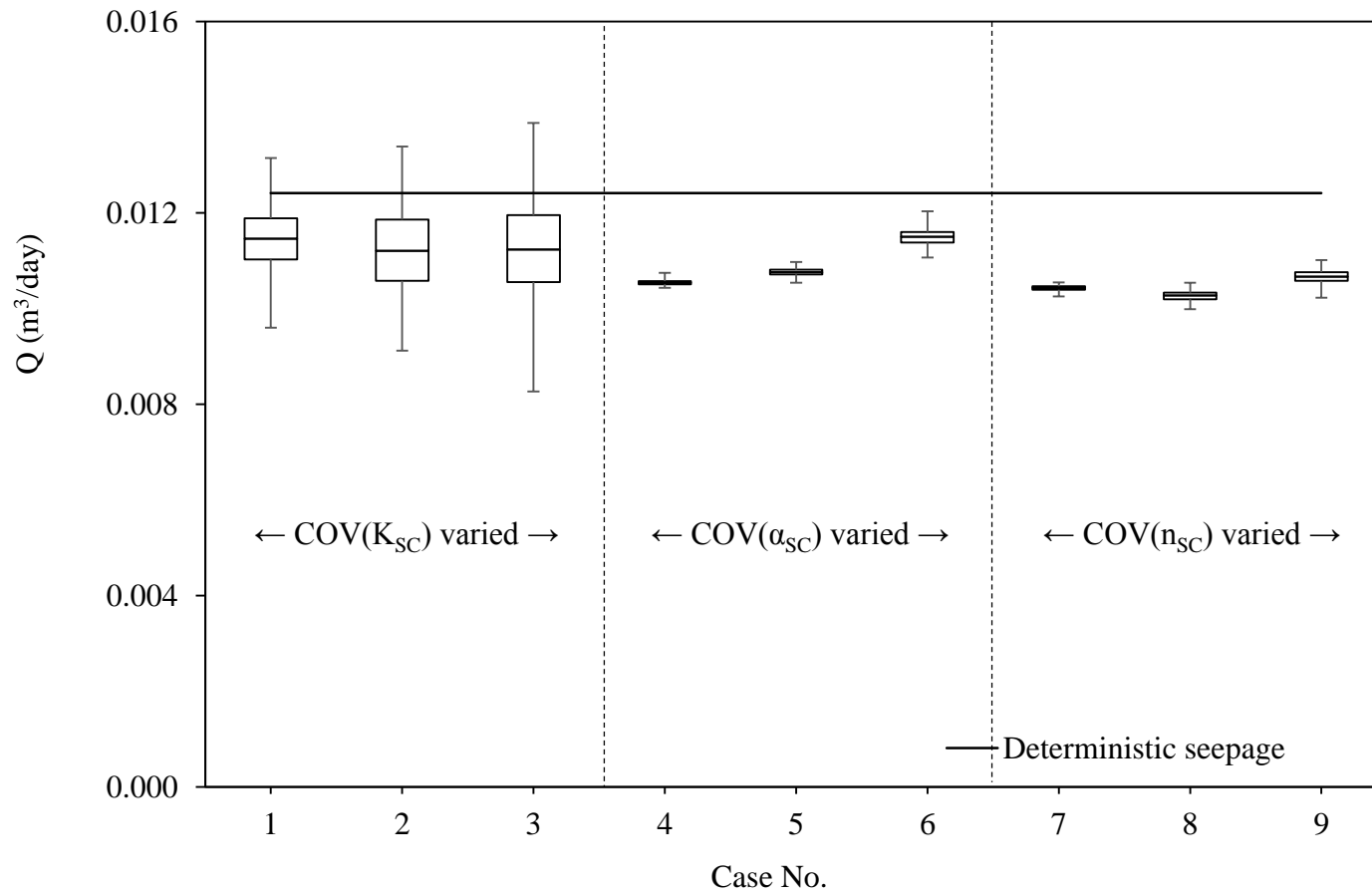


Figure 5.21 The box-plots of stochastic seepage for rapid drawdown when  $t=2500$  days at Section 5.

## 5.2 Rapid Fill Case

For the rapid fill case, a total head of 1 m is assigned to the upstream face of the embankment dam given in Figure 5.1 as an initial condition. Then the total head is increased from 1 m to 23 m in two days, linearly. The boundary condition is presented graphically in Figure 5.22. Such a filling rate is common for flood detention dams, whose reservoir is almost empty prior to the occurrence of a flood. Water level in the reservoir is considered to rapidly increase during the rising stage of a single flood.

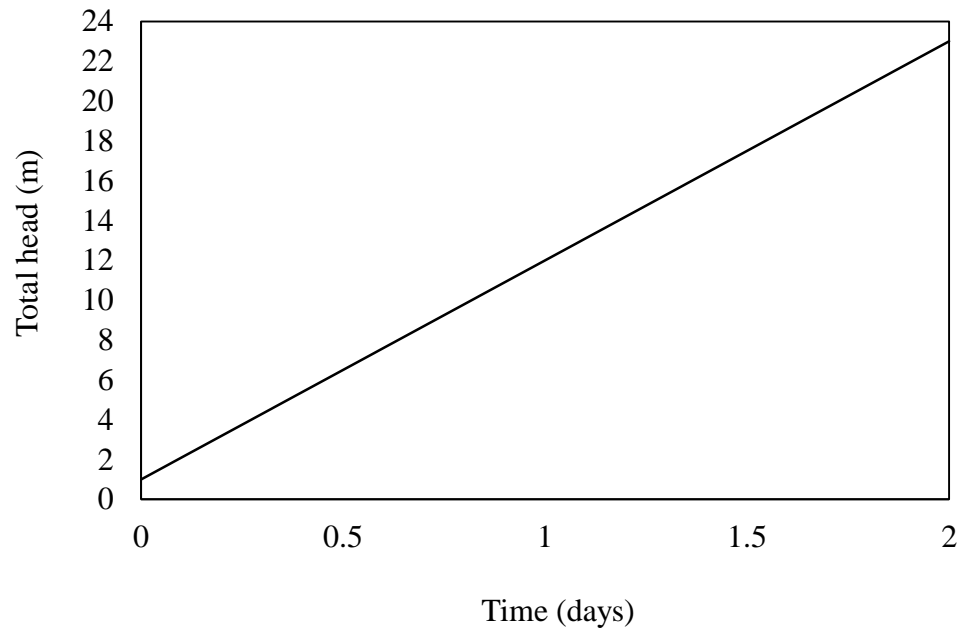


Figure 5.22 The upstream boundary condition for the rapid fill case.

The simulation duration is selected as 1000 days, which is sufficient time for the flow to reach a condition where almost no changes are observed between two successive time steps in all sections. In other words, at the end of the simulation, almost steady-state conditions are observed for the flow. The simulation duration of the analysis is determined from the deterministic model of the problem. The change of the deterministic seepage rate with respect to time at sections are given in

Figure 5.23 for the case. It clear from this figure that after 1000 days, the seepage rate at sections do not change with respect to time.

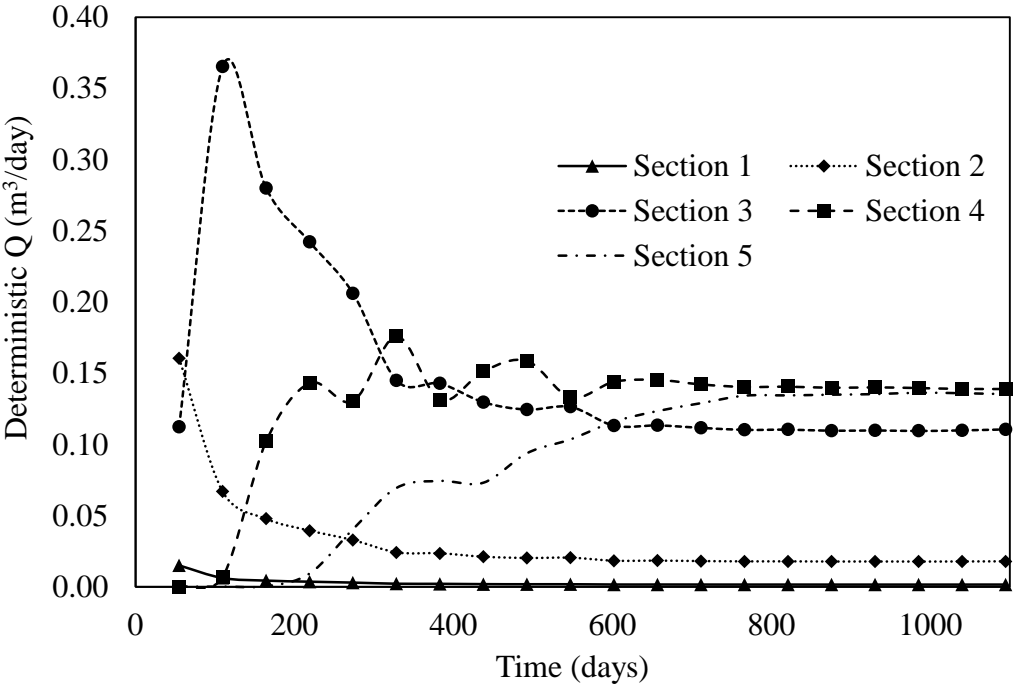


Figure 5.23 The change of the deterministic flow rate with respect to time for the rapid fill case.

First, the problem is solved deterministically to obtain the seepage tendency of the dam with respect to rapid fill case. The results are demonstrated in Figure 5.24 to Figure 5.26 with the free surface of the flow and velocity vectors for times  $t= 50$  days, 500 days and 1000 days, which correspond to 5%, 50% and 100% of the total simulation duration, respectively. It is seen that the velocity vectors at Section 1 and Section 3 to 5 when  $t=50$  days are negligibly small, resulting in almost no flows in these sections. A similar situation is also observed at Section 1 when  $t=500$  and 1000 days. Similar results are expected and obtained for these sections and mentioned times from the stochastic solution of the problem.

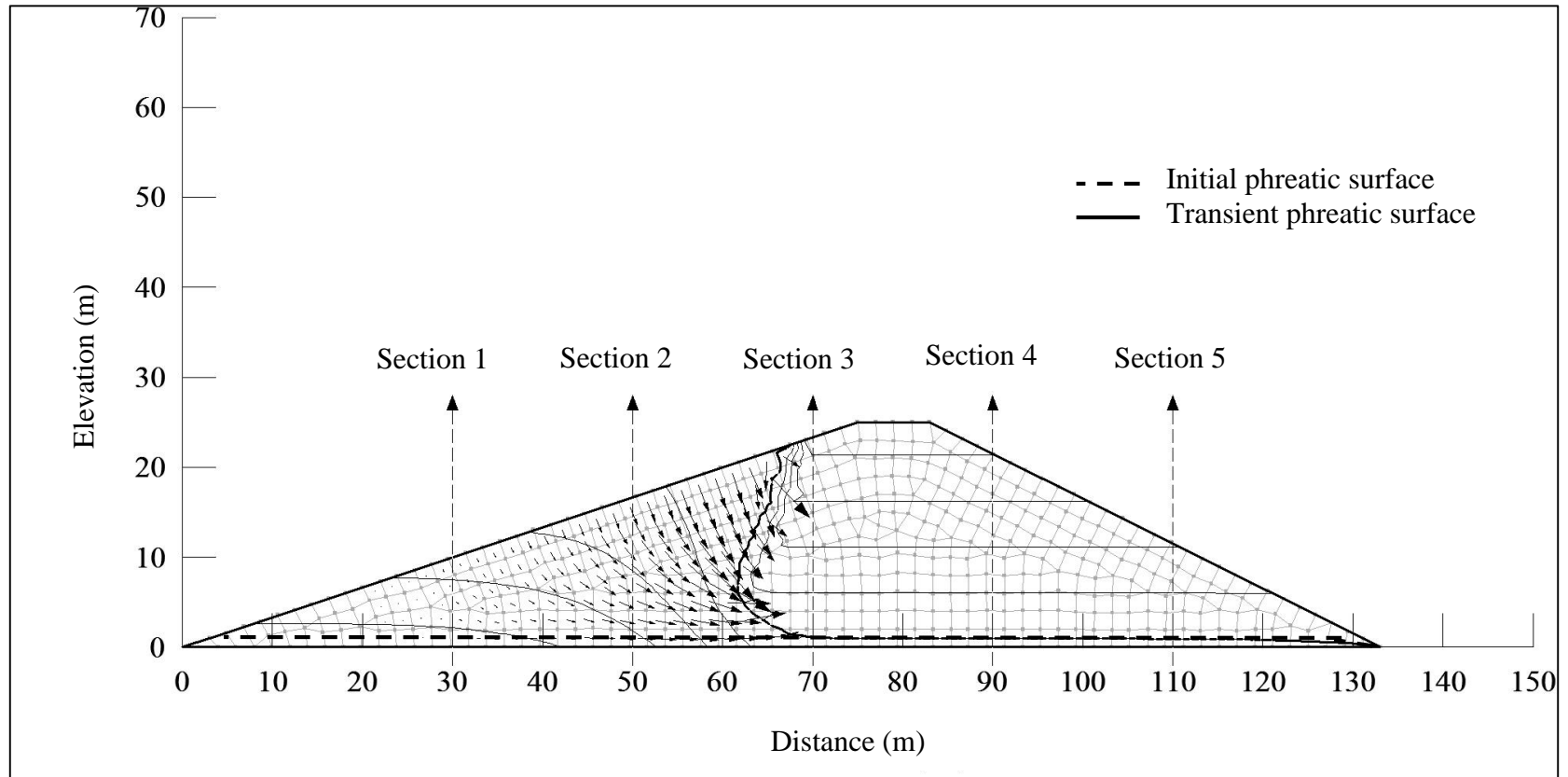


Figure 5.24 The phreatic surface, pore water pressure contours and velocity vectors of deterministic seepage for rapid fill when  $t=50$  days.

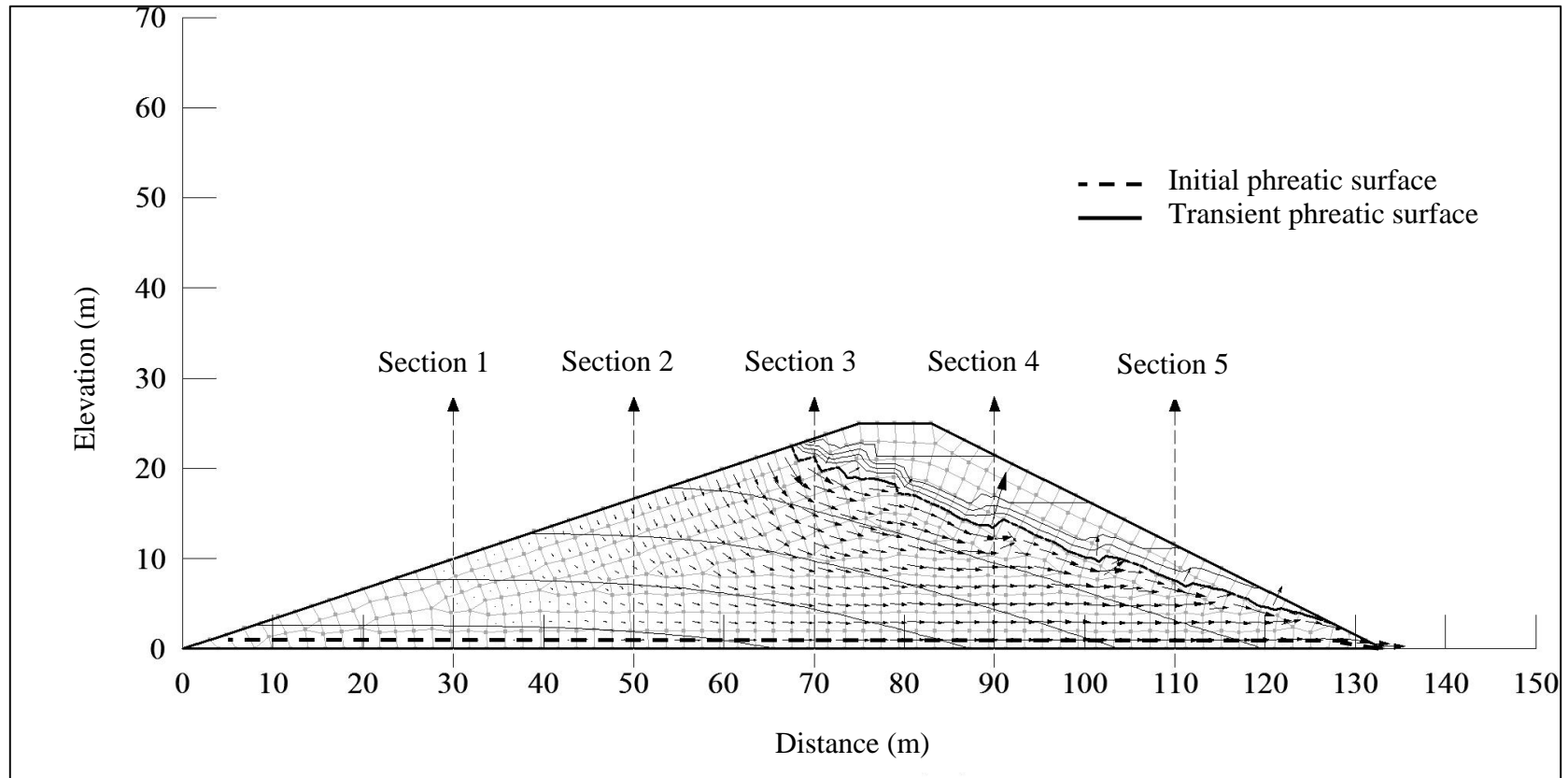


Figure 5.25 The phreatic surface, pore water pressure contours and velocity vectors of deterministic seepage for rapid fill when  $t=500$  days.

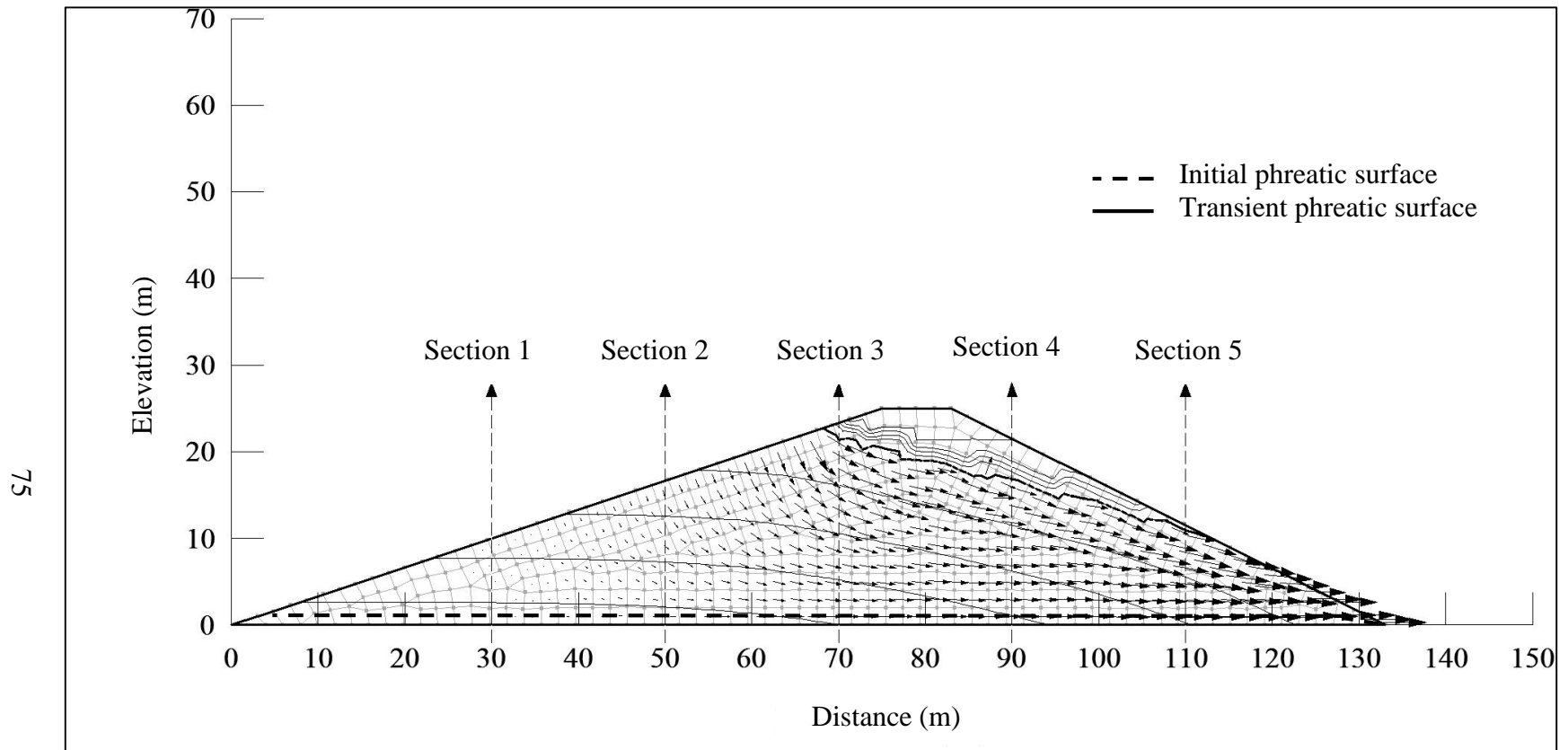


Figure 5.26 The phreatic surface and velocity vectors of deterministic seepage for rapid fill when  $t=1000$  days.

The box-plots of the seepage rate for the rapid fill condition are given for Case 1 to 9 in Figure 5.27 to Figure 5.31 for  $t=50$  days, Figure 5.32 to Figure 5.36 for  $t=500$  days and Figure 5.37 to Figure 5.41 for  $t=1000$  days. The deterministically calculated flow rates are shown by continuous lines for comparison purposes on these figures.

Inspection of box-plots reveals that the variation of hydraulic conductivity has minor effects on the flow rate at the beginning of the simulation (see Case 1 to 3 in Figure 5.27 to Figure 5.31). However, the effects increase with increasing time (see Case 1 to 3 in Figure 5.32 to Figure 5.41). When time increases, the seepage quantity increases for a given section and effects of  $K$  variation increases. Similar findings were presented in the sensitivity analysis conducted for the rapid drawdown case. Besides, the increase in the variation of hydraulic conductivity results in a decrease in the mean flow rate and increase in the range of the computed flow rates. Also, from the first and third quartiles of the box-plots, it can be understood that, the skewness of the probability distributions increases with the increase of  $COV(K)$ .

The variation of van Genuchten parameters has almost no effects on seepage: the mean flow rates computed for Case 4 to 9 are very close to that is obtained from the deterministic solution. Slight changes are observed for the mean flow rates computed for Case 4 to 9 when  $t$  equals to 500 days. However, these changes disappeared when the flow reached to its steady-state condition at  $t=1000$  days. Therefore, it can be said that ignoring the variation of  $\alpha$  and  $n$  does not introduce significant changes in transient seepage results for the given rapid fill condition for the tested  $COV$  ranges.

It should be noted that the box-plots for Section 1 and Section 3 to 5 at  $t=50$  days and Section 1 for all selected times of the simulation may be misleading in evaluating the effects produced by random parameters, because there exist insignificantly low flow rates at these sections for given times. Therefore, very small flow rates are considered as “no flow” case and no interpretation is made accordingly.

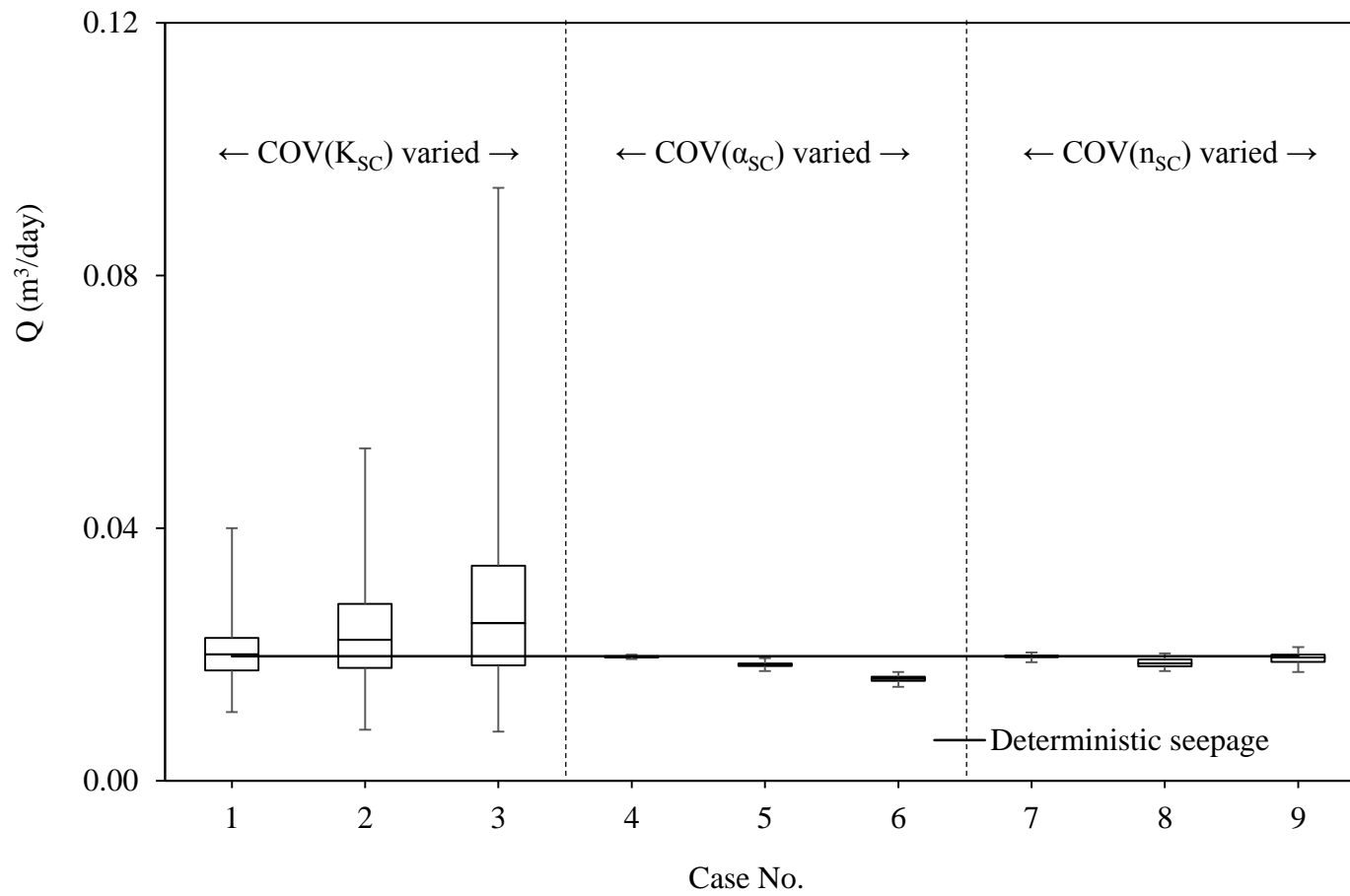


Figure 5.27 The box-plots of stochastic seepage for rapid fill when  $t=50$  days at Section 1.

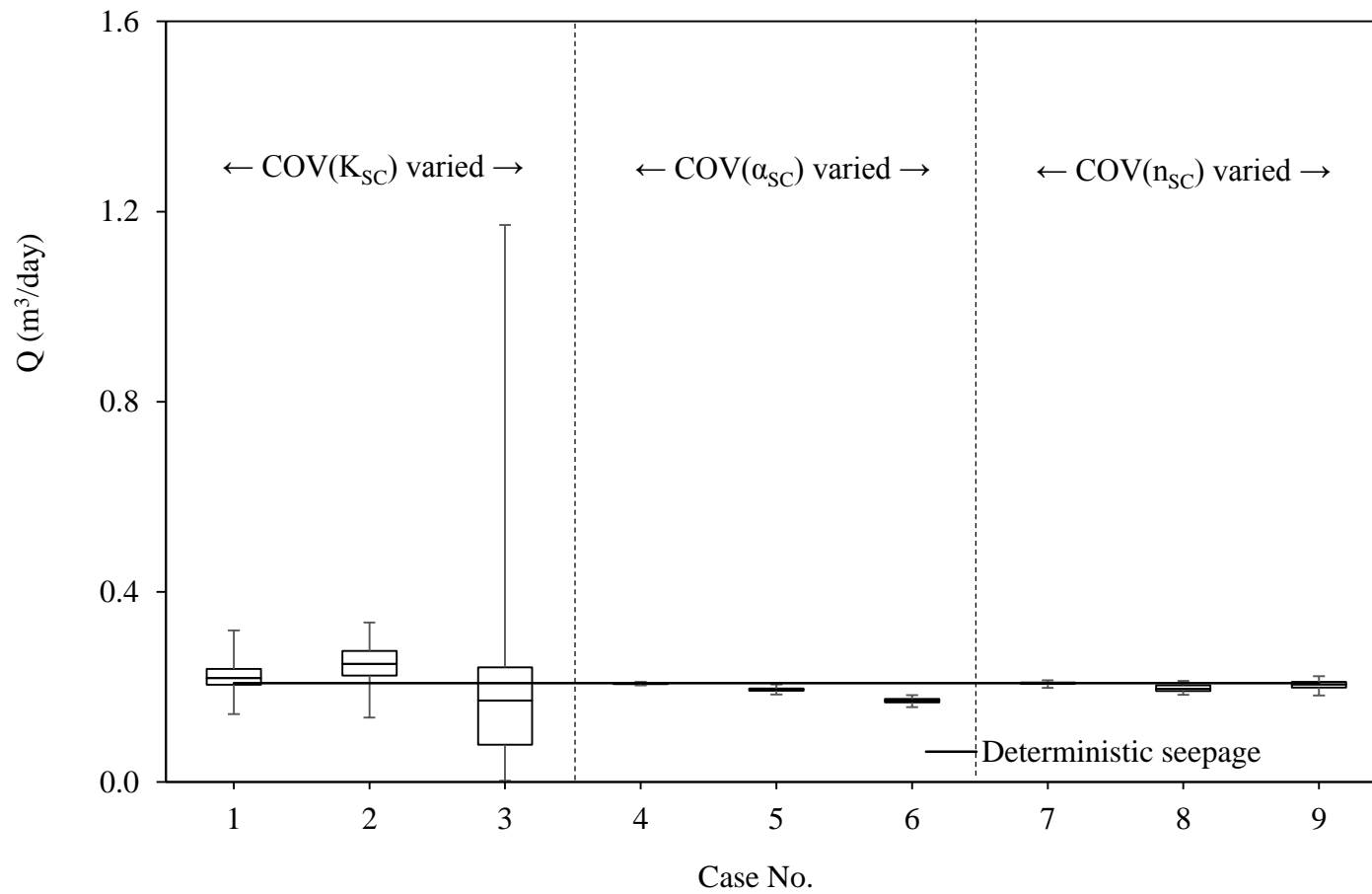


Figure 5.28 The box-plots of stochastic seepage for rapid fill when  $t=50$  days at Section 2.

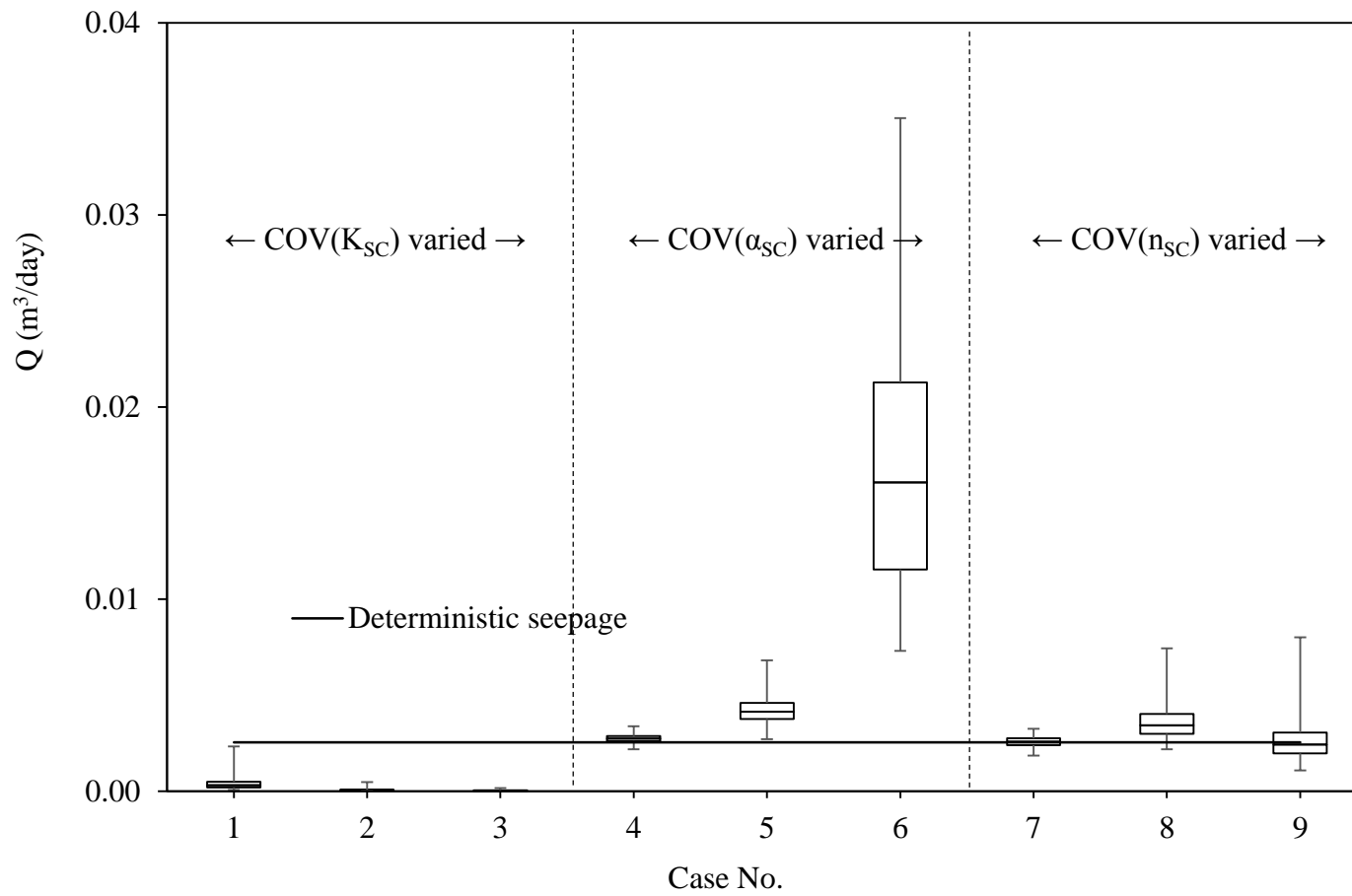


Figure 5.29 The box-plots of stochastic seepage for rapid fill when  $t=50$  days at Section 3.

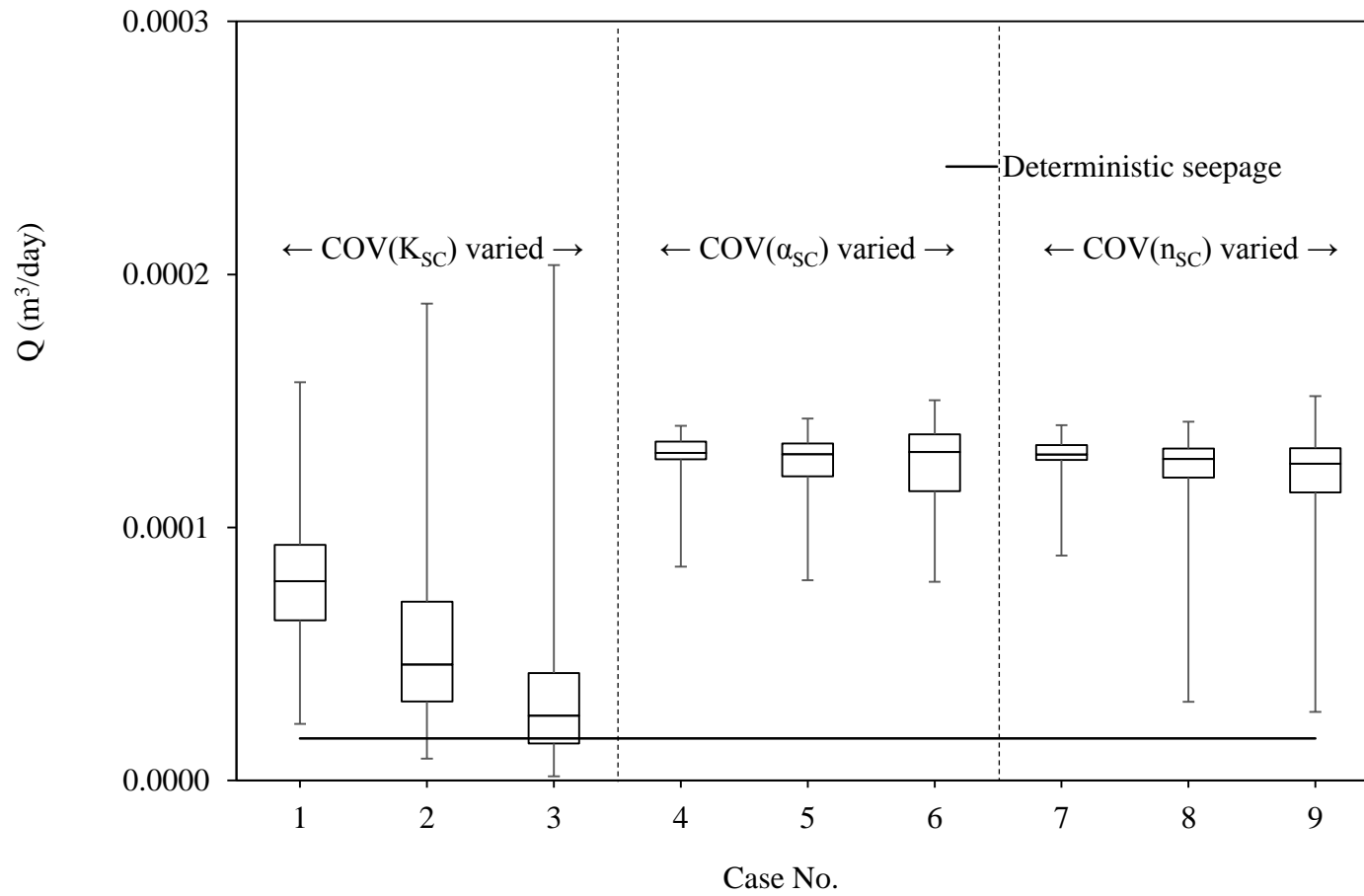


Figure 5.30 The box-plots of stochastic seepage for rapid fill when  $t=50$  days at Section 4.

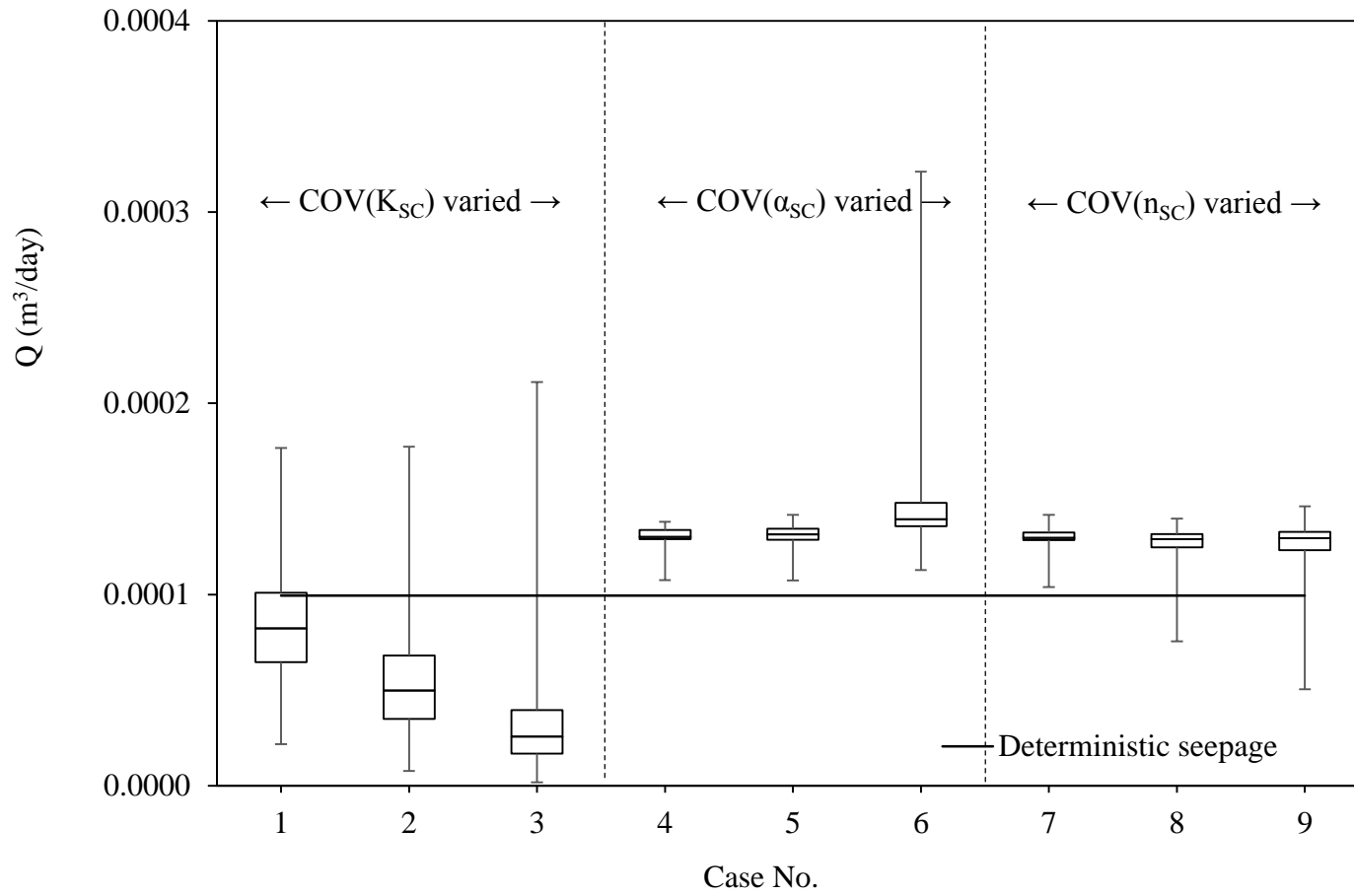


Figure 5.31 The box-plots of stochastic seepage for rapid fill when  $t=50$  days at Section 5.

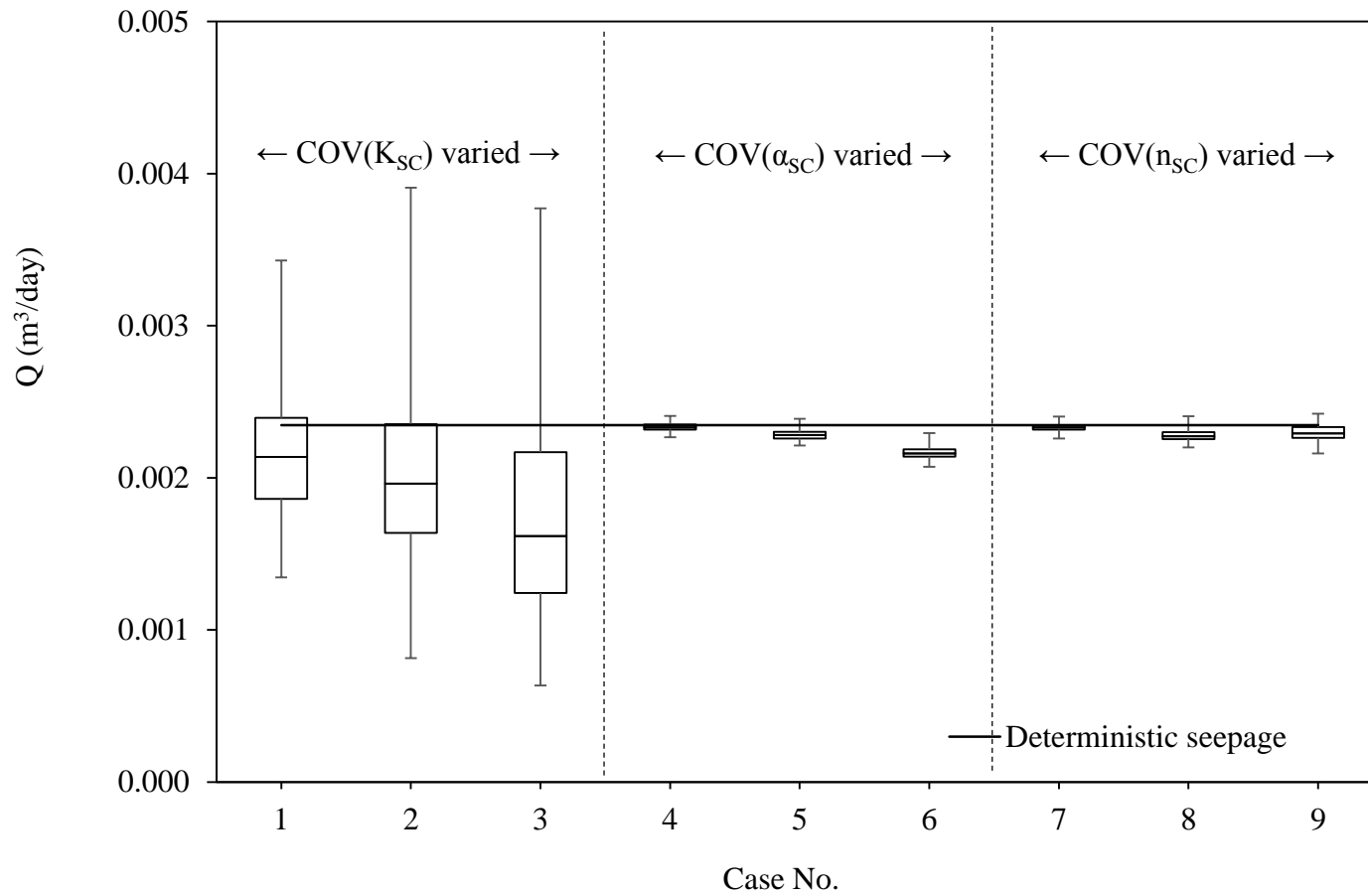


Figure 5.32 The box-plots of stochastic seepage for rapid fill when  $t=500$  days at Section 1.

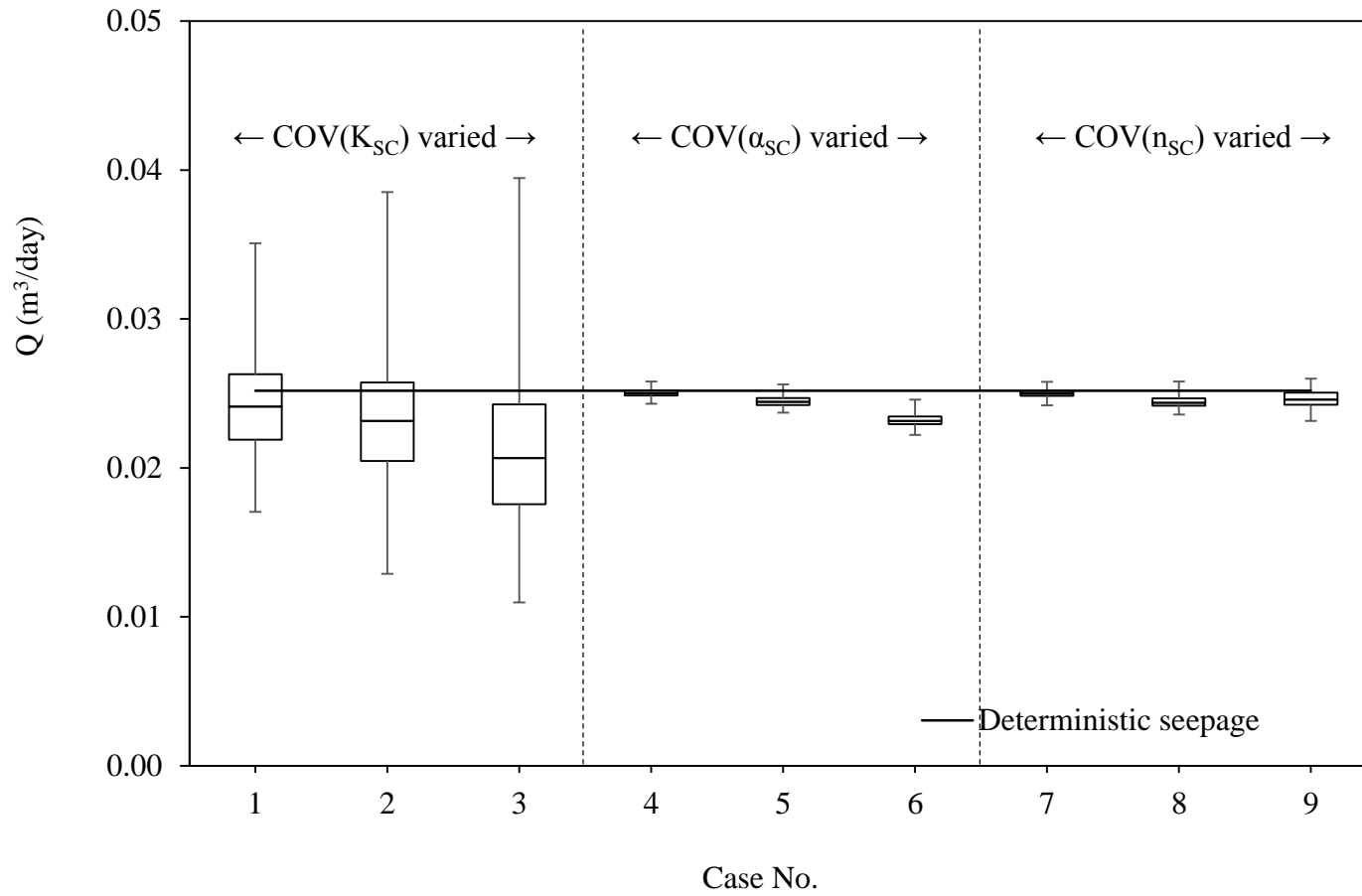


Figure 5.33 The box-plots of stochastic seepage for rapid fill when  $t=500$  days at Section 2.

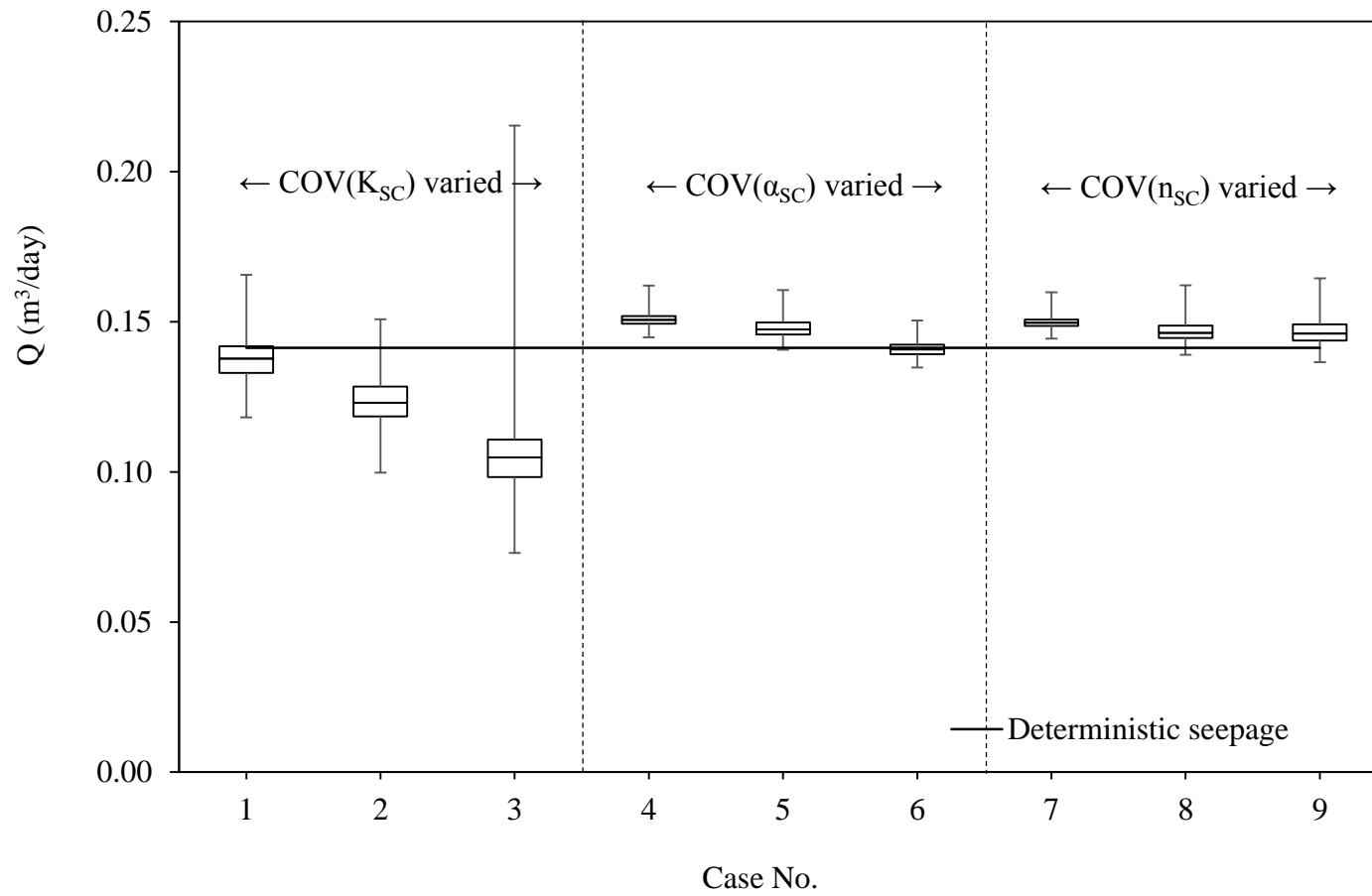


Figure 5.34 The box-plots of stochastic seepage for rapid fill when  $t=500$  days at Section 3.

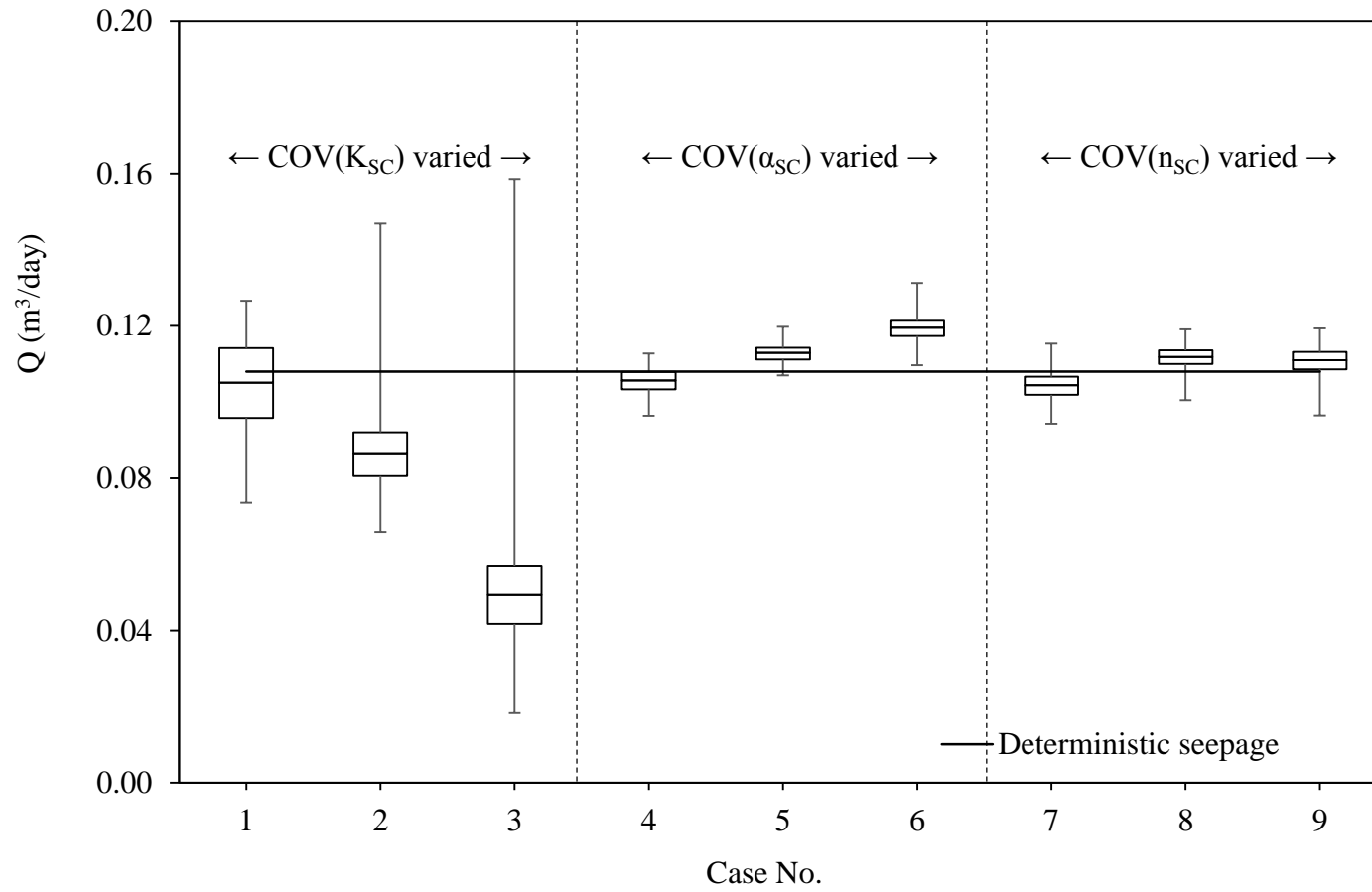


Figure 5.35 The box-plots of stochastic seepage for rapid fill when  $t=500$  days at Section 4.

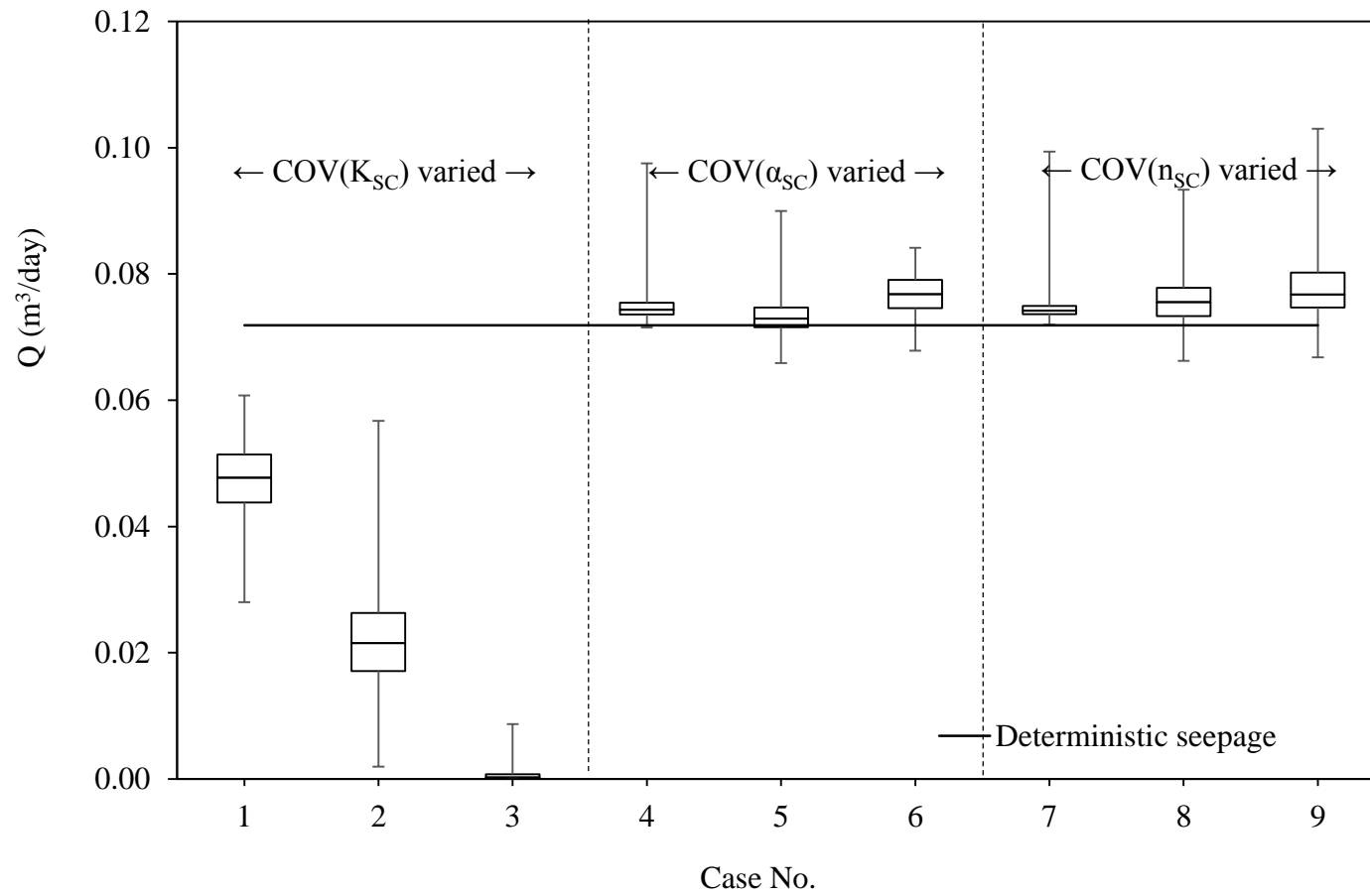


Figure 5.36 The box-plots of stochastic seepage for rapid fill when  $t=500$  days at Section 5.

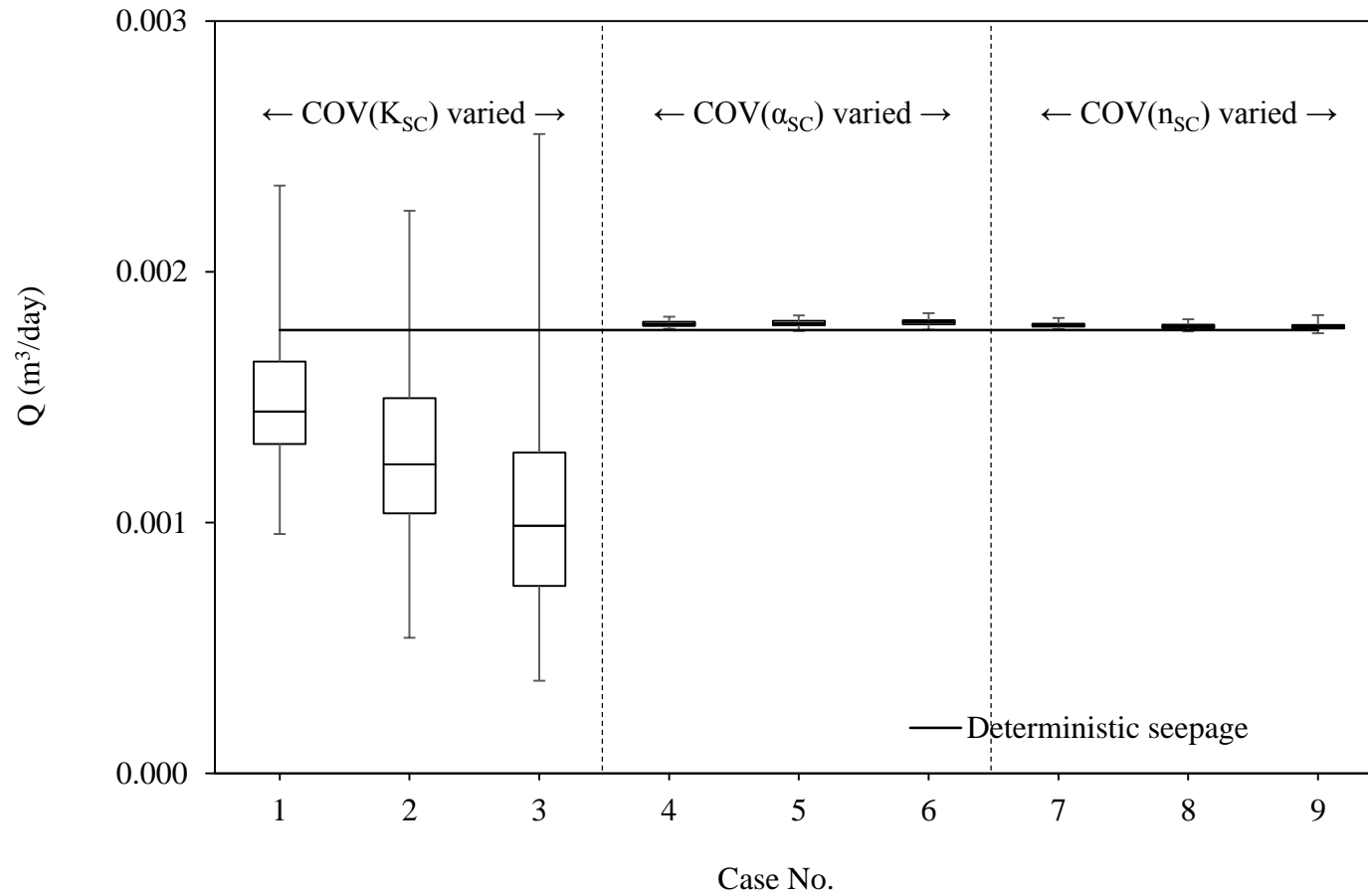


Figure 5.37 The box-plots of stochastic seepage for rapid fill when  $t=1000$  days at Section 1.

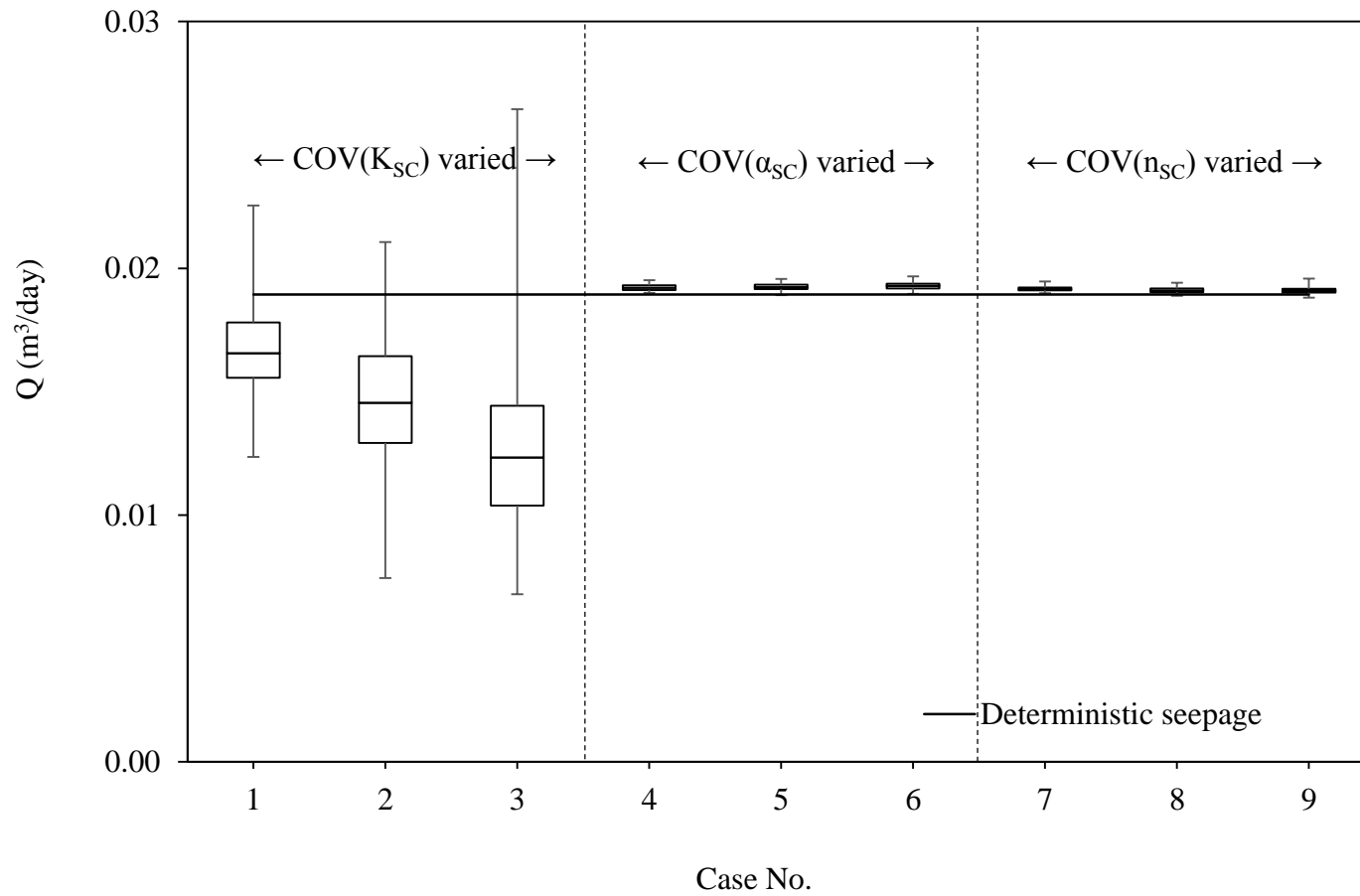


Figure 5.38 The box-plots of stochastic seepage for rapid fill when  $t=1000$  days at Section 2.

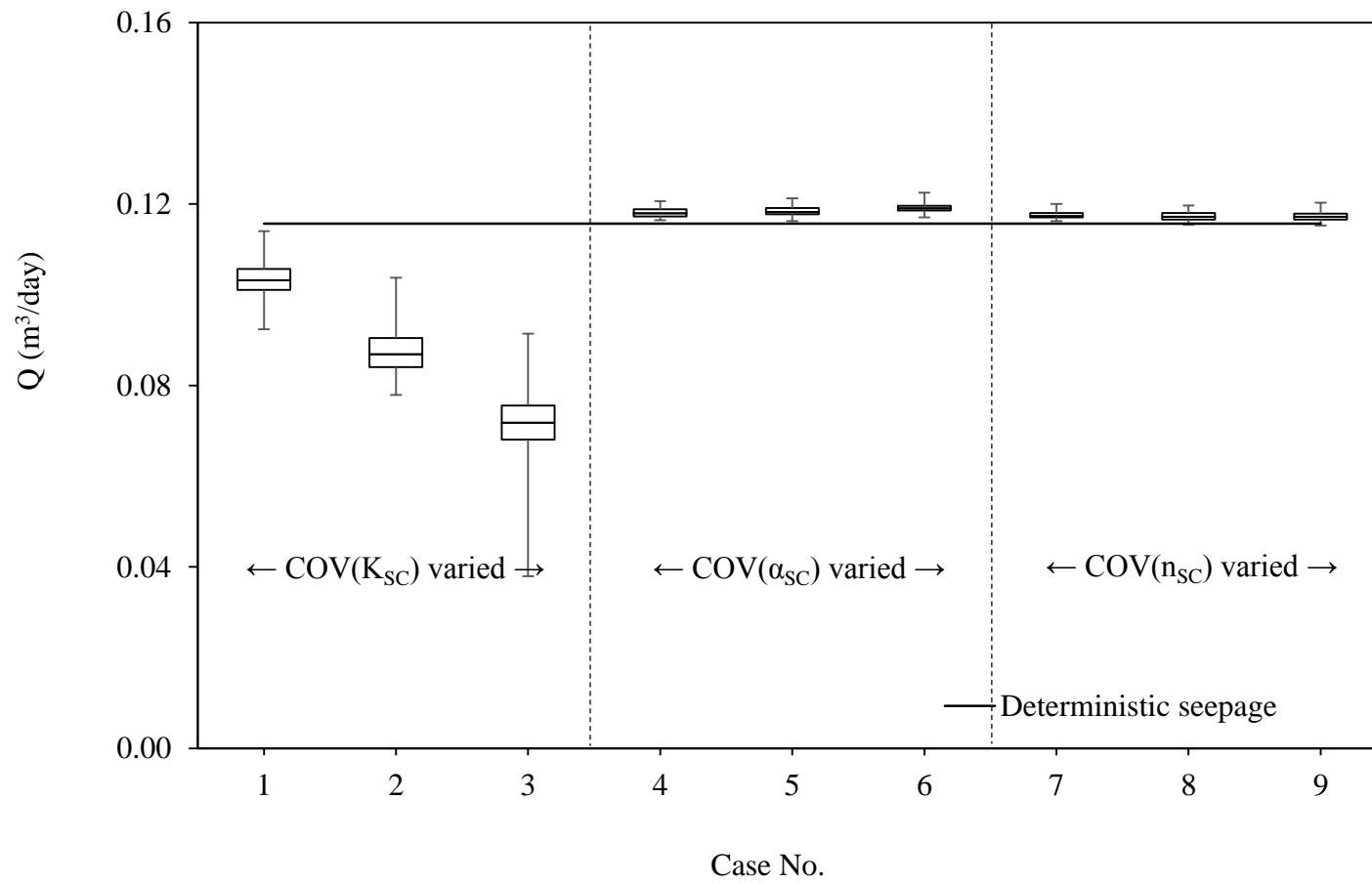


Figure 5.39 The box-plots of stochastic seepage for rapid fill when  $t=1000$  days at Section 3.

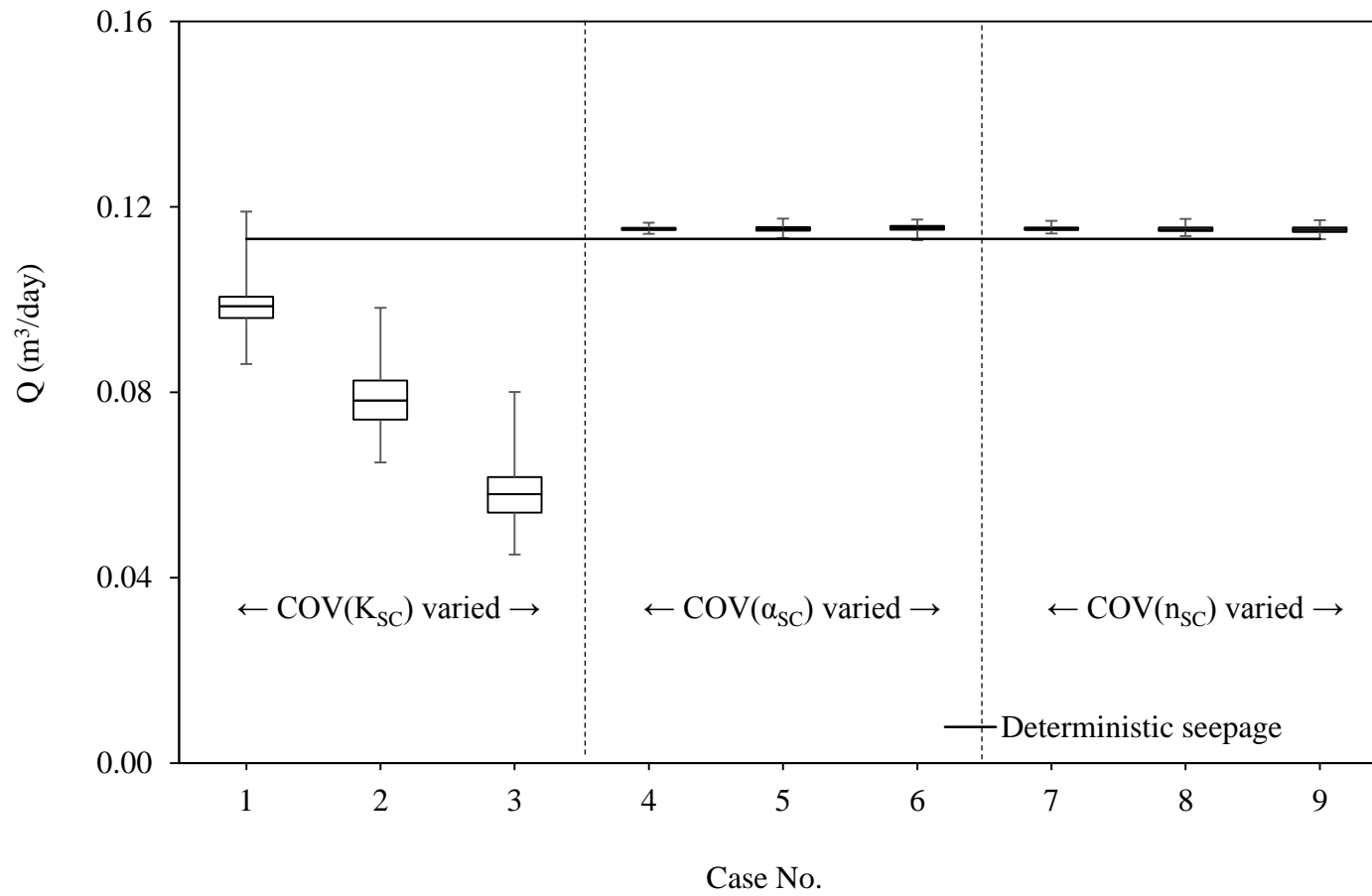


Figure 5.40 The box-plots of stochastic seepage for rapid fill when  $t=1000$  days at Section 4.

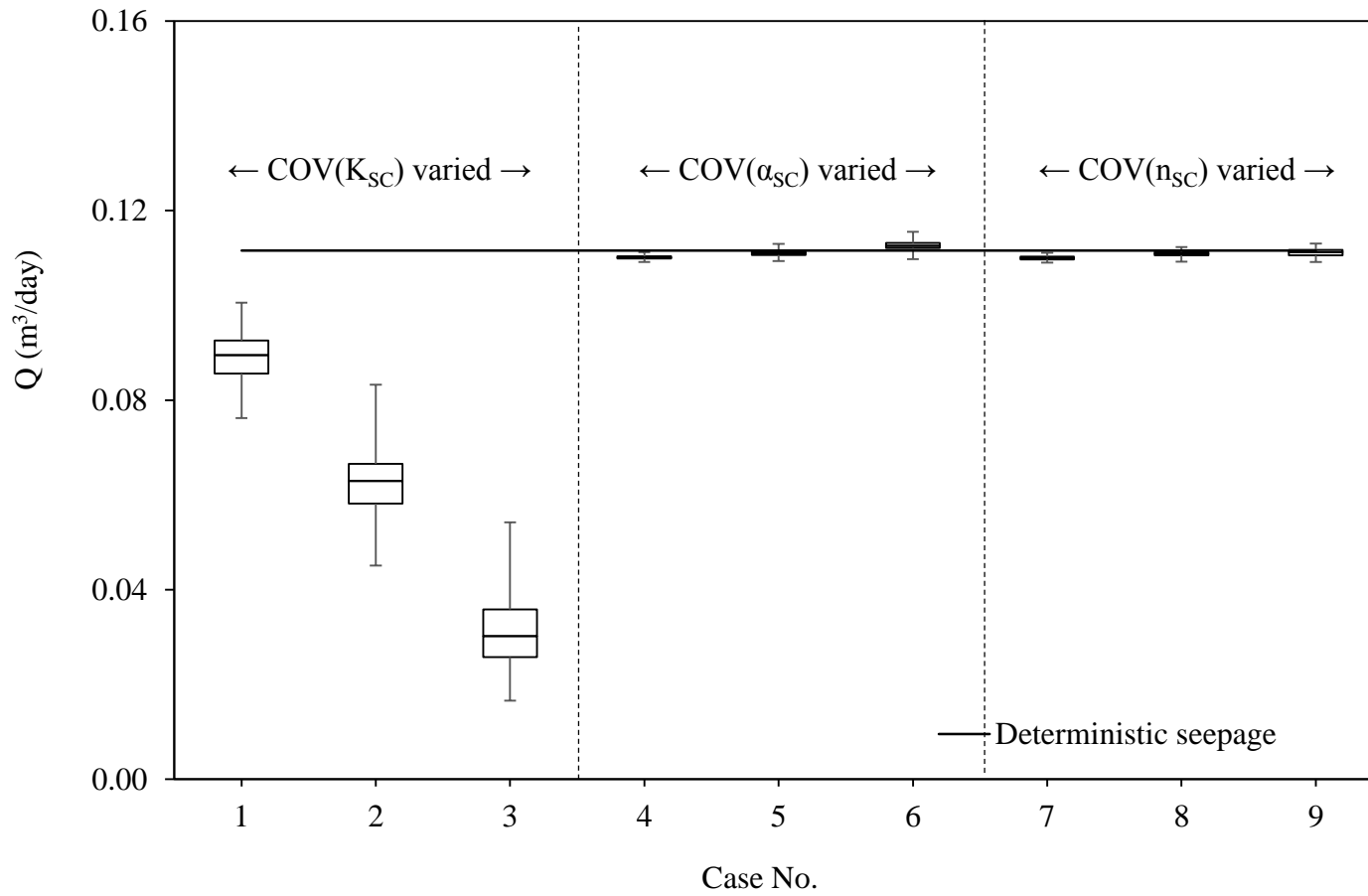


Figure 5.41 The box-plots of stochastic seepage for rapid fill when  $t=1000$  days at Section 5.

### 5.3 Discussion

For both rapid drawdown and fill cases, the variation of hydraulic conductivity is found to have crucial effect on the transient seepage. The increase in the variation of hydraulic conductivity,  $K$  results in decrease in the mean seepage rates. Similar findings are presented for the sensitivity analysis carried out for steady-state seepage. The degree of the decrease in the mean flow is seen to be dependent on time for both cases. For the rapid drawdown case the degree of decrease in the mean flow decreases with time, whereas for the rapid fill case the degree of decrease increases with time.

It can be concluded that the transient seepage is extremely sensitive to the variation of hydraulic conductivity. Therefore, the randomness in  $K$  should be included in transient seepage analyses.

The variation effects of van Genuchten parameters ( $\alpha$  and  $n$ ) have shown to be slighter for both transient cases. The effects are more apparent in the rapid drawdown case. The mean seepage rate slightly decreases when  $\alpha$  or  $n$  are randomly varied over the flow domain. This may be caused by the unsaturated hydraulic conductivity changing from one point to another in the flow domain resulting in extended flow paths and smaller flow rates. Besides, the flow rates observed for the case are relatively small and this may make the variability impacts of the parameters more visible for the case. Generally, the variations of van Genuchten parameters resulted in smaller influences on the seepage of the rapid fill case.

The increase in COV values of  $\alpha$  from 0.32 to 1.26 and  $n$  from 0.04 to 0.16 do not result in a change in the mean seepage rate. Also, the variation of both  $\alpha$  and  $n$  has similar effects on the seepage. Therefore it can be said that, there is no relative importance between two parameters in view of their uncertainties.

Consequently, the transient seepage can be said to be sensitive to the variation of fitting parameters in a relatively small degree. For practical applications, the deterministic treatment of  $\alpha$  and  $n$  may be reasonable. This may not introduce major

errors in seepage analysis. However, for more accurate estimations of probabilistic behavior of the transient seepage they should be considered as stochastic variables. In the next chapter, they are treated as random variables to completely investigate the behavior and probabilistic properties of the seepage through embankment dams under uncertainty.



## CHAPTER 6

### APPLICATIONS

The degree of uncertainty and statistical randomness of the seepage through embankment dams are the issues to be investigated for understanding the probabilistic nature of the phenomenon. The applications of the study investigate the statistical and probabilistic properties of the seepage via some statistical analyses and interpretations.

The findings of the sensitivity analyses showed that the uncertainty of hydraulic conductivity significantly affects the seepage, whereas the variability of van Genuchten fitting parameters have slighter effects. These outcomes are considered in the application problems. All parameters, which are  $K$ ,  $\alpha$  and  $n$ , are treated as random variables. Then, seepage analyses are conducted for different problems using the stochastic approach proposed in the study.

The seepage rate computed considering the randomness of  $K$ ,  $\alpha$  and  $n$  is also random and its properties need to be defined. The data set of the seepage rate can be described by determining its statistical moments, i.e. mean, variance, skewness and kurtosis, and type of its statistical distribution. These properties can be used when dealing with the uncertainty of the seepage.

The distribution fitting is used to select the statistical distribution that best fits to the data set. Using statistical distributions, the uncertainty of the seepage can be quantified. In addition, the level of risk of failure due to seepage can be estimated if

a threshold value is known. Also, the determination of the distribution type for seepage rate may provide an important mean for reliability-based safety assessments. To this end, the frequency histograms of the seepage are derived and statistical distributions are fitted to seepage data sets of application problems in the study. The validity of the assumed distribution type is verified using goodness of fit tests. Two common tests are used for this purpose: the Kolmogorov-Smirnov and Chi-square methods. In the Kolmogorov-Smirnov method, the observed cumulative distribution function (CDF) is compared with the assumed theoretical CDF. The hypothesis is rejected if the maximum difference between the observed and theoretical functions ( $D_{max}$ ) exceeds the value which is determined by the level of significance,  $\alpha'$ . The level of significance is the probability of  $D_{max}$  exceeding a critical value (Massey Jr. 1951). The maximum  $D_{max}$  can be computed using (Ang and Tang 1975):

$$D_{max} = |F(x) - S(x)| \quad (6.1)$$

where  $F(x)$  is the proposed theoretical CDF and  $S(x)$  is the stepwise CDF of the observed data.

The Chi-square test based on the comparison between the observed frequencies with those obtained from the assumed theoretical distribution. The Chi-square statistics is defined with the following expression (Ang and Tang 1975):

$$X^2 = \sum_{i=1}^k \frac{(O_i - E_i)^2}{E_i} \quad (6.2)$$

in which,  $k$  is the number of intervals used in dividing the entire range of the data,  $O_i$  is the observed frequency, and  $E_i$  is the expected frequency for the interval  $i$ . The hypothesis is rejected at the chosen significance level if the Chi-square statistics is greater than the critical value.

In this study, the goodness of fit tests are conducted using a software named EasyFit (Mathwave 2013). The statistical distributions are determined for the seepage rates of the application problems. In distribution fitting process, commonly used

functions in water resources engineering, which are normal (N), three-parameter gamma (G-3P), three-parameter log-normal (LN-3P), generalized extreme value (GEV) and log-Pearson type 3 (LPT3) probability density functions are tested for goodness of fit using Kolmogorov-Smirnov and Chi-square tests. The hypotheses are tested at the significance levels of 5% and 10%. The test results are used to assess typical statistical distribution types for the seepage quantity.

The descriptive statistics, including the range, COV and the first four moments (i.e. the mean, standard deviation, skewness and kurtosis), of the seepage rate are derived at different sections of the embankment dams for different durations of the transient flow. For the sections having no flow during certain times of the transient simulation, the values of degree of uncertainty, skewness and kurtosis are not computed. Also, no PDF is assigned to the seepage data of these sections.

The application problems are composed of the homogeneous embankment dam defined in Chapter 5 with the rapid drawdown and rapid fill transient conditions. An additional complex boundary condition (i.e. a combined fill and drawdown case) is also considered for the dam. Finally, the complex boundary condition is applied on a simple zoned embankment dam.

## 6.1 Rapid Drawdown Case

This application problem deals with the degree of uncertainty and statistical randomness of the seepage through the embankment dam shown in Figure 5.1, having the same boundary condition defined in Section 5.1 (i.e. the rapid drawdown case in which the upstream initial head of 23 m is decreased to 1 m in four days). Different than the sensitivity analysis held in Section 5.1, in this application all parameters,  $K$ ,  $\alpha$  and  $n$  are kept random having the statistical properties presented in Table 6.1.

Table 6.1 The statistical properties of the dam material considered for the application problems given in Section 6.1, Section 6.2 and Section 6.3.1 of Chapter 6.

Parameter	$\mu$	COV	Reference
$K$ (m/s)	$3.33 \times 10^{-7}$	2.33	(Carsel and Parrish 1988; Fredlund 2005)
$\alpha$ (cm <sup>-1</sup> )	0.027	0.63	
$n$	1.23	0.08	

For the application problem, a total of 1000 Monte Carlo simulations are conducted. Similar to the sensitivity analysis, the total duration of each simulation is selected as 2500 days. The seepage rate is computed at five different sections for three time steps of the simulation duration. The descriptive statistics of the seepage rate are given in Table 6.2. Also, the change of expected values of the flow rate with respect to time and the change of the dispersions from the expected values are given in Figure 6.1 (a) and (b), respectively. Accordingly, the mean seepage rate decreases with respect to time for all sections. There exists negligibly small flow rates at Section 3 which makes the uncertainty analysis of the flow insignificant at this section. Similarly, the standard deviation decreases with time for all sections. The spread of the distributions decreases with the decrease in flow rate. Besides, the coefficient of variation of the flow does not significantly vary with time for the rapid drawdown case. It can be said that the degree of uncertainty (i.e. COV) of the

seepage does not considerably change for constantly decreasing flows with respect to time.

The descriptive statistics showed that the probability distributions of the seepage are always skewed positively (i.e. skewed to left) or negatively (i.e. skewed to right), and leptokurtic (i.e. kurtosis $>0$ ) or platykurtic (i.e. kurtosis $<0$ ) in some degree. Specifically, the most of the distributions are positively skewed. It is seen that there is no relation between time and both skewness and kurtosis.

The hydraulic conductivity has the maximum coefficient of variation among other input parameters with a value of 2.33. The maximum computed COV for the seepage rate is 0.14, which is much smaller than that of hydraulic conductivity. It can be said that the degree of variation of the input parameter is decreased by the system.

Table 6.2 The descriptive statistics of the seepage rate for the rapid drawdown case.

Time	Sect.	Max (Q)	Min (Q)	$\mu$ (Q)	$\sigma$ (Q)	COV (Q)	Skewness	Kurtosis
		(m <sup>3</sup> /day)						
t=68 days	1	0.12	0.04	0.06	0.007	0.12	0.57	3.09
	2	0.08	0.05	0.06	0.004	0.07	0.11	0.10
	3	0.02	0.00	0.00	0.004	-	0.28	-0.19
	4	0.07	0.05	0.06	0.004	0.07	0.11	-0.32
	5	0.11	0.05	0.08	0.007	0.09	0.13	0.27
t=1152 days	1	0.03	0.02	0.02	0.001	0.06	0.14	-0.01
	2	0.02	0.01	0.01	0.001	0.09	0.06	-0.22
	3	0.01	0.00	0.00	0.001	-	-	-
	4	0.02	0.01	0.01	0.002	0.11	0.10	-0.44
	5	0.03	0.02	0.03	0.002	0.06	0.28	0.51
t=2500 days	1	0.01	0.01	0.01	0.001	0.07	-0.10	0.04
	2	0.01	0.00	0.01	0.001	0.13	-0.17	-0.12
	3	0.00	0.00	0.00	0.001	-	-	-
	4	0.01	0.00	0.01	0.001	0.14	-0.46	0.33
	5	0.01	0.01	0.01	0.001	0.07	0.20	0.05

The proposed PDFs are tested for goodness of fit to the seepage. The results of tests are presented in Table 6.3. The overall decision of a probability density function depends on the acceptance of the hypothesis from both Kolmogorov-Smirnov and Chi-square methods at the specified significance levels. If the hypothesis is rejected by either method, the overall decision of a fit is assumed to be non-acceptable. According to the test results, the seepage rate during rapid drawdown can be represented by generalized extreme value (GEV) or normal (N) distributions. Specifically, the most common fitted probability distribution type for the case is GEV distribution. The frequency histograms of the seepage, fitted probability density functions and the overall decision of the goodness of fit tests are given in Figure 6.2 to Figure 6.14 for the application problem.

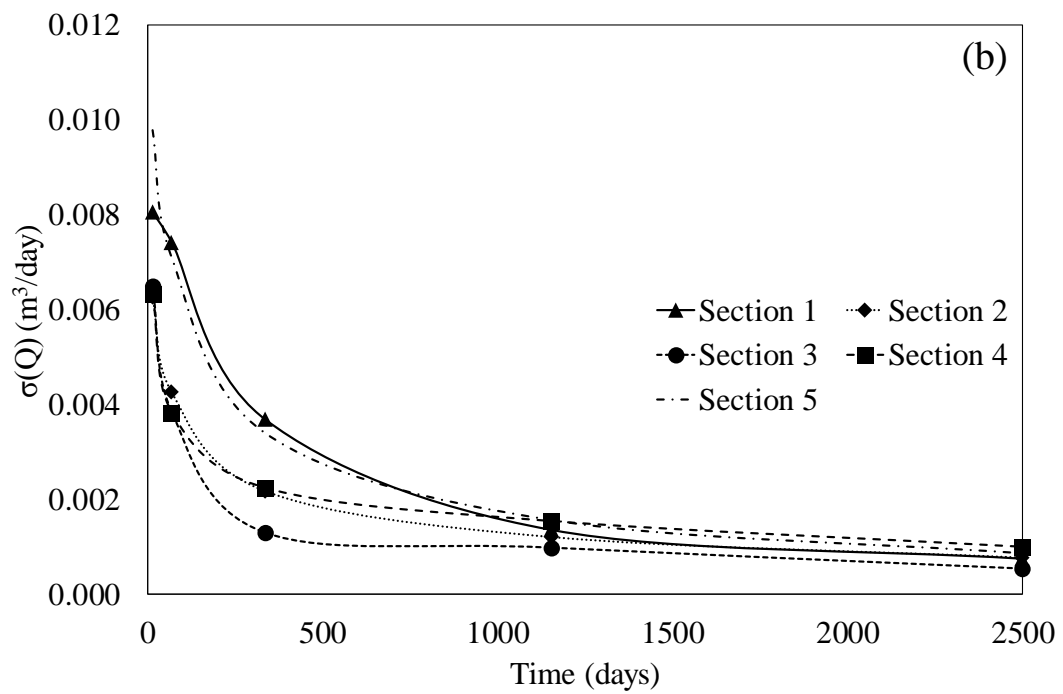
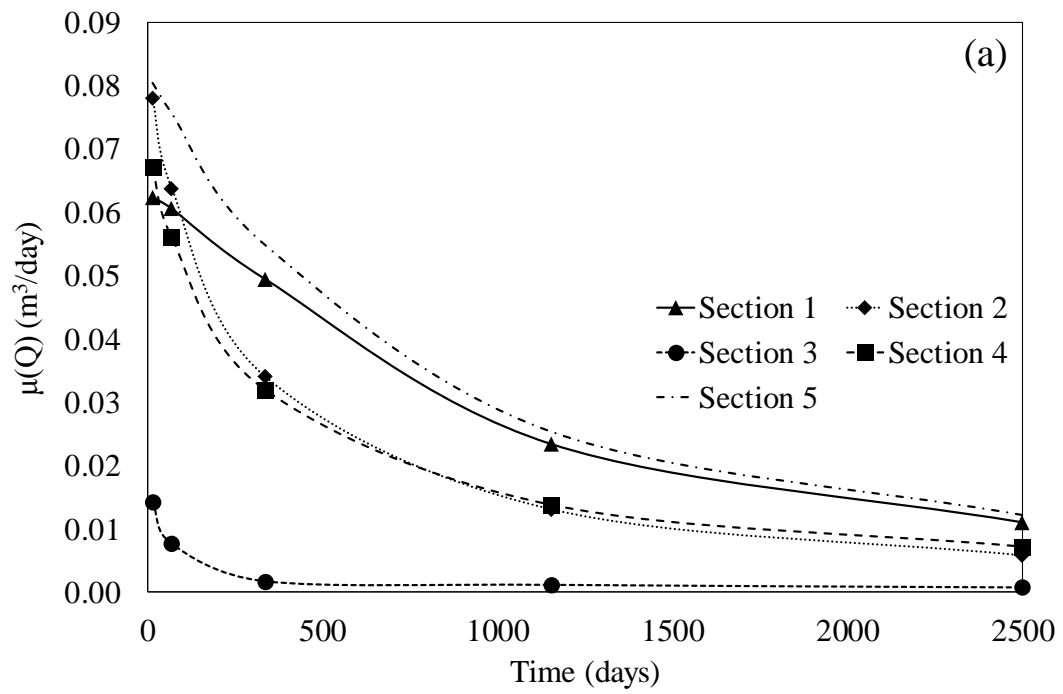


Figure 6.1 The change of (a)  $\mu(Q)$  and (b)  $\sigma(Q)$  with respect to time for the rapid drawdown case.

Table 6.3 Goodness of fit results for PDFs of the seepage for the rapid drawdown case.

Time	Sect.	PDF type	Kolmogorov-Smirnov ( $D_{max}$ )			Chi-square ( $X^2$ )			Overall decision
			Critical value for $\alpha'=0.1$ is 0.039 Critical value for $\alpha'=0.05$ is 0.043			Critical value for $\alpha'=0.1$ is 14.684 Critical value for $\alpha'=0.05$ is 16.919			
			Computed value	Decision		Computed value	Decision		
$\alpha'=0.1$	$\alpha'=0.05$	$\alpha'=0.1$		$\alpha'=0.05$					
t=68 days	1	GEV	0.020	Accept	Accept	N/A	N/A	N/A	Accept
	2	N	0.018	Accept	Accept	8.602	Accept	Accept	Accept
	3	GEV	0.018	Accept	Accept	11.314	Accept	Accept	Accept
	4	GEV	0.015	Accept	Accept	7.027	Accept	Accept	Accept
	5	GEV	0.013	Accept	Accept	N/A	N/A	N/A	Accept
t=1152 days	1	GEV	0.020	Accept	Accept	2.466	Accept	Accept	Accept
	2	N	0.014	Accept	Accept	1.576	Accept	Accept	Accept
	3	-	-	-	-	-	-	-	-
	4	GEV	0.019	Accept	Accept	4.150	Accept	Accept	Accept
	5	GEV	0.020	Accept	Accept	7.467	Accept	Accept	Accept
t=2500 days	1	GEV	0.018	Accept	Accept	N/A	N/A	N/A	Accept
	2	GEV	0.018	Accept	Accept	N/A	N/A	N/A	Accept
	3	-	-	-	-	-	-	-	-
	4	GEV	0.021	Accept	Accept	N/A	N/A	N/A	Accept
	5	GEV	0.021	Accept	Accept	3.585	Accept	Accept	Accept

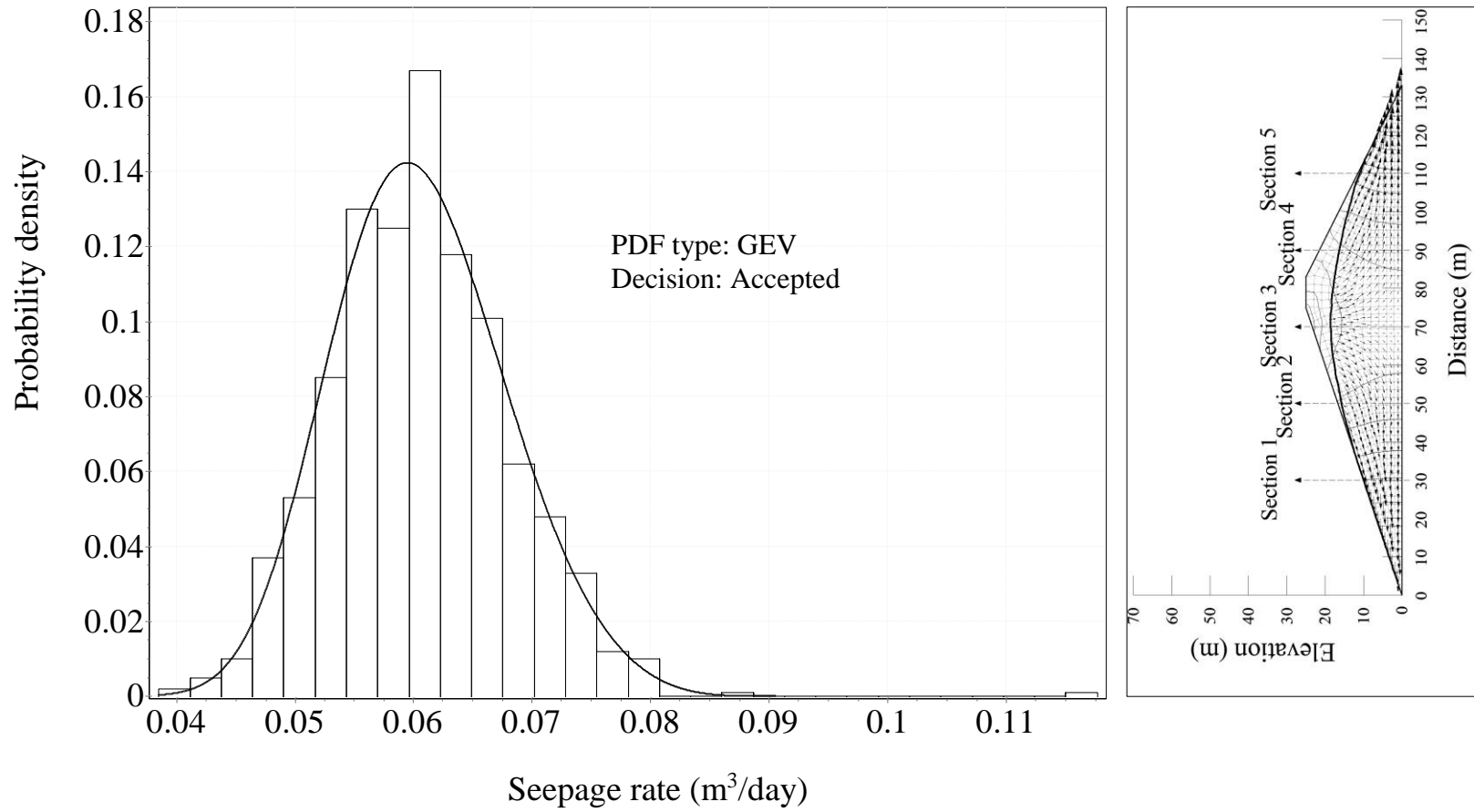


Figure 6.2 Frequency histogram of Q for rapid drawdown case when t=68 days at Section 1.

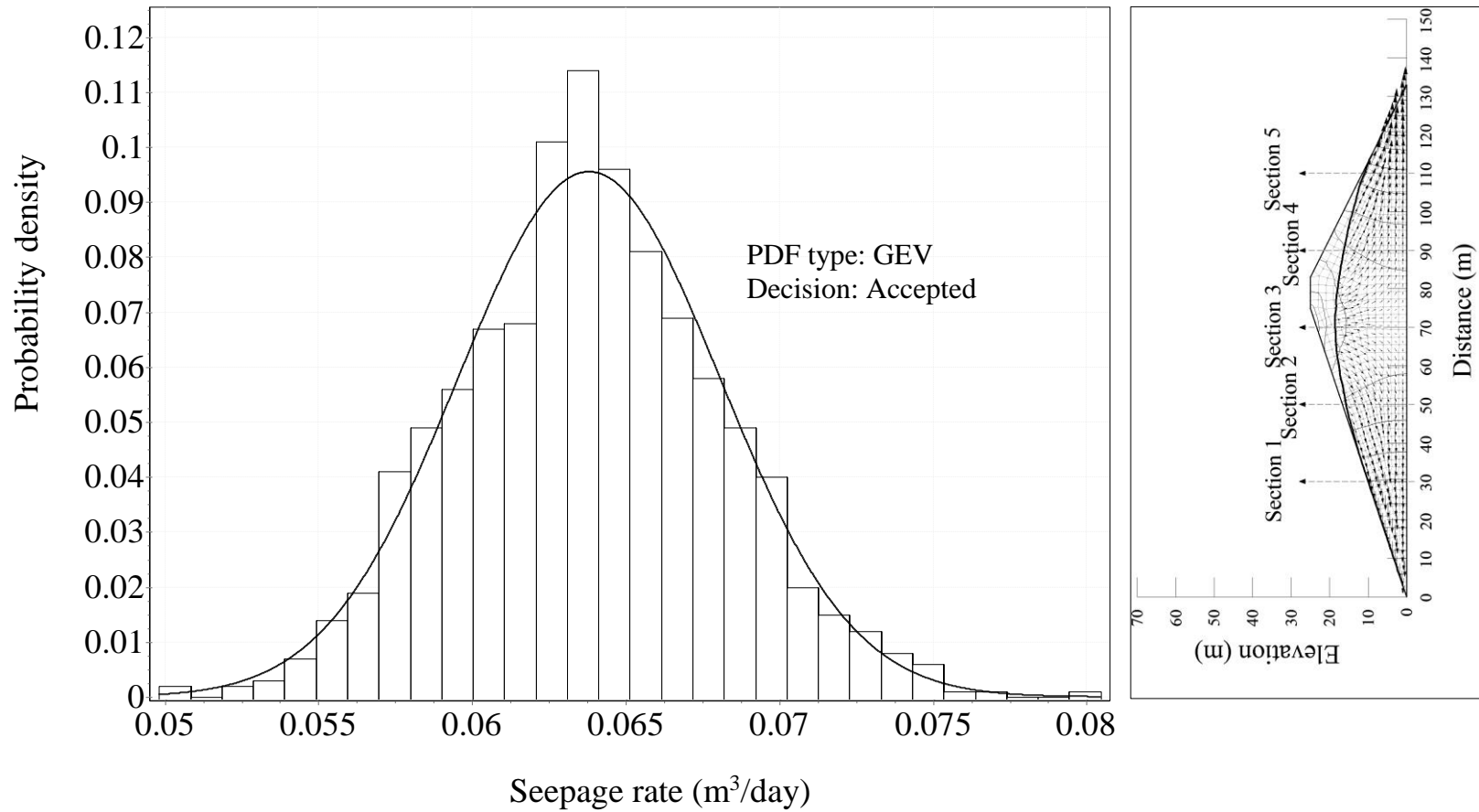


Figure 6.3 Frequency histogram of  $Q$  for rapid drawdown case when  $t=68$  days at Section 2.

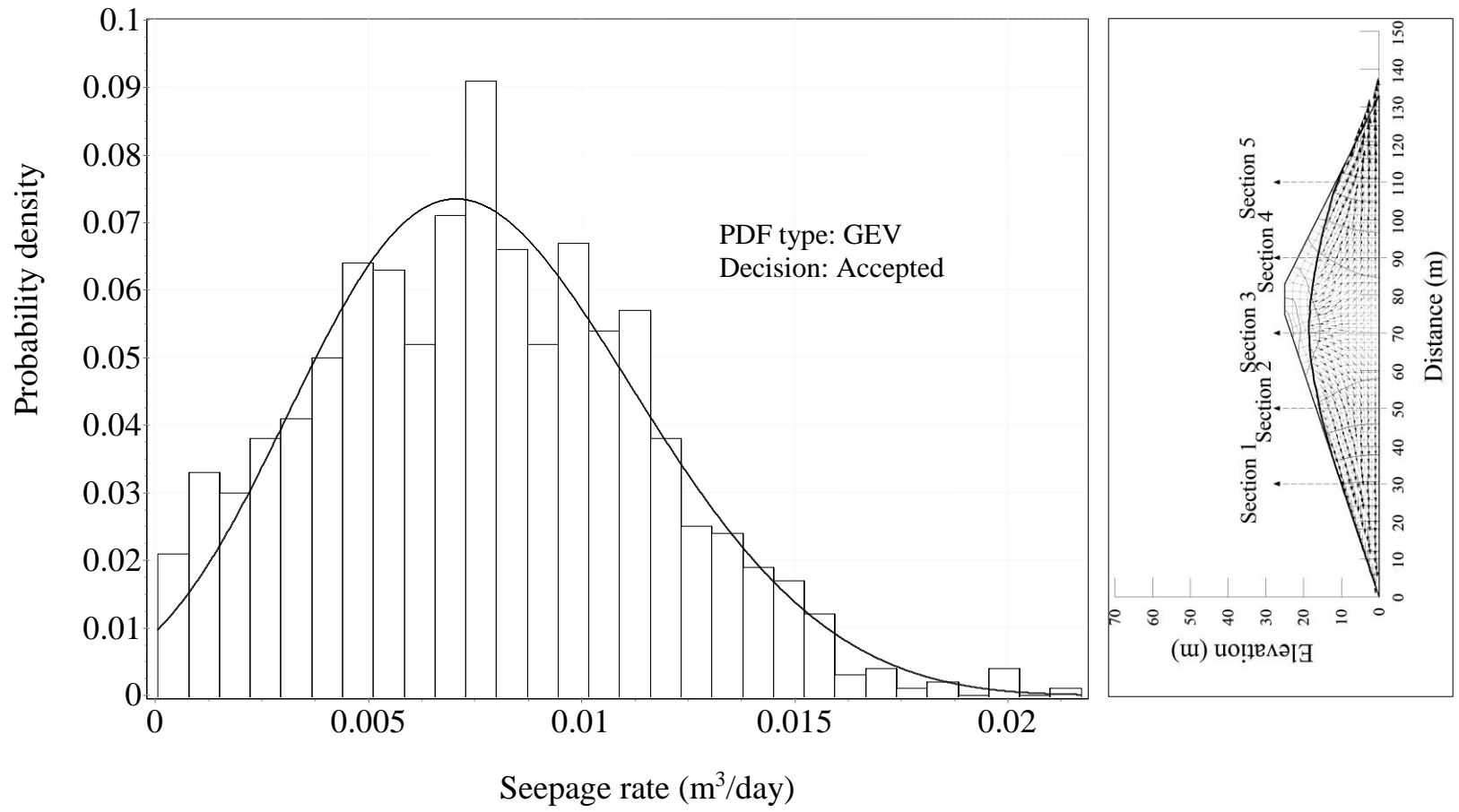


Figure 6.4 Frequency histogram of  $Q$  for rapid drawdown case when  $t=68$  days at Section 3.

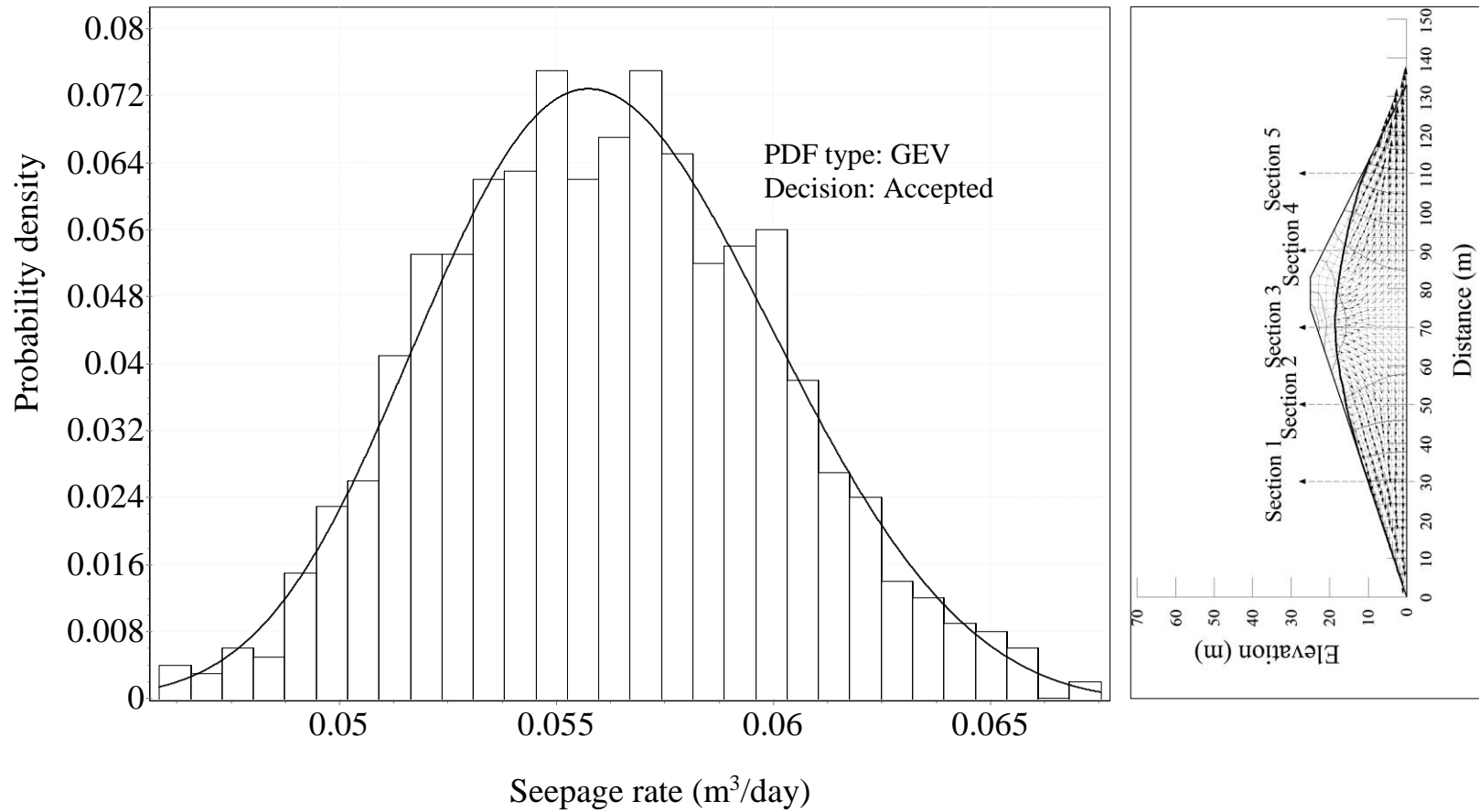


Figure 6.5 Frequency histogram of  $Q$  for rapid drawdown case when  $t=68$  days at Section 4.

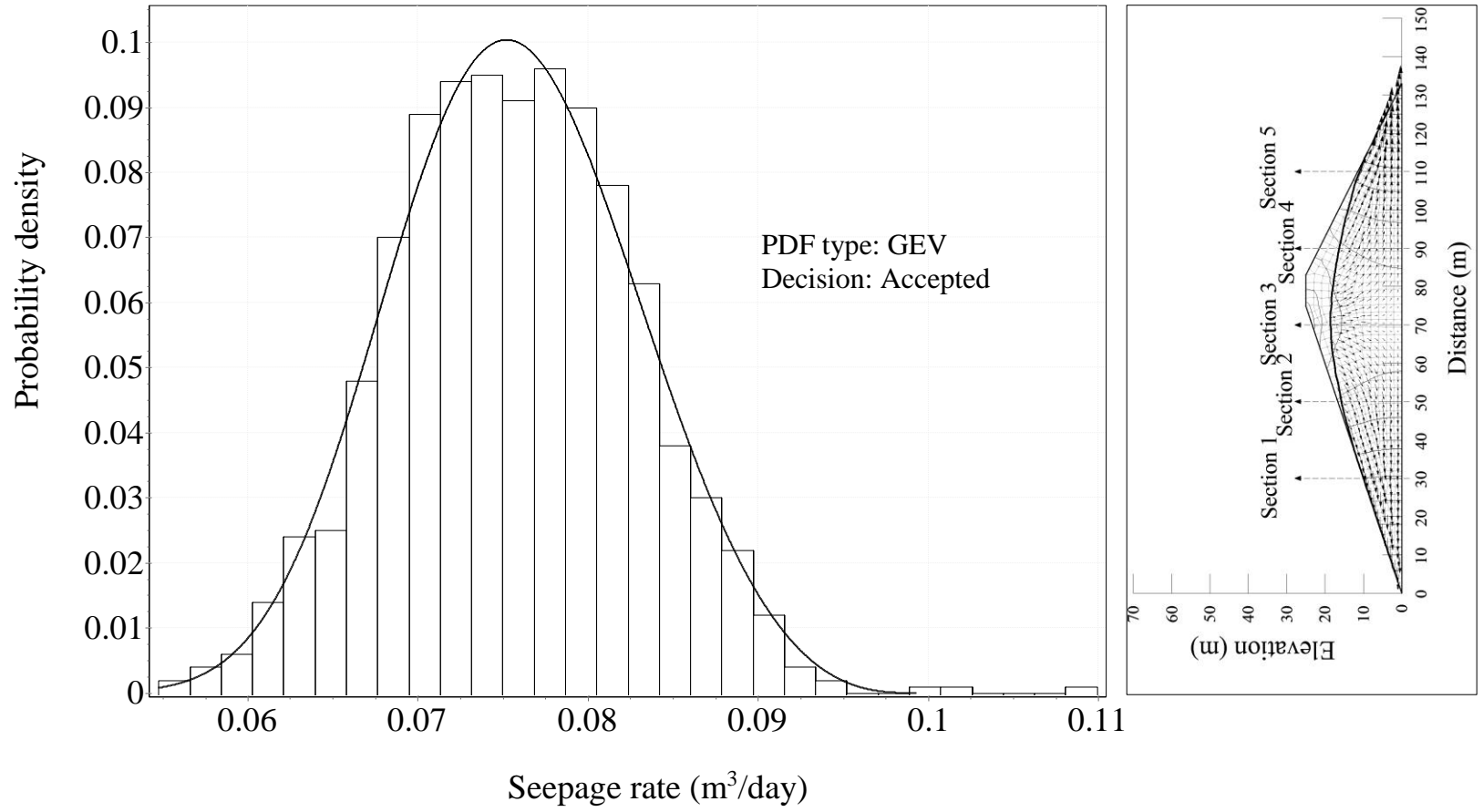


Figure 6.6 Frequency histogram of Q for rapid drawdown case when t=68 days at Section 5.

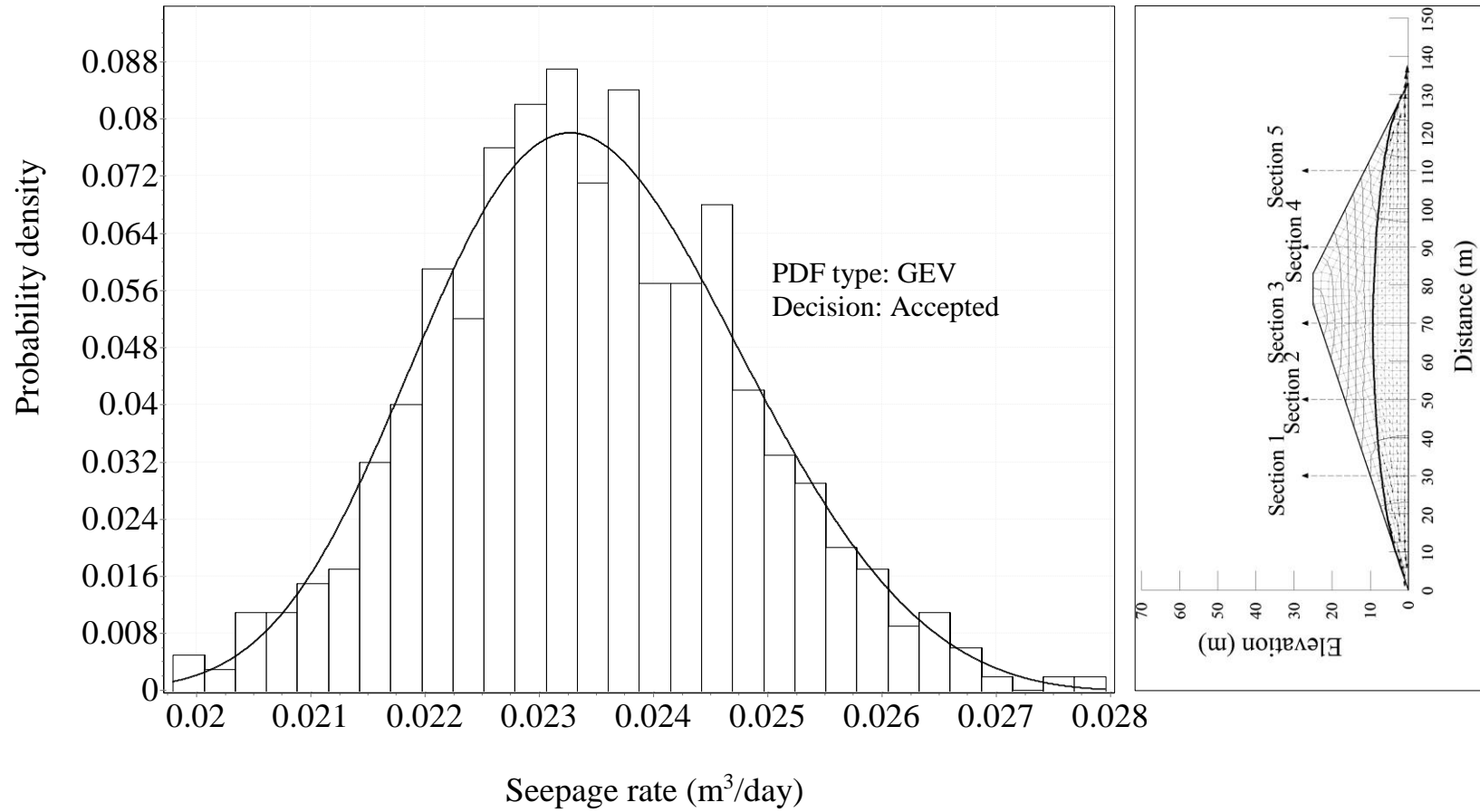


Figure 6.7 Frequency histogram of  $Q$  for rapid drawdown case when  $t=1152$  days at Section 1.

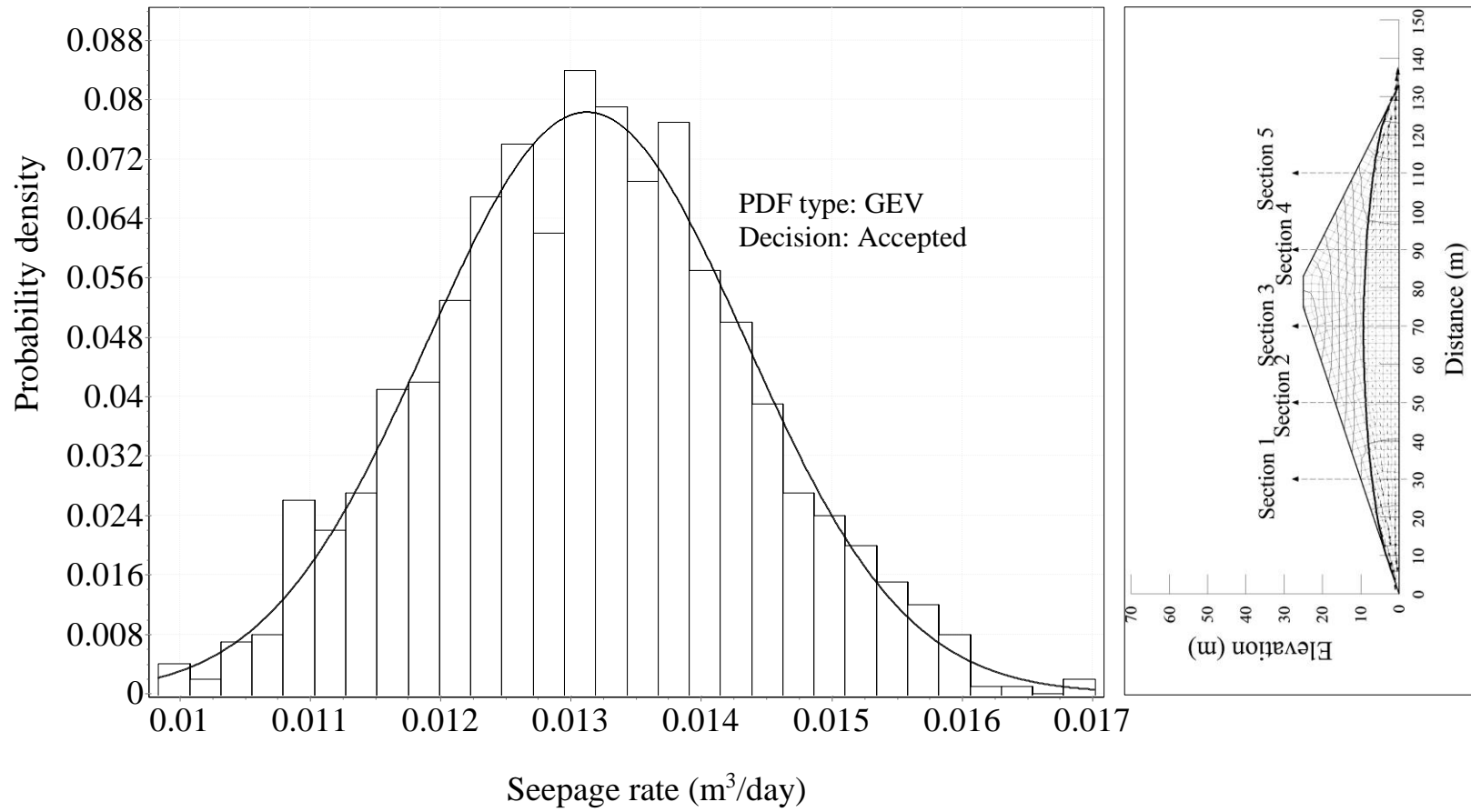


Figure 6.8 Frequency histogram of Q for rapid drawdown case when t=1152 days at Section 2.

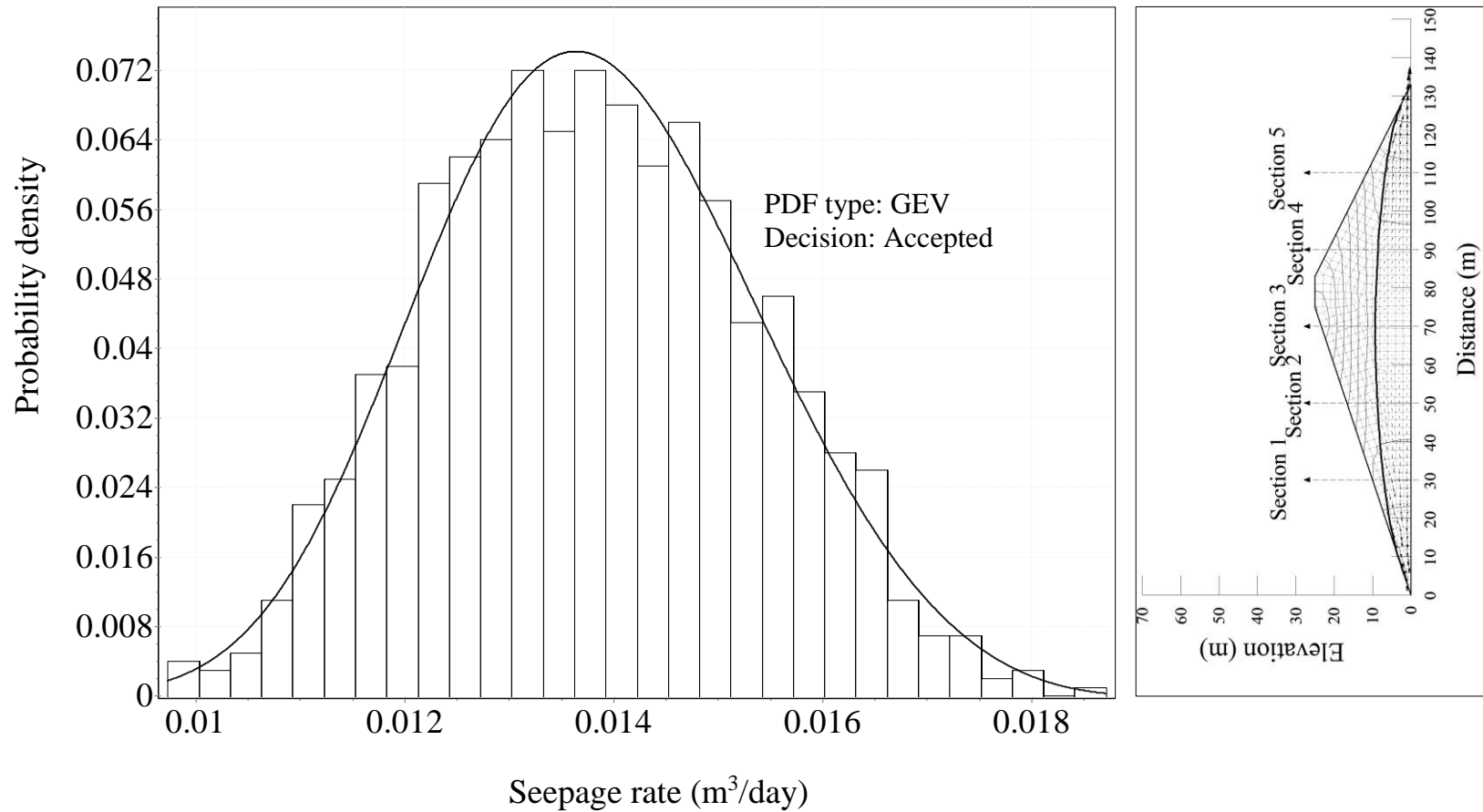


Figure 6.9 Frequency histogram of  $Q$  for rapid drawdown case when  $t=1152$  days at Section 4.

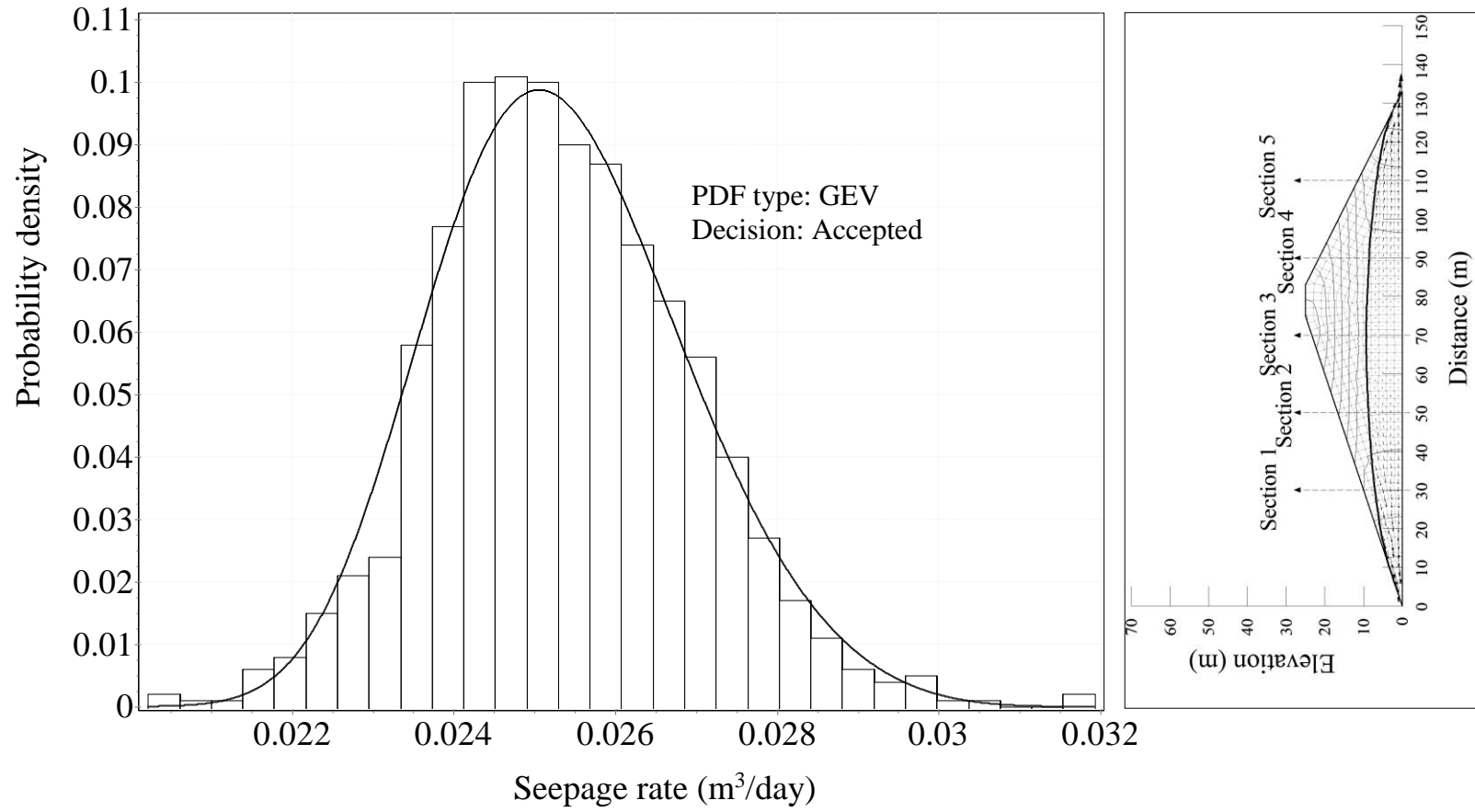


Figure 6.10 Frequency histogram of  $Q$  for rapid drawdown case when  $t=1152$  days at Section 5.

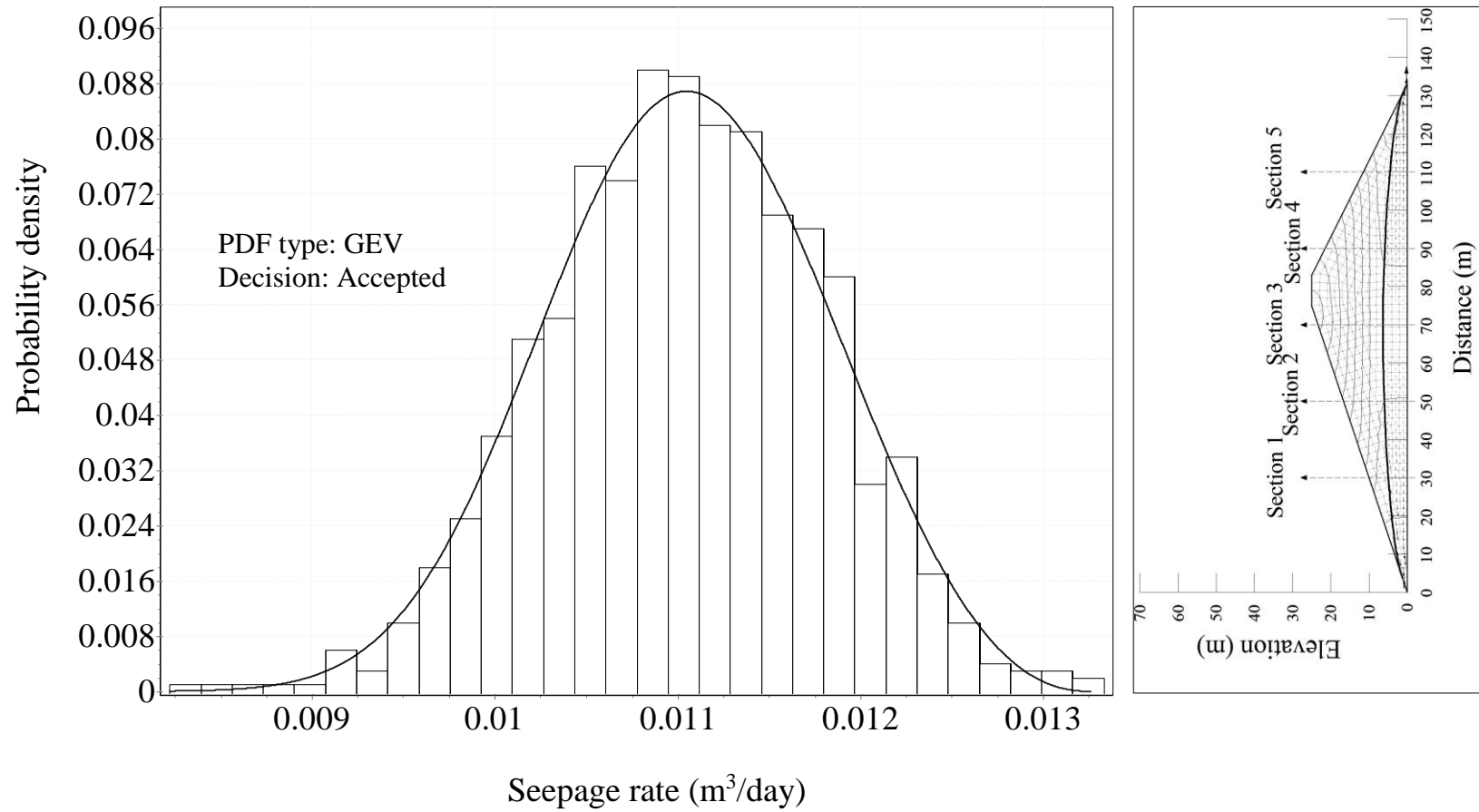


Figure 6.11 Frequency histogram of  $Q$  for rapid drawdown case when  $t=2500$  days at Section 1.

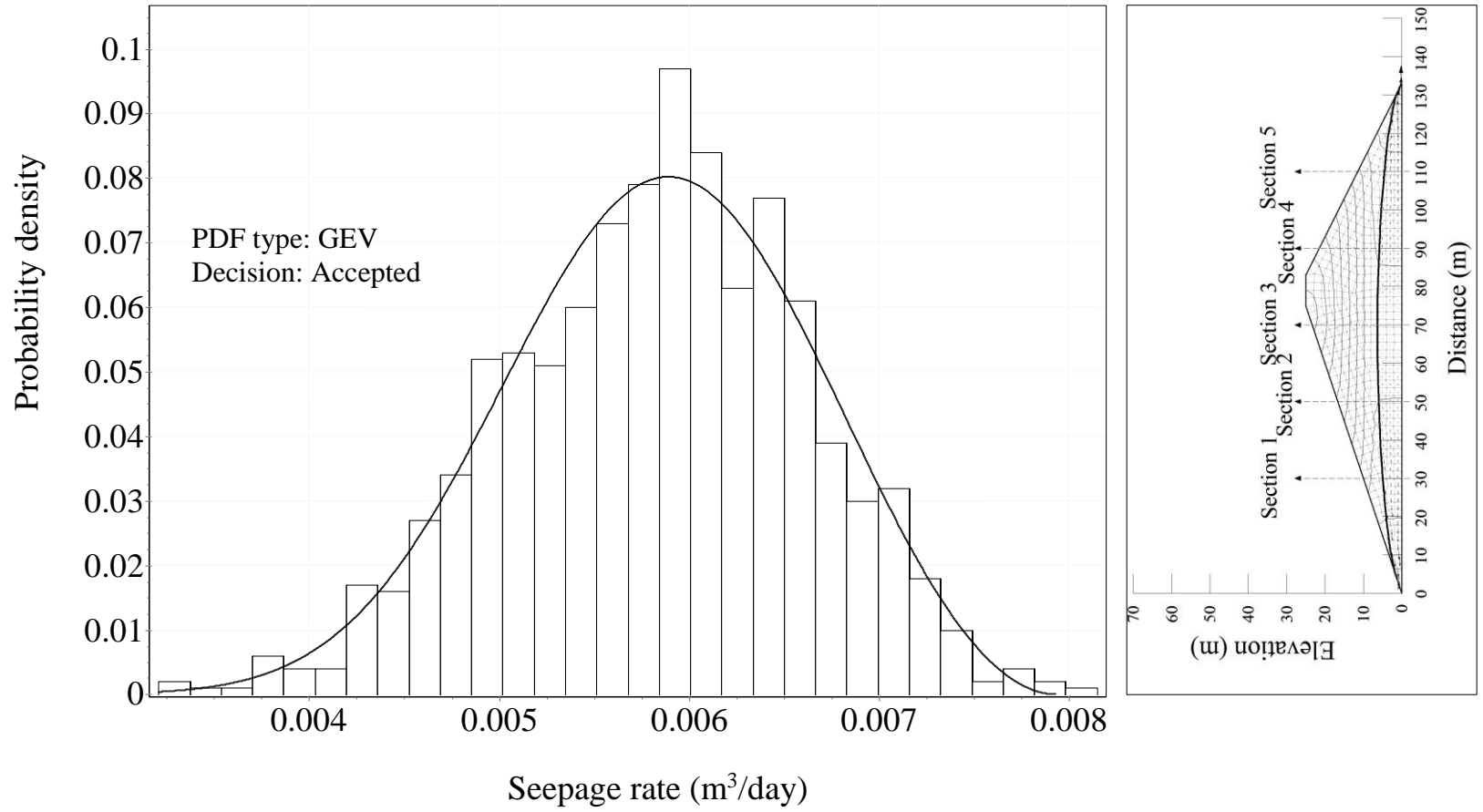


Figure 6.12 Frequency histogram of  $Q$  for rapid drawdown case when  $t=2500$  days at Section 2.

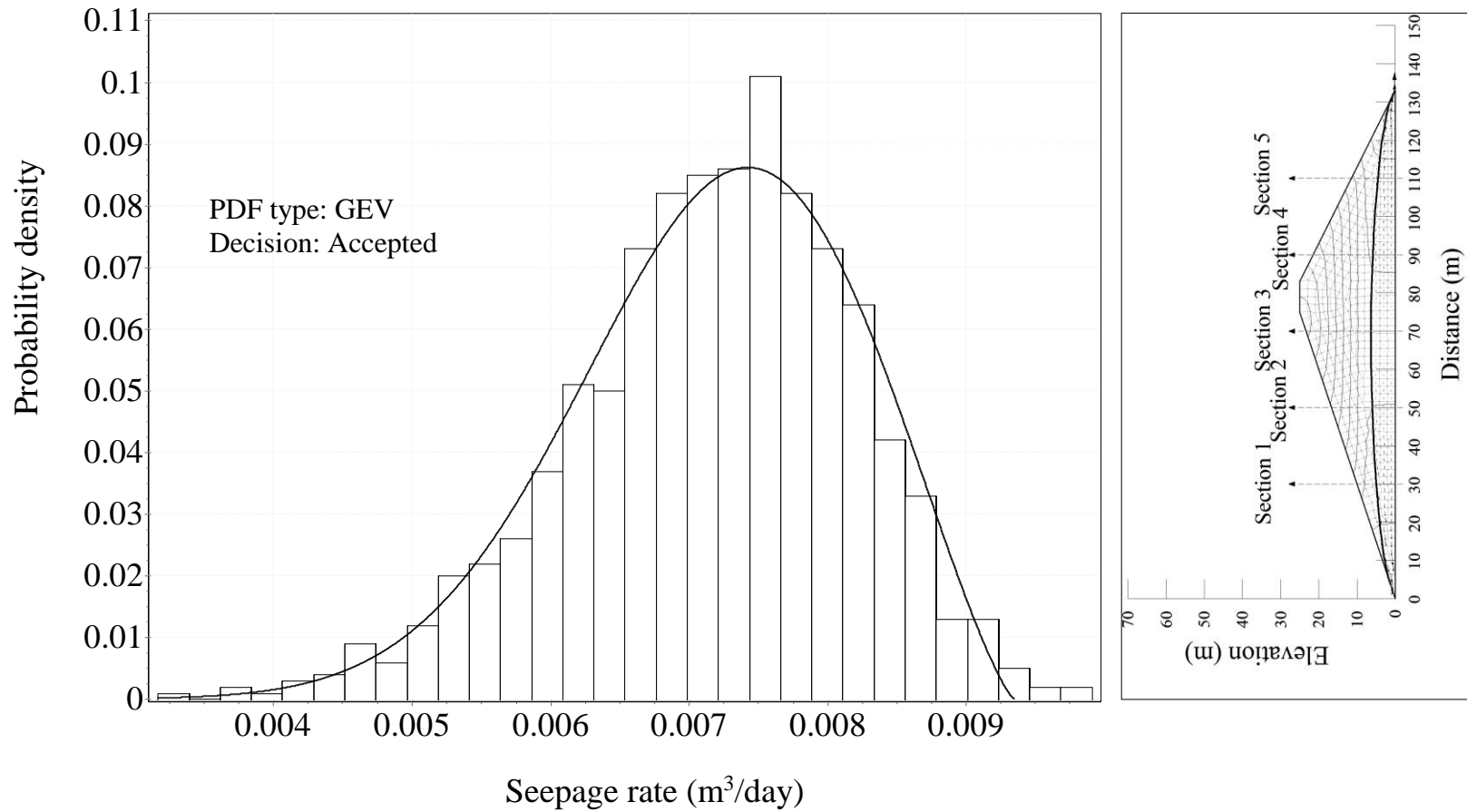


Figure 6.13 Frequency histogram of  $Q$  for rapid drawdown case when  $t=2500$  days at Section 4.

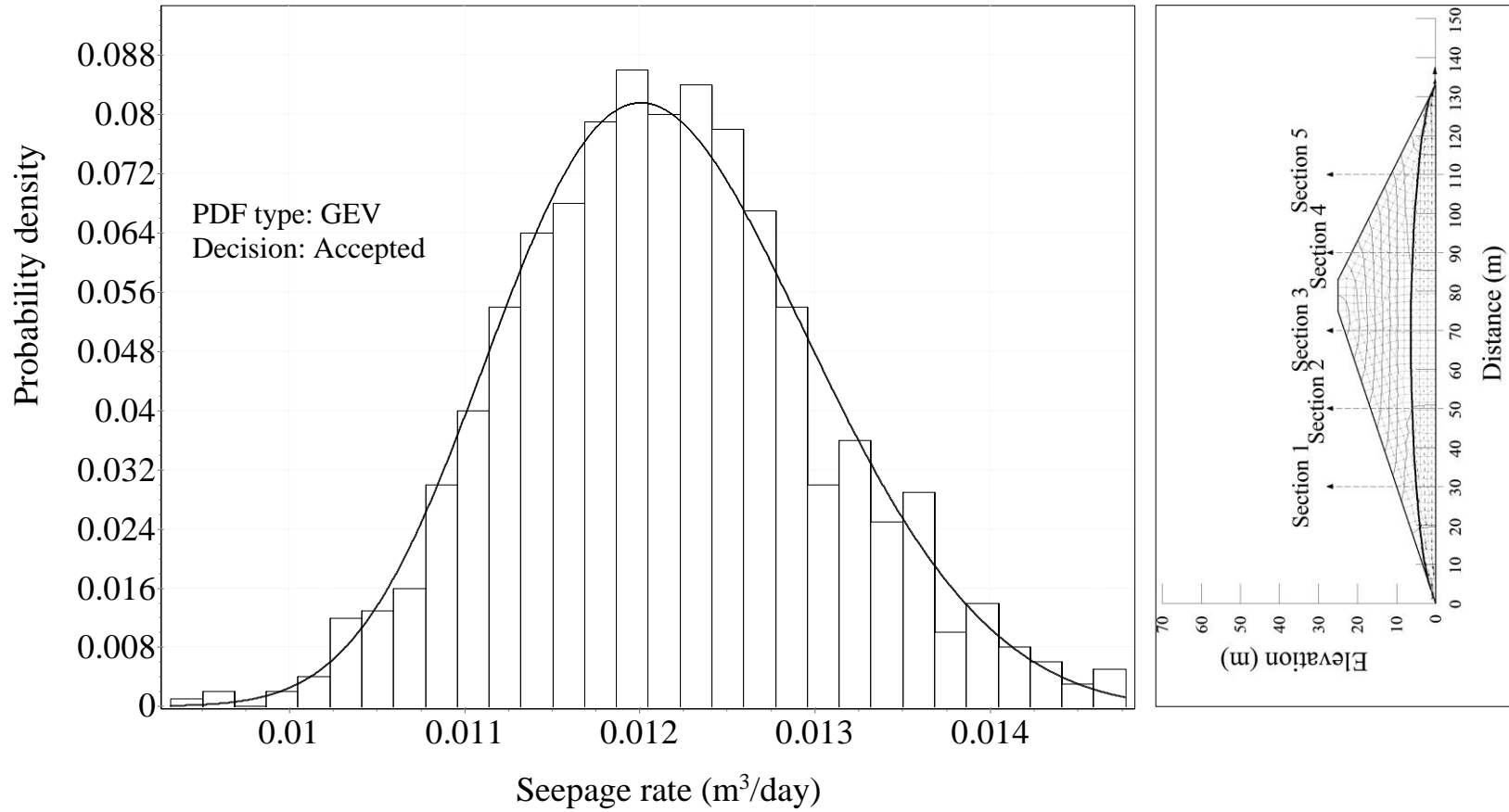


Figure 6.14 Frequency histogram of  $Q$  for rapid drawdown case when  $t=2500$  days at Section 5.

## 6.2 Rapid Fill Case

In the present part, the seepage statistics and its probabilistic properties are investigated for the embankment dam presented in Figure 5.1 with the boundary condition described in Section 5.2 (i.e. the rapid fill case in which the upstream initial head of 1 m is increased to 23 m in two days). All of the input soil parameters are considered to be random having the statistical properties given in Table 6.1. The seepage through the dam is stochastically analyzed conducting 1000 MCS. The obtained data sets of the flow rate at different sections of the dam for different simulation durations are statistically analyzed. Similar to the sensitivity analysis held in Section 5.2, the duration of the simulation is selected as 1000 days.

The descriptive statistics of the flow is summarized in Table 6.4. Besides, the change of the mean and the standard deviation of the seepage rate with respect to time are illustrated in Figure 6.15 (a) and (b), respectively. The results show that during the simulation, for Section 1 to 4, at first the mean flow increases to a certain level; then, it starts to decrease. The standard deviation of flows follow a similar trend; the increase in values are followed by a decrease. Then they stabilize with time. Besides, the degree of variability (i.e. COV) of the seepage rate decreases with time. There exists almost no flow at specific sections for specific durations of the simulation. It is clear that the uncertainty quantification for the flow are inapplicable for these sections. Therefore, no statistical moment computations are performed for them.

It is seen that almost all of the probability distributions are positively skewed. Generally, the skewness decreases with time for a given section. In other words, the symmetry of probability distributions of an individual section changes from left-skewed to symmetric shape with time. Similar to skewness, commonly the kurtosis of probability distributions decrease with the time. The shape of the probability distributions change from peaked to flat shapes with respect to time.

It is seen that the maximum COV value for the seepage rate is computed as 0.80 (see Table 5.4), whereas the maximum COV value of input parameters is 2.33.

Similar to the rapid drawdown case, the variation degree of the input parameter is decreased by the system in the rapid fill case.

Table 6.4 The descriptive statistics of the seepage rate for the rapid fill case.

Time	Sect.	Max (Q)	Min (Q)	$\mu$ (Q)	$\sigma$ (Q)	COV (Q)	Skewness	Kurtosis
		(m <sup>3</sup> /day)						
t=28 days	1	0.13	0.02	0.06	0.020	0.32	0.69	0.38
	2	0.52	0.00	0.08	0.066	0.80	2.51	10.47
	3	0.00	0.00	0.00	0.000	-	-	-
	4	0.00	0.00	0.00	0.000	-	-	-
	5	0.00	0.00	0.00	0.000	-	-	-
t=461 days	1	0.00	0.00	0.00	0.001	-	-	-
	2	0.04	0.01	0.02	0.004	0.18	0.39	0.01
	3	0.18	0.09	0.13	0.008	0.07	0.37	1.89
	4	0.24	0.05	0.09	0.013	0.14	3.66	39.65
	5	0.05	0.00	0.02	0.008	0.50	0.54	0.08
t=1000 days	1	0.00	0.00	0.00	0.000	-	-	-
	2	0.02	0.01	0.01	0.003	0.18	0.37	0.14
	3	0.11	0.07	0.09	0.005	0.06	0.34	0.87
	4	0.16	0.06	0.08	0.007	0.09	2.82	26.63
	5	0.09	0.04	0.06	0.007	0.11	-0.07	-0.07

The frequency histograms of the seepage rate is plotted and prospective probability density functions are fitted to the flow data. Tests for goodness of fit are conducted and the results are listed in Table 6.5. Considering the tests results, it can be said that the seepage rate for the rapid fill case can be represented by a generalized extreme value (GEV) distribution for most of the times of simulation. The seepage rates whose assigned PDF is rejected in Table 6.5 also cannot be described by other type of probability distributions considered in the study and any other type of distribution functions. For the rapid fill case, the frequency histograms of the seepage, fitted probability density functions, and the overall decision of the goodness of fit test are shown in Figure 6.16 to Figure 6.25.

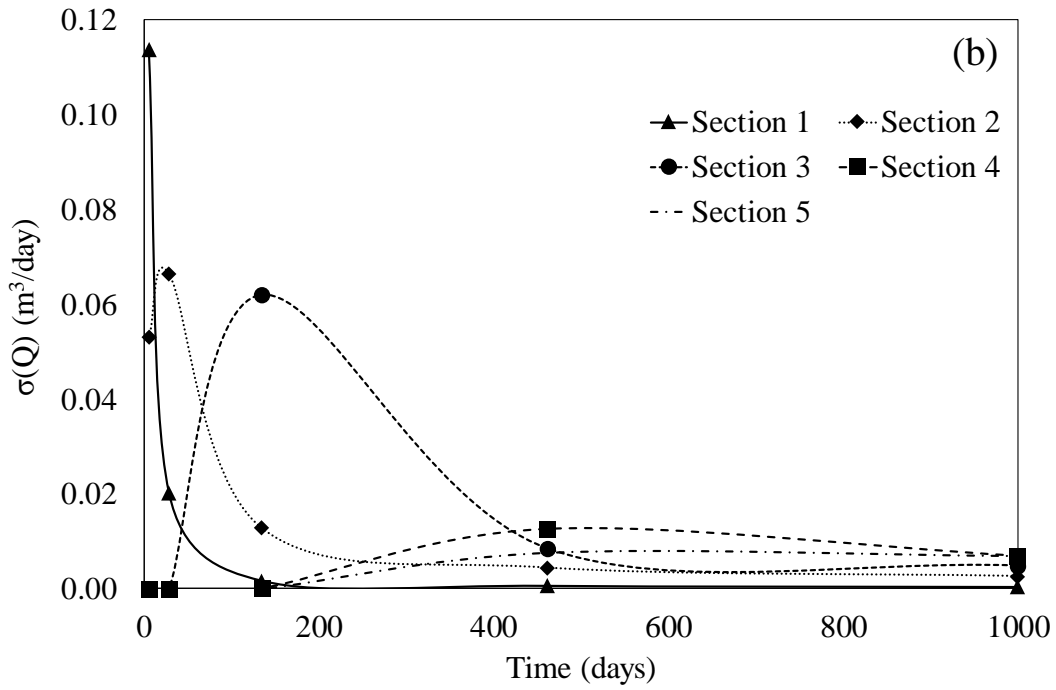
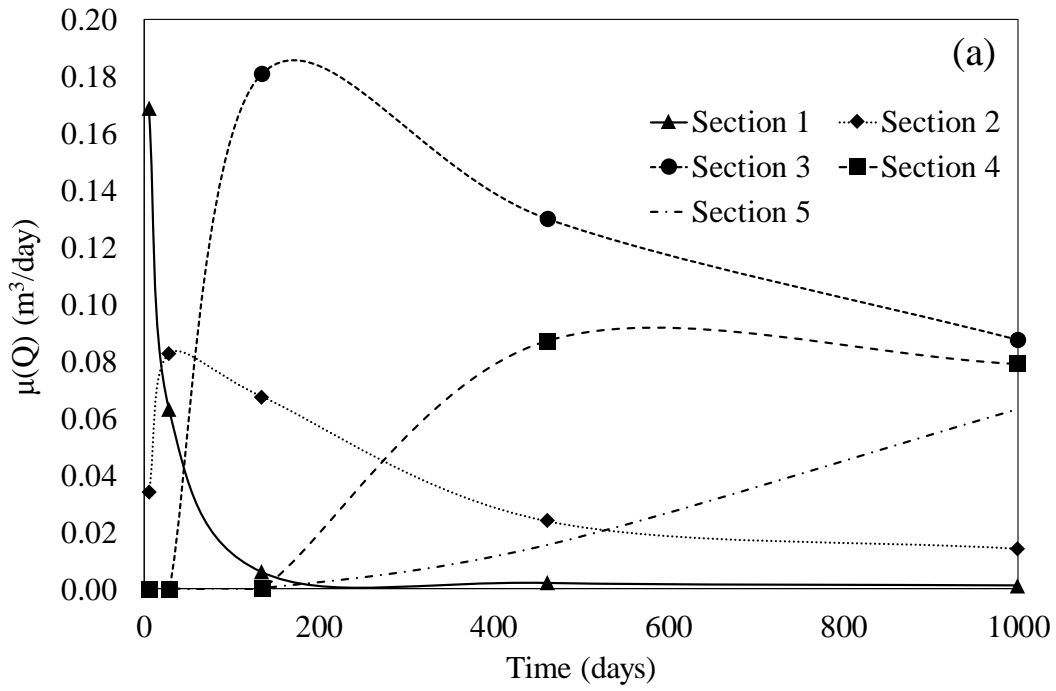


Figure 6.15 The change of (a)  $\mu(Q)$  and (b)  $\sigma(Q)$  with respect to time for the rapid fill case.

Table 6.5 Goodness of fit results for PDFs of the seepage for the rapid fill case.

Time	Sect.	PDF type	Kolmogorov-Smirnov ( $D_{max}$ )			Chi-square ( $X^2$ )			Overall decision
			Critical value for $\alpha'=0.1$ is 0.039 Critical value for $\alpha'=0.05$ is 0.043			Critical value for $\alpha'=0.1$ is 14.684 Critical value for $\alpha'=0.05$ is 16.919			
			Computed value	Decision		Computed value	Decision		
$\alpha'=0.1$	$\alpha'=0.05$	$\alpha'=0.1$		$\alpha'=0.05$					
t=28 days	1	GEV	0.022	Accept	Accept	18.303	Reject	Reject	Reject
	2	GEV	0.024	Accept	Accept	16.955	Reject	Reject	Reject
	3	-	-	-	-	-	-	-	-
	4	-	-	-	-	-	-	-	-
	5	-	-	-	-	-	-	-	-
t=461 days	1	-	-	-	-	-	-	-	-
	2	GEV	0.014	Accept	Accept	5.058	Accept	Accept	Accept
	3	GEV	0.021	Accept	Accept	N/A	N/A	N/A	Accept
	4	GEV	0.037	Accept	Accept	N/A	N/A	N/A	Accept
	5	GEV	0.024	Accept	Accept	10.469	Accept	Accept	Accept
t=1000 days	1	-	-	-	-	-	-	-	-
	2	GEV	0.015	Accept	Accept	3.904	Accept	Accept	Accept
	3	GEV	0.015	Accept	Accept	N/A	N/A	N/A	Accept
	4	GEV	0.031	Accept	Accept	N/A	N/A	N/A	Accept
	5	GEV	0.020	Accept	Accept	N/A	N/A	N/A	Accept

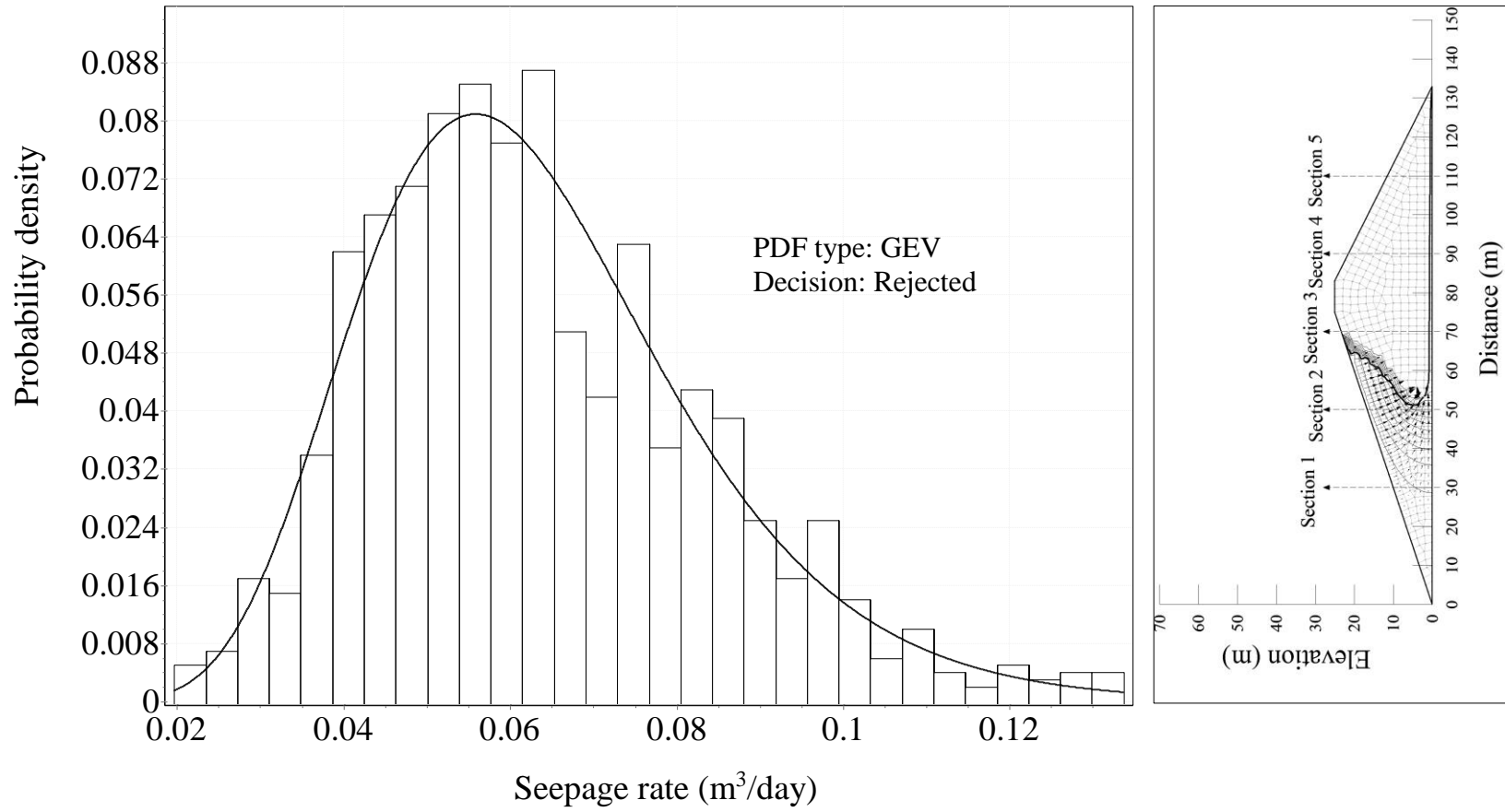


Figure 6.16 Frequency histogram of  $Q$  for rapid fill case when  $t=28$  days at Section 1.

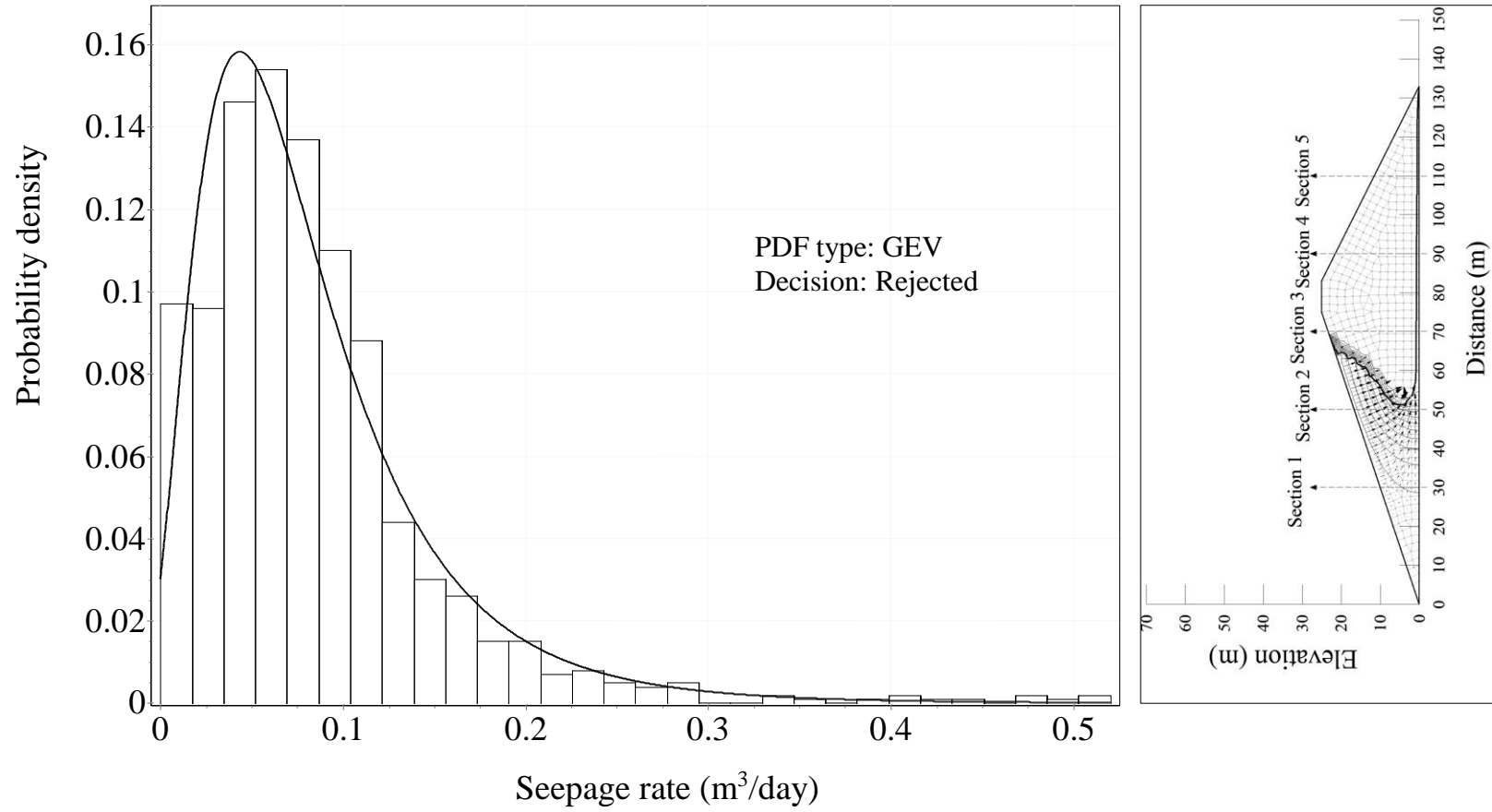


Figure 6.17 Frequency histogram of  $Q$  for rapid fill case when  $t=28$  days at Section 2.

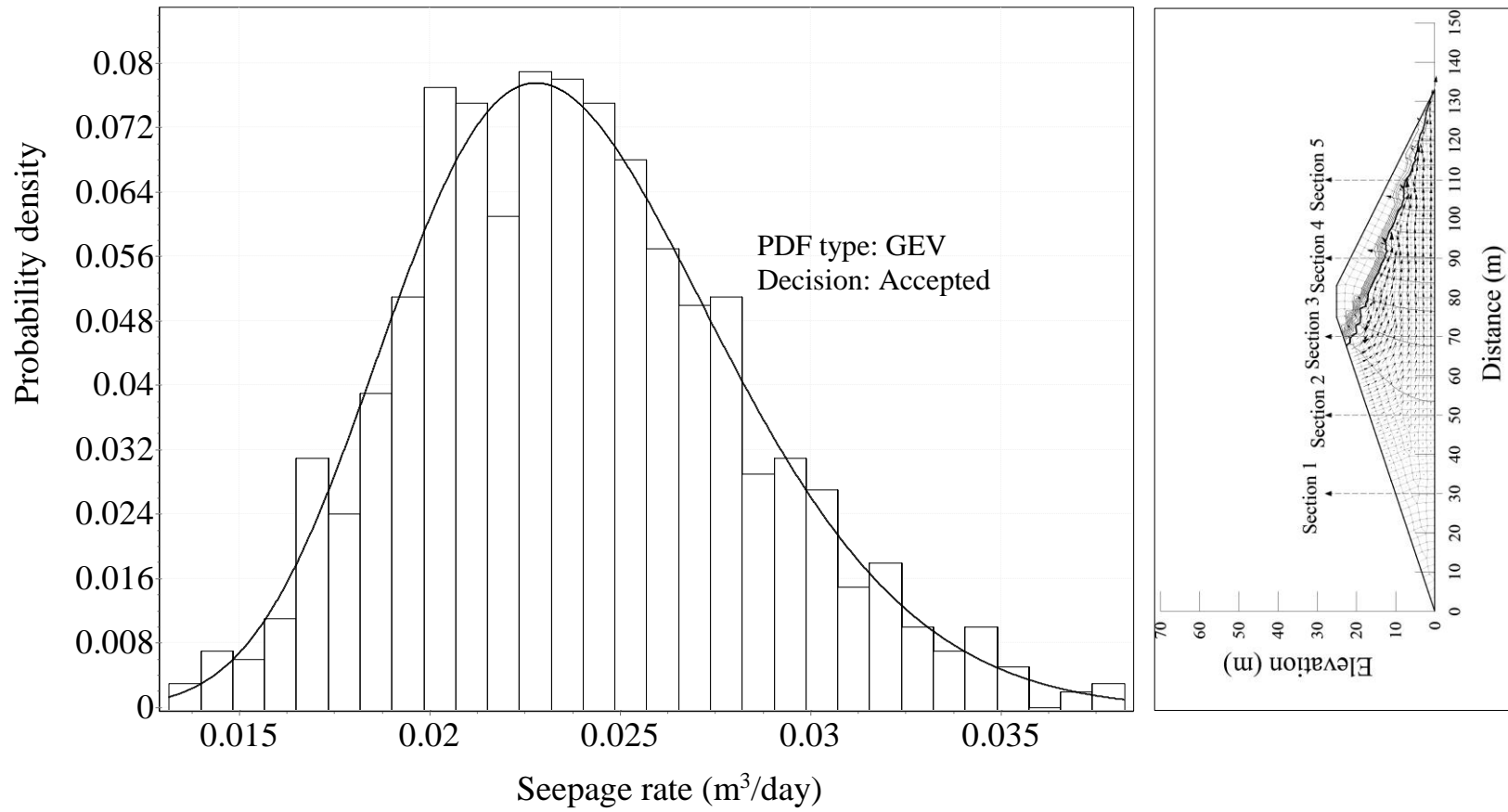


Figure 6.18 Frequency histogram of  $Q$  for rapid fill case when  $t=461$  days at Section 2.

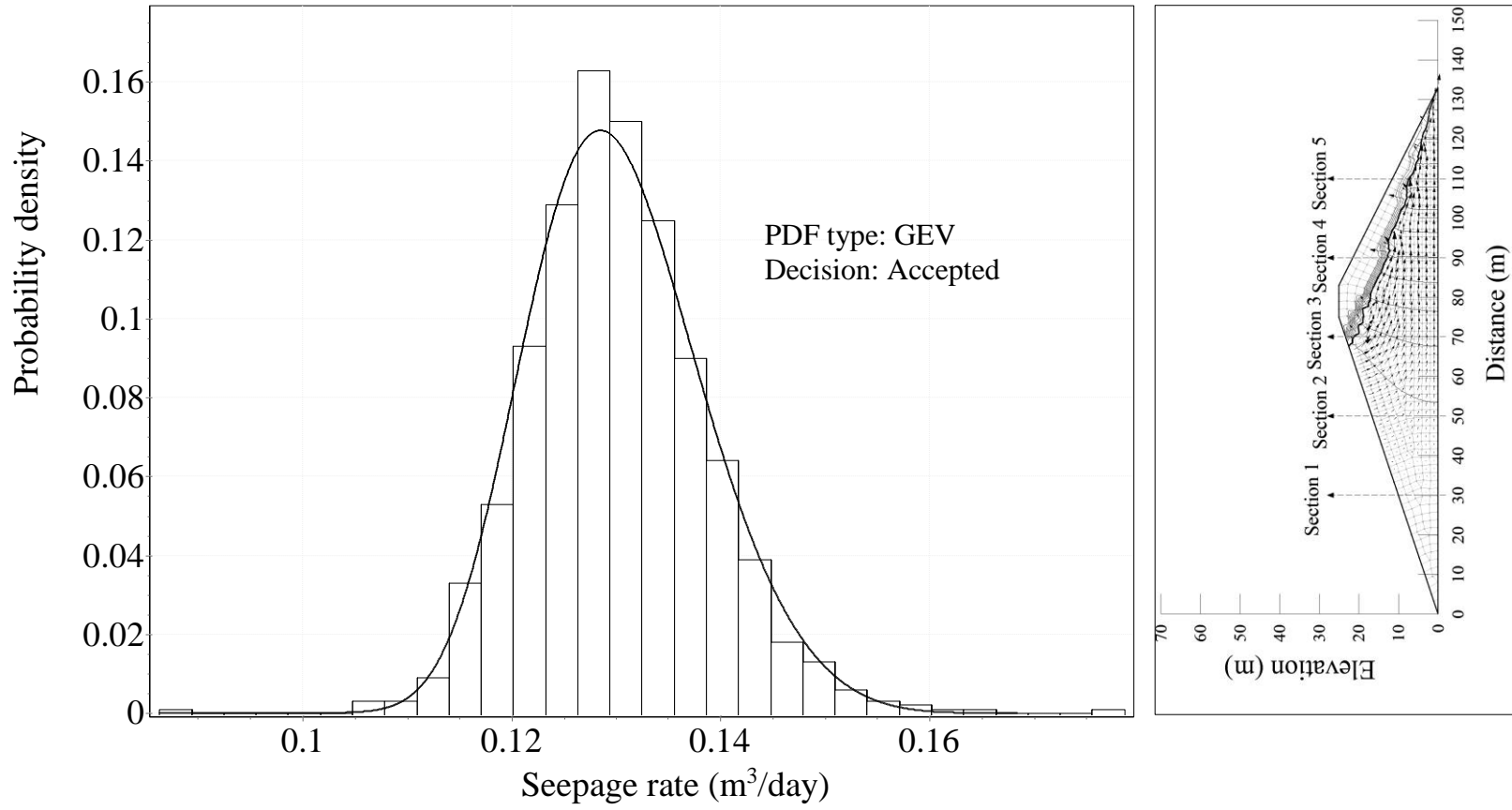


Figure 6.19 Frequency histogram of  $Q$  for rapid fill case when  $t=461$  days at Section 3.

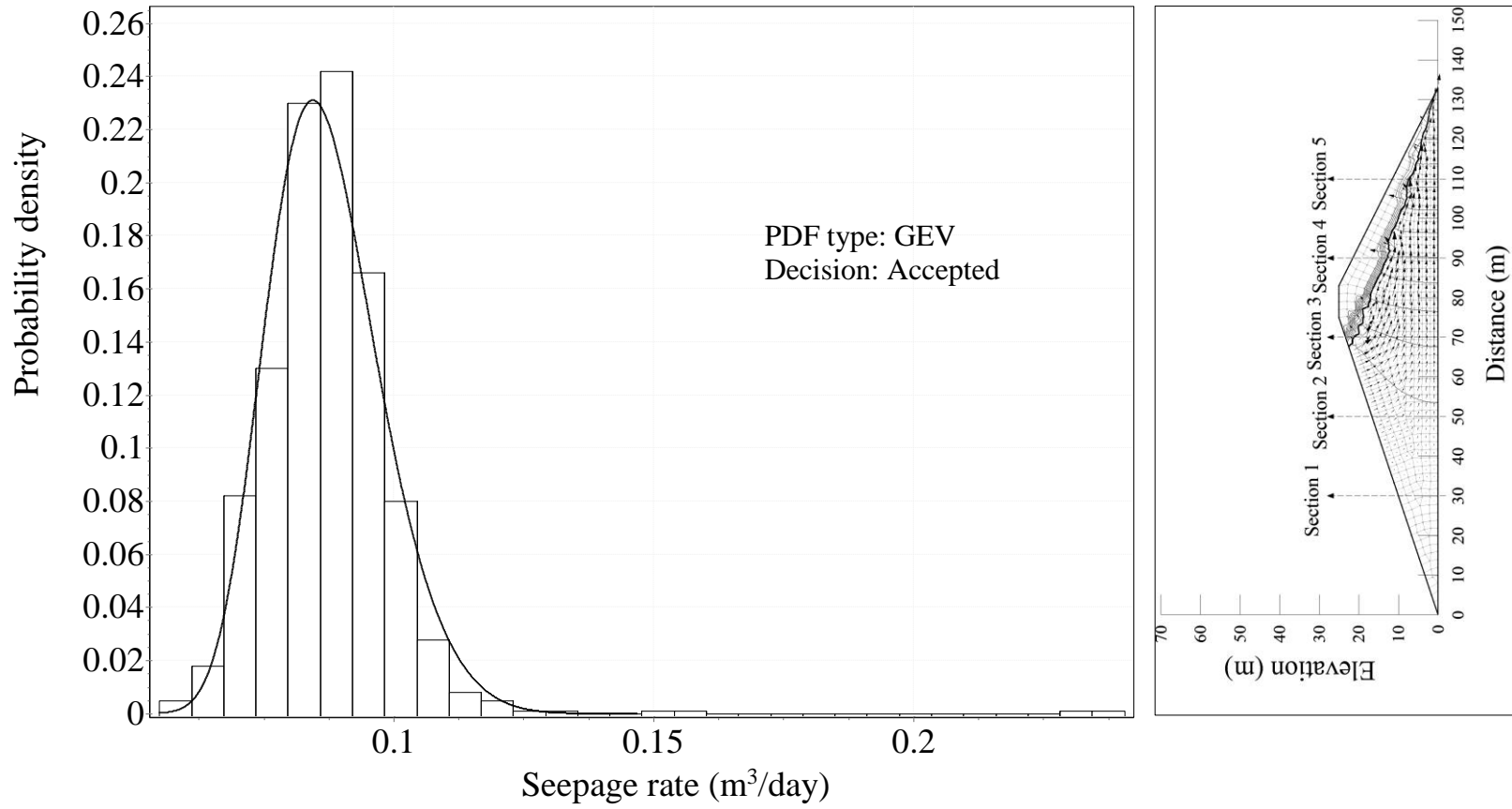


Figure 6.20 Frequency histogram of Q for rapid fill case when t=461 days at Section 4.

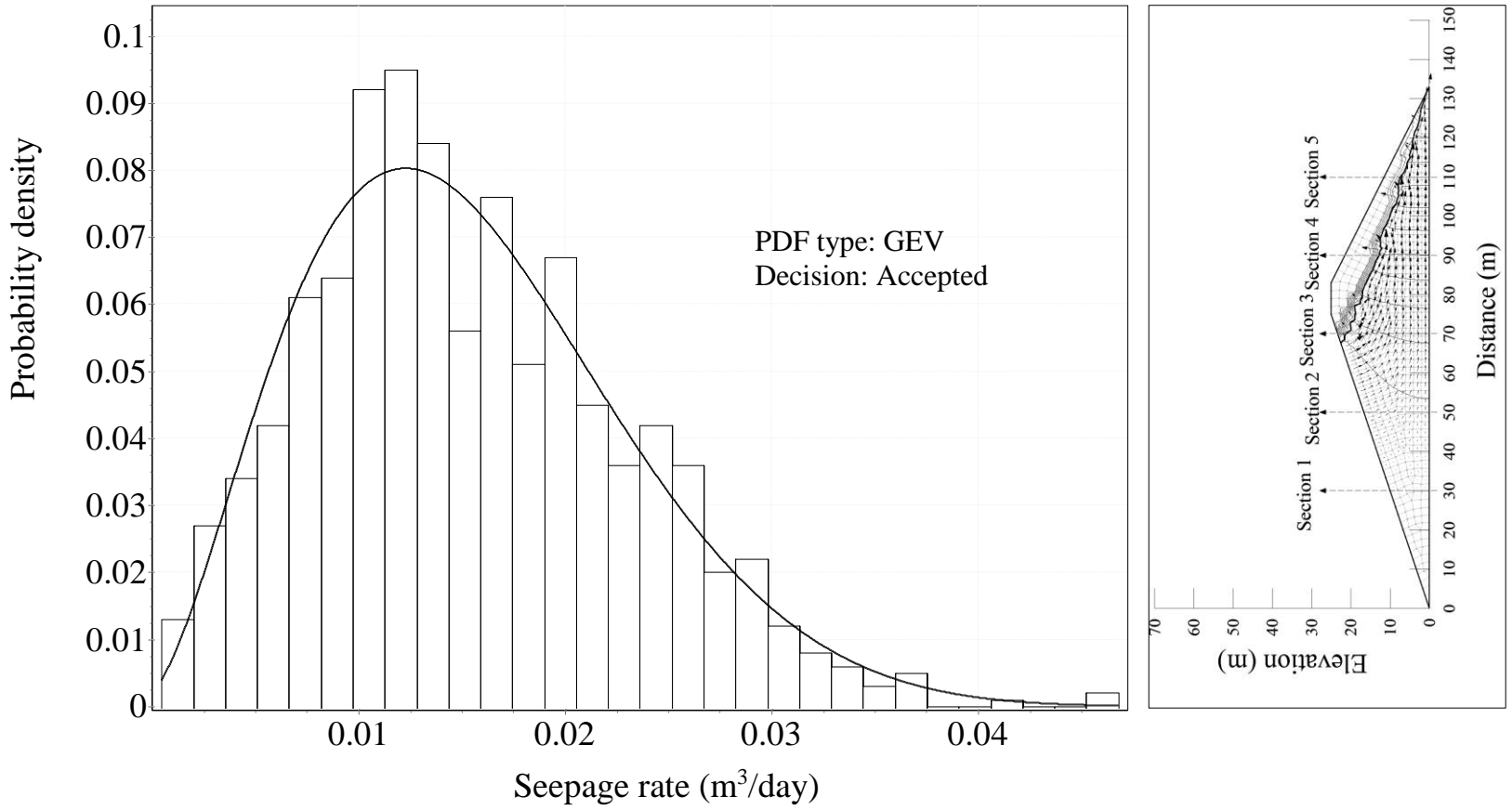


Figure 6.21 Frequency histogram of Q for rapid fill case when t=461 days at Section 5.

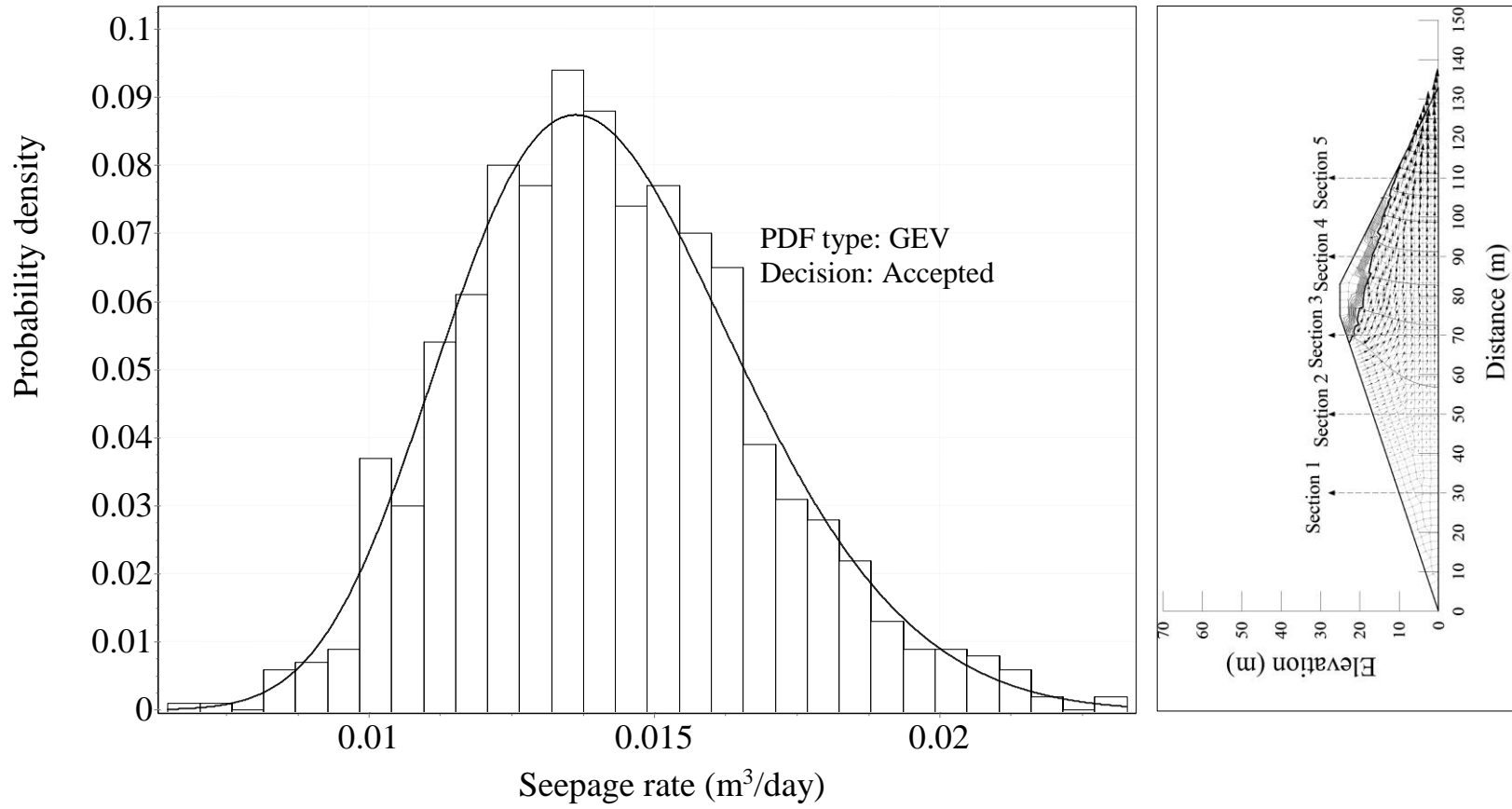
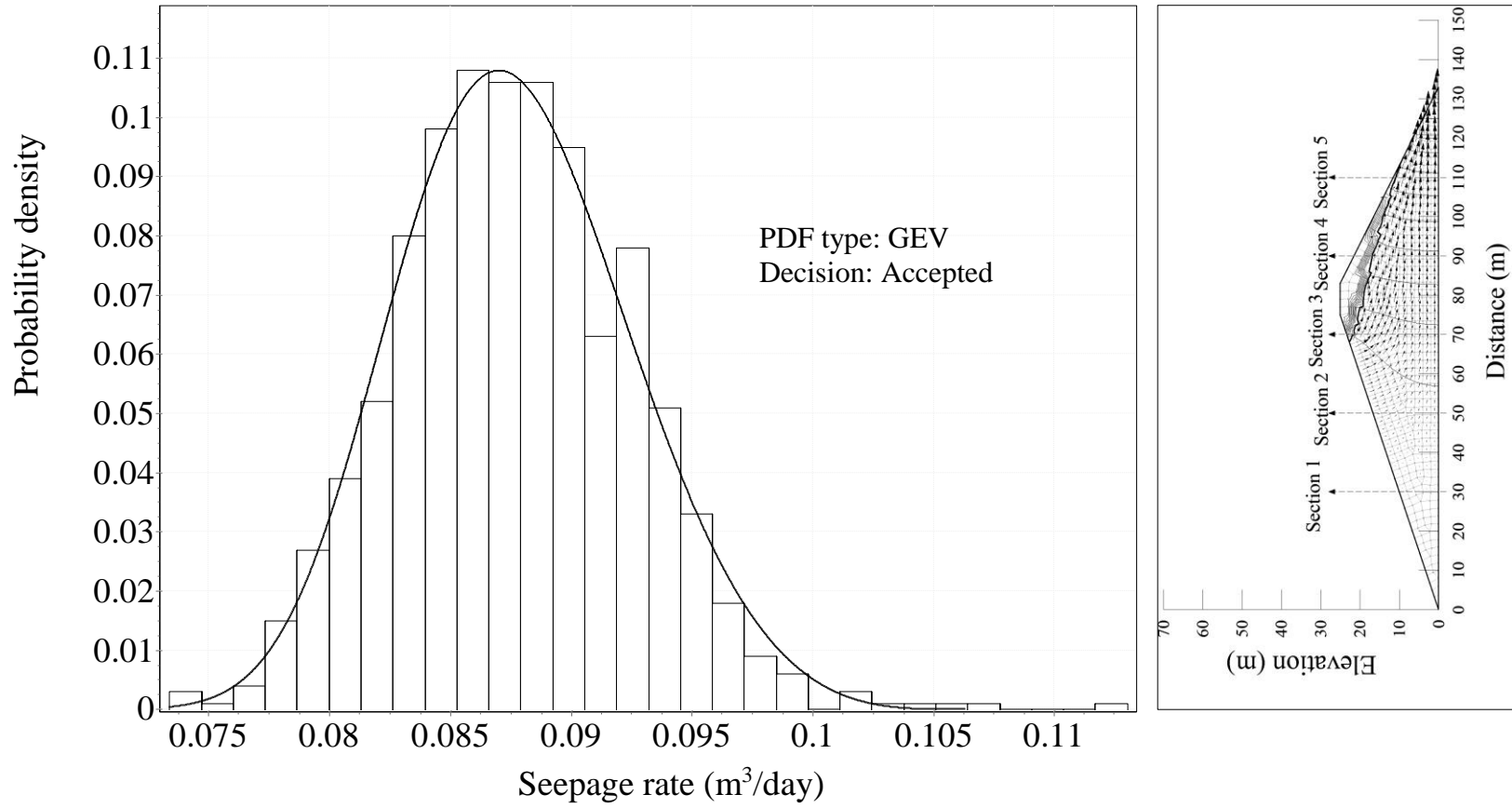


Figure 6.22 Frequency histogram of  $Q$  for rapid fill case when  $t=1000$  days at Section 2.



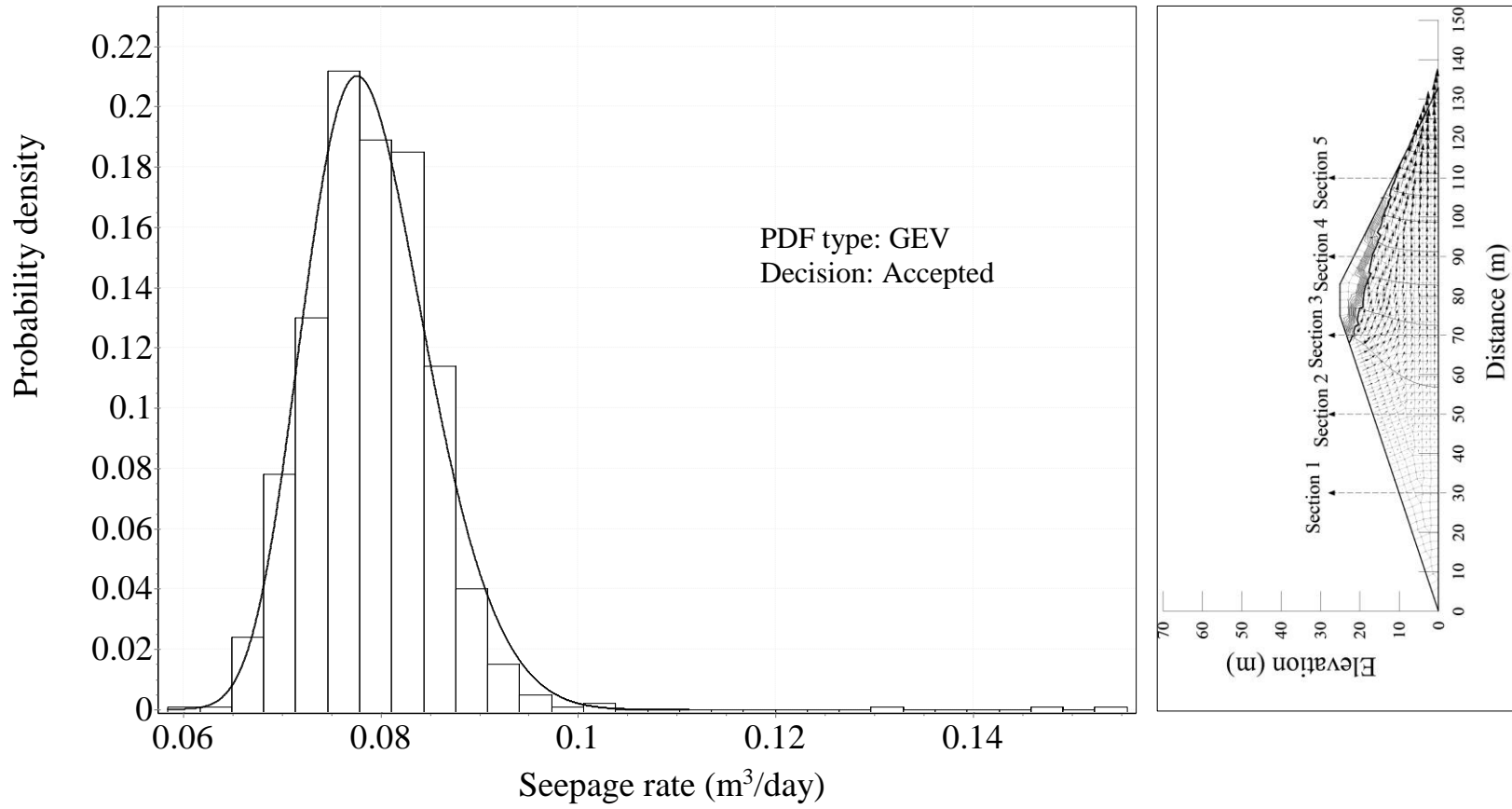


Figure 6.24 Frequency histogram of  $Q$  for rapid fill case when  $t=1000$  days at Section 4.

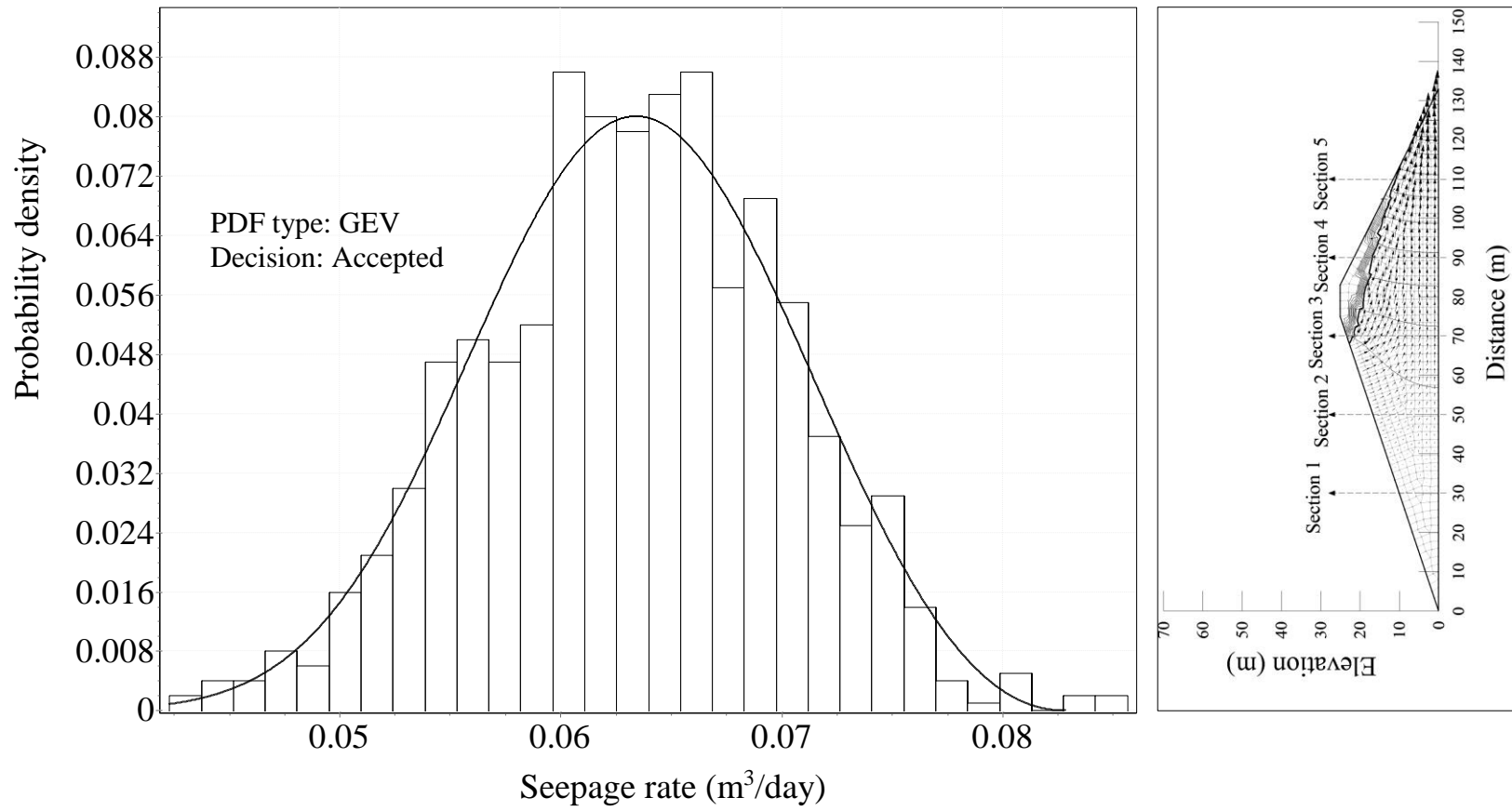


Figure 6.25 Frequency histogram of  $Q$  for rapid fill case when  $t=1000$  days at Section 5.

### 6.3 Combined Fill and Drawdown Case

This case normally refers to the accommodation of a single flood event in the reservoir. With almost empty reservoir condition for a flood detention dam, reservoir level increases rapidly during the rising stage of the flood. After the time to peak value of the flood hydrograph, reservoir level decreases during the recession period of the flood. Parallel to the physical nature of floods, the rate of increase of water level in the reservoir is greater than the rate of the water level decrease (see Figure 6.26). For the application problems subject to combined fill and drawdown case, the initial upstream total head is assumed to be 1 m. The total head increases to 23 m in two days. Then, it is decreases to again 1 m in four days. The graphical representation of the upstream boundary condition is given in Figure 6.26.

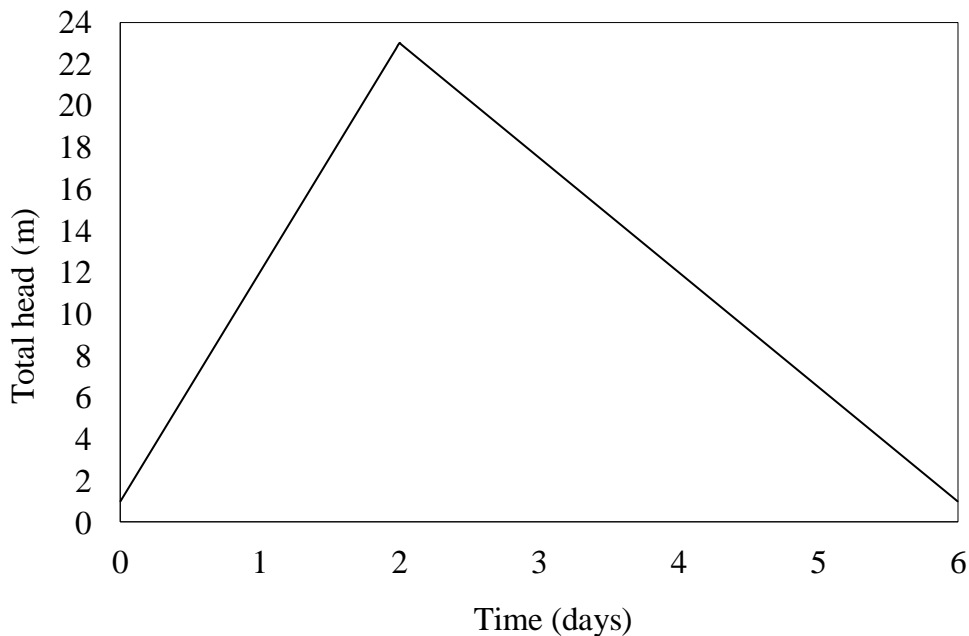


Figure 6.26 The upstream boundary condition for the combined fill and drawdown case.

### 6.3.1 Homogeneous Embankment Dam

This section investigates the degree of variation of the seepage and its probabilistic properties for the embankment dam given in Figure 5.1 with the complex boundary condition, combined fill and drawdown case. The uncertainty of the dam material is taken into account considering the soil properties supplied in Table 6.1.

The total simulation duration is determined to be 500 days, which is a sufficient time for the flow to reach its steady state condition. A sequence of 1000 analyses, each having spatially varying soil properties are held. Then, the data sets of the flow at the sections are obtained and analyzed statistically.

The descriptive statistics of the flow are determined and presented in Table 6.6. The changes in  $\mu(Q)$  and  $\sigma(Q)$  are plotted in Figure 6.27 (a) and (b), respectively. It is seen from the mean flow rates that there is considerable flow rate at Section 1. The mean flow rate increases at the very beginning of the simulation. Then, it decreases with time and approaches to zero at this section. The flow fluctuates at insignificantly small rates at Section 2; and there is no flow at Section 3 to 5. Besides, similar tendencies are observed for the standard deviations of flows at all sections. The dispersion of the flow increases with the increase in the mean flow rate, and decreases as the flow rate decreases at Section 1. The flow dispersion at Section 2 is relatively minor, and no dispersion is observed for the flow rates at Section 3 to 5 since there is no flow at these sections.

The COV of the flow rate at Section 1 decreases with time. The maximum coefficient of variation of the flow rate is computed as 1.90 and it is observed during the filling part of the boundary condition. The maximum COV value of the input parameters is 2.33. Similarly, the degree of variation of the input parameter decreases by the system.

The probability density functions for the seepage through the dam are determined by goodness of fit tests. The results are given in Table 6.7. According to the results, the most of the seepage through sections can be statistically defined by three-

parameter log-normal distribution (LN-3P). The seepage rates whose fitted PDF is rejected by goodness tests also cannot be described by the other type of probability distributions considered in this study and any other type of distribution functions.

For this application problem, the frequency histograms of the seepage, fitted probability density functions and the overall decision of the goodness of fit test are given in Figure 6.28 to Figure 6.34.

Table 6.6 The descriptive statistics of the seepage through the homogeneous dam for the combined fill and drawdown case.

Time	Sect.	Max (Q)	Min (Q)	$\mu$ (Q)	$\sigma$ (Q)	COV (Q)	Skewness	Kurtosis
		(m <sup>3</sup> /day)						
t=1 days	1	1.99	0.01	0.12	0.181	1.47	4.97	34.02
	2	0.00	0.00	0.00	0.000	-	-	-
	3	0.00	0.00	0.00	0.000	-	-	-
	4	0.00	0.00	0.00	0.000	-	-	-
	5	0.00	0.00	0.00	0.000	-	-	-
t=2 days	1	1.86	0.00	0.28	0.232	0.82	1.56	3.63
	2	0.32	0.00	0.01	0.019	1.90	7.02	81.00
	3	0.00	0.00	0.00	0.000	-	-	-
	4	0.00	0.00	0.00	0.000	-	-	-
	5	0.00	0.00	0.00	0.000	-	-	-
t=4 days	1	0.44	0.00	0.05	0.032	0.66	2.69	23.03
	2	0.15	0.00	0.00	0.006	-	17.97	403.56
	3	0.00	0.00	0.00	0.000	-	-	-
	4	0.00	0.00	0.00	0.000	-	-	-
	5	0.00	0.00	0.00	0.000	-	-	-
t=6 days	1	0.06	0.00	0.00	0.007	-	2.88	11.31
	2	0.07	0.00	0.00	0.003	-	17.65	395.03
	3	0.00	0.00	0.00	0.000	-	-	-
	4	0.00	0.00	0.00	0.000	-	-	-
	5	0.00	0.00	0.00	0.000	-	-	-

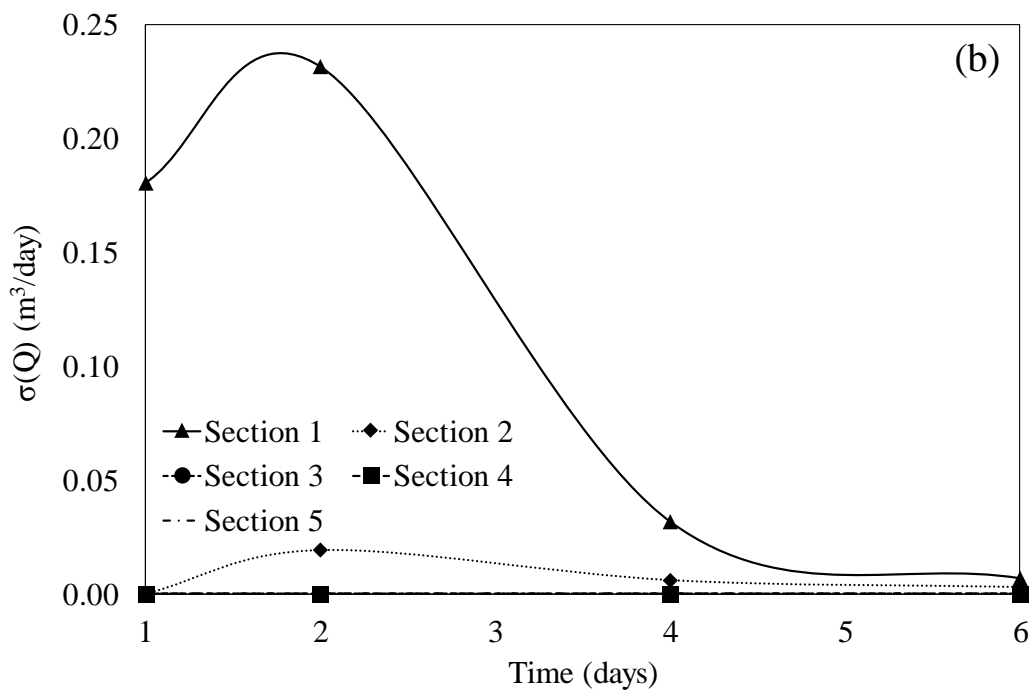
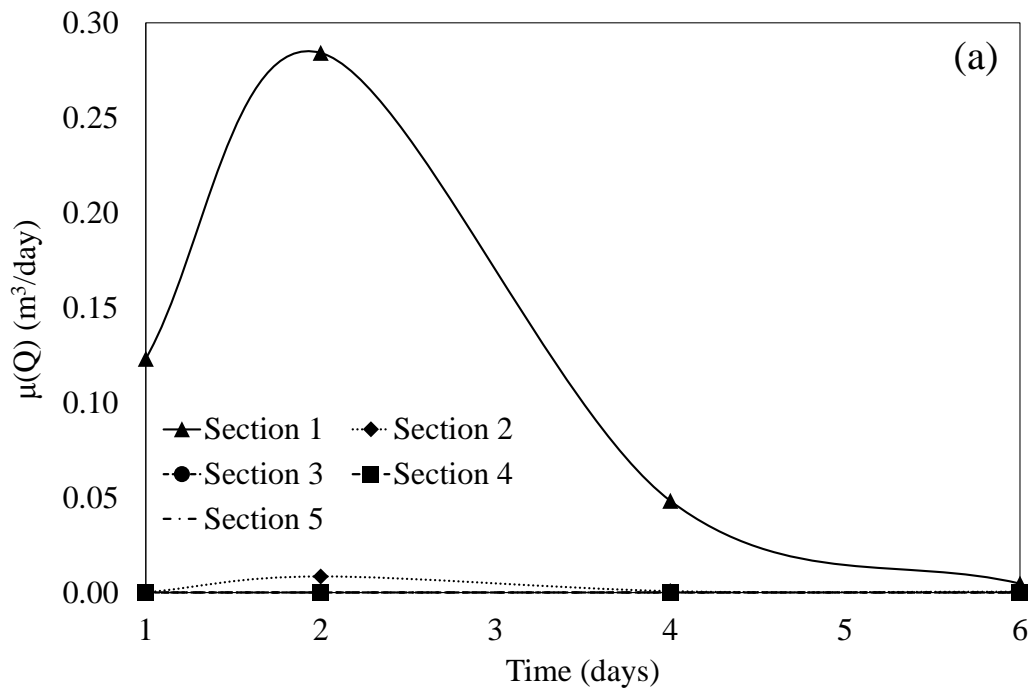


Figure 6.27 The change of (a)  $\mu(Q)$  and (b)  $\sigma(Q)$  with respect to time for homogeneous dam subjected to combined fill and drawdown case.

Table 6.7 Goodness of fit results for PDFs of seepage through the homogeneous dam for the combined fill and drawdown case.

Time	Sect.	PDF type	Kolmogorov-Smirnov ( $D_{max}$ )			Chi-square ( $X^2$ )			Overall decision
			Critical value for $\alpha'=0.1$ is 0.039 Critical value for $\alpha'=0.05$ is 0.043			Critical value for $\alpha'=0.1$ is 14.684 Critical value for $\alpha'=0.05$ is 16.919			
			Computed value	Decision		Computed value	Decision		
$\alpha'=0.1$	$\alpha'=0.05$	$\alpha'=0.1$		$\alpha'=0.05$					
t=1 days	1	LN-3P	0.021	Accept	Accept	11.557	Accept	Accept	Accept
	2	-	-	-	-	-	-	-	-
	3	-	-	-	-	-	-	-	-
	4	-	-	-	-	-	-	-	-
	5	-	-	-	-	-	-	-	-
t=2 days	1	LN-3P	0.054	Reject	Reject	40.825	Reject	Reject	Reject
	2	LN-3P	0.018	Accept	Accept	3.294	Accept	Accept	Accept
	3	-	-	-	-	-	-	-	-
	4	-	-	-	-	-	-	-	-
	5	-	-	-	-	-	-	-	-
t=4 days	1	LN-3P	0.034	Accept	Accept	12.068	Accept	Accept	Accept
	2	LN-3P	0.105	Reject	Reject	131.650	Reject	Reject	Reject
	3	-	-	-	-	-	-	-	-
	4	-	-	-	-	-	-	-	-
	5	-	-	-	-	-	-	-	-
t=6 days	1	LN-3P	0.047	Reject	Reject	31.307	Reject	Reject	Reject
	2	LN-3P	0.102	Reject	Reject	113.660	Reject	Reject	Reject
	3	-	-	-	-	-	-	-	-
	4	-	-	-	-	-	-	-	-
	5	-	-	-	-	-	-	-	-

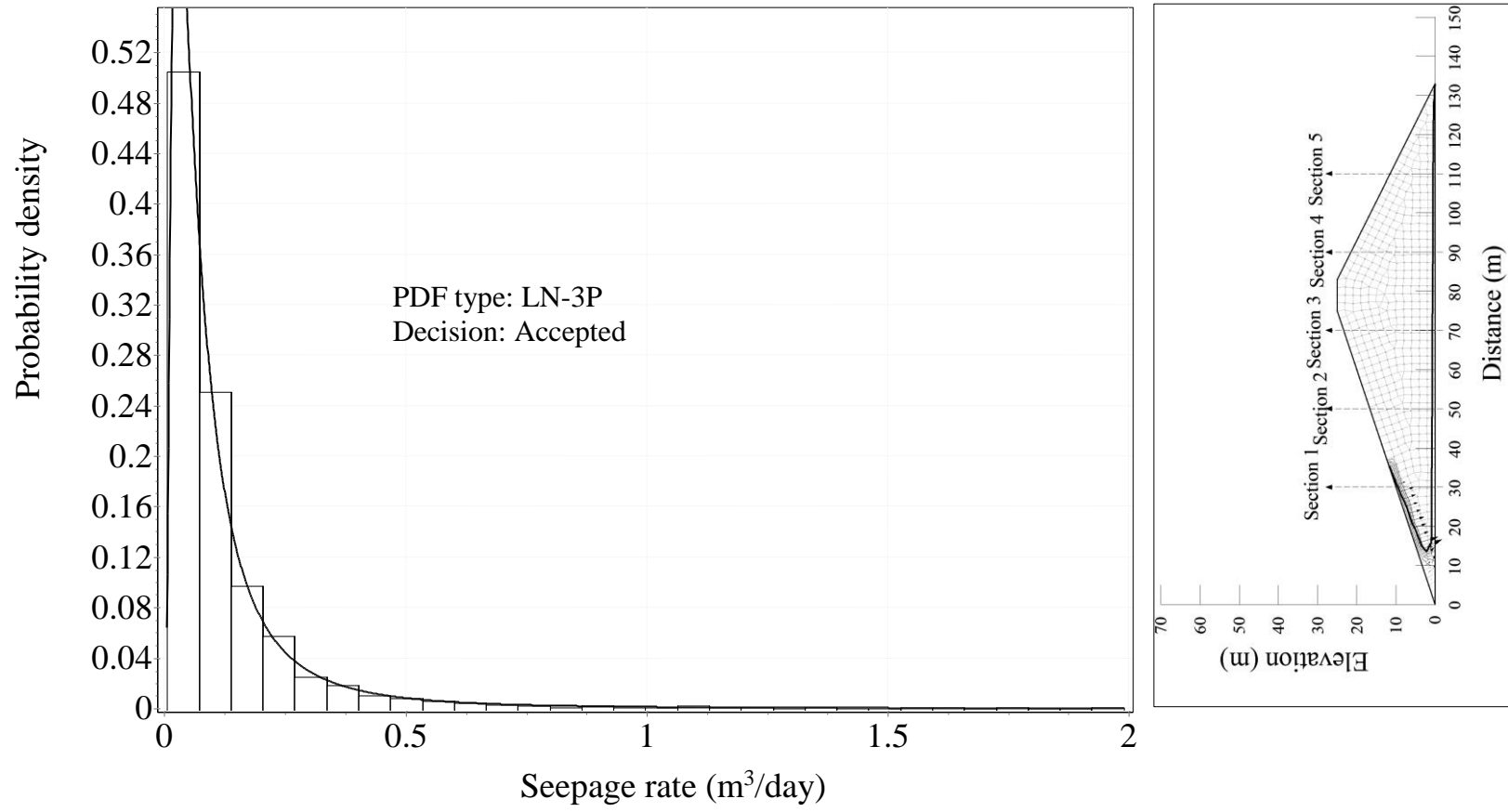


Figure 6.28 Frequency histogram of  $Q$  through the homogeneous dam for the combined fill and drawdown case when  $t=1$  days at Section 1.

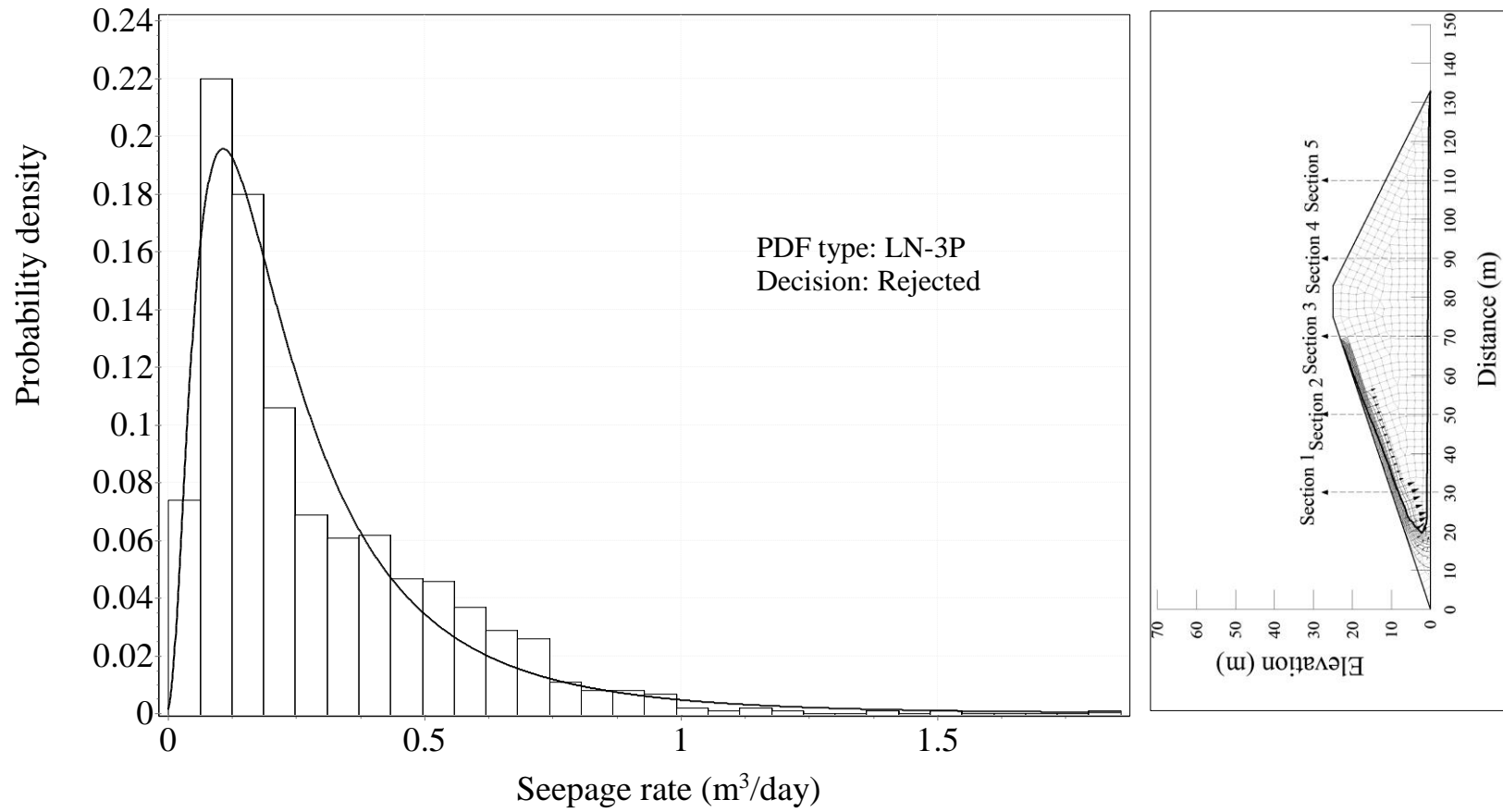


Figure 6.29 Frequency histogram of  $Q$  through the homogeneous dam for the combined fill and drawdown case when  $t=2$  days at Section 1.

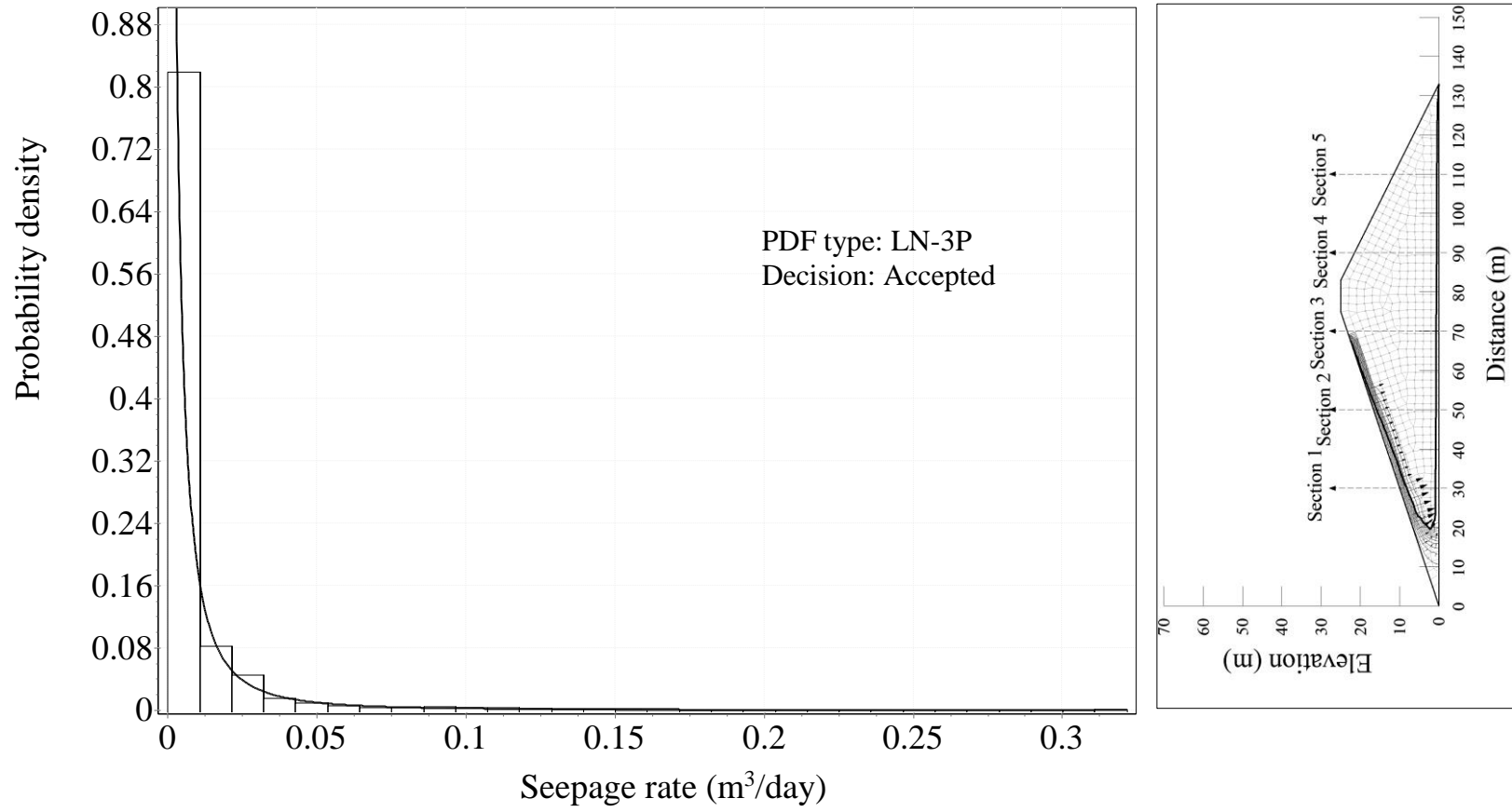


Figure 6.30 Frequency histogram of  $Q$  through the homogeneous dam for the combined fill and drawdown case when  $t=2$  days at Section 2.

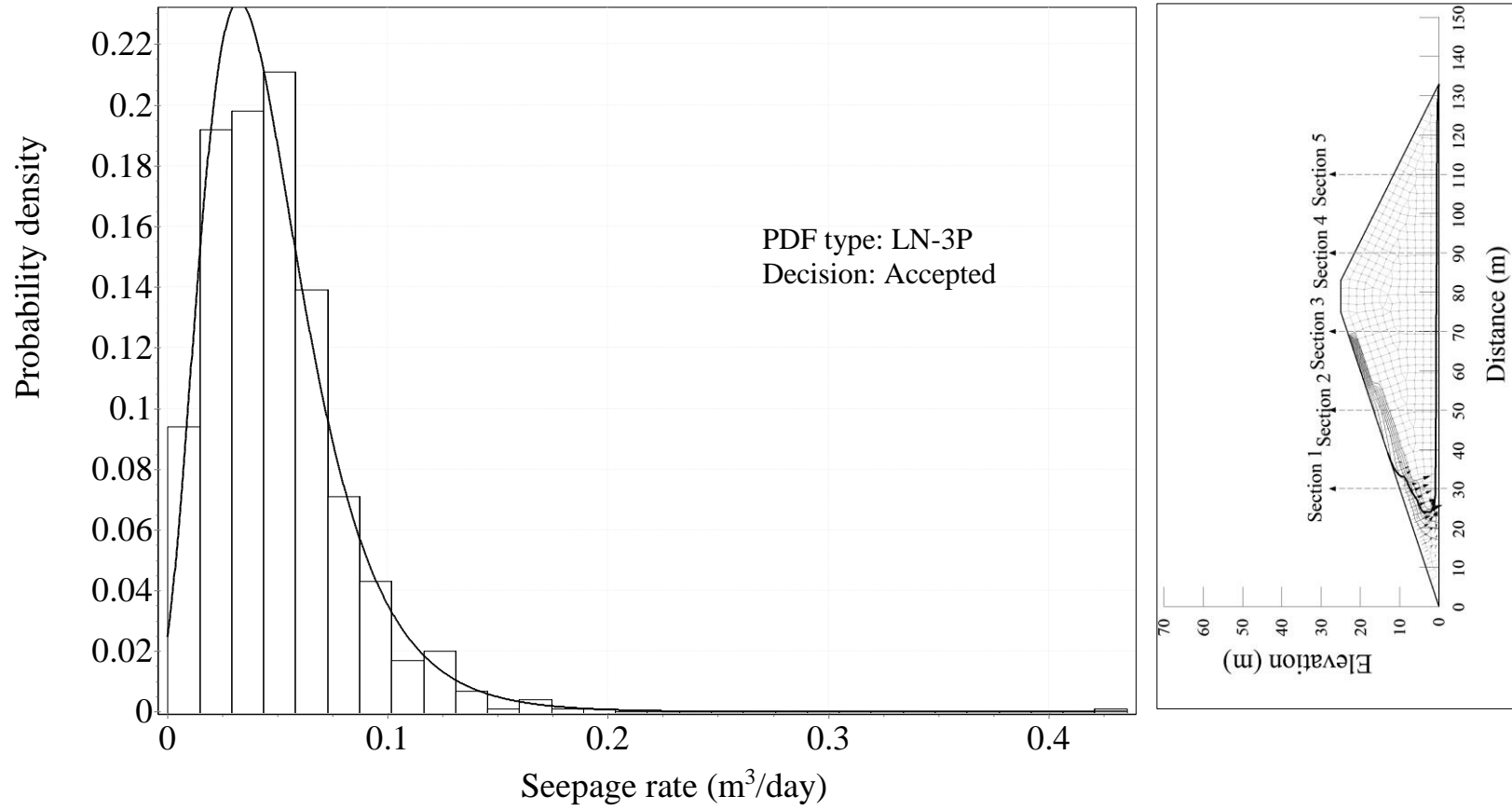


Figure 6.31 Frequency histogram of  $Q$  through the homogeneous dam for the combined fill and drawdown case when  $t=4$  days at Section 1.

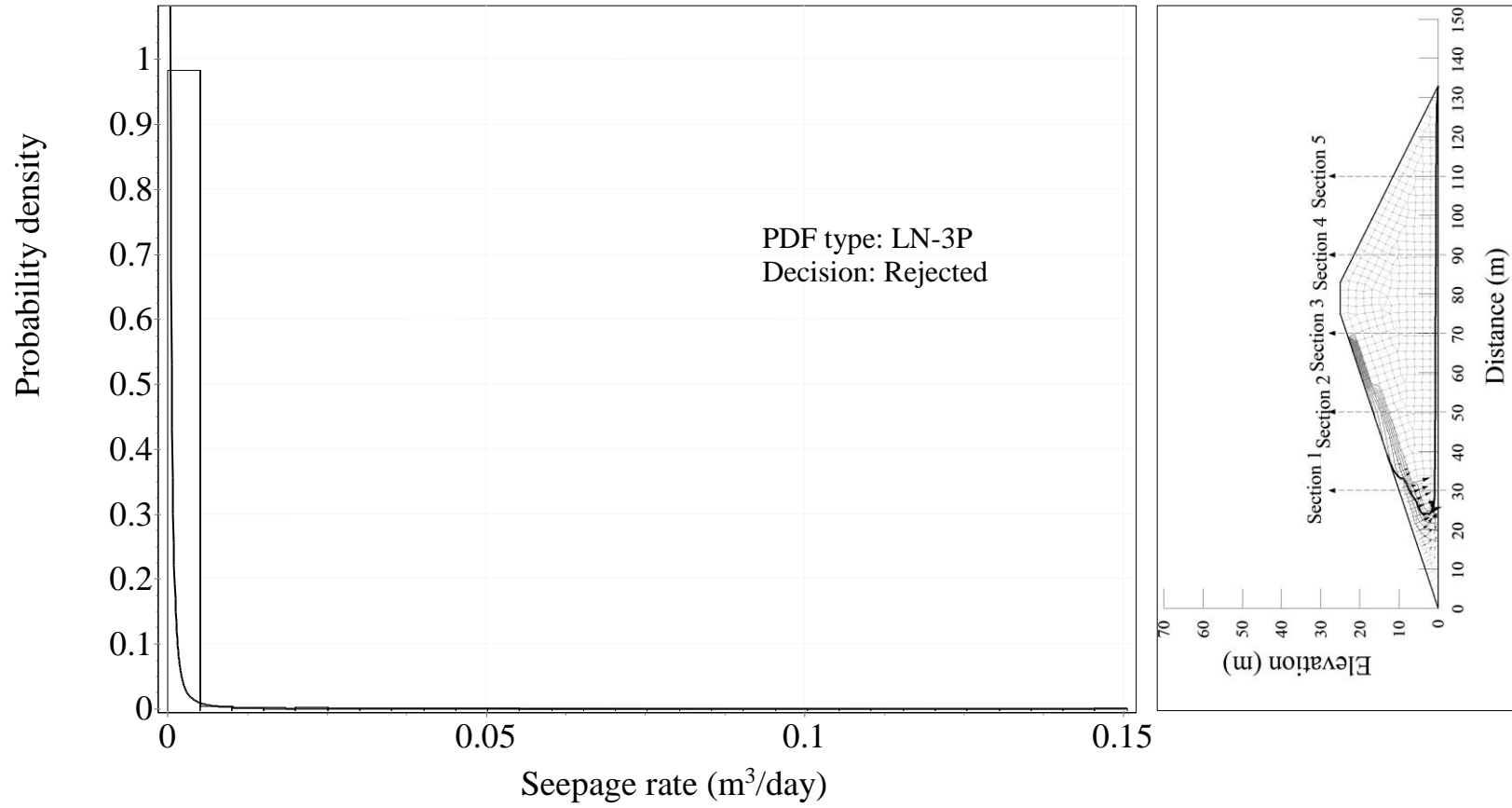


Figure 6.32 Frequency histogram of Q through the homogeneous dam for the combined fill and drawdown case when t=4 days at Section 2.

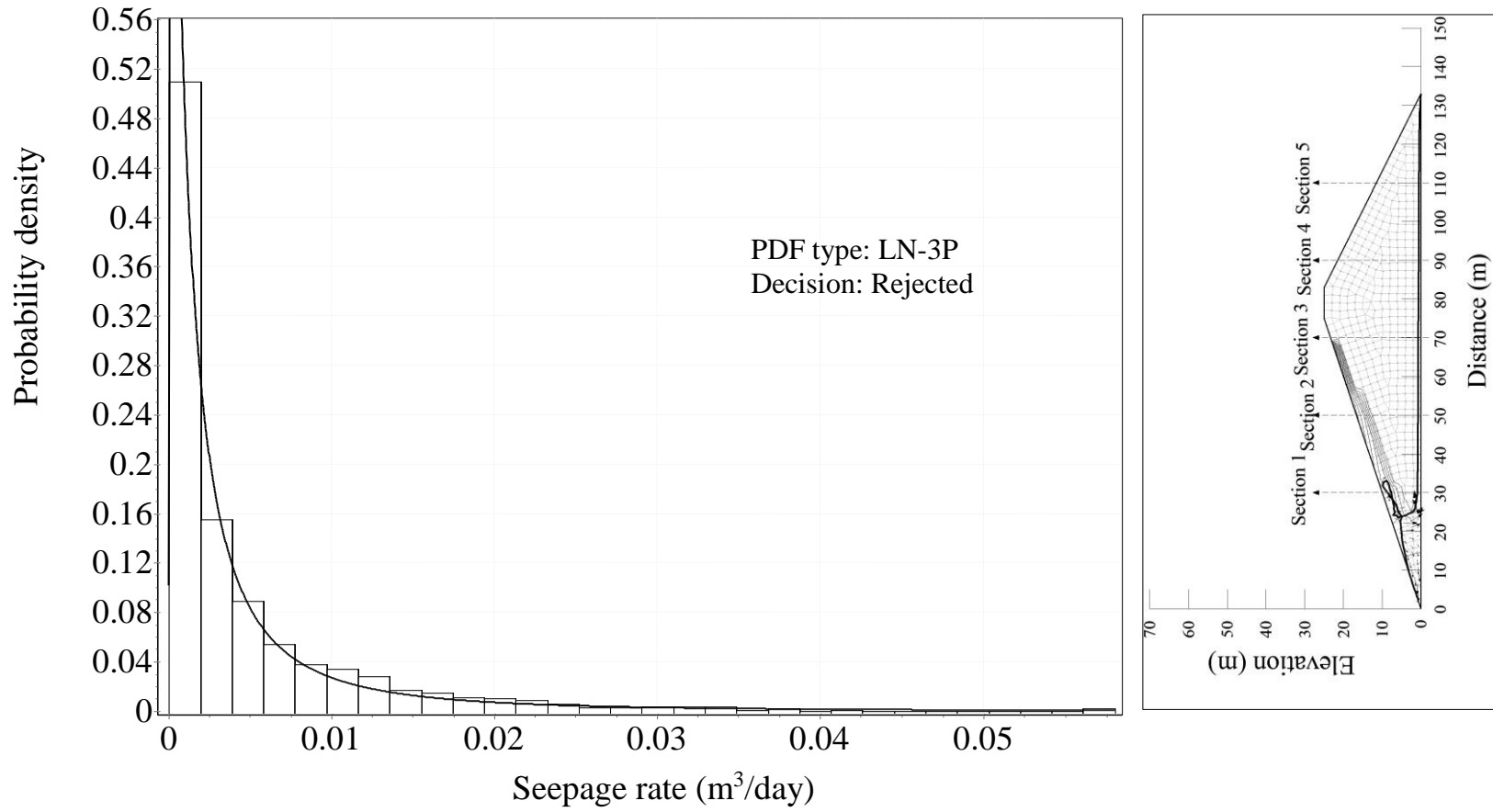


Figure 6.33 Frequency histogram of  $Q$  through the homogeneous dam for the combined fill and drawdown case when  $t=6$  days at Section 1.

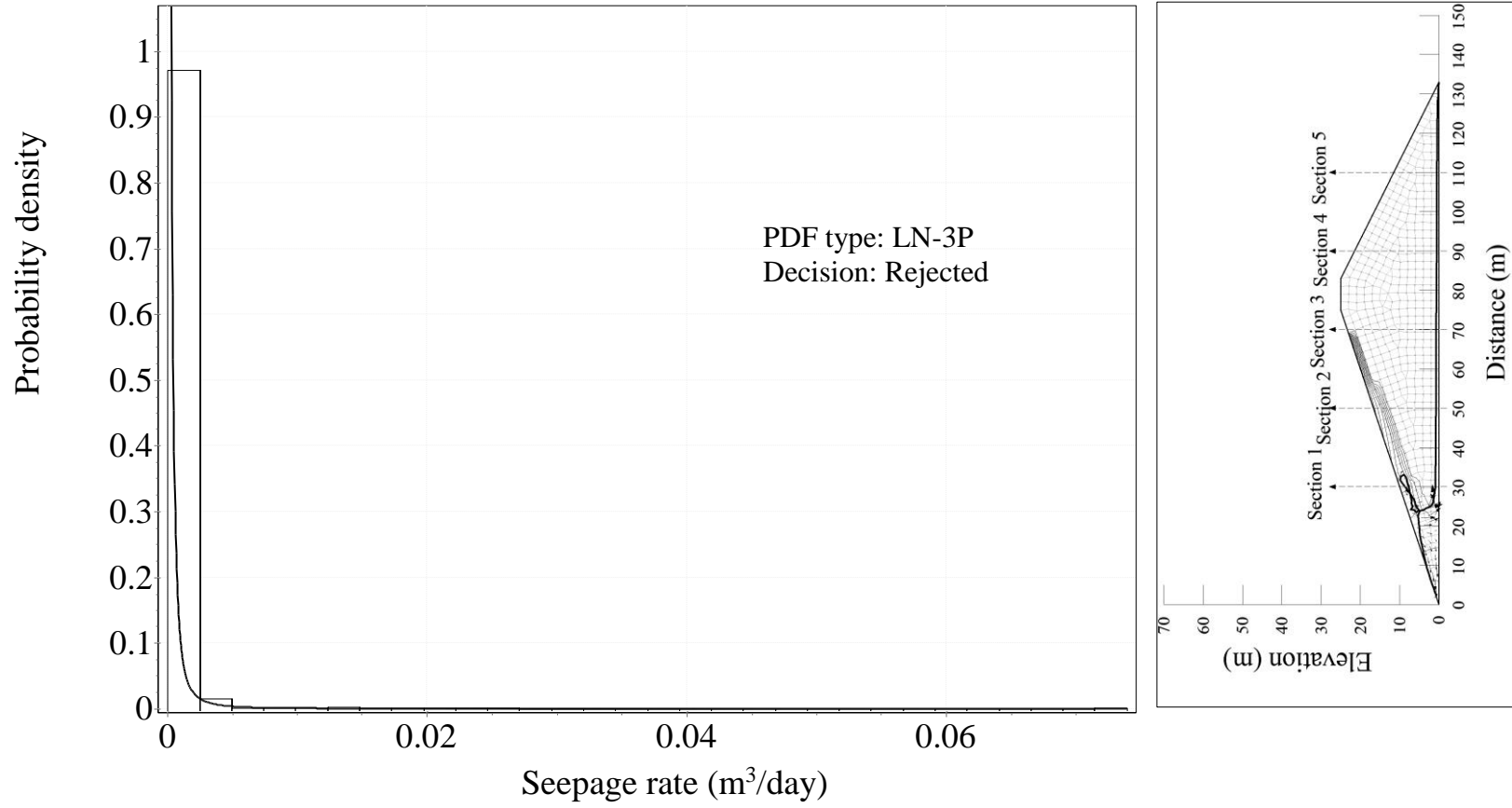


Figure 6.34 Frequency histogram of  $Q$  through the homogeneous dam for the combined fill and drawdown case when  $t=6$  days at Section 2.

### 6.3.2 Simple Zoned Embankment Dam

For comparison purposes, the seepage is stochastically analyzed and the results evaluated statistically for the simple zoned embankment dam given in Figure 6.35 having the upstream boundary condition given in Figure 6.26. The main geometry of the dam, the locations of sections and the initial boundary condition at the upstream are kept the same with the former application problem (i.e. the homogeneous embankment dam defined in Section 6.3.1). However, a new material configuration is considered. The embankment is supposed to be composed of a shell and a core structure. The shell and core materials are determined to be gravelly sand and clay, respectively. The statistical properties of soils are given in Table 6.8 for both material types. With this analysis, it is aimed to assess effect of type of material on the uncertainty and randomness of the flow.

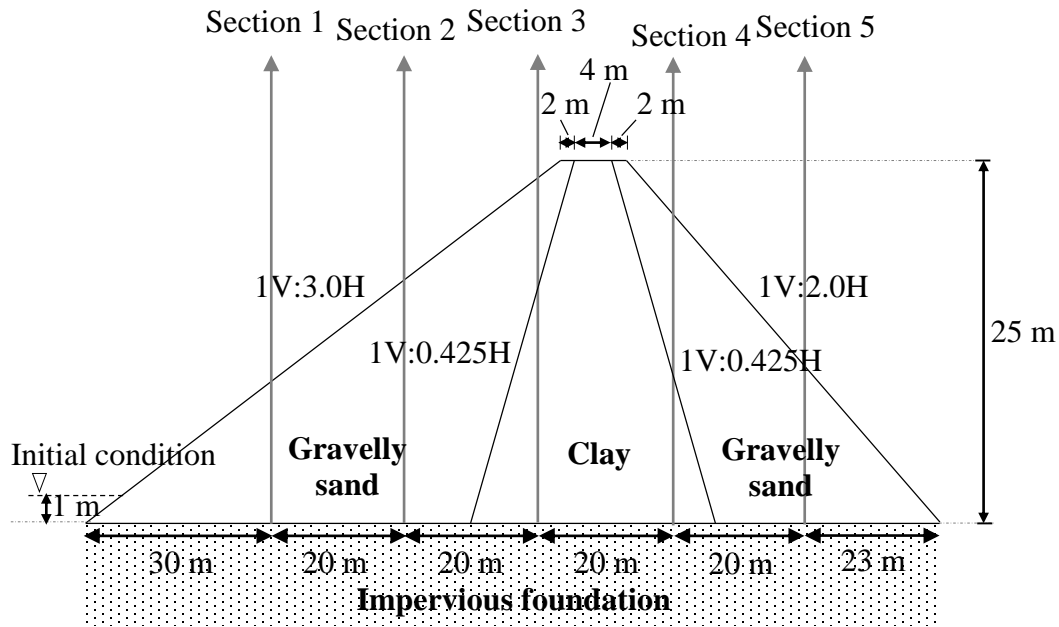


Figure 6.35 The geometry, sections and initial conditions of the simple zoned dam considered for combined fill and drawdown case.

The total time for the simulation of transient seepage is selected as 500 days, which is an adequate duration for the flow to reach its steady-state condition for the given embankment dam and boundary conditions. The transient seepage is analyzed stochastically with 1000 numbers of MCS.

Table 6.8 The statistical properties of the simple zoned dam material considered for the combined fill and drawdown case.

	Parameter	$\mu$	COV	Reference
Clay	K (m/s)	$7.22 \times 10^{-7}$	2.70	(Carsel and Parrish 1988; Fredlund 2005)
	$\alpha$ (cm <sup>-1</sup> )	0.02	0.80	
	n	1.31	0.07	
Gravelly sand	K (m/s)	$8.80 \times 10^{-5}$	0.040	(Zeng et al. 2012)
	$\alpha$ (cm <sup>-1</sup> )	0.08	0.040	
	n	2.45	0.044	

Firstly, the results are statistically analyzed. Then, the frequency histograms of the flow rates are derived and probability distributions are fitted to the data. The descriptive statistics of the flow rates are given in Table 6.9. The mean and standard deviation change of the flow rates with respect to time are given in Figure 6.36 (a) and (b), respectively. The descriptive statistics showed that the mean flow rate at;

- (a) Section 1 rapidly reaches to a relatively high rate as the hydraulic conductivity of the gravelly sand is relatively greater. Then, it sharply decreases until the water at the upstream reaches to its maximum level. With the drawdown of the total head, water starts to drain from the dam body which cause another increase in the flow at Section 1.
- (b) Section 2 and 3 increases with the fill part of the boundary condition and then decreases with the drain of water. The mean flow rates at Section 2 are greater than those of Section 3. Because the former one rests inside the gravelly sand whose hydraulic conductivity is relatively greater.
- (c) Section 4 and 5 are almost zero throughout the simulation.

The standard deviations of the flow rate at Section 1 and 2 are relatively smaller. The material (i.e. gravelly sand) of these sections has slighter coefficient of variation values for its properties; this results in smaller dispersions in flow through the material. Similar findings were obtained in the sensitivity analysis conducted in Section 4.2.3. However, for Section 3 whose biggest part rests inside the clay material, the standard deviation of the flow rate is much greater than that of Section 1 and 2. The higher variation in clay properties resulted in higher dispersions in the flow.

Besides, the COV of the flow rate is relatively small and does not vary with time at Section 1 and 2. However, the variation degree of the flow rate at Section 3 decreases with time during the filling part. Similar results were found for Section 1 of the application problem analyzed for the rapid fill case. The uncertainty of seepage at Section 4 and 5 are insignificant since there is no flow at these sections throughout the simulation.

The maximum coefficient of variation of the flow rate is computed as 0.51 and it is observed at Section 3 during the filling part of the boundary condition. The maximum COV value of the input parameters is 2.70. Similar to the former application problems, the degree of variation of the input parameter is decreased by the system in this case.

The PDFs of the seepage through the dam are determined by goodness of fit tests. The fitted PDF types and decisions on hypotheses are shown in Table 6.10. The findings of the tests showed that the seepage through almost all sections and for all times can be described by generalized extreme value distribution. It is seen that, the seepage rates whose PDF is rejected by fit tests also cannot be described by other type of probability distributions considered in the study and any other type of distribution functions.

The frequency histograms of the seepage rate through the simple zoned embankment dam and fitted PDFs with the overall decision are given in Figure 6.38 to Figure 6.49.

Table 6.9 The descriptive statistics of the seepage through the simple zoned dam for the combined fill and drawdown case.

Time	Sect.	Max (Q)	Min (Q)	$\mu$ (Q)	$\sigma$ (Q)	COV (Q)	Skewness	Kurtosis
		(m <sup>3</sup> /day)						
t=1 days	1	27.94	26.37	27.14	0.240	0.01	-0.16	-0.05
	2	3.33	2.70	3.05	0.126	0.04	-0.25	-0.73
	3	0.00	0.00	0.00	0.001	-	-	-
	4	0.00	0.00	0.00	0.001	-	-	-
	5	0.00	0.00	0.00	0.002	-	-	-
t=2 days	1	1.18	0.95	1.06	0.033	0.03	0.48	0.92
	2	13.23	10.43	11.77	0.368	0.03	0.45	0.91
	3	44.43	5.45	11.08	5.685	0.51	2.71	9.39
	4	0.00	0.00	0.00	0.001	-	-	-
	5	0.00	0.00	0.00	0.007	-	-	-
t=4 days	1	2.80	2.67	2.72	0.019	0.01	0.15	0.02
	2	7.31	6.67	6.96	0.123	0.02	0.32	-1.01
	3	0.69	0.36	0.51	0.049	0.10	-0.06	-0.23
	4	0.03	0.00	0.00	0.002	-	3.44	22.73
	5	0.02	0.00	0.00	0.003	-	-	-
t=6 days	1	7.35	6.98	7.12	0.070	0.01	1.25	0.85
	2	4.03	3.85	3.90	0.028	0.01	1.24	1.66
	3	0.25	0.11	0.17	0.019	0.11	0.31	0.50
	4	0.08	0.00	0.00	0.008	-	3.17	17.07
	5	0.03	0.00	0.00	0.005	-	-	-

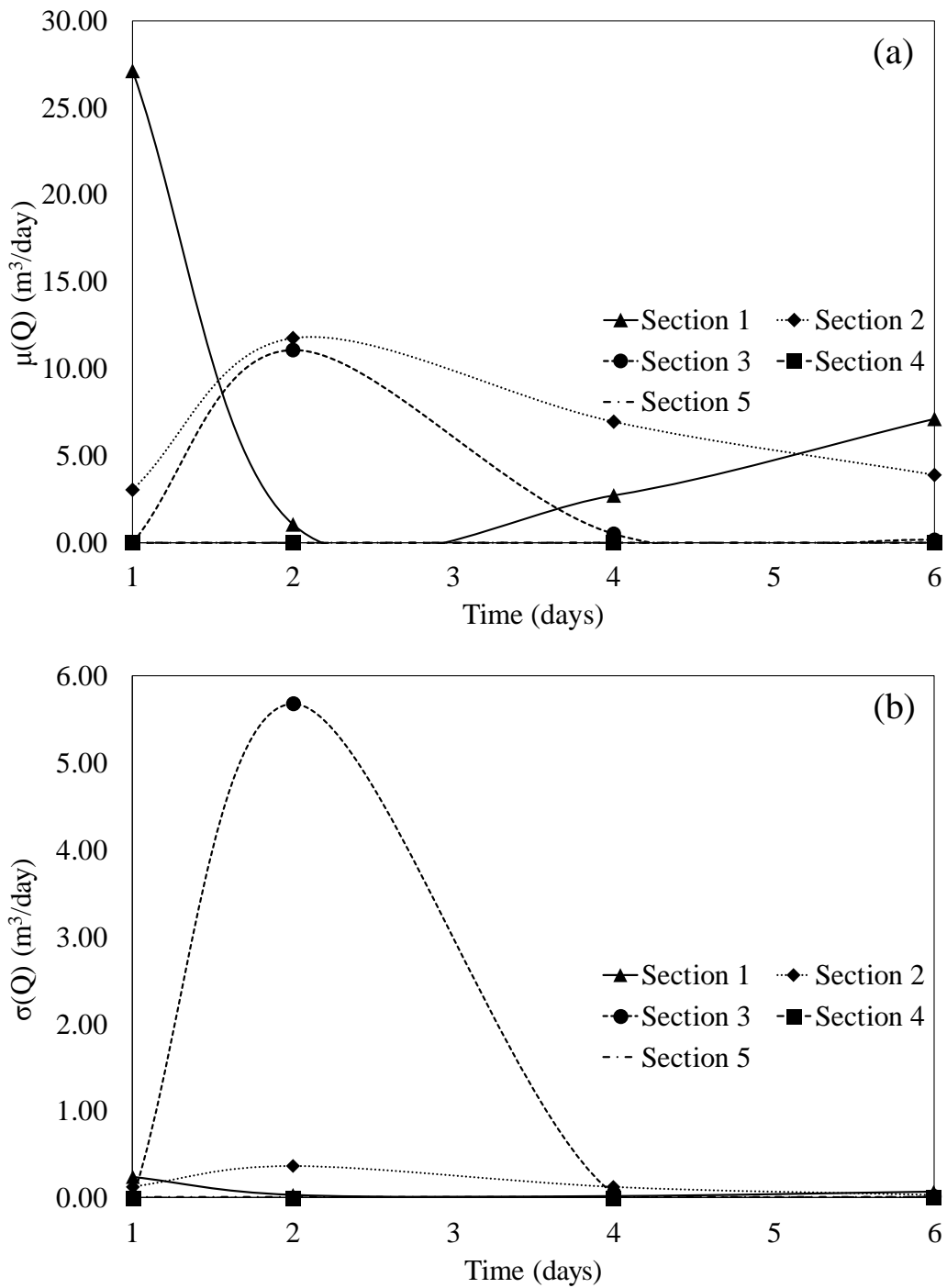


Figure 6.36 The change of (a)  $\mu(Q)$  and (b)  $COV(Q)$  with respect to time for simple zoned dam subjected to combined fill and drawdown case.

Table 6.10 Goodness of fit results for PDFs of seepage through the simple zoned dam for the combined fill and drawdown case.

Time	Sect.	PDF type	Kolmogorov-Smirnov ( $D_{max}$ )			Chi-square ( $X^2$ )			Overall decision
			Critical value for $\alpha'=0.1$ is 0.039 Critical value for $\alpha'=0.05$ is 0.043			Critical value for $\alpha'=0.1$ is 14.684 Critical value for $\alpha'=0.05$ is 16.919			
			Computed value	Decision		Computed value	Decision		
$\alpha'=0.1$	$\alpha'=0.05$	$\alpha'=0.1$		$\alpha'=0.05$					
t=1 days	1	GEV	0.019	Accept	Accept	N/A	N/A	N/A	Accept
	2	GEV	0.032	Accept	Accept	17.714	Reject	Reject	Reject
	3	-	-	-	-	-	-	-	-
	4	-	-	-	-	-	-	-	-
	5	-	-	-	-	-	-	-	-
t=2 days	1	GEV	0.027	Accept	Accept	6.978	Accept	Accept	Accept
	2	GEV	0.032	Accept	Accept	16.308	Reject	Accept	Accept
	3	GEV	0.127	Reject	Reject	464.360	Reject	Reject	Reject
	4	-	-	-	-	-	-	-	-
	5	-	-	-	-	-	-	-	-
t=4 days	1	GEV	0.015	Accept	Accept	N/A	N/A	N/A	Accept
	2	GEV	0.083	Reject	Reject	97.578	Reject	Reject	Reject
	3	GEV	0.020	Accept	Accept	N/A	N/A	N/A	Accept
	4	GEV	0.038	Accept	Accept	13.730	Accept	Accept	Accept
	5	-	-	-	-	-	-	-	-
t=6 days	1	GEV	0.067	Reject	Reject	138.370	Reject	Reject	Reject
	2	GEV	0.028	Accept	Accept	14.044	Accept	Accept	Accept
	3	GEV	0.016	Accept	Accept	N/A	N/A	N/A	Accept
	4	GEV	0.019	Accept	Accept	5.535	Accept	Accept	Accept
	5	-	-	-	-	-	-	-	-

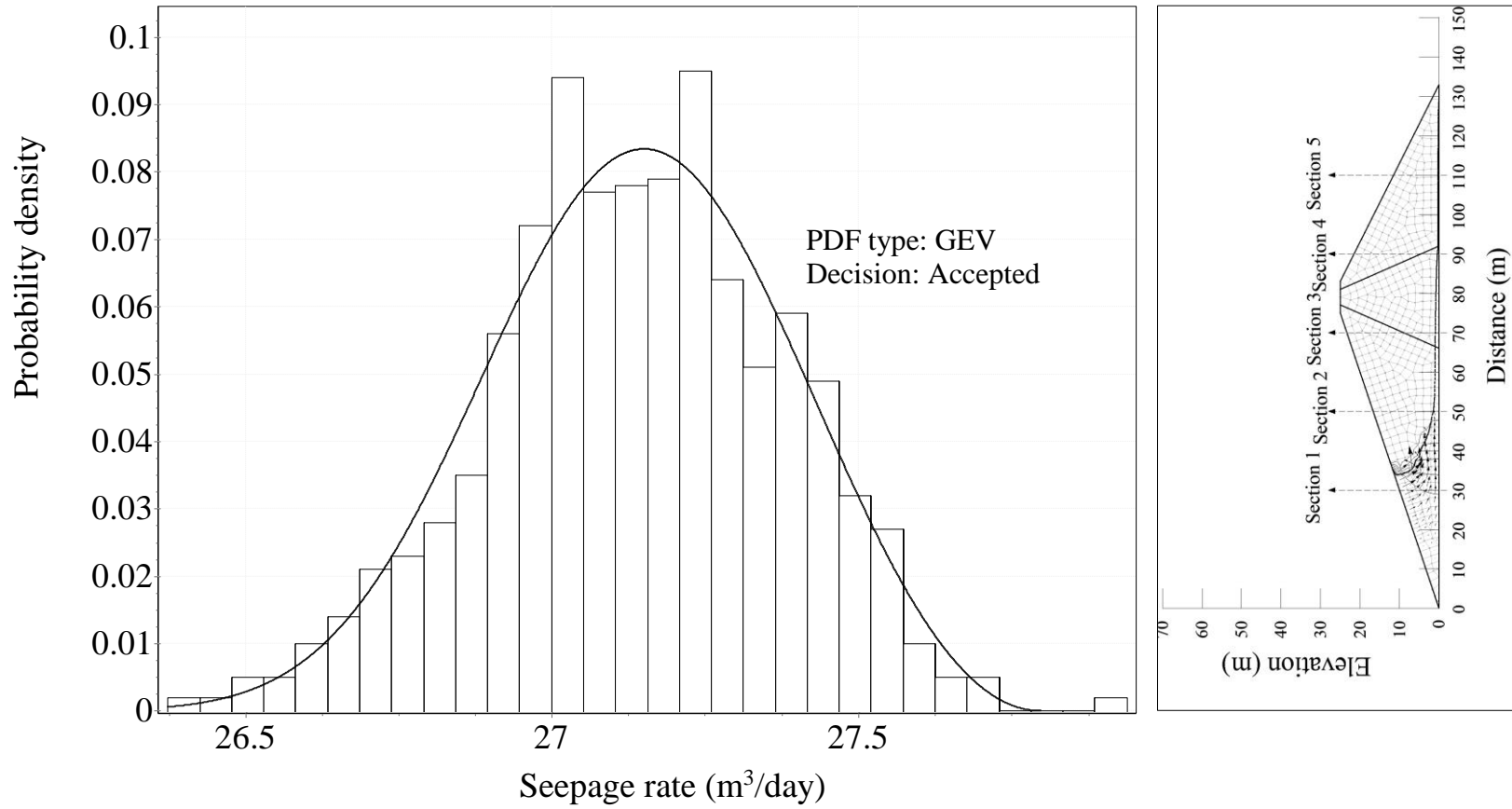


Figure 6.37 Frequency histogram of Q through the simple zoned dam for the combined fill and drawdown case when t=1 days at Section 1.

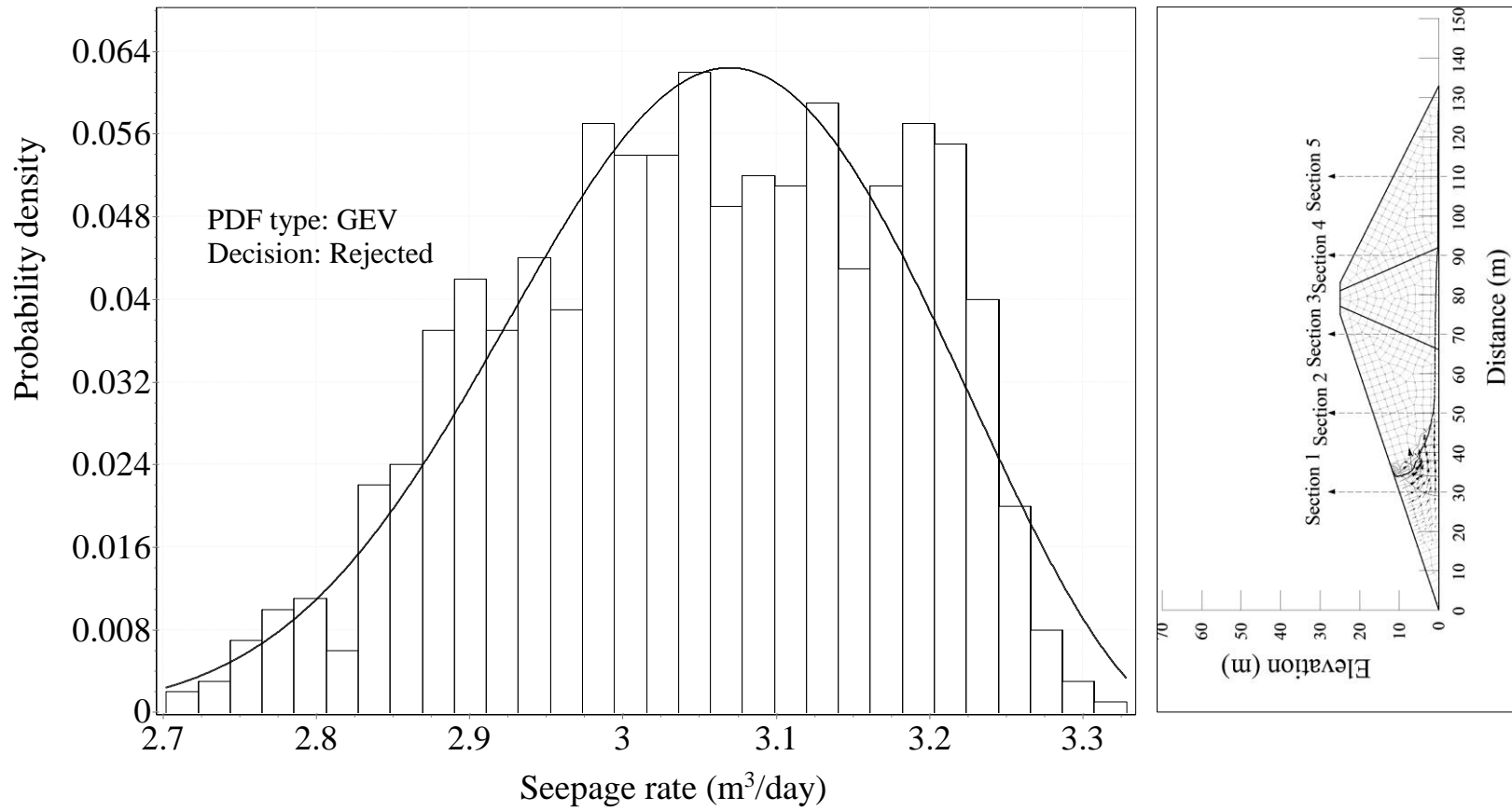


Figure 6.38 Frequency histogram of  $Q$  through the simple zoned dam for the combined fill and drawdown case when  $t=1$  days at Section 2.

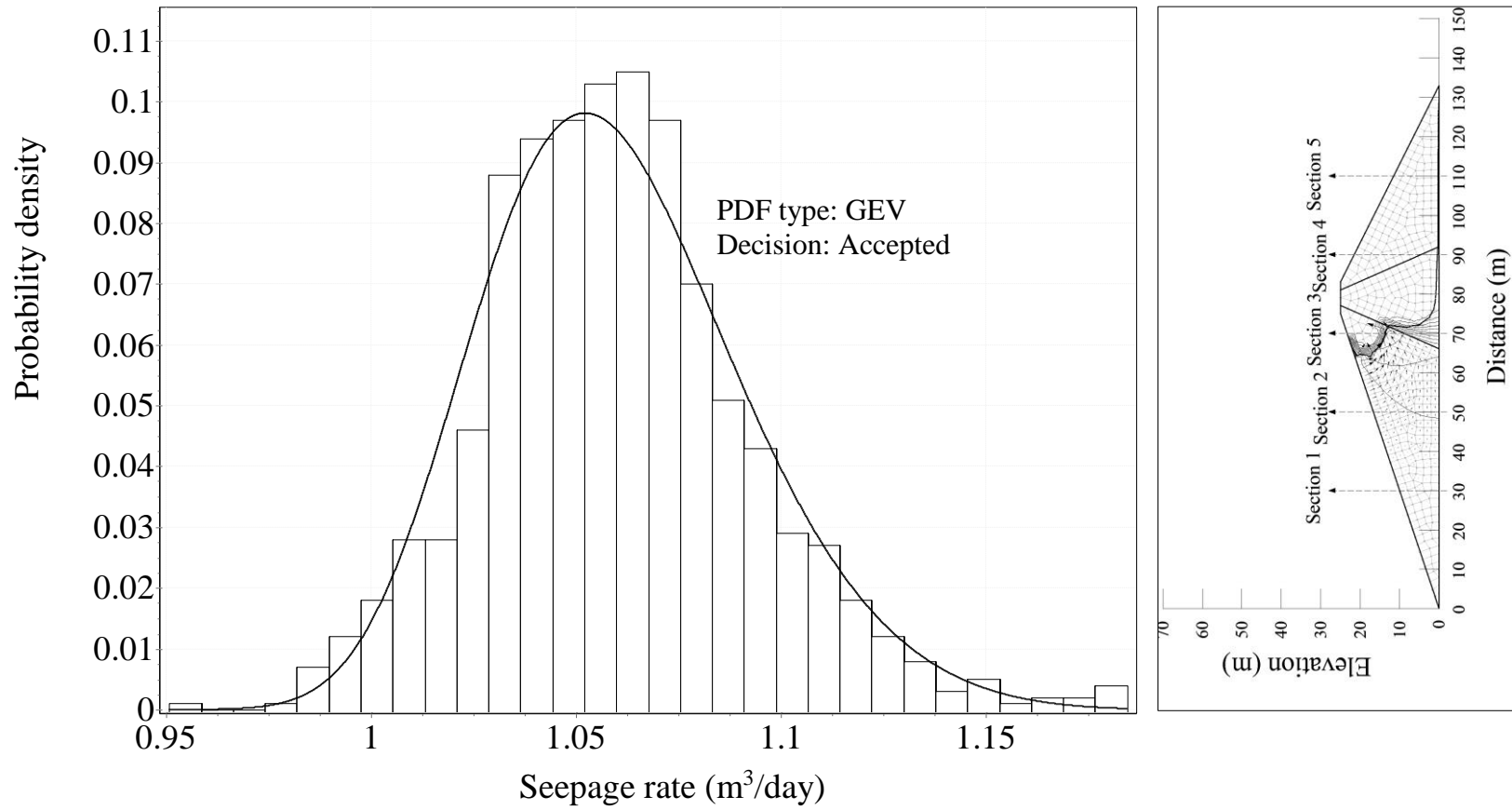


Figure 6.39 Frequency histogram of  $Q$  through the simple zoned dam for the combined fill and drawdown case when  $t=2$  days at Section 1.

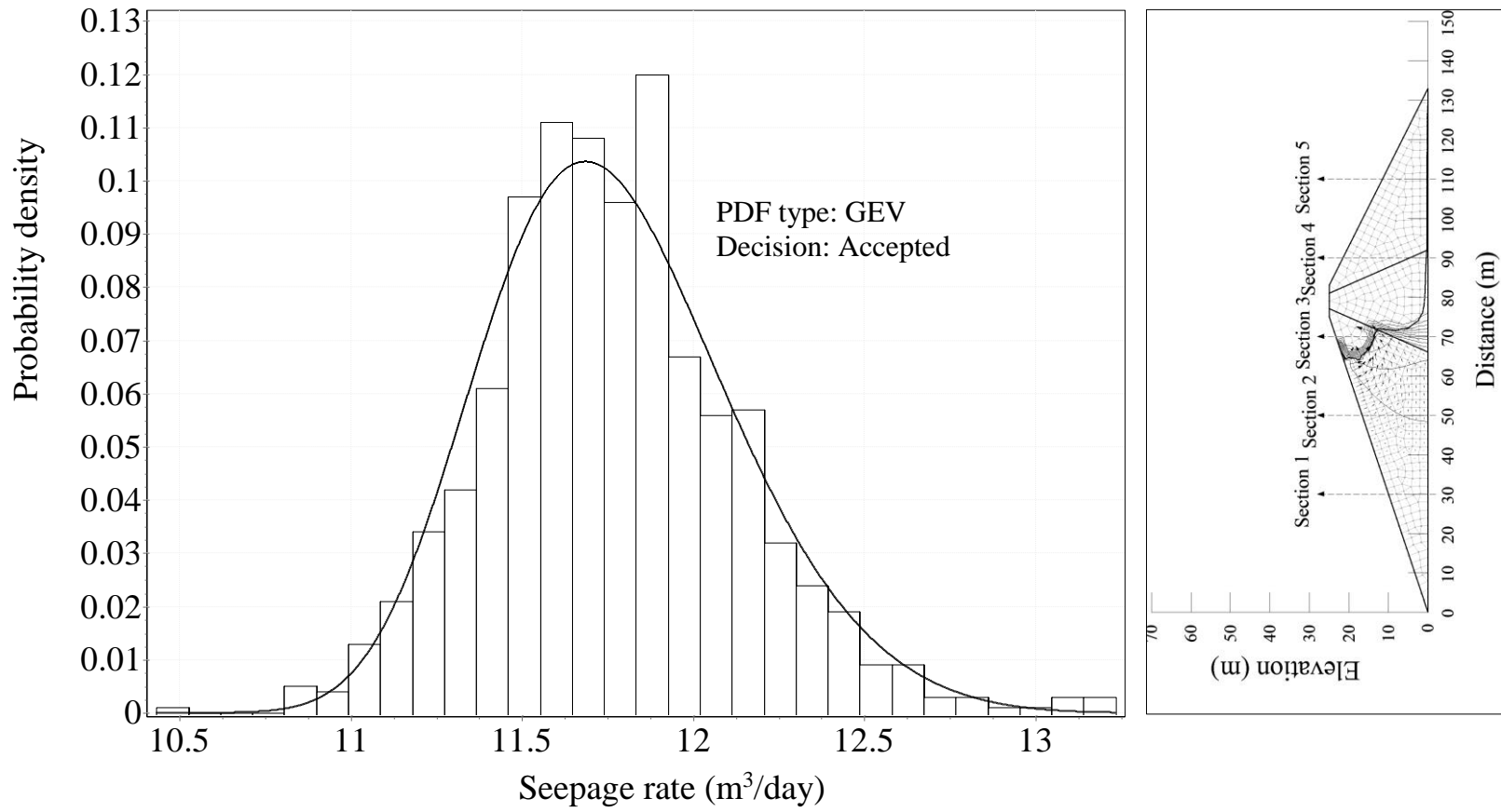


Figure 6.40 Frequency histogram of  $Q$  through the simple zoned dam for the combined fill and drawdown case when  $t=2$  days at Section 2.

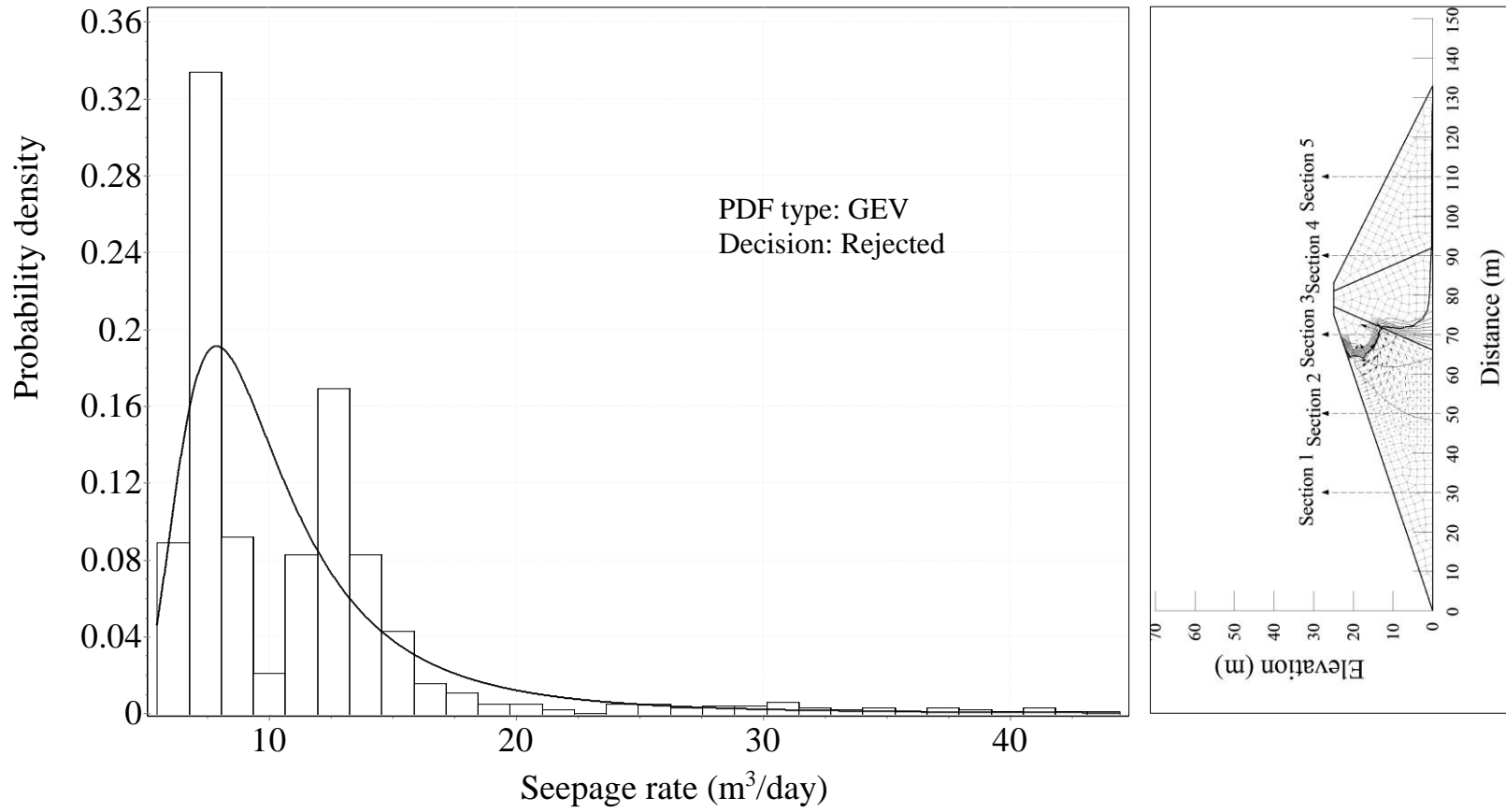


Figure 6.41 Frequency histogram of  $Q$  through the simple zoned dam for the combined fill and drawdown case when  $t=2$  days at Section 3.

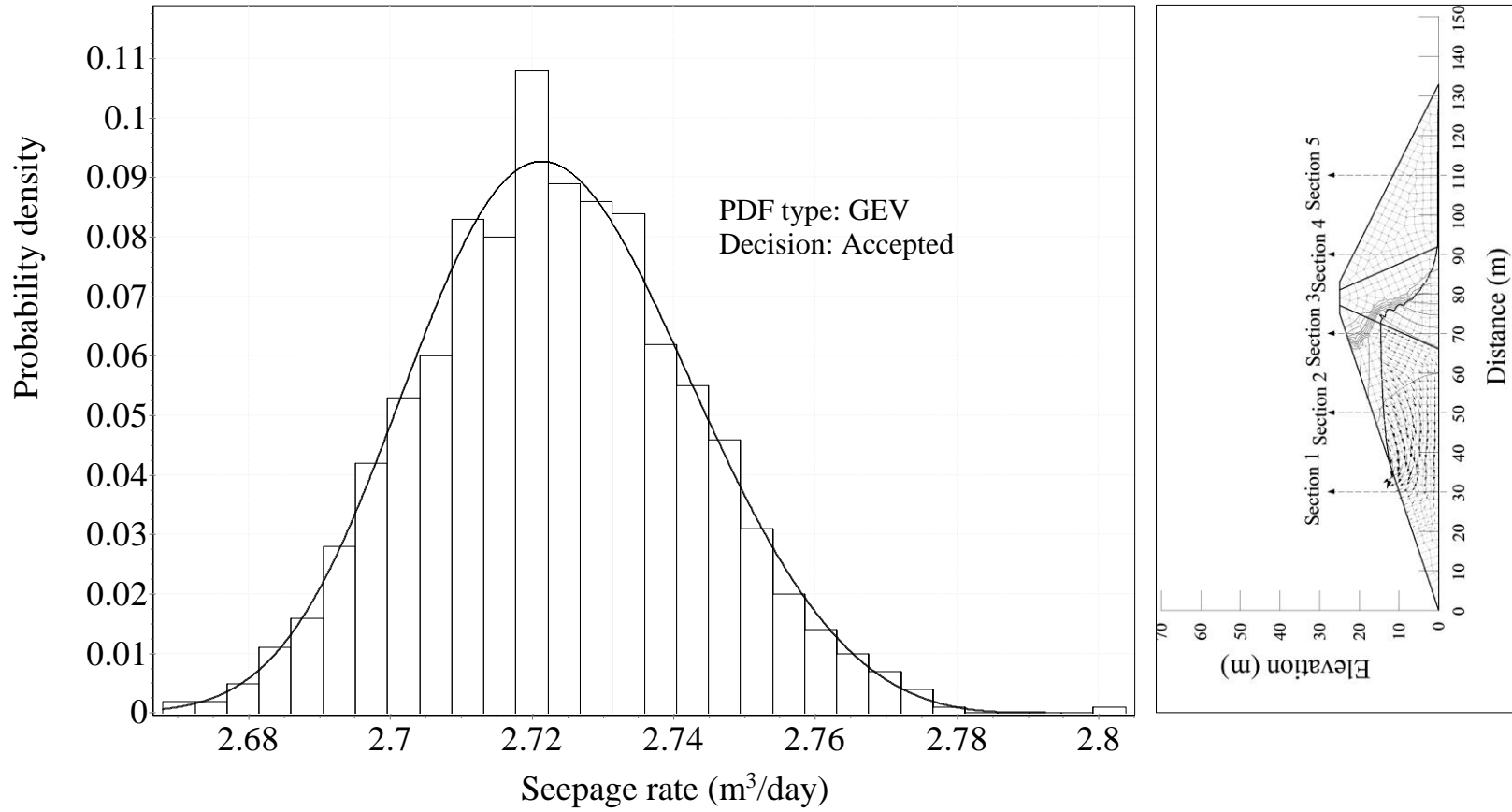


Figure 6.42 Frequency histogram of  $Q$  through the simple zoned dam for the combined fill and drawdown case when  $t=4$  days at Section 1.

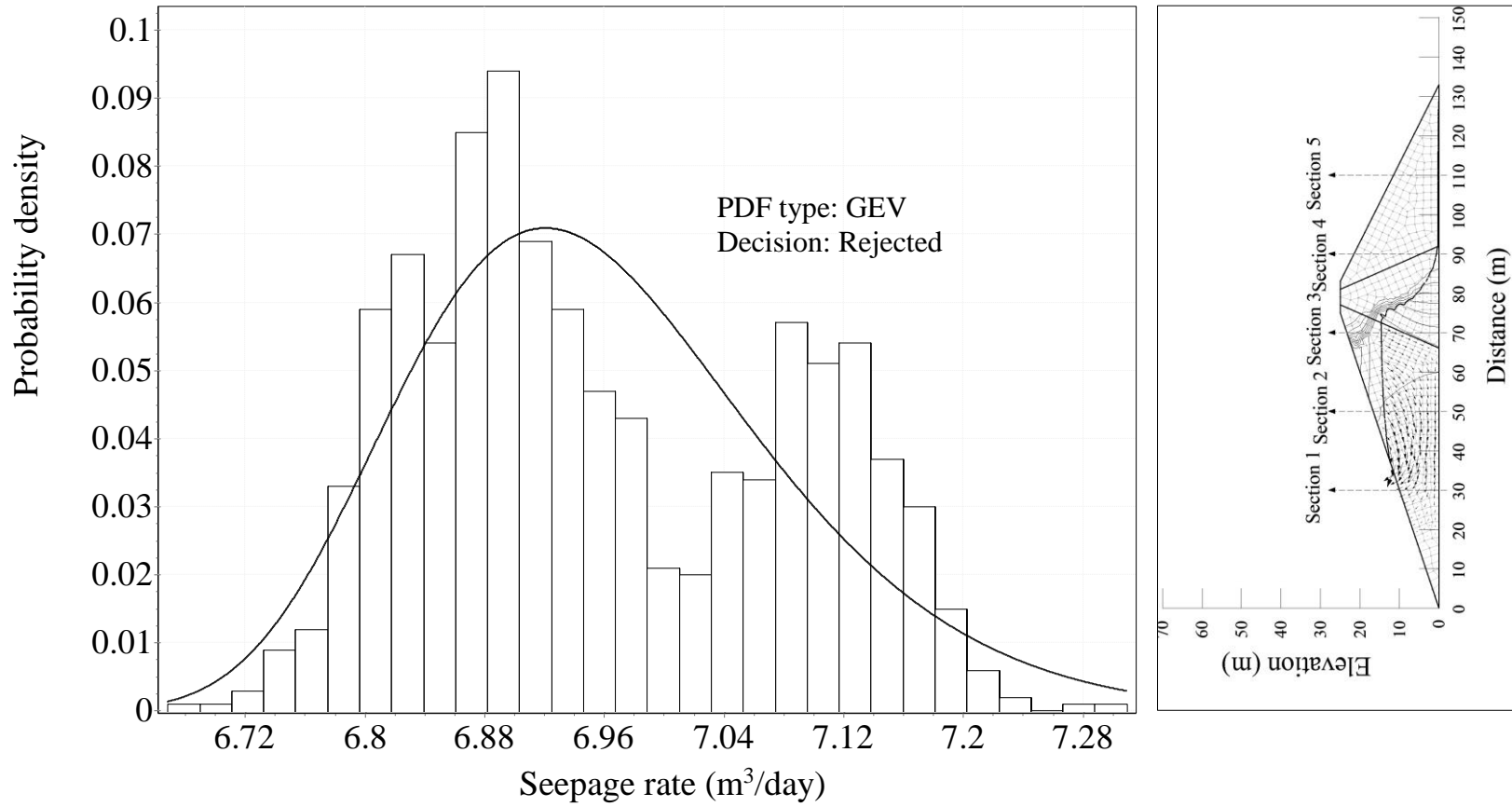


Figure 6.43 Frequency histogram of Q through the simple zoned dam for the combined fill and drawdown case when t=4 days at Section 2.

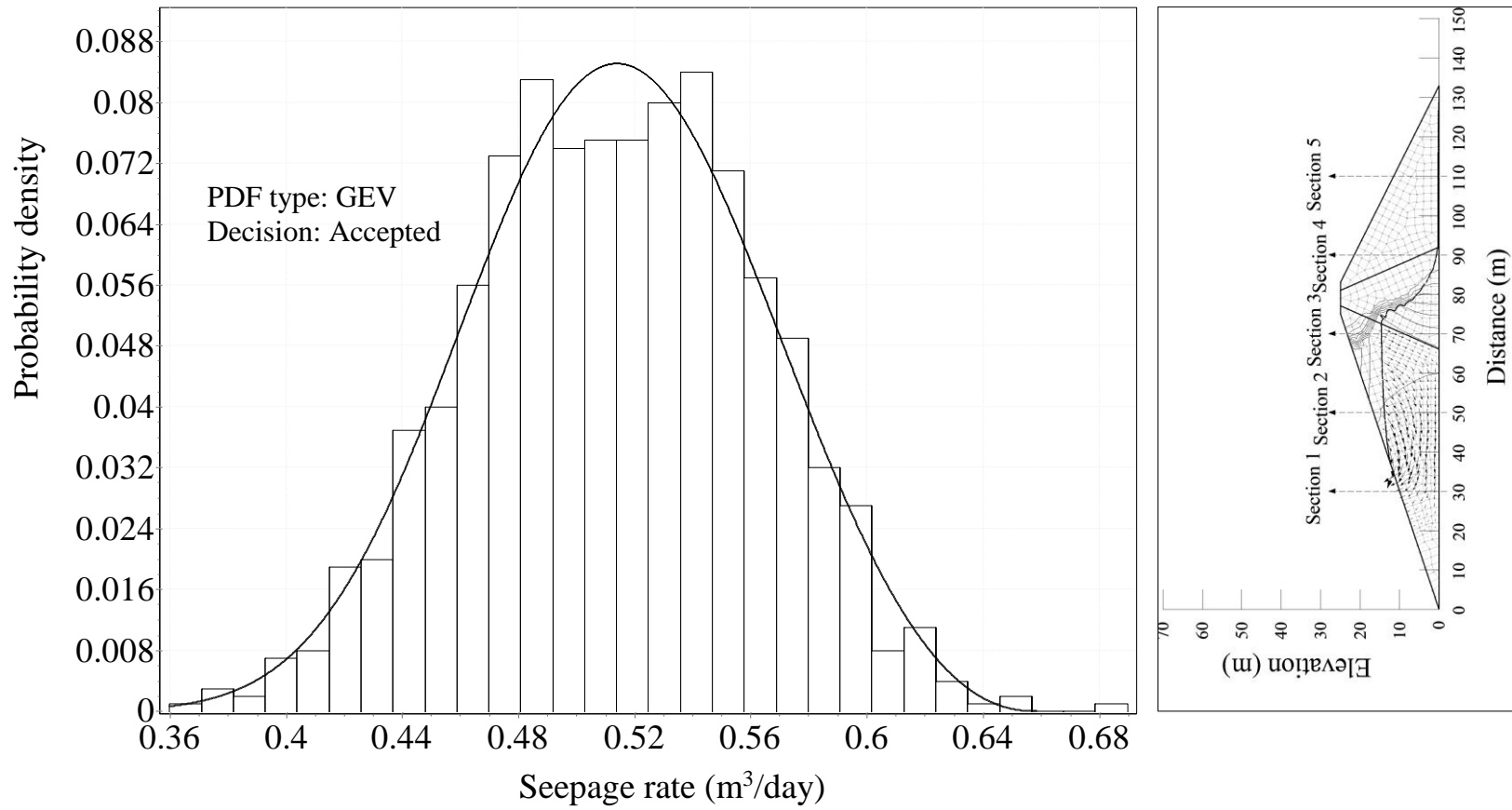


Figure 6.44 Frequency histogram of  $Q$  through the simple zoned dam for the combined fill and drawdown case when  $t=4$  days at Section 3.

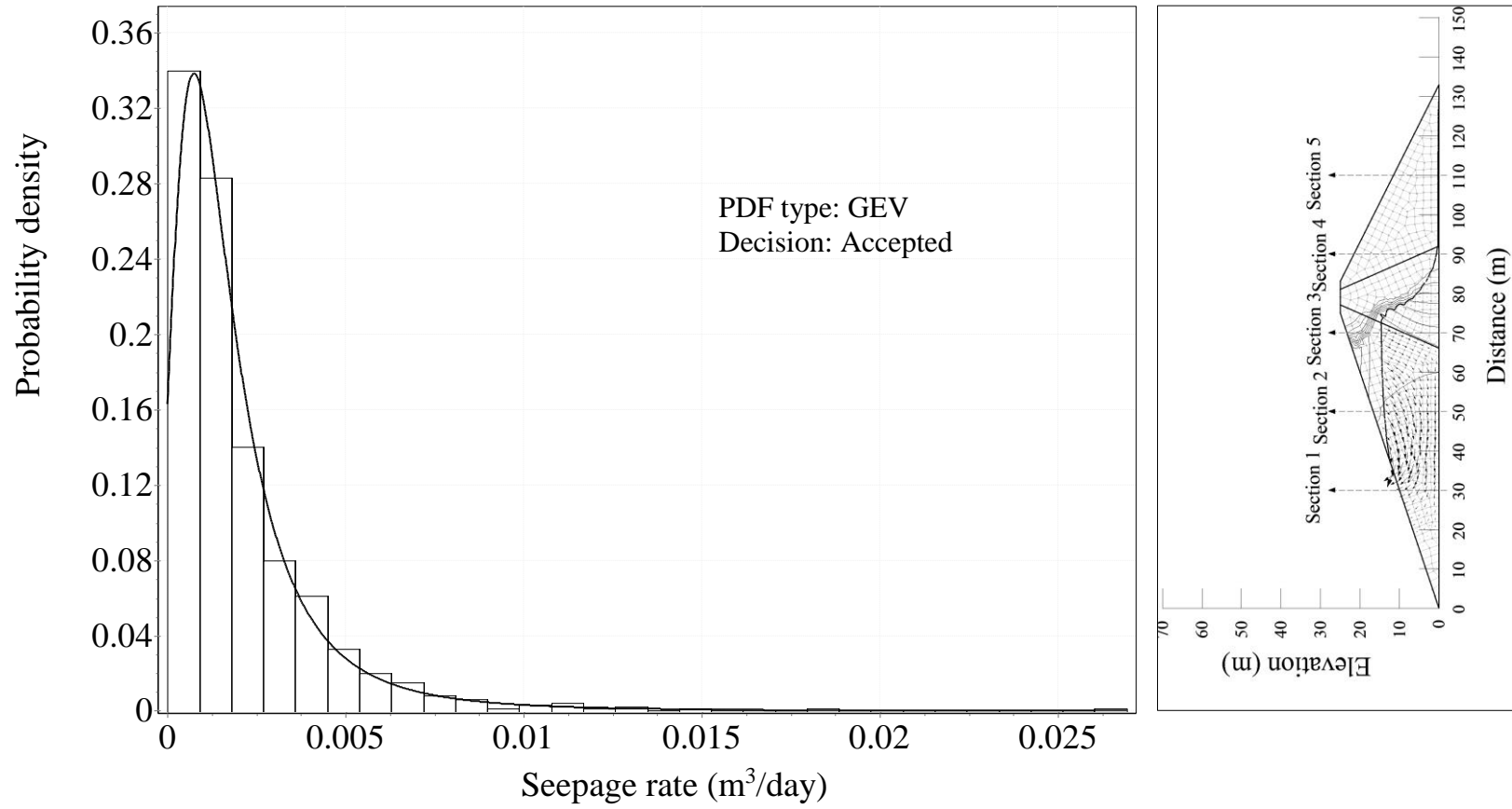


Figure 6.45 Frequency histogram of Q through the simple zoned dam for the combined fill and drawdown case when t=4 days at Section 4.

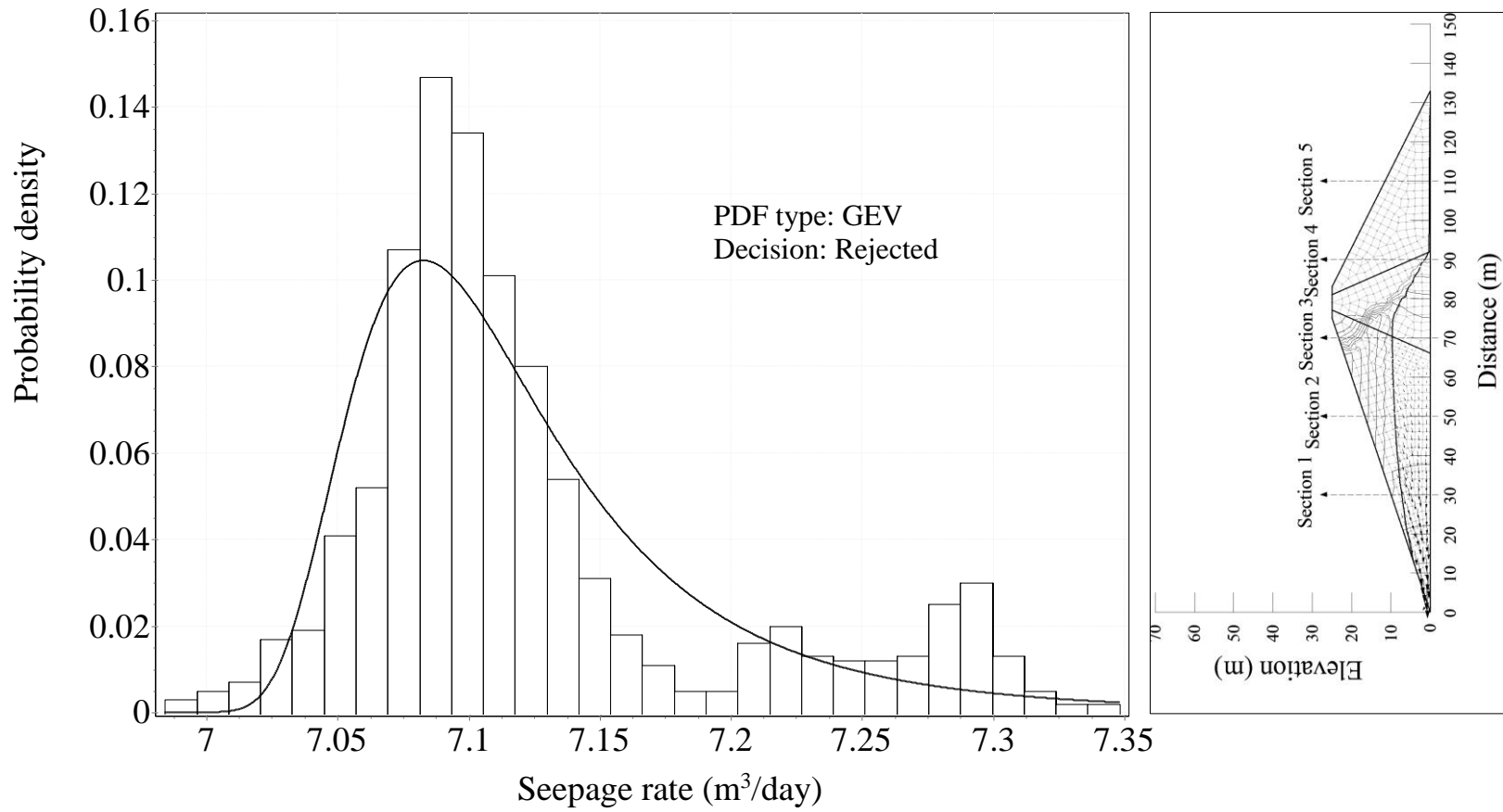


Figure 6.46 Frequency histogram of  $Q$  through the simple zoned dam for the combined fill and drawdown case when  $t=6$  days at Section 1.

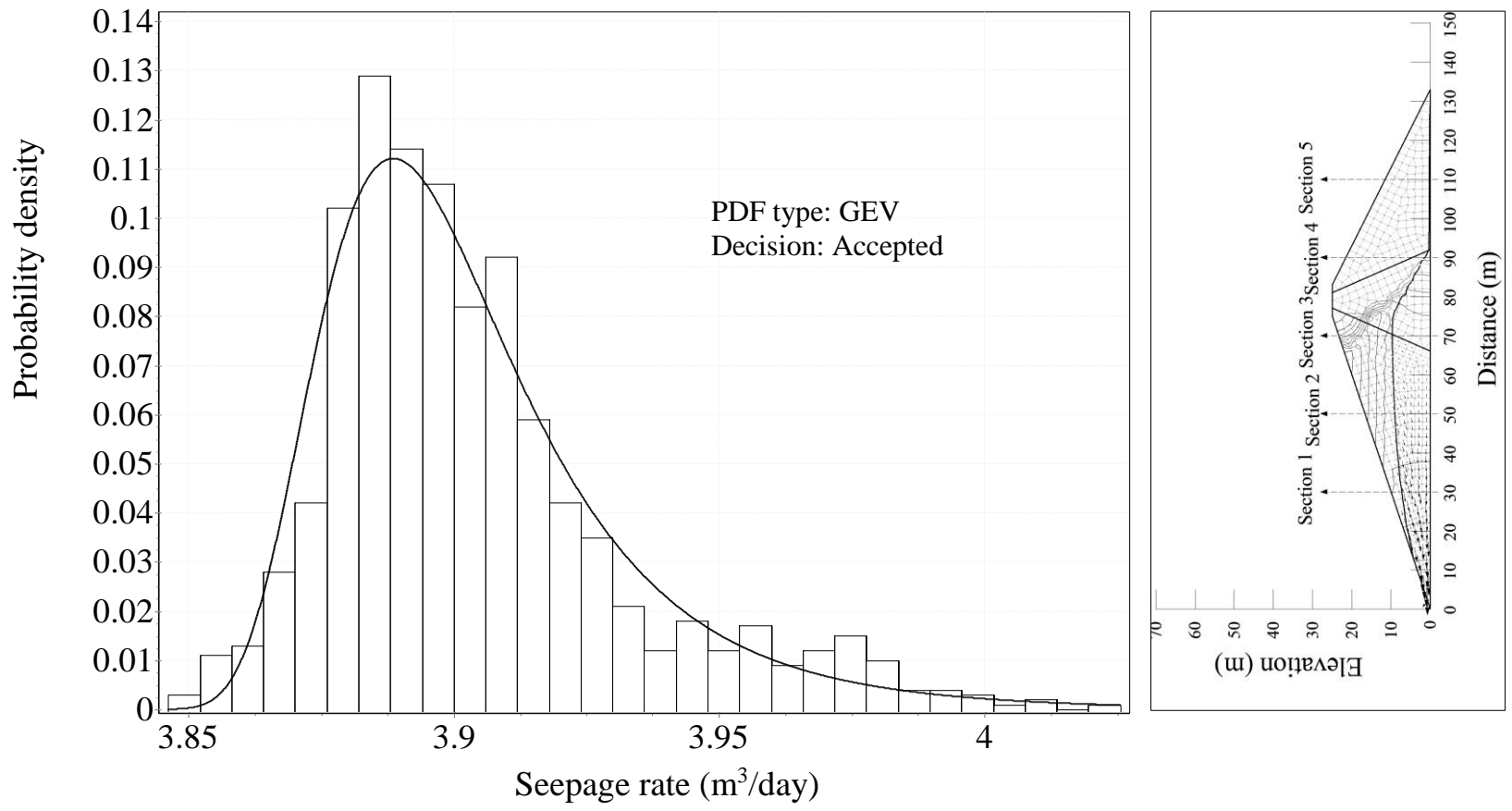


Figure 6.47 Frequency histogram of Q through the simple zoned dam for the combined fill and drawdown case when t=6 days at Section 2.

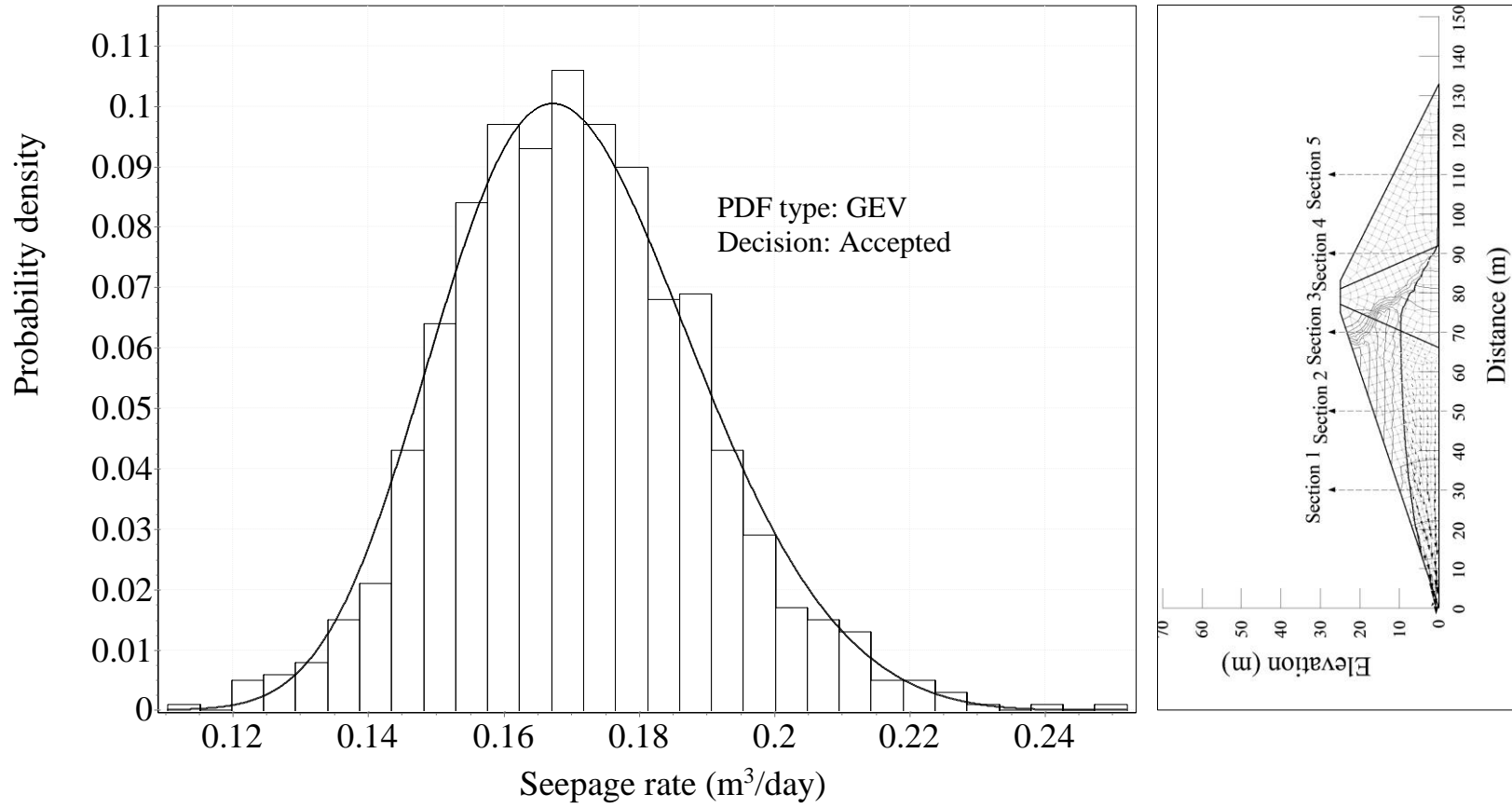


Figure 6.48 Frequency histogram of Q through the simple zoned dam for the combined fill and drawdown case when t=6 days at Section 3.

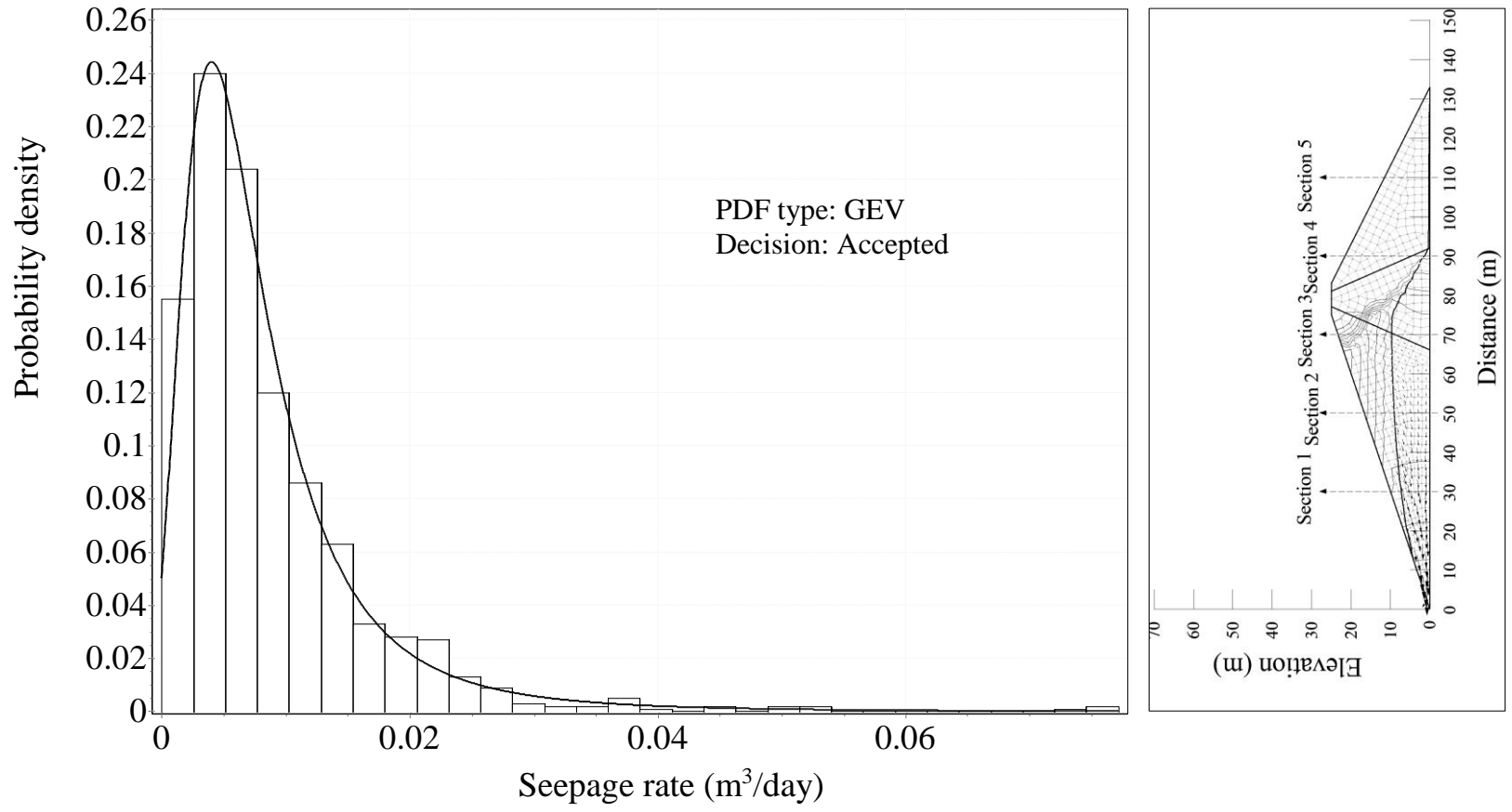


Figure 6.49 Frequency histogram of  $Q$  through the simple zoned dam for the combined fill and drawdown case when  $t=6$  days at Section 4.

## CHAPTER 7

### DISCUSSION

The present study is aimed to investigate effect of uncertainties in soil characteristics in seepage through embankment dams. This is achieved via the findings of the following two parts of the study:

- The sensitivity analyses that are conducted for steady and unsteady seepage presented the individual variation effects of the random parameters,
- The application problems revealed the probabilistic properties and randomness of the seepage rate for various boundary conditions and embankment dam types.

The uncertainty of soil properties are limited with the randomness of hydraulic conductivity and van Genuchten fitting parameters for SWCC,  $\alpha$  and  $n$ .

The results of the sensitivity analyses presented the variation effects of hydraulic conductivity,  $\alpha$  and  $n$ . According to the results:

- The assumption of random variable model for hydraulic conductivity resulted in seepage rates smaller than that obtained from the deterministic solution. This is observed for all values of  $COV(K)$  and for both steady and transient seepage conditions. Also, the mean seepage rate decreases with the increase in  $COV(K)$ . When the  $COV(K)$  is doubled, the mean seepage rate decreases up to 50% depending on the material type, boundary conditions and type of the embankment. Because, when the hydraulic conductivity

substantially changes from one point to another neighboring point, the flow path tends to extend to follow regions having higher hydraulic conductivities. This causes a decrease in the flow rate. Similar findings were also presented by Ahmed (2009) and it was suggested that there might not be a need for a core if the embankment dam is made of materials having high degree of variability. However, the mean seepage rate is presented to be not affected by the variation of hydraulic conductivity if the embankment material is coarse grained. For the case, when  $COV(K)$  is increased, even if it is doubled, only the range of the computed seepage rate and  $COV(Q)$  increases; the mean flow rate does not change. This can be attributed to the low variation degree of coarse grained materials. Due to small variability, hydraulic conductivity tends to be uniform across the dam body for this type of materials.

- The mean steady-state flow rate is not sensitive to variations in  $\alpha$  and  $n$ . In other words, the changes in  $COV(\alpha)$  and  $COV(n)$  do not affect the mean flow rate. However, the mean flows computed for transient flow conditions are shown to be susceptible to the random variation of fitting parameters. There is no relative importance between two parameters; their variation have similar impacts. The impacts are shown to be minor.

In the light of above findings, the randomness of hydraulic conductivity is strongly suggested to be considered in seepage modeling. Some exceptional cases may occur if the coefficient of variation of hydraulic conductivity is smaller than 0.05, which can be considered as a very small degree in both geotechnical engineering (Jones et al. 2002) and hydraulic engineering applications (Johnson 1996). It is reasonable to adopt deterministic models and keep the hydraulic conductivity constant for those cases.

The treatment of  $\alpha$  and  $n$  as deterministic variables may not be misleading in estimation of the steady-state seepage rate. For practical applications, one may compute also the transient seepage considering them as deterministic variables. This

may not introduce major errors. However, a proper theoretical investigation of the transient seepage properties in embankments needs stochastic definitions for these parameters.

The application problems of the present study illustrated that the uncertainties of input parameters produce uncertainty in the seepage rate which can be represented by probability distributions. These distributions are defined with statistical moments and probability density functions. The goodness of fit tests are conducted to represent the range of the flow data obtained from Monte Carlo simulation. The investigation of the statistical moments and the probability distributions of the flow may help understanding the variability of the seepage:

- For the rapid fill case,  $COV(Q)$  is found to decrease with time; however, it is not substantially affected by time for the rapid drawdown case. Also, it is presented to be higher for the rapid fill case. Therefore, the behavior of the degree of seepage rate variability (i.e.  $COV(Q)$ ) strongly depends on time and boundary conditions.
- The seepage through coarse grained materials is shown to have smaller  $COV$  values. This can be explained by the fact that coarse grained materials exhibit low variability. Then, it can be said that  $COV(Q)$  also depends on the material and embankment dam type.
- The variation coefficient of the response parameter decreases when it is compared with that of the input parameters. The  $COV(Q)$  is found to be smaller than the maximum variability degree of the input parameters (i.e.  $K$ ,  $\alpha$  and  $n$ ) for all application problems. This means, the embankment dam systems decreases the uncertainty degree of the input parameter.
- Commonly, good fits are provided by generalized extreme value (GEV) and three-parameter log-normal (LN-3P) density functions for the seepage rate. The seepage rate distributions which are shown to be rejected by goodness of fit tests, also cannot be fitted by other common probability density

functions. The hypotheses are generally rejected when excessive skewness or peakedness are observed due to flow extremities. This is mainly observed for insignificantly small flow rates. However, even for the rejected hypotheses, GEV and LN-3P distributions are seen to reasonably capture the peak, asymmetry and curvature of the tails of the probability distributions of the seepage. Similarly, Le et al. (2012) studied the probability distribution of the transient seepage and they concluded that the seepage data can be well represented using log-normal distribution. It should be noted that log-normal distribution is a common function used in describing geotechnical parameters. Besides, the generalized extreme value distribution is a common function used in hydraulic engineering, particularly used in describing hydrological variables (Martins and Stedinger 2000).

The findings of the research have clearly demonstrated the uncertainty effects of soil parameters, variation degree of the seepage rate and possible probability density distributions used to describe the flow. The findings of the sensitivity analyses may provide design engineers conducting seepage analysis guidance in determining which parameters to treat as stochastic and which others as deterministic. Also, one may benefit from probability density functions in assessing the reliability of the embankment dams with respect to some tendencies, such as piping. However, it should be noted that further estimations and computations are needed for risk assessment studies. Finally, the results on variation degree of the seepage rate give awareness to professionals working on the subject that each seepage problem in embankment dams is unique.

## CHAPTER 8

### CONCLUSIONS

#### 8.1 Summary

The actual field conditions of soils exhibit variations in some degree in space. The variability leads to uncertainties in material properties of soils, and this is a governing factor in their seepage, stability, and consolidation behavior. In most of the practical hydraulic and geotechnical engineering applications, the variability of soil properties is ignored in the analyses. In particular, seepage analysis through embankment dams is handled using deterministic models assuming constant soil properties. However, the seepage through embankments involves uncertainties due to the lack of knowledge of soil's hydraulic and physical properties. In this context, this study investigates the effects of uncertainties of hydraulic conductivity and soil-water characteristic curve fitting parameters,  $\alpha$  and  $n$  on the seepage through embankments. The Monte Carlo simulation technique having a random variable generator is coupled with finite element modeling software SEEP/W. Using the proposed methodology, uncertainty based analyses are conducted on steady and transient seepage through embankment dams. The parameters whose variability has significant effects on the seepage rate are determined. Then, the statistical properties of the flow rate are investigated by some application problems.

## 8.2 Novelty of the Study

The merit of the study is based on the consideration and inclusion of the following items, analyses and results:

- The water flow through the unsaturated part (i.e. the part above of the phreatic surface of seepage) of the embankment dam is taken into consideration regarding the uncertainties in soil-water content function fitting parameters. The variability of  $\alpha$  and  $n$  and their effects on the seepage are not widely studied in the previous studies.
- The statistical properties of fitting parameters,  $\alpha$  and  $n$  is extensively investigated using the related literature and the data of 203 different soils obtained from a large database system (SoilVision software) allocating the properties (including hydraulic and geotechnical properties) of several soil types gathered from many sites all over the world. At first, the dependence and correlation between  $\alpha$  and  $n$  is investigated and it is determined that they can be assumed as uncorrelated variables. Then, their statistical moments including the mean and coefficient of variation values are determined and justified using both the literature and the data of soil samples. Previous studies dealing with stochastic seepage analysis were mainly based on hypothetical statistical properties or the use of limited number of soil data obtained from limited sites. Therefore, it can be said that this study increased the statistical significance on random soil parameters.
- For the random variable generation of hydraulic conductivity, and fitting parameters  $\alpha$  and  $n$ , a C# code is developed. The code consists of two sub-functions and two main parts for random variable generation. The sub-functions computes the relative hydraulic conductivity and water content function of the soil, whereas the main part generates random variables for the parameters and call the sub-functions. This code runs as an add-in in SEEP/W and gives the software the capability of modeling soil uncertainties.

This is an enhancement made by the study for practical applications using SEEP/W as a tool for seepage analysis.

- The capability of conducting Monte Carlo simulations is brought to the software SEEP/W via some batch files written in Windows command line. This is also an enhancement for practical applications using SEEP/W as a tool for seepage analysis.
- The study included sensitivity analyses for hydraulic conductivity and fitting parameters  $\alpha$  and  $n$  to investigate the relative importance of variability of the parameters on both steady-state and transient seepage. The individual variation effects of the parameters are presented. No previous study has highlighted these effects before.
- Considering the outcomes of the conducted sensitivity analyses, time-dependent variations in seepage conditions, such as the case of rapid drawdown and rapid fill are investigated considering random variations of aforementioned parameters. The seepage rate statistics of embankment dams are examined determining descriptive statistics of the flow rate and deriving their frequency histograms. Also, probability density functions are fitted to describe the seepage rate. A further process on the probability distributions of the flow may yield the probability of occurrence of internal erosion, piping, etc. if threshold values are known for these cases.

### **8.3 Conclusions**

The main findings and contributions of the study to the field can be summarized as follows:

- The variation of hydraulic conductivity of fine grained materials has significant effects on the steady-state seepage. The mean flow rate decreases with the increase of hydraulic conductivity variation. If highly variable fine grained materials are used as embankment material the decrease in the flow

may allow redesign of a prospective core. However, hydraulic conductivity variation effects of coarse grained materials are found to be minor since they generally have low variability. Also, the variations of van Genuchten SWCC fitting parameters are demonstrated to have negligible impacts for the steady-state seepage through both fine and coarse grained materials.

- The findings of the sensitivity analyses on transient seepage presented the substantial effects of hydraulic conductivity variation on the flow for both rapid drawdown and fill cases. The seepage is sensitive to the variation of van Genuchten fitting parameters in a small degree.
- The degree of uncertainty of the seepage rate is found to be dependent on boundary conditions, time and embankment material type. It does not significantly change with time during the rapid drawdown case; however, it decreases with time for the rapid fill case. Besides, the seepage variability is found to be higher in rapid fill case when it is compared with that of the rapid drawdown case. It is also shown to have smaller values if the embankment material is made of coarse grained materials.
- Finally, log-normally distributed random input variables produces probability density functions for the seepage rate which are most commonly defined by generalized extreme value (GEV) and three-parameter log-normal (LN-3P) distributions.

#### **8.4 Suggested Future Research**

Through the course of this study, several aspects of unsaturated flow modeling, random parameter assumption and random input generation came into the picture. However, due to the research limitations considered some of them were not included in the scope of the study. Consideration of these aspects is thought to be beneficial for the future research on uncertainty based analysis of seepage through embankment dams. Brief descriptions of these aspects are given below for the researchers and professionals working on the subject:

- The hysteresis effect in unsaturated soil results in different behaviors during wetting and drying processes of the soil. The further research considering the hysteresis effect would investigate the transient unsaturated seepage behavior of the embankment more realistically. Also, the uncertainty of SWCC fitting parameters of both wetting and drying curves is suggested to be considered in the further research.
- Compacted clay soil may exhibit anisotropy. Its hydraulic conductivity may vary in x and y directions with different statistical properties. The anisotropy of clay cores of embankment dams may be considered in a future stochastic seepage analysis.
- For very long durations of transient cases, the water evaporating from the body of the embankment dam changes the water content of the soil. This may result in a change in the behavior of its unsaturated part. The effect of evaporation on the seepage through embankment dams may be the subject of a future study.
- The transient unsaturated seepage analysis needs definition of saturated and residual water contents of the soil. Further research may consider the uncertainties in these two water content parameters of the soil. This may help definition of unsaturated soil properties more realistically, and more accurate investigations can be made for the probabilistic nature of the seepage.
- The uncertainties in the analysis of seepage through embankment dams is limited to the uncertainty of some soil properties in the study. However, the hydrological parameters in a basin and the inflow into a reservoir of an embankment dam are also uncertain, resulting in randomness in boundary conditions. Consideration of the uncertainties in boundary conditions would aid investigation of probabilistic behavior of the seepage more accurate.
- The author is aware of the physical difference between random variable model and random field assumption. The random field assumption considers

the correlation in the random variable, whereas the random variable model assumes no correlation in the field; parameters are generated without dependence. Random field model generate varying parameters with distance, which is identified with a scale of fluctuation or correlation distance. It is clear that the latter one is more realistic in defining soil properties. Therefore, it is suggested for future stochastic seepage studies which will be based on the procedure of the current study to consider the correlation in the random fields of their parameters.

## REFERENCES

- Ahmed, A. (2008). "Saturated-Unsaturated Flow through Leaky Dams." *Journal of Geotechnical and Geoenvironmental Engineering*, American Society of Civil Engineers, 134(10), 1564–1568.
- Ahmed, A. (2012). "Stochastic Analysis of Seepage under Hydraulic Structures Resting on Anisotropic Heterogeneous Soils." *Journal of Geotechnical and Geoenvironmental Engineering*, American Society of Civil Engineers, 139(6), 1001–1004.
- Ahmed, A. A. (2009). "Stochastic analysis of free surface flow through earth dams." *Computers and Geotechnics*, 36(7), 1186–1190.
- Ahmed, A., McLoughlin, S., and Johnston, H. (2014). "3D Analysis of Seepage under Hydraulic Structures with Intermediate Filters." *Journal of Hydraulic Engineering*, American Society of Civil Engineers, 6014019.
- Ang, A. H.-S., and Tang, W. H. (1975). *Probability Concepts in Engineering Planning and Design Vol. 1: Basic Principles*. John Wiley & Sons, New York.
- Aral, M., and Maslia, M. (1983). "Unsteady Seepage Analysis of Wallace Dam." *Journal of Hydraulic Engineering*, American Society of Civil Engineers, 109(6), 809–826.
- Bakr, A. A., Gelhar, L. W., Gutjahr, A. L., and MacMillan, J. R. (1978). "Stochastic analysis of spatial variability in subsurface flows: 1. Comparison of one- and three-dimensional flows." *Water Resour. Res.*, AGU, 14(5), 953–959.
- Bathe, K.-J., and Khoshgoftaar, M. R. (1979). "Finite element free surface seepage analysis without mesh iteration." *International Journal for Numerical and Analytical Methods in Geomechanics*, John Wiley & Sons, Ltd, 3(1), 13–22.
- Bennion, D. W., and Griffiths, J. C. (1966). "A Stochastic Model for Predicting Variations in Reservoir Rock Properties." *SPE Journal*, Society of Petroleum Engineers, 6(1), 9–16.

- Box, G. E. P., and Muller, M. E. (1958). "A Note on the Generation of Random Normal Deviates." *The Annals of Mathematical Statistics*, 29(2), 610–611.
- Bresler, E., and Dagan, G. (1983a). "Unsaturated flow in spatially variable fields: 2. Application of water flow models to various fields." *Water Resources Research*, 19(2), 421–428.
- Bresler, E., and Dagan, G. (1983b). "Unsaturated flow in spatially variable fields: 3. Solute transport models and their application to two fields." *Water Resources Research*, 19(2), 429–435.
- Brooks, R. H., and Corey, A. T. (1964). "Properties of Porous Media Affecting Fluid Flow." *ASCE Journal of the Irrigation and Drainage Division*, 92(2), 61–90.
- Brutsaert, W. (1966). "Probability laws for pore size distributions." *Soil Science*, 101, 85–92.
- Bulnes, A. C. (1946). "An Application of Statistical Methods to Core Analysis Data of Dolomitic Limestone." *Transactions of the AIME, Society of Petroleum Engineers*, 165(1), 223–240.
- Burdine, N. T. (1953). "Relative permeability calculations from pore size distribution data." *Journal of Petroleum Engineering*, 5, 71–78.
- Caffisch, R. E. (1998). "Monte Carlo and quasi-Monte Carlo methods." *Acta Numerica*, 1–49.
- Carsel, R. F., and Parrish, R. S. (1988). "Developing joint probability distributions of soil water retention characteristics." *Water Resources Research*, 24(5), 755–769.
- Chalermyanont, T., and Benson, C. (2004). "Reliability-Based Design for Internal Stability of Mechanically Stabilized Earth Walls." *Journal of Geotechnical and Geoenvironmental Engineering*, American Society of Civil Engineers, 130(2), 163–173.
- Chang, C., Tung, Y., and Yang, J. (1994). "Monte Carlo Simulation for Correlated Variables with Marginal Distributions." *Journal of Hydraulic Engineering*, American Society of Civil Engineers, 120(3), 313–331.
- Cheng, Y., Phoon, K., and Tan, T. (2008). "Unsaturated Soil Seepage Analysis Using a Rational Transformation Method with Under-Relaxation." *International Journal of Geomechanics*, American Society of Civil Engineers, 8(3), 207–212.

- Cho, S. E. (2007). "Effects of spatial variability of soil properties on slope stability." *Engineering Geology*, 92(3-4), 97-109.
- Cho, S. E. (2012). "Probabilistic analysis of seepage that considers the spatial variability of permeability for an embankment on soil foundation." *Engineering Geology*, 133-134(0), 30-39.
- Chu-Agor, M., Wilson, G., and Fox, G. (2008). "Numerical Modeling of Bank Instability by Seepage Erosion Undercutting of Layered Streambanks." *Journal of Hydrologic Engineering*, American Society of Civil Engineers, 13(12), 1133-1145.
- Dagan, G., and Bresler, E. (1983). "Unsaturated flow in spatially variable fields: 1. Derivation of models of infiltration and redistribution." *Water Resources Research*, 19(2), 413-420.
- Elkateb, T., Chalaturnyk, R., and Robertson, P. K. (2003). "An overview of soil heterogeneity: quantification and implications on geotechnical field problems." *Canadian Geotechnical Journal*, NRC Research Press, 40(1), 1-15.
- Eykholt, G. R., Elder, C. R., and Benson, C. H. (1999). "Effects of aquifer heterogeneity and reaction mechanism uncertainty on a reactive barrier." *Journal of Hazardous Materials*, 68(1-2), 73-96.
- Fenton, G., and Griffiths, D. (1996). "Statistics of Free Surface Flow through Stochastic Earth Dam." *Journal of Geotechnical Engineering*, ASCE, 122(6), 410-427.
- Fenton, G., and Griffiths, D. (1997). "Extreme Hydraulic Gradient Statistics in Stochastic Earth Dam." *Journal of Geotechnical and Geoenvironmental Engineering*, American Society of Civil Engineers, 123(11), 995-1000.
- Fenton, G., and Vanmarcke, E. (1990). "Simulation of Random Fields via Local Average Subdivision." *Journal of Engineering Mechanics*, American Society of Civil Engineers, 116(8), 1733-1749.
- Foster, D., Bole, D., and Deere, T. (2014). "Rio Grande Dam - Seepage Reduction Design and Construction." *Rocky Mountain Geo-Conference 2014*, American Society of Civil Engineers, 31-58.
- Foster, M., Fell, R., and Spannagle, M. (2000). "The statistics of embankment dam failures and accidents." *Canadian Geotechnical Journal*, NRC Research Press, 37(5), 1000-1024.

- Fredlund, D. G., and Morgenstern, N. R. (1976). "Constitutive relations for volume change in unsaturated soils." *Canadian Geotechnical Journal*, NRC Research Press, 13(3), 261–276.
- Fredlund, D. G., and Morgenstern, N. R. (1977). "Stress State Variables for Unsaturated Soils." *Journal of the Geotechnical Engineering Division*, 103(5), 447–466.
- Fredlund, D. G., and Xing, A. (1994). "Equations for the soil-water characteristic curve." *Canadian Geotechnical Journal*, NRC Research Press, 31(4), 521–532.
- Fredlund, M. (2005). "SoilVision-A Knowledge Based Database System for Saturated/Unsaturated Soil Properties." SoilVision Systems Ltd., Saskatchewan.
- Freeze, R. A. (1975). "A stochastic-conceptual analysis of one-dimensional groundwater flow in nonuniform homogeneous media." *Water Resour. Res.*, AGU, 11(5), 725–741.
- Fu, J., and Jin, S. (2009). "A study on unsteady seepage flow through dam." *Journal of Hydrodynamics, Ser. B*, 21(4), 499–504.
- Gardner, W. (1956). "Mathematics of isothermal water conduction in unsaturated soils." *International Symposium on Physico-Chemical Phenomenon in Soils*, Washington, D.C., 78–87.
- Geo-Slope Int Ltd. (2013). *Seepage Modeling with SEEP/W*. Geo-Slope International Ltd., Calgary.
- Geo-Slope Int Ltd. (2014). "Groundwater Seepage Analysis with SEEP/W." <<http://www.geo-slope.com/products/seepw.aspx>>.
- Geo-Slope Int. Ltd. (2012). *GeoStudio Add-Ins Programming Guide and Reference*. Geo-Slope International Ltd., Calgary, 61.
- Ghanbarian-Alavijeh, B., Liaghat, A., Huang, G.-H., and van Genuchten, M. T. (2010). "Estimation of the van Genuchten Soil Water Retention Properties from Soil Textural Data." *Pedosphere*, 20(4), 456–465.
- Golder, E. R., and Settle, J. G. (1976). "The Box-Muller Method for Generating Pseudo-Random Normal Deviates." *Journal of the Royal Statistical Society. Series C (Applied Statistics)*, Wiley for the Royal Statistical Society, 25(1), 12–20.

- Griffiths, D., and Fenton, G. (1997). "Three-Dimensional Seepage through Spatially Random Soil." *Journal of Geotechnical and Geoenvironmental Engineering*, American Society of Civil Engineers, 123(2), 153–160.
- Griffiths, D., and Fenton, G. (1998). "Probabilistic Analysis of Exit Gradients due to Steady Seepage." *Journal of Geotechnical and Geoenvironmental Engineering*, American Society of Civil Engineers, 124(9), 789–797.
- Griffiths, D., and Fenton, G. (2004). "Probabilistic Slope Stability Analysis by Finite Elements." *Journal of Geotechnical and Geoenvironmental Engineering*, American Society of Civil Engineers, 130(5), 507–518.
- Griffiths, D., Huang, J., and Fenton, G. (2009). "Influence of Spatial Variability on Slope Reliability Using 2-D Random Fields." *Journal of Geotechnical and Geoenvironmental Engineering*, American Society of Civil Engineers, 135(10), 1367–1378.
- Griffiths, D. V., and Fenton, G. A. (1993). "Seepage beneath water retaining structures founded on spatially random soil." *Géotechnique*, 43(4), 577–587.
- Gui, S., Zhang, R., Turner, J., and Xue, X. (2000). "Probabilistic Slope Stability Analysis with Stochastic Soil Hydraulic Conductivity." *Journal of Geotechnical and Geoenvironmental Engineering*, American Society of Civil Engineers, 126(1), 1–9.
- Gutjahr, A. L., and Gelhar, L. W. (1981). "Stochastic models of subsurface flow: infinite versus finite domains and stationarity." *Water Resources Research*, 17(2), 337–350.
- Gutjahr, A. L., Gelhar, L. W., Bakr, A. A., and MacMillan, J. R. (1978). "Stochastic analysis of spatial variability in subsurface flows: 2. Evaluation and application." *Water Resources Research*, 14(5), 953–959.
- Hoa, N. T., Gaudu, R., and Thirriot, C. (1977). "Influence of the hysteresis effect on transient flows in saturated-unsaturated porous media." *Water Resources Research*, 13(6), 992–996.
- Husein Malkawi, A. I., Hassan, W. F., and Abdulla, F. A. (2000). "Uncertainty and reliability analysis applied to slope stability." *Structural Safety*, 22(2), 161–187.
- Jacobson, T. (2013). "An Analysis on Soil Properties on Predicting Critical Hydraulic Gradients for Piping Progression in Sandy Soils." Utah State University.

- Jiang, S., Li, D., Cao, Z., Zhou, C., and Phoon, K. (2014). "Efficient System Reliability Analysis of Slope Stability in Spatially Variable Soils Using Monte Carlo Simulation." *Journal of Geotechnical and Geoenvironmental Engineering*, American Society of Civil Engineers, 4014096.
- Johnson, P. (1996). "Uncertainty of Hydraulic Parameters." *Journal of Hydraulic Engineering*, American Society of Civil Engineers, 122(2), 112–114.
- Jones, A. L., Kramer, S. L., and Arduino, P. (2002). *Estimation of Uncertainty in Geotechnical Properties for Performance-Based Earthquake Engineering*. Berkeley, 104.
- L'Ecuyer, P. (2012). "Random Number Generation." *Handbook of Computational Statistics SE - 3*, Springer Handbooks of Computational Statistics, J. E. Gentle, W. K. Härdle, and Y. Mori, eds., Springer Berlin Heidelberg, 35–71.
- Lam, L., and Fredlund, D. G. (1984). "Saturated-Unsaturated Transient Finite Element Seepage Model for Geotechnical Engineering." *Finite Elements in Water Resources SE - 10*, J. P. Laible, C. A. Brebbia, W. Gray, and G. Pinder, eds., Springer Berlin Heidelberg, 113–122.
- Law, J. (1944). "A Statistical Approach to the Interstitial Heterogeneity of Sand Reservoirs." *Transactions of the AIME*, Society of Petroleum Engineers, 155(1), 202–222.
- Le, T. M. H., Gallipoli, D., Sanchez, M., and Wheeler, S. J. (2012). "Stochastic analysis of unsaturated seepage through randomly heterogeneous earth embankments." *International Journal for Numerical and Analytical Methods in Geomechanics*, John Wiley & Sons, Ltd, 36(8), 1056–1076.
- Li, W., Lu, Z., and Zhang, D. (2009). "Stochastic analysis of unsaturated flow with probabilistic collocation method." *Water Resources Research*, 45(8), W08425.
- Likos, W., Lu, N., and Godt, J. (2014). "Hysteresis and Uncertainty in Soil Water-Retention Curve Parameters." *Journal of Geotechnical and Geoenvironmental Engineering*, American Society of Civil Engineers, 140(4), 4013050.
- Lin, G.-F., and Chen, C.-M. (2004). "Stochastic analysis of spatial variability in unconfined groundwater flow." *Stochastic Environmental Research and Risk Assessment*, Springer-Verlag, 18(2), 100–108.
- Liu, G. R., and Quek, S. S. (2003). *Finite Element Method: A Practical Course*. Butterworth Heinemann.

- Lu, N., and Godt, J. (2008). "Infinite slope stability under steady unsaturated seepage conditions." *Water Resources Research*, 44(11), W11404.
- Lu, N., and Likos, W. J. (2004). *Unsaturated Soil Mechanics*. John Wiley & Sons, Inc., New Jersey.
- Mantoglou, A. (1992). "A theoretical approach for modeling unsaturated flow in spatially variable soils: Effective flow models in finite domains and nonstationarity." *Water Resources Research*, 28(1), 251–267.
- Mantoglou, A., and Gelhar, L. W. (1987). "Stochastic modeling of large-scale transient unsaturated flow systems." *Water Resources Research*, 23(1), 37–46.
- Maqsoud, A., Bussiere, B., Chaire, M. M., and Chaire, M. A. (2004). "Hysteresis Effects On The Water Retention Curve: A Comparison Between Laboratory Results And Predictive Models ." *57TH Canadian Geotechnical Conference*, 8–15.
- Martins, E. S., and Stedinger, J. R. (2000). "Generalized maximum-likelihood generalized extreme-value quantile estimators for hydrologic data." *Water Resources Research*, 36(3), 737–744.
- Massey Jr., F. J. (1951). "The Kolmogorov-Smirnov Test for Goodness of Fit." *Journal of the American Statistical Association*, Taylor & Francis, Ltd. on behalf of the American Statistical Association, 46(253), 68–78.
- Mathwave. (2013). "EasyFit – Distribution Fitting Software." <<http://www.mathwave.com/en/home.html>>.
- McMillan, W. D. (1966). *Theoretical analysis of groundwater basin operations*. Hydraulic Laboratory, University of California, Berkeley, 167.
- Meunier, A. (2005). *Clays*. Springer, Berlin, 472p.
- Money, R. (2006). "Comparison of 2D and 3D Seepage Model Results for Excavation near Levee Toe." *GeoCongress 2006*, American Society of Civil Engineers, 1–4.
- Mualem, Y. (1976). "A new model for predicting the hydraulic conductivity of unsaturated porous media." *Water Resources Research*, 12(3), 513–522.
- Neuman, S. (1973). "Saturated-Unsaturated Seepage by Finite Elements." *ASCE Journal of the Hydraulics Division*, 99(12), 2233–2250.

- Neuman, S. P., and Witherspoon, P. A. (1970). "Finite Element Method of Analyzing Steady Seepage with a Free Surface." *Water Resources Research*, 6(3), 889–897.
- Neuman, S. P., and Witherspoon, P. A. (1971). "Analysis of Nonsteady Flow with a Free Surface Using the Finite Element Method." *Water Resources Research*, 7(3), 611–623.
- Ng, C. W. W., and Shi, Q. (1998a). "Influence of rainfall intensity and duration on slope stability in unsaturated soils." *Quarterly Journal of Engineering Geology*, 31(2), 105–113.
- Ng, C. W. W., and Shi, Q. (1998b). "A numerical investigation of the stability of unsaturated soil slopes subjected to transient seepage." *Computers and Geotechnics*, 22(1), 1–28.
- Oh, W. T., and Vanapalli, S. K. (2010). "Influence of rain infiltration on the stability of compacted soil slopes." *Computers and Geotechnics*, 37(5), 649–657.
- Papagianakis, A. T., and Fredlund, D. G. (1984). "A steady state model for flow in saturated–unsaturated soils." *Canadian Geotechnical Journal*, NRC Research Press, 21(3), 419–430.
- Pearson, K. (1895). "Note on Regression and Inheritance in the Case of Two Parents." *Proceedings of the Royal Society of London*, 58 (347-352), 240–242.
- Pham, H. Q., Fredlund, D. G., and Barbour, S. L. (2005). "A study of hysteresis models for soil-water characteristic curves." *Canadian Geotechnical Journal*, NRC Research Press, 42(6), 1548–1568.
- Phoon, K., Santoso, A., and Quek, S. (2010). "Probabilistic Analysis of Soil-Water Characteristic Curves." *Journal of Geotechnical and Geoenvironmental Engineering*, American Society of Civil Engineers, 136(3), 445–455.
- Richards, L. A. (1931). "Capillary conduction of liquids through porous mediums." *Journal of Applied Physics*, 1(5), 318–333.
- Rumsey, D. J. (2011). *Statistics for Dummies*. Wiley Publishing Inc., New Jersey, 384.
- Sako, K., and Kitamura, R. (2006). "A Practical Numerical Model for Seepage Behavior of Unsaturated Soil." *SOILS AND FOUNDATIONS*, 46(5), 595–604.

- Sillers, W. S., Fredlund, D., and Zakerzaheh, N. (2001). "Mathematical attributes of some soil–water characteristic curve models." *Geotechnical & Geological Engineering*, Kluwer Academic Publishers, 19(3-4), 243–283.
- Singh, V. P., Jain, S. K., and Tyagi, A. (2007). *Risk and Reliability Analysis: A Handbook for Civil and Environmental Engineers*. American Society of Civil Engineers Press, Virginia, U.S.
- Smith, L., and Freeze, R. A. (1979a). "Stochastic analysis of steady state groundwater flow in a bounded domain: 1. One-dimensional simulations." *Water Resour. Res.*, AGU, 15(3), 521–528.
- Smith, L., and Freeze, R. A. (1979b). "Stochastic analysis of steady state groundwater flow in a bounded domain: 2. Two-dimensional simulations." *Water Resour. Res.*, 15(6), 1543–1559.
- SoilVision Systems Ltd. (2014). "SoilVision - Soil Database Software." <<http://www.soilvision.com/subdomains/soildatabase.com/databases.shtml>>.
- Soleymani, S., and Akhtarapur, A. (2011). "Seepage Analysis for Shurijeh Reservoir Dam Using Finite Element Method." *ASCE Proceedings*, ASCE.
- Soraganvi, V., Mohan Kumar, M. S., and Muthineni, S. (2005). "Modeling of seepage flow through layered soils." *Unsaturated Soils: Numerical and Theoretical Approaches SE - 22*, Springer Proceedings in Physics, T. Schanz, ed., Springer Berlin Heidelberg, 313–325.
- Srivastava, A., and Babu, G. L. S. (2009). "Effect of soil variability on the bearing capacity of clay and in slope stability problems." *Engineering Geology*, 108(1–2), 142–152.
- Tan, T., Phoon, K., and Chong, P. (2004). "Numerical Study of Finite Element Method Based Solutions for Propagation of Wetting Fronts in Unsaturated Soil." *Journal of Geotechnical and Geoenvironmental Engineering*, American Society of Civil Engineers, 130(3), 254–263.
- Tani, M. (1982). "The properties of a water-table rise produced by a one-dimensional, vertical, unsaturated flow." *Journal of Japan for Society*, 64, 409–418.
- Tartakovsky, D. M. (1999). "Stochastic modeling of heterogeneous phreatic aquifers." *Water Resources Research*, 35(12), 3941–3945.

- Taylor, R. (1990). "Interpretation of the Correlation Coefficient: A Basic Review." *Journal of Diagnostic Medical Sonography*, 6(January/February), 35–39.
- Thieu, N. T. M., Fredlund, M. D., Fredlund, D. G., and Hung, V. Q. (2001). "Seepage Modeling in a Saturated/Unsaturated Soil System." *International Conference on Management of the Land and Water Resources*, Hanoi, Vietnam.
- United States Bureau of Reclamation (USBR). (1987). *Design of Small Dams*. USBR, Washington.
- Van Genuchten, M. T. (1980). "A Closed-form Equation for Predicting the Hydraulic Conductivity of Unsaturated Soils<sup>1</sup>." *Soil Science Society of America Journal*, 44(5), 892–898.
- Vanmarcke, E. H. (1980). "Probabilistic stability analysis of earth slopes." *Engineering Geology*, 16(1-2), 29–50.
- Vanmarcke, E. H. (2010). *Random Fields: Analysis and Synthesis*. World Scientific Publishing, Singapore.
- Warren, J. E., and Price, H. S. (1961). "Flow in Heterogeneous Porous Media." *SPE Journal*, Society of Petroleum Engineers, 1(3), 153–169.
- Willardson, L. S., and Hurst, R. L. (1965). "Sample Size Estimates in Permeability Studies." *Journal of the Irrigation and Drainage Division*, ASCE, 91(1), 1–10.
- Williamson, D. F., Parker, R. ., and Kendrick, J. S. (1989). "The Box Plot: A Simple Visual Method to Interpret Data." *Annals of Internal Medicine*, 110(11), 916.
- Wu, T. H., Vyas, S. K., and Chang, N. Y. (1973). "Probabilistic Analysis of Seepage." *Journal of the Soil Mechanics and Foundations Division*, ASCE, 99(4), 323–340.
- Yang, C., Sheng, D., Carter, J., and Huang, J. (2013). "Stochastic Evaluation of Hydraulic Hysteresis in Unsaturated Soils." *Journal of Geotechnical and Geoenvironmental Engineering*, American Society of Civil Engineers, 139(7), 1211–1214.
- Yang, C., Sheng, D., and Carter, J. P. (2012). "Effect of hydraulic hysteresis on seepage analysis for unsaturated soils." *Computers and Geotechnics*, 41(0), 36–56.

- Yates, S. R., van Genuchten, M. T., and Leij, F. J. (1989). "Analysis of Predicted Hydraulic Conductivities using RETC." *Proceedings of the International Workshop on Indirect Methods for Estimating the Hydraulic Properties of Unsaturated Soils*, 273–283.
- Yeh, T.-C. J., Gelhar, L. W., and Gutjahr, A. L. (1985a). "Stochastic Analysis of Unsaturated Flow in Heterogeneous Soils: 1. Statistically Isotropic Media." *Water Resources Research*, 21(4), 457–464.
- Yeh, T.-C. J., Gelhar, L. W., and Gutjahr, A. L. (1985b). "Stochastic Analysis of Unsaturated Flow in Heterogeneous Soils: 2. Statistically Anisotropic Media With Variable  $\alpha$ ." *Water Resources Research*, 21(4), 457–464.
- Zeng, C., Wang, Q., and Zhang, F. (2012). "Evaluation of Hydraulic Parameters Obtained by Different Measurement Methods for Heterogeneous Gravel Soil." *Terrestrial, Atmospheric & Oceanic Sciences*, Chinese Geoscience Union (CGU), 23(5), 585–596.
- Zhang, D. (1999). "Nonstationary stochastic analysis of transient unsaturated flow in randomly heterogeneous media." *Water Resources Research*, 35(4), 1127–1141.
- Zhang, D., and Lu, Z. (2002). "Stochastic analysis of flow in a heterogeneous unsaturated-saturated system." *Water Resources Research*, 38(2), 10–15.
- Zhang, L. L., Zhang, L. M., and Tang, W. H. (2005). "Rainfall-induced slope failure considering variability of soil properties." *Géotechnique*, 55(Volume 55, Issue 2), 183–188(5).



## APPENDICES

### APPENDIX A: The C# code

The C# code used for the application of van Genuchten method and random variable generation for hydraulic conductivity and van Genuchten fitting parameters  $\alpha$  and  $n$  are given below:

```
// This is a C# code, which is used as an Add-In function in SEEP/W.
// The code contains two general functions to calculate unsaturated
// hydraulic conductivity, and volumetric water content using
// van Genuchten method. There are two a random number generation function.

using System;

public class My_General_Functions
{
    // This general function is used under the "Random_Van_G_K_Unsat"
    function.

    public static Random autoRand = new Random();

    // The following function applies the van Genuchten method.
    // It takes a pressure and returns the van Genuchten K value
    // with a,n,m and Ksat values.

    public static double Van_G_K_Unsat( double pressure, double fa, double
fn, double fm,
        double fKsat )
    {

        // returned K value
        double fKx;

        // temporary variables
        double fTemp1, fTemp2, fTemp3, fTemp4, fTemp5, fTemp6;

        if(pressure < 0.0) // if in the unsaturated side of the function
        {
            double fSuction = Math.Abs (pressure);
```

```

        fTemp1 = fSuction*fa;
        fTemp2 = (Math.Pow((1.0 + Math.Pow(fTemp1, fn)),
(fm/2)));

        fTemp3 = Math.Pow(fTemp1, (fn-1));
        fTemp4 = (1.0 + Math.Pow(fTemp1, fn));
        fTemp5 = Math.Pow(fTemp4, -fm);
        fTemp6 = Math.Pow((1.0 - fTemp3 * fTemp5), 2.0);
        fKx = fKsat * (fTemp6/fTemp2);
    }
    else // use the user input Ksat if pwp are zero or positive
        fKx = fKsat;

    return fKx;
}

// This is the second general function in this file. It is called by
// "Van_Genuchten_VWC" function.
public static double Van_G_VWC( double pressure, double fa, double
fn, double fm, double fPorosity, double fResidualWC )
{
    double fWC, suction; // returned K value
    double fTemp1, fTemp2; // temporary variables

    if(pressure < 0.0) // if in the unsaturated side of the
function
    {
        suction = Math.Abs (pressure);
        fTemp1 = suction*fa;
        fTemp2 = Math.Pow( 1.0 / (1.0 + Math.Pow(fTemp1, fn)
) , fm );

        fWC = fResidualWC + (fPorosity-fResidualWC) * fTemp2;
    }
    else // use the user input porosity if pwp are zero or
positive
        fWC = fPorosity;

    return fWC;
}
} // end of the sub-function.

// The following function generates random hydraulic conductivity variables
// using random van Genuchten "a" parameter and van Genuchten "n" parameter.

public class Random_Van_G_K_Unsat : Gsi.Function
{
    public double muK; //mean of the hydraulic conductivity
    public double COVK; //coefficient of variation of hydraulic conductivity
    public double malpha; // mean of the van G "a" parameter in units of
1/pressure
    public double COValpha; //coefficient of variation of van G "a"
parameter
    public double mn; // mean of the van G "n" parameter

```

```

    public double COVn;      //coefficient of variation of the van G "n"
parameter
    double u1, u2, u3, u4, u5, u6;

    public Random_Van_G_K_Unsat()
    {

        u1 = My_General_Functions.autoRand.NextDouble();
        u2 = My_General_Functions.autoRand.NextDouble();
        u3 = My_General_Functions.autoRand.NextDouble();
        u4 = My_General_Functions.autoRand.NextDouble();
        u5 = My_General_Functions.autoRand.NextDouble();
        u6 = My_General_Functions.autoRand.NextDouble();
    }

    public double Calculate( double pressure )
    {

        double sigmaa, sigmalna, r1, alpha, sigman, sigmalnn, r2, n, m,
sigmaK, sigmalnK, r3;

// Generation of random variables of van Gencuhten "a" parameter

        sigmaa = COValpha * malpha;
        sigmalna = Math.Sqrt(Math.Log(1 + Math.Pow((sigmaa / malpha), 2)));

        r1 = Math.Sqrt(-2.0 * Math.Log(u1)) * Math.Sin(2.0 * Math.PI * u2);

        alpha = Math.Log(malpha) - 0.5 * Math.Pow(sigmalna, 2) + sigmalna *
r1;
        alpha = Math.Exp(alpha);

// Generation of random variables of van Gencuhten "n" parameter

        sigman = COVn * mn;
        sigmalnn = Math.Sqrt(Math.Log(1 + Math.Pow((sigman / mn), 2)));

loop:
        r2 = Math.Sqrt(-2.0 * Math.Log(u3)) * Math.Sin(2.0 * Math.PI * u4);

        n = Math.Log(mn) - 0.5 * Math.Pow(sigmalnn, 2) + sigmalnn * r2;
        n = Math.Exp(n);
        if (n < 1.0)
        {
            u3 = My_General_Functions.autoRand.NextDouble();
            u4 = My_General_Functions.autoRand.NextDouble();
            goto loop;
        }
        m = 1 - (1 / n);

// Calculation of random hydraulic conductivity

```

```

        double fKx = My_General_Functions.Van_G_K_Unsat(pressure, alpha, n,
m, muK);

        if (pressure < 0.0)
        {
            return fKx;
        }
        else

        fKx = Math.Log(fKx);

        sigmaK = COVK * muK;
        sigmaLnK = Math.Sqrt(Math.Log(1 + Math.Pow((sigmaK / muK), 2)));

        r3 = Math.Sqrt(-2.0 * Math.Log(u5)) * Math.Sin(2.0 * Math.PI * u6);
        fKx = fKx - 0.5 * Math.Pow(sigmaLnK, 2) +sigmaLnK * r3;

        return Math.Exp(fKx);

    }

}

// The following function is used to compute volumetric water content of the
// soil using random van Genuchten "a" parameter and van Genuchten "n"
// parameter

public class Van_Genuchten_VWC : Gsi.Function
{
    public double Porosity; //Saturated water content
    public double Residual_WC; //Residual water content
    public double malpha; // mean of the van G "a" parameter in units
of 1/pressure
    public double COValpha; //coefficient of variation of van G "a"
parameter
    public double mn; // mean of the van G "n" parameter
    public double COVn; //coefficient of variation of the van G "n"
parameter
    double u1, u2, u3, u4;

    public Van_Genuchten_VWC()
    {

        u1 = My_General_Functions.autoRand.NextDouble();
        u2 = My_General_Functions.autoRand.NextDouble();
        u3 = My_General_Functions.autoRand.NextDouble();
        u4 = My_General_Functions.autoRand.NextDouble();

    }
}

```

```

public double Calculate( double pressure )
{
    double sigmaa, sigmalna, r1, alpha, sigman, sigmalnn, r2, n, m;

    // Generation of random variables of van Gencuhten "a" parameter for
water content function
    sigmaa = COValpha * malpha;
    sigmalna = Math.Sqrt(Math.Log(1 + Math.Pow((sigmaa / malpha), 2)));

    r1 = Math.Sqrt(-2.0 * Math.Log(u1)) * Math.Sin(2.0 * Math.PI * u2);

    alpha = Math.Log(malpha) - 0.5 * Math.Pow(sigmalna, 2) + sigmalna *
r1;
    alpha = Math.Exp(alpha);

    // Generation of random variables of van Gencuhten "n" parameter for
water content function
    sigman = COVn * mn;
    sigmalnn = Math.Sqrt(Math.Log(1 + Math.Pow((sigman / mn), 2)));

loop:
    r2 = Math.Sqrt(-2.0 * Math.Log(u3)) * Math.Sin(2.0 * Math.PI * u4);

    n = Math.Log(mn) - 0.5 * Math.Pow(sigmalnn, 2) + sigmalnn * r2;
    n = Math.Exp(n);
    if (n < 1.0)
    {
        u3 = My_General_Functions.autoRand.NextDouble();
        u4 = My_General_Functions.autoRand.NextDouble();
        goto loop;
    }
    m = 1 - (1 / n);

    double fWC = My_General_Functions.Van_G_VWC(pressure,
        alpha, n, m, Porosity, Residual_WC);
    return fWC;
}
}

```

## APPENDIX B: Supplementary codes

A sample code written in Windows command line (i.e. an “.exe” file) to generate copies of SEEP/W simulation files:

```
@echo off
for /L %%i IN (1,1,1000) do call :docopy %%i
goto end
:docopy
set FN=%1
set FN=%FN:~-4%
copy "C:\Users\Calamak\Desktop\Case studies\Transient seepage\Rapid
drawdown\RD_25.04.2014.gsz" "C:\Users\Calamak\Desktop\Case
studies\Transient seepage\Rapid drawdown\RD_25.04.2014-%%FN%.gsz"
:end
```

A sample code written in Windows command line (i.e. an “.exe” file) to solve individual SEEP/W simulation files:

```
for /L %%i IN (1,1,1000) do call :dosolve %%i

goto end

:dosolve

set FN=%1

set FN=%FN:~-4%

"C:\Program Files\GEO-SLOPE\GeoStudio2007\Bin\Geostudio.exe" "/solve:all"
"C:\Users\Calamak\Desktop\Case      studies\Transient      seepage\Rapid
drawdown\RD_25.04.2014-%%FN%.gsz"

:end
```

A sample code written in Windows command line (i.e. an “.exe” file) to extract each SEEP/W simulation files to get seepage flow results:

```
for /L %%i IN (1,1,1000) do call :dounrar %%i

goto end

:dounrar

set FN=%1

set FN=%FN:~-4%

"C:\Program Files\7-Zip\7z.exe" x -r -x!*.mrk -x!*.xml -x!*.bmp -aou
"C:\Users\Calamak\Desktop\Case studies\Transient seepage\Rapid
drawdown\RD_25.04.2014-%%FN%.gsz"

:end
```

A sample code written in Visual Basic language, which runs as an add-in inside Microsoft Excel, to get the seepage flow results inside one final Microsoft Excel file:

```
Sub CopyFluxes()  
    Sheets("Fluxes").Activate  
    Range("C1").Select  
    Dim I As Integer  
    For I = 1 To 1000  
        Workbooks.Open          Filename:="C:\Users\Calamak\Desktop\Case  
studies\Transient seepage\Rapid drawdown\Transient Seepage\001\flux_" & I  
        Range("B:B").Copy  
        ThisWorkbook.Activate  
        ActiveCell.Offset(0, 1).Select  
        ActiveSheet.Paste  
        Application.CutCopyMode = False  
        Workbooks("flux_" & I).Close  
    Next I  
End Sub
```



## **CURRICULUM VITAE**

### **PERSONAL INFORMATION**

Surname, Name: Çalamak, Melih

Nationality: Turkish (TC)

Date and Place of Birth: 26 December 1986, Ankara, Turkey

Marital Status: Single

### **EDUCATION**

<b>Degree</b>	<b>Institution</b>	<b>Year of Graduation</b>
M.S.	METU Civil Engineering	2010
B.S.	Gazi Univ. Civil Engineering	2008
High School	İncesu Anadolu High School	2004

### **PROFESSIONAL EXPERIENCE**

<b>Year</b>	<b>Place</b>	<b>Enrollment</b>
2008-present	METU Civil Engineering Dept.	Research Assistant

### **HONOURS AND AWARDS**

2014	Outstanding Teaching Assistant, awarded by Department of Civil Engineering, Middle East Technical University.
2013	Photo contest winner of Annual Conference of Canadian Dam Association, Montreal, Canada.

### **FOREIGN LANGUAGES**

Advanced English

## PUBLICATIONS

### Journal Papers

- 1) **Calamak, M.** & Bozkus, Z. (2013). Comparison of performance of two run-of-river plants during transient conditions. *ASCE Journal of Performance of Constructed Facilities*, 27(5), 624–632. [http://dx.doi.org/10.1061/\(ASCE\)CF.1943-5509.0000370](http://dx.doi.org/10.1061/(ASCE)CF.1943-5509.0000370)
- 2) **Calamak, M.**, & Bozkus, Z. (2012). Protective measures against waterhammer in run-of-river hydropower plants. *Teknik Dergi/Technical Journal of Turkish Chamber of Civil Engineers*, 23(December), 1623-1636. <http://www.scopus.com/inward/record.url?eid=2-s2.0-84873891366&partnerID=tZOtx3y1>

### Conference Papers

- 1) **Calamak, M.** & Yanmaz, A. M. (2014). A study on effects of filter gradation uncertainty on seepage through embankment dams (in Turkish). *Proc. 4<sup>th</sup> National Symposium on Dam Safety*, pp. 127-137, Elazig, Turkey. <http://dx.doi.org/10.13140/2.1.1960.9282>
- 2) **Calamak, M.** & Yanmaz, A. M. (2014). Probabilistic assessment of slope stability for earth-fill dams having random soil parameters. *In Hydraulic structures and society - Engineering challenges and extremes (pp. 1–9)*. The University of Queensland. <http://dx.doi.org/10.14264/uql.2014.16>
- 3) **Calamak, M.**, Arici, Y. & Yanmaz, A. M. (2013). An assessment on dam engineering in Turkey (in Turkish). *Proc. 3<sup>rd</sup> Hydraulic Structures Symposium*, pp. 73-83, Ankara, Turkey. <http://dx.doi.org/10.13140/2.1.2943.9686>
- 4) **Calamak, M.**, Kentel, E., & Yanmaz, A. M. (2013). Spatial variability in seepage flow through earth-fill dams. *USB Proc. Canadian Dam Association Annual Conference 2013*, Montreal, Quebec, Canada. <http://dx.doi.org/10.13140/2.1.1245.3769>
- 5) **Calamak, M.**, & Bozkus, Z. (2012). Numerical investigation of operation levels in a surge tank of a small hydropower plant. *CD Proc. 10<sup>th</sup> International Congress on Advances in Civil Engineering*, Middle East Technical University, Ankara, Turkey. <http://dx.doi.org/10.13140/2.1.1769.6648>
- 6) **Calamak, M.**, Kentel, E., & Yanmaz, A. M. (2012). Seepage analysis of earth-fill dams having random fields. *CD Proc. 10<sup>th</sup> International Congress on Advances in Civil Engineering*, Middle East Technical University, Ankara, Turkey. <http://dx.doi.org/10.13140/2.1.3866.8169>

- 7) **Calamak, M.** (2011). SCADA system, automation and remote control in run-of-river hydropower plants (in Turkish). *Proc. 2<sup>nd</sup> Hydraulic Structures Symposium*, pp. 97-103, Diyarbakir, Turkey.  
<http://dx.doi.org/10.13140/2.1.1764.3204>

## **HOBBIES**

Photography, Trekking, Camping, Travelling, Reading